# Reward-related memory and interindividual variability in structural and functional brain networks

A thesis submitted to the Degree of Doctor of Philosophy

School of Psychology, Cardiff University

May 2021

Vera Dehmelt

# Thesis Summary

On any given day we only remember a fraction of what we experience. An event's salience will influence the probability of remembering. Extrinsic reward has been shown to introduce salience and facilitate memory. Yet, memory modulation through reward varies between individuals. This thesis aims to investigate: the brain networks associated with variability in reward-modulated memory; how reward influences hippocampus-dependent memory such as recollection, temporal order, and associative memory; how reward influences consolidation of intentionally memorised information; and how variability within brain networks associated with rewarded memory formation relates to variability in the influence of reward on different types of memory. Chapter 2 examined the effect of reward on temporal order memory and whether this effect was dependent on the type of post-encoding period. Comparing a distractor and a wakeful rest, temporal order memory was better for high than low reward items only when a distractor task filled the post-encoding period. Chapters 3 and 4 investigated the structural and functional connections underlying variability in reward-modulated temporal order memory. In Chapter 3, variability in the reward-related enhancement of temporal order memory was found to be associated with variability in the microstructure of the right inferior longitudinal fasciculus. Chapter 4 indicated a relationship between resting-state functional connectivity within a right hemispheric semantic network and variability in the reward-related temporal order memory benefit. Chapters 5 and 6 investigated the structural and functional connections underlying variability in immediate versus 24-hour delayed intentional memory. In Chapter 5, variability in delayed memory was related to variability in fornix microstructure. Chapter 6 indicated a relationship between variability in reward-related memory enhancement at delayed memory test and variability in resting-state functional connectivity between nucleus accumbens and hippocampus.

Together, these findings contribute to a better understanding of how individual variability in structural and functional connections relate to reward-modulated memory enhancements.

# Declaration and Statements

Statement 1

This thesis is being submitted in partial fulfilment of the requirements for the degree of Doctor of Philosophy.

Signed _____ Date: 17.05.2021

Statement 2

This work has not been submitted in substance for any other degree or award at this or any other university or place of learning, nor is it being submitted concurrently for any other degree or award (outside of any formal collaboration agreement between the University and a partner organisation).

Signed _____ Date: 17.05.2021

Statement 3

I hereby give consent for my thesis, if accepted, to be available in the University's Open Access repository (or, where approved, to be available in the University's library and for inter-library-loan), and for the title and summary to be made available to outside organisations, subject to the expiry of the University approved bar on access if applicable.

Signed _____ Date: 17.05.2021

Declaration

This thesis is the result of my own independent work, except where otherwise stated, and the views expressed are my own. Other sources are acknowledged by explicit reference. This thesis has not been edited by a third party beyond what is permitted by Cardiff University's Use of Third Party Editors by Research Degree Students Procedure.

Signed _____ Date: 17.05.2021

# Acknowledgements

I would like to express my gratitude to the following people, without their kindness and support the completion of this thesis would not have been possible. First, I would like to thank my primary supervisor, Matthias Gruber. His enthusiasm for science and sustained belief in my work enabled me to pursue my interests and continue to hone on my skills. His ongoing support throughout the new challenges of remote research has been invaluable. He helped me develop as a researcher and continues to share his knowledge and skills to further my path along my academic endeavours. I would also like to thank my second supervisor, John Aggleton, whose thorough feedback, encouraging discussions, and pushes forward I greatly value.

My thanks go to all the people at CUBRIC, whom I miss deeply. Thank you to Caz for the immense part she took in creating the great atmosphere at CUBRIC. I am thankful to my desk-neighbour Mark Postans for encouraging me when I got stuck on a problem. My thanks also go to Greg Parker, whose expertise in DTI I greatly appreciate. Thank you to Peter Hobden for his help in MRI data collection and for training me to become an MRI scanning operator. Thank you to Charlotte for her guidance on resting-state analysis, for providing insightful feedback, and for her encouragement in the final stages of this thesis. I would also like to express my gratitude to Duarte and Julia for their support during my unplanned departure from Cardiff. I would like to thank the other members of the lab; Danlu, Kathrin, and Hiki for their valuable feedback. I want to especially thank Ash for starting this journey towards our PhDs with me and for her sustained help and encouragement, but above all for her friendship. Our little group of friends, including Amy, Emily, Emma, and Laura, was an integral part to the enjoyment of my life in Cardiff. My thanks also go to the School of Psychology at Cardiff University for funding my PhD.

I want to thank my family for their support from the Continent. Thanks to Laura, Carina, Oma Else, Oma Rita, and Karl. I cannot express how grateful I am to my Mutti and Papa for their love, encouragement and believe in me, even when my believe in myself was low. Finally, thanks to Jake for his love, his confidence in me, for feeding me, and for spending his time off work reading this thesis.

# Contents page

# List of Figures

# List of Tables

# List of Formulas

# List of Abbreviations

| | |
|---|---|
| ATL | Anterior temporal lobe |
| BOLD | Blood-oxygen level dependent |
| CI | Confidence interval |
| CSF | Cerebrospinal fluid |
| DTI | Diffusion tensor imaging |
| DWI | Diffusion-weighted imaging |
| ECoG | Electrocorticogram |
| EPI | Echoplanar imaging |
| ErC | Entorhinal cortex |
| FA | Fractional anisotropy |
| FDR | False discovery rate |
| fMRI | Functional magnetic resonance imaging |
| fODF | Fibre orientation density function |
| FWE | Free-water elimination |
| FWE | Family-wise error rates |
| FWHM | Full-width-half-maximum |
| GLM | General linear model |
| HARDI | High angular resolution diffusion imaging |
| HC | Hippocampus |
| ICA | Independent component analysis |
| IFOF | Inferior fronto-occipital fasciculus |
| ILF | Inferior longitudinal fasciculus |
| ISI | Inter-stimulus interval |
| ITG | Inferior temporal gyrus |
| LFP | Local field potential |
| LTM | Long-term memory |
| LTP | Long-term potentiation |
| MD | Mean diffusivity |
| MID | Monetary incentive task |
| MRI | Magnetic resonance imaging |
| MTG | Middle temporal gyrus |
| MTL | Medial temporal lobe |
| NAcc | Nucleus accumbens |
| NODDI | Neurite orientation dispersion and density imaging |
| OFC | Orbitofrontal cortex |
| OLS | Ordinary least squares |
| PCA | Principal component analysis |
| PFC | Prefrontal cortex |
| PHC | Parahippocampal cortex |

| | |
|---|---|
| PrC | Perirhinal cortex |
| ROI | Region of interest |
| RSC | Retrosplenial cortex |
| RSFC | Resting-state functional connectvitiy |
| RT | Reaction time |
| SD | Semantic dementia |
| SD | Standard deviation |
| SE | Standard error |
| SN | Substantia nigra |
| STG | Superior temporal gyrus |
| TFC | Temporal fusiform cortex |
| TPM | Tissue probability map |
| UF | Uncinate fasciculus |
| VTA | Ventral tegmental area |

# Chapter 1: General Introduction

Do you remember what you did last Saturday? Maybe you took your favourite walk around the lake. You were enjoying the sun on your face, passing the usual spots; nothing out of the ordinary until you ran into an old friend you had not seen in a long time. You and your friend were having a nice chat and you decided to meet again soon before you parted ways. How will the rest of your walk unfold? How will you remember and retell your encounter later that evening or in a week? Will you remember more or less details because something special happened during an ordinary experience? Tulving (2002) likens the ability to "consciously re-experience past experiences" (Tulving, 2002, p.6) to time travel; we are viewing ourselves as subjects in the time of the re-experienced memory and present in the act of remembering. This illustrates one important feature of episodic memory, the form of declarative memory related to our own experiences: its relationship to time.

Events in episodic memory are often characterised by their sequential structure. A series of incidents, interactions, and objects are bound into episodic events by their context or the similarities in our experiencing of them. We certainly do not remember everything we experience. Crucially, an event's salience or value, as well as our emotional or motivational state during the experience will influence the probability of remembering it (e.g., Shohamy & Adcock, 2010; Tambini, Rimmele, Phelps, & Davachi, 2017). In the following paragraphs I will provide an overview of psychological and neurocognitive models of memory, influences of reward, sleep, or rest on memory, how these processes are proposed to interact, and how they are thought to be implemented in brain structure and function.

## 1.1 Theories of episodic memory – brain and behaviour

Two systems of declarative memory have been suggested, episodic and semantic memory (Polster, Nadel, & Schacter, 1991; Tulving, 1984; Squire, 1992). The two systems are proposed to differ in the content of the information they process and store. Episodic memory describes an individual's memory for personal autobiographic events

or episodes. They are spatiotemporal in their structure and have spatiotemporal relationships to each other. Semantic memory refers to a person's factual knowledge about the world, concepts, and even themselves (Tulving, 1984; 2002). Within this psychological framework, an episodic experience creates a memory *engram* within the brain where it is "stored" with different fidelity and for different lengths. The *engram* is retrieved after an effective memory cue and thereby an event is remembered (Tulving, 2002; Tulving & Thomson, 1973). However, not all *engrams* are effectively stored and remembered. An event's salience and its motivational as well as emotional context influence how and whether it is remembered. This promotes memory in support of adaptive behaviours (Shohamy & Adcock, 2010). These descriptions highlight three components central to memory research: consolidation, representation, and memory systems. A number of fields concerned with the human experience like philosophy, psychology, medicine, and neuroscience have investigated how memories are formed, stored, and retrieved. Varying methods are employed to investigate memory within and across these fields. These methods include observations, behavioural experiments, the study of amnesic patients, and research in the animal model. Within the long history of the research of memory formation, these fields have shared information reciprocally (Polster et al., 1991).

The questions of memory representations and memory systems have often informed each other. This is exemplified in the study of amnesic patients. Patients present with particular memory deficits. For example, Cohen and Squire (1980) have demonstrated that amnesic patients were able to learn new procedural skills without explicit memory of said learning. This exemplifies different memory systems, a difference between "knowing how" and "knowing that", between knowledge that you cannot and can declare (Cohen & Squire, 1980). These deficits are frequently accompanied by particular brain damages. For example, the patient K.C. who has been thoroughly investigated in Tulving's lab (Tulving, 2002; Rosenbaum et al., 2005). K.C. suffered memory loss and deficits after a traumatic brain injury. He displayed deep anterograde amnesia, the inability to create new memories. His retrograde amnesia, the loss of already acquired memory, was extremely asymmetric. This asymmetry is represented in K.C.'s display of normal cognitive abilities. His knowledge about the

world was comparable to his educational background. He recognised his friends and family. He was even able to recall knowledge about his life on a factual basis. Nevertheless, he lacked any memory for events in his life, independent of the importance of the events or the regularity with which they occurred (Tulving, 2002). In a series of experiments Tulving and colleagues were able to show that K.C. was capable to slowly acquire new semantic knowledge without explicit memory of the events of coming to the lab and training the task (Hayman, Macdonald, & Tulving, 1993; Tulving, Hayman, & Macdonald, 1991). K.C.'s severe anterograde amnesia and his asymmetric retrograde episodic memory loss were accompanied by disproportional (in comparison to his diffuse cortical atrophy) necrosis of the bilateral hippocampus, the left mammillary bodies, and the left amygdala. Within the medial temporal lobes (MTL), the entorhinal cortex (ErC), perirhinal cortex (PrC), and parahippocampal cortex (PHC) displayed structural magnetic resonance imaging (MRI) abnormalities that suggest necrosis (Rosenbaum et al., 2005). This illustrates that even though cases of "pure" episodic memory deficit are rare, studies of memory deficits in amnesic patients point to the overlap between theories about memory systems and representation. Amnesic patients display distinctive deficits pointing towards separable memory systems and their amnesias are related to distinctive damages of memory representations in the brain, often mainly within the MTL.

Researchers employ different types of tasks in the investigation of declarative memory, including free recall, cued recall, or recognition memory tasks. Recognition memory itself is separable into two components, recollection and familiarity (Brown & Aggleton, 2001). During recollection, contextual details of the previous episodic event are retrieved while familiarity is not accompanied by this detailed explicit remembering and reflects a sense of knowing. For example, when encountering a person on the street, you might have the feeling that you know them. Although you cannot put your finger on where you met them, they are familiar to you. Or you might see a dog and their owner on the street, and you can recall the last time you encountered this pair. You remember that you noticed them three days ago in the park, you remember that you were on a walk with a friend and pointed the dog's interesting colouring out to them. You are able to recall the contextual details of the first time you encountered this dog; in your mind,

you can travel back in time to that specific event. Hence, recollection is reflecting the sensation of remembering and familiarity the sensation of knowing (Stern & Hasselmo, 2008). According to dual-process theories, recollection and familiarity are distinct processes that are supported via separable regions within the MTL (Brown & Aggleton, 2001; Eichenbaum, Yonelinas, & Ranganath, 2007). In the animal model, the behaviour of rats and monkeys on different memory tasks can be interpreted as reflecting different processes akin to recollection and familiarity memory in human subjects (Eichenbaum, Sauvage, Fortin, Komorowski, & Lipton, 2012). Thus, investigation of memory in the animal model, lesion and amnesia studies as well as functional imaging studies provide bases for theories into the neurocognitive – brain/mind – underpinnings of memory.

According to one dual-process theory (see Brown & Aggleton, 2001; Davachi, 2006; Eichenbaum et al., 2012), the hippocampal formation and the surrounding entorhinal (ErC), perirhinal (PrC), and parahippocampal (PHC) cortices that make up the MTL are believed to subserve different aspects of memory. The hippocampal formation refers to the hippocampus proper (the CA fields), the subiculum as the primary output structure of the hippocampus, and the dentate gyrus. The hippocampus receives information about percepts from unimodal and polymodal sensory areas along the so-called “what-stream” via the PrC and lateral ErC. Visuospatial context information reaches the hippocampus from the “where-stream” via the PHC and the medial ErC. Within the hippocampus, object and space/context information is then integrated into a coherent episodic trace. The episodic trace comprises objects or behavioural events in their spatial or temporal contexts, or both. Following this theory, familiarity is supported by the PrC while recollection and especially associative memory are subserved by the hippocampus. Selective lesions in the animal model as well as amnesia and functional imaging studies in humans support this distinction (Brown & Aggleton, 2001; Davachi, 2006; Eichenbaum et al., 2007; Eichenbaum et al., 2012). In an extension of these models, Ranganath and Ritchey (2012) propose that information about objects, faces, or entities and their importance/value/reward-predictive properties is processed in an anterior system. Information about context is processed in a posterior system. The hippocampus integrates information from the anterior and the posterior system. The anterior system comprises the PrC in the MTL and the regions it connects to, including

the orbitofrontal cortex (OFC) and the amygdala. The posterior system comprises the PHC within the MTL memory system and the retrosplenial cortex (RSC) and the regions they connect to. The functionalities of these systems are described not only by the involvement of their main constituents in certain tasks, including memory as well as perception, but also by the constituent's connections within the hippocampus and the cortex (Ranganath & Ritchey, 2012). Other models suggest that familiarity and recollection are not separable processes of recognition memory per se but merely an expression of different levels of memory strength supported by the same process (Kirwan, Wixted, & Squire, 2008; Wais, Squire, & Wixted, 2010; Wixted & Squire, 2011). Investigation of these models is beyond the scope of this thesis. But models of the form of representation and contributions of subregions in the MTL provide points of access into the investigation of episodic memory within this work.

Episodic memory is distinct in that it connects "the 'what' with the 'where' and the 'when' of the memory" (Manns, Howard, & Eichenbaum, 2007, p. 530) and Tulving (2002) emphasizes the recollective flavour of episodic memory. These associative and recollective aspects should especially involve processing in the hippocampus (e.g., Brasted, Bussey, Murray, & Wise, 2003; Davachi & DuBrow, 2015; Tompary, Duncan, & Davachi, 2016; Tubridy & Davachi, 2011). Another important aspect of episodic memory is its relationship to time.

### 1.1.1 Time and memory

The relationship between time and memory can be well described via the hippocampus. The hippocampus displays specific time, order, and scene representations sometimes within specific cell populations (Eichenbaum, 2013; O'Keefe & Nadel, 1978; MacDonald, Lepage, Eden, & Eichenbaum, 2011; Murray, Wise, & Graham, 2018). Along the evolutionary family tree from early vertebrates, via mammals and primates, to humans, the hippocampus developed from subserving simple "map-like" representations supporting navigation, via representations supporting associative, recency, and recollective memory to scene perception underlying learning about complex events (Murray et al., 2018). Investigation of episodic-like temporal memory in

the animal model can provide insight into how the temporal structure of memory is represented in the brain (Dere, Huston, & De Souza Silva, 2005).

In a study by Manns et al. (2007), rats had to remember the position and order of different odours. The rats experienced sequences of five pots that contained differently smelling sand. Every new smell constituted a new object in the sequence and with every new object/smell the position was switched. After the sequence-encoding, an object/smell pair was presented to the animal and the rats would find reward in the pot with the earlier smell of the sequence. Therefore, the rats had to make a correct "which came first?" temporal order discrimination to be rewarded. In recordings of the animal's hippocampus cells during this task, hippocampal CA1-cells carried information about the identity of single odours. Other cells displayed similarity for different smells experienced at the same position (spatial specificity) while again other cells fired more similar for smells experienced closer together (lag; temporal specificity). However, the largest population of hippocampus-cells exhibited a combination of this behaviour. Their population firing patterns showed spatial specificity while growing more dissimilar across the time of the experiment and even across lags of one trial. This temporal specificity (linearly growing dissimilarity of population patterns for space) was related to successful memory for the sniffing-event structure (Manns et al., 2007; for a similar finding in humans, see Dimsdale-Zucker, Ritchey, Ekstrom, Yonelinas, & Ranganath, 2018). In a study by Fortin and colleagues (2002), rats with hippocampal lesions, tested on a similar temporal order task, showed chance level performance compared to control animals, independent of the lag (number of intervening objects/cups) between pairs. Nevertheless, these lesioned animals performed well on a recognition memory test and were able to identify odour cups that were not presented in the sequence (Fortin, Agster, & Eichenbaum, 2002).

Additional examples of studies in non-human primates illustrate that rhesus monkeys are able to make temporal order decisions, capturing aspects of episodic memory, and that they discriminate temporal order based on order representations specifically as opposed to the strength of the memory, position coding, or coding for time passed (Templer & Hampton, 2013). Monkeys with ablations limited to the

hippocampal formation (hippocampus proper, subiculum, dentate gyrus) were impaired on associative memory tasks, independent of modality (Moss, Mahut, & Zola-Morgan, 1981). In a study by Charles, Gaffan, and Buckley (2004), monkeys were trained on a recency discrimination task. The monkeys were presented with a sequence of five clipart images and then tested on an image pair. They received reward for choosing the image they had seen later in the sequence. The monkeys displayed recency as well as lag effects. They made fewer errors if the target image was later in the sequence and therefore closer to the test. They also made fewer errors if the lag between the images of the pair was larger, if, for example, the object pair that was tested included image 2 and 4 as opposed to image 2 and 3. Monkeys with dissection of the fornix, a major output pathway of the hippocampus, displayed a similar pattern but made overall significantly more errors on the temporal order task than control monkeys. Contrastingly, fornix-dissected and control monkeys behaved the same on memory tests on object pairs containing old and novel images, reliably choosing the old image (Charles et al., 2004). These effects described in the animal model outline the importance of the hippocampus in associative and temporal order memory tasks, a central aspect of episodic memory, specifically.

As described above, investigation within amnesic patients informs theories of memory systems and representations as well as the animal model. This tradition is based on early reported case studies of Korsakoff syndrome (Rosenbaum et al., 2005). Korsakoff syndrome usually results from untreated Wernicke's encephalopathy (Kopelman, Thomson, Guerrini, & Marshall, 2009). Wernicke's encephalopathy itself is the result of a thiamine (vitamin B1) deficiency due to a poor diet and compromised thiamine absorption in chronic alcoholism (Sullivan & Pfefferbaum, 2008). This makes these two memory disorders unusual in that they are caused by a distinct neurochemical pathology (Kopelman et al., 2009). Thiamine deficiency results in the neuropsychiatric symptoms of Wernicke's encephalopathy due to its importance as a co-factor in carbohydrate metabolism within various neurotransmitter systems. Long-lasting thiamine deficiency will result in lesions within the mammillary bodies, the thalamus, the hypothalamic nuclei, the periventricular nuclei among others. Due to these lesions

patients present with symptoms like ophthalmoplegia (weakness of the eye muscles), nystagmus (eye shaking), ataxia, and a confusional state.

Wernicke's encephalopathy can be treated with vitamin B repletion. If untreated, it can result in Korsakoff syndrome which is characterised by profound episodic memory impairments and most likely chronic (Kopelman et al., 2009; Sullivan & Pfefferbaum, 2008). Neuropathology within Korsakoff syndrome is reflected in damage to regions within the midline diencephalon, e.g., the mammillary bodies, anterior thalamic nuclei, and midline thalamus (Aggleton, Dumont, & Warburton, 2011; Downes, Mayes, MacDonald, & Hunkin, 2002; Kopelman et al., 2009). In a comparison of Korsakoff syndrome patients with healthy controls on a spatial and temporal order recall test, Postma and colleagues (2006) found that patients were impaired on both spatial as well as temporal order recall (Postma, van Asselen, Keuper, Wester, & Kessels, 2006). Amnesic patients were similarly impaired whether the spatial or temporal feature was presented and tested alone, whether the presentation was spatiotemporal but only one of the features had to be remembered, or whether presentation and test were spatiotemporal. Contrastingly, controls displayed a decline in memory performance from single feature presentation and test to a combined presentation and single feature test to spatiotemporal presentation and test. This pattern is interpretated as a deficit in binding of different contextual information in Korsakoff patients (Postma et al., 2006). In another comparison of patients with organic amnesia and healthy control subjects by Downes and colleagues (2002), patients with Korsakoff syndrome and MTL-amnesia were significantly impaired on a temporal order memory task while performing like control subjects on a recognition memory task. Patients with Korsakoff syndrome and MTL-amnesia did not significantly differ from each other in their memory test performance despite their differences in affected brain regions. Brain damage within the Korsakoff syndrome affects the midline diencephalon and typically spares the hippocampus. Brain damage within the MTL-amnesic patients affected mainly the hippocampus and the ErC, PrC, and PHC partially. That midline diencephalic and hippocampal damage both led to specifically impaired temporal order memory led the authors to conclude their results to be in line with Aggleton and Brown's (1999) theory of an extended hippocampal system (Downes et al., 2002).

Although brain damages within Korsakoff syndrome generally spare the hippocampus, hippocampal atrophy or dysfunction have sometimes been seen in Korsakoff syndrome patients (Postma et al., 2006; Sullivan & Pfefferbaum, 2008). Studies of amnesic patients with hippocampal and broader MTL damage represent a second large group of investigations. In a case study of a patient with selective bilateral hippocampal damage, the patient displayed severe temporal order memory deficits on a variety of memory tasks in comparison to healthy controls (Mayes et al., 2001). The bilateral hippocampal lesion in the patient was not accompanied by extensive MTL damage. The diencephalon and the frontal cortex of the patient did not show damage. Healthy controls were matched to the amnesic patient on age, gender, and IQ. The MTL-amnesic patient displayed severe temporal order memory deficits while performing at a mostly normal level in recognition memory tests. The amnesic patient was even able to recognise item pairs as old, but she was unable to remember their order correctly, independent of whether she was instructed to specifically memorise the order during encoding or not. Her temporal order memory deficit was also evident in forced-choice recognition tests of the sequence (correct order presented together with foils of wrong order) as well as in a reordering paradigm (Mayes et al., 2001). In another study of serial free recall in patients with MTL-amnesia in comparison to healthy controls, Palombo and colleagues (2018) demonstrated that MTL-amnesic patients were unable to reinstate the temporal context in which an item was encoded. This means that recall of one item did not become a critical cue for neighbouring items. Contrarily, controls displayed a pattern where recall of one item led to the increased probability of recalling following as well as previous items in the list. This demonstrated that MTL damage and its associated amnesia leads to a deficit to jump back in time, the exact descriptor of episodic memory (Palombo, Di Lascio, Howard, & Verfaellie, 2018).

During episodic encoding, our continuous experience needs to be parsed into episodic events for memory. Breaks in perceptual, temporal, or conceptual information introduce event boundaries that underly this process (Davachi & DuBrow, 2015; Kurby & Zacks, 2008). Studies that investigate the influence of these event boundaries on memory in human participants introduce these boundaries by a change in the object category displayed or in the colour that frames the to-be-encoded objects for example.

These investigations were able to show that associative memory between objects and their context was increased at the event boundary while temporal order memory was found to be stronger for object pairs within events (not crossing a boundary) than across events (across a boundary) (DuBrow & Davachi, 2014; Ezzyat & Davachi, 2011; Heusser, Ezzyat, Shiff, & Davachi, 2018). Like the macaques, human subjects display an effect of lag where the temporal order between object pairs at longer lags is better discriminated than at shorter lags or for neighbouring objects. In the study by DuBrow and Davachi (2014), functional MRI was acquired during a temporal order memory task involving study-test cycles. They employed multivoxel pattern analysis to investigate the relationship between the pattern of functional brain activation and memory performance. The amount of similarity in the activation pattern of the hippocampus between the two objects of the pair at encoding was related to successful temporal order memory. Furthermore, hippocampal reactivation of the pattern to intervening items during retrieval was related to memory success (DuBrow & Davachi, 2014). By contrast, dissimilarity in hippocampal encoding patterns between the two objects of tested object pairs was related to correct high confidence temporal order memory in a study by Jenkins and Ranganath (2016). Participants had to make “which came first” temporal order discriminations on object pairs from previously encoded sequences and were instructed to rate their confidence in their decision. The dissimilarity in hippocampal patterns between the two objects separated by six objects during successful encoding was interpreted as temporal discrimination being supported by contextual information and dissimilarity patterns like in the study by Manns et al. (2007). In a second study, DuBrow and Davachi (2016) employed a similar encoding task with a serial recall memory test. They found that within-event (not crossing an event boundary) serial recall was related to increased functional connectivity between the hippocampus and the ventromedial prefrontal cortex (PFC). Contrastingly, univariate BOLD signal during encoding within the medial hippocampus and the ventrolateral PFC was related to serial recall across event boundaries (DuBrow & Davachi, 2016). Patterns of within-event binding and across-event segmentation introduced by an event boundary have been demonstrated in the fMRI signal of the ventromedial PFC and areas within the MTL (Ezzyat & Davachi, 2011). Jenkins and Ranganath (2010) demonstrated that encoding activity within the MTL and the PFC related to accuracy in a temporal order memory

test. Whereas fine-grained temporal order memory was supported by encoding activity in the MTL, coarse temporal order memory was supported by encoding activity in the PFC (Jenkins & Ranganath, 2010). It has been suggested that the PFC and the hippocampus facilitate temporal order memory formation independently as well as together. The representation of contextual information in the lateral PFC supports relational binding in episodic memory formation (Clewett & Davachi, 2017).

Whether temporal order memory is supported by hippocampal pattern dissimilarity (Jenkins & Ranganath, 2010; 2016; Manns et al., 2007), pattern similarity (DuBrow & Davachi, 2014; Ezzyat & Davachi, 2014), or other hippocampal mechanisms like memory strength is beyond the scope of this thesis. It has been suggested that how exactly the hippocampus encodes and remembers order might depend on the task (Davachi & DuBrow, 2015; Jenkins & Ranganath, 2016). What remains of interest is that the human MTL and hippocampus specifically as well as the frontal cortex support memory for temporal structure (Heusser, Poeppel, Ezzyat, & Davachi; 2016; Hsieh, Gruber, Jenkins, & Ranganath, 2014; Jenkins & Ranganath, 2010; Tubridy & Davachi, 2011).

One important feature of episodic memory formation lies in its contribution to adaptive behaviour. Every day we make decisions based on the perceived value of the predicted outcome of that decision. Episodic memory is of importance for this because often just one specific experience can form the basis for future decision-making (Wimmer & Büchel, 2016). Following this, the motivational value of an event will influence the probability of remembering or forgetting it (e.g., Shohamy & Adcock, 2010). Reward as an external motivator can introduce motivational value to an event. Additionally, laboratory investigations of reward- or novelty-modulated memory have shown that these memories share features with episodic memory events; for example, their rich contextual detail and the experienced confidence in memory (Shohamy & Adcock, 2010). Episodic memory events are also often temporal in nature but the investigation of temporal order memory in humans often lacks reward. In the following sections, I will outline how reward influences memory before I introduce the aims of this study in 1.3.

Throughout this thesis, the term “salience” refers to the property of reward that is not directly reflected in its value-component. The salience components of reward are proposed to elicit orienting responses (Schultz, 2015). Rewards, which can be a stimulus, an object, or an event, are salient due to their physical intensity, their novelty and surprise as well as due to their motivational properties (Schultz, 2015). The value and salience components of rewards have been proposed to interact (Madan & Spetch, 2012). In free recall following value learning, memory enhancements reflected an interaction of salience and value in that memory for the extremes was enhanced for high as well as low value items. This was based on the range of values experienced (Madan & Spetch, 2012). Within the framework of this thesis, both value and salience aspects of reward are believed to interact to generate motivational significance; reward is salient because it signals value, and a higher reward is more salient because it signals more value within the range of values that are experienced.

### 1.1.2 Reward and memory

Long-term potentiation (LTP) is described as the neural mechanism underlying long-term memory (LTM) formation through changes in synaptic plasticity (Lisman & Grace, 2005; Tubridy & Davachi, 2011; Shohamy & Adcock, 2010; Wallenstein, Hasselmo, & Eichenbaum, 1998). These changes can be induced by reward- and novelty-related firing of dopaminergic cells and a dopamine-transmitted pathway was proposed to include the hippocampus (Figure 1.1; Düzel, Bunzeck, Guitart-Masip, & Düzel, 2010; Lisman & Grace, 2005).

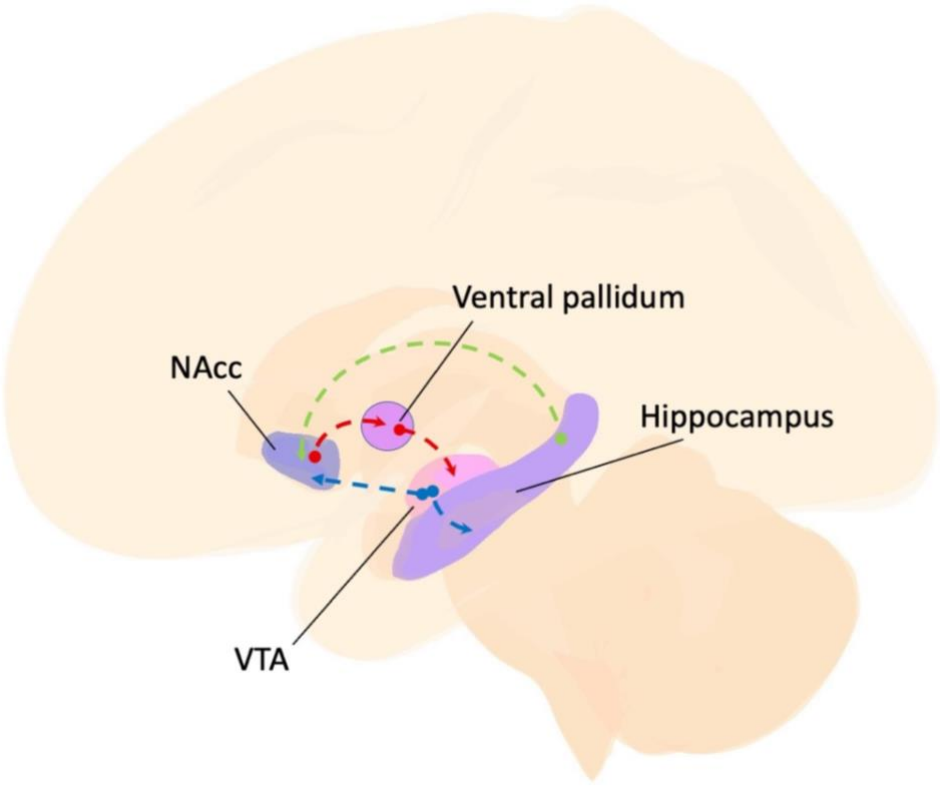


**Figure 1.1 The hippocampal-VTA loop.** The hippocampus receives dopaminergic input from the VTA, which also has excitatory dopamine connections to the NAcc. The hippocampus provides excitatory (glutamatergic) input to the NAcc, which projects to the ventral pallidum. Thereby the inhibitory effect of the ventral pallidum to the VTA is reduced and the loop closed. Lines denote input. Green = glutamatergic excitatory input. Red = inhibitory GABAergic input. Blue = dopaminergic input. Hippocampus and NAcc ROIs from Grabner et al. (2006). Probabilistic binarised VTA ROI from Murty et al. (2014). *(See Düzel et al., 2010; Lisman & Grace, 2005; Shohamy & Adcock, 2010; Figure adapted from Gruber, Valji, & Ranganath, 2019)*.

The hippocampus, the ventral tegmental area (VTA), and the nucleus accumbens (NAcc) are intrinsically connected (Kahn & Shohamy, 2013). These regions form a functional loop via dopamine- and other transmitter-related synapses (Düzel et al., 2010; Lisman & Grace, 2005). Hippocampal LTP depends on targeted and layer-specific direct dopaminergic projections from the substantia nigra (SN) and the VTA. The hippocampus also has a polysynaptic pathway back to the VTA. Excitatory connections from the subiculum, the output structure of the hippocampus, to the NAcc can lead to inhibitory output from the NAcc to the ventral pallidum. Inhibition of the ventral pallidum in turn releases its inhibition of the VTA. The VTA in turn excites the hippocampus and the NAcc via dopamine. Novelty-signal along this pathway is compared with information about behavioural relevance (e.g., via reward). Depending on those comparisons, LTM formation will be induced or not. Dopaminergic dysfunction

within this system impairs episodic memory consolidation (Düzel et al., 2010; Lisman & Grace, 2005). Functionality of this system at encoding has been shown to influence memory (Shohamy & Adcock, 2012; Wittmann et al., 2005).

#### 1.1.2.1 Reward and encoding processes

Though the hippocampal-VTA loop (Lisman & Grace, 2005) and NOMAD (Novelty-related Motivation of Anticipation and exploration by Dopamine; Düzel et al., 2010) models are concerned with novelty, they also point towards the importance of motivational factors like reward to regulate novelty responses. Furthermore, both novelty and reward have been shown to modulate activity within this network (e.g., Bunzeck, Dayan, Dolan, & Düzel, 2010). In a spatial decision task, rats learned a path across four decision points towards reward (van der Meer, Johnson, Schmitzer-Torbert, & Redish, 2010). Whereas the first three decision points were of low risk when a false decision led to a dead end, the final decision point was associated with a higher risk, when a wrong decision led back to the start and rats lost reward. Cell recordings in the hippocampus, the dorsal, and the ventral striatum were made during learning. Learning was fast, rats reached asymptotic behaviour after ten laps. During learning, especially at the early stages of learning, cells in the rats' ventral striatum, which includes the NAcc, represented upcoming rewards at decision points. Hippocampal cells fired relatively uniformly across the track, exemplifying its function as processing a map-like representation of the path. Rats need to represent and remember reward outcomes as well as the spatiotemporal configuration of the path to learn this task. Therefore, hippocampus and striatal processing enable learning encouraged by reward (van der Meer et al., 2010).

In a study by Adcock and colleagues (2006), participants received high or low reward for correctly remembering a scene in a delayed memory test. Regions within the NAcc and the VTA were independently localised for reward-responsiveness. Activity within the NAcc, the VTA, and the hippocampus during the reward-cue was related to subsequent memory. The reward-cue was followed by the to-be-remembered scenes. Activity in the NAcc, the VTA, and the hippocampus during reward anticipation (during cue) was increased for subsequently remembered as opposed to forgotten scenes but

only during high reward anticipation. This was accompanied by better high than low reward memory. Furthermore, higher functional connectivity between the VTA and the hippocampus was related to the reward-related memory enhancement (Adcock, Thangavel, Whitfield-Gabrieli, Knutson, & Gabrieli, 2006). Similarly, other studies have shown that encoding-related activity and connectivity within the hippocampal-VTA loop are connected to memory enhancement through reward (Murty & Adcock, 2014; Wittman et al., 2005; Wolosin, Zeithamova, & Preston, 2012). In addition, studies have demonstrated that changes within this system during post-encoding are similarly important. I will outline some of these findings below.

#### 1.1.2.2 Reward and post-encoding processes

The investigation of episodic-like memory in animals includes animals traveling along a path. Replay of the path information in the hippocampus during wakeful rest (Davidson, Kloostermann, & Wilson, 2009; Karlsson & Frank, 2009; Singer & Frank, 2009) or sleep (Dupret, O'Neill, Pleydell-Bouverie, & Csicsvari, 2010; Lansink et al., 2008; Lee & Wilson, 2002; Peyrache, Khamassi, Benchenane, Wiener, Battaglia, 2009) has been found to be related to successful memory.

In human participants, reward-motivated encoding (high versus low monetary reward for encoding task performance) led to memory benefits for objects from high rewarding contexts in an immediate memory test (Gruber, Ritchey, Wang, Doss, & Ranganath, 2016). These reward-related memory benefits were related to post-encoding increases in functional connectivity between VTA and hippocampus. Additionally, they found hippocampal reactivation of those high reward contexts during post-encoding rest to be related to better memory for objects encoded within this context (Gruber et al., 2016). A study by Murty, Tompary, Adcock, and Davachi (2017) showed that not only post-encoding processes within this network are related to reward-enhanced memory. Functional connectivity between the hippocampus and the cortex during post-encoding rest was associated with overall memory performance on the task, while functional connectivity between VTA and the cortex was specific for high reward memory in a 24-hour delayed associative memory test for pictures and their names (Murty et al., 2017). In another study of associative binding and reward, Wimmer

and Shohamy (2012) first paired two items reliably with each other in a statistical learning paradigm. In a second step, they then employed classical conditioning to pair one of the two with reward. Finally, in the third step, participants were presented with object pairs and were instructed to pick the object they felt was “luckier”. The pairs comprised objects from the first step that were not presented during the second phase. Participants displayed a bias towards picking items that in the first step were paired with subsequently, in the second step, rewarded items over items paired with ones that were not rewarded in the second step. This bias occurred for the one item of the item-pair that was never presented during the reward-phase and without participants’ conscious memory of the item pairing. In the hippocampus, this decision bias was related to reactivation of patterns exhibited during the first encoding step in the second reward phase (Wimmer & Shohamy, 2012). A study by Igloi and colleagues (2015) demonstrated that long-term memory retention for high reward information is accompanied by increased striatal-hippocampal connectivity as well as the presence of sleep spindles during a post-encoding nap (Igloi, Gaggioni, Sterpenich, & Schwartz, 2015). Thus, Igloi et al. demonstrated that prioritised sleep-dependent memory consolidation supports high reward memory.

#### 1.1.2.3 Reward and semantic processing

An important function of declarative memory formation is the abstraction of valuable decision-making heuristics from episodic events (Wimmer & Büchel, 2010; Wimmer & Shohamy, 2012). It is adaptive that more than one process subserves preferential episodic memory formation based on motivational value due to its importance for future behaviour. LTM formation supported by the dopaminergic functioning of the hippocampal-VTA loop is one process and elaborative and strategic encoding supported by the semantic network is another. Cohen and colleagues (Cohen, Cheng, Paller, & Reber, 2019; Cohen, Rissman, Suthana, Castel, & Knowlton, 2014; 2016) found that memory for high-value information was supported by encoding activity in regions involved in semantic processing like the inferior frontal cortex and posterior lateral temporal cortex. They employed different memory tasks typically utilised in investigations of episodic memory. This included a recollection memory test (Cohen et al., 2014), free recall (Cohen et al., 2016), and a complex association memory test

(Cohen et al., 2019). A relationship between encoding-activity in semantic processing areas and memory was found across all of these investigations (Cohen et al., 2019; Cohen et al., 2014; 2016). Activation in classic reward processing areas was also found but only in young not in older adults during the cuing period (Cohen et al., 2016) or this activation was unspecific, related to correctly remembered items independent of value (Cohen et al., 2019). These results display that the strategic engagement of semantic processing capacities, maybe related to task-requirements, should be investigated in studies concerned with reward and memory.

### 1.1.3 Interindividual differences in reward-related memory

How much a certain reward can incentivise varies between individuals (Berridge, 2007; Cohen, Young, Baek, Kessler, & Ranganath, 2005). Furthermore, some of the studies reviewed above show that modulation of memory through reward varies between individuals. For example, Adcock et al. (2006) found that interindividual differences in the activation of the VTA during reward-anticipation correlated with high confidence recognition memory. Wolosin et al. (2012) showed that interindividual variability in reward-modulated (high – low-value) hippocampal subfield encoding-activity correlated with variability in the reward-related memory benefit for object pairs in a cued recall test (Wolosin et al., 2012). Within the semantic network, Cohen and colleagues (2014) showed that variability in participants' memory performance in a free recall test correlated with reward-modulated (high > low) activation of regions within the temporal cortex (Cohen et al., 2014). In their review of highly superior and severely deficient autobiographical memory, Palombo, Sheldon, and Levine (2018) propose that "autobiographical memory, like other cognitive domains, can be considered a 'trait' that reflects stable individual differences in the manner in which people tend to access their past" (p. 588). Investigations of these trait-like interindividual differences in autobiographical as well as episodic-like memory in their extremes and their nuances are suggested of importance for our understanding of adaptive memory formation (Palombo, Sheldon et al., 2018). The examples put forth here demonstrate the value of investigating between-subject variability when studying memory.

In the following paragraphs I will outline the neuroimaging methods employed in this thesis before outlining its aims. Tractography measured via diffusion-weighted imaging (DWI) and resting-state functional connectivity (RSFC) are employed to investigate the neuroanatomical and functional underpinnings of reward-modulated memory.

## 1.2 Magnetic resonance imaging methods

### 1.2.1 Diffusion-weighted magnetic resonance imaging

Diffusion-weighted imaging (DWI) is employed during Magnetic Resonance Imaging (MRI) to measure Brownian motion, the random thermal motion of molecules, within tissue (Le Bihan et al., 2001). DWI of brain tissue specifically measures the motion of water molecules within brain tissue. Movement of water molecules is free within cerebrospinal fluid (CSF) and more restricted in grey and white matter (Huisman, 2010). Restriction to the diffusion of water molecules within brain tissue is introduced by, for example, myelination, axonal diameter, fibre density, crossing/bending fibres etc. Therefore, the direction of the diffusion within brain tissue can also be measured. Diffusion varies between isotropy, where the degree of diffusion is spread equally, and anisotropy, where the movement of the water molecules is restricted to one direction. Isotropic diffusion can be illustrated by a sphere and anisotropic diffusion by an ellipsoid (Alexander, Lee, Lazar, & Field, 2007; Huisman, 2010).

The Diffusion Tensor Model is one way the diffusion measured with DWI is modelled, which is then called Diffusion Tensor Imaging (DTI; Basser, Mattiello, & Le Bihan, 1994). In DTI, diffusion weighted images are acquired along three perpendicular orientations called eigenvectors. DTI uses a Gaussian approximation of diffusion. While isotropic diffusion is the same in all directions, anisotropic diffusion is fastest along the directions of what hinders diffusion, such as fibres. Anisotropic diffusion is slower along the axes perpendicular to the principal (fast) diffusion axis. DTI applies the measurement of diffusion along the principal and perpendicular axes to measure within each voxel fast and slow diffusion along the eigenvectors. Eigenvectors are mathematically quantified by eigenvalues. The principal diffusion direction, the fastest (i.e., longitudinal axis) is

expressed by the eigenvalue λ1. λ2 and λ3 are the eigenvalues that describe the slower diffusion along the directions perpendicular to the principal diffusion (i.e., the radial axes; Assaf & Pasternak, 2007; Le Bihan & Iima, 2015; Le Bihan et al., 2001; Mori & Zhang, 2006).

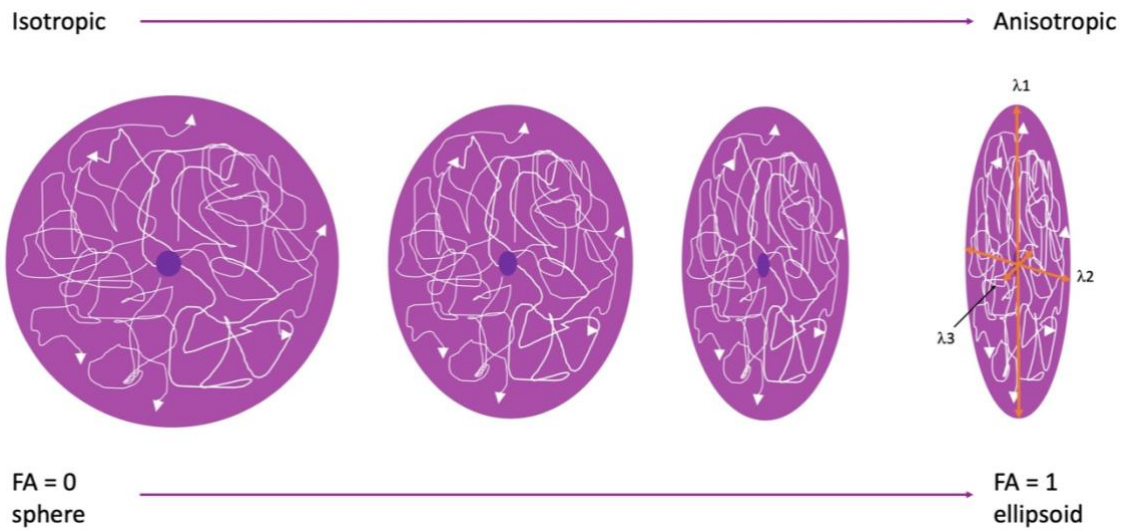


**Figure 1.2. Illustration of isotropic and anisotropic diffusion and the diffusion tensor.** Equal diffusion in all directions is observed in complete isotropic diffusion represented by a sphere. A narrow ellipsoid represents complete anisotropic diffusion where diffusion is predominant along the direction parallel to the longitudinal axis (λ1) and restricted along the perpendicular (radial) axes (λ2 and λ3). λ represent the eigenvalues of the diffusion tensor. Orange arrows represent the principal and radial diffusion axes. White lines and arrows represent the random motion of water molecules. *Figure adapted from Huisman, 2010 and Lerner et al., 2014.*

The diffusion tensor's eigenvalues are used to calculate parameters believed to describe underlying microstructural properties of white matter (Jones, 2008; Mori & Zhang, 2006). Two parameters of interest in this thesis are mean diffusivity (MD) and fractional anisotropy (FA). Mean diffusivity is the average of the three eigenvalues of the tensor within each voxel. A greater MD usually reflects higher diffusion along all three directions, less restriction, and higher water content in the tissue (Le Bihan, 2003). Fractional anisotropy describes the amount of anisotropy in the tissue. The amount of fast diffusion along the principal axis and slow diffusion along the radial axes. FA only varies between 0 and 1 where 0 reflects isotropic diffusion and values closer to 1 indicate more restricted diffusion. Restricted diffusion in turn indicates stronger myelination and axonal coherence (Beaulieu, 2002; Le Bihan, 2003; O'Donnell & Westin, 2011; Soares, Marques, Alves, & Sousa, 2013).

#### 1.2.1.1 Tractography

One way to utilise the information collected with DTI is to describe white matter pathways via their three-dimensional reconstruction from fibre trajectories with tractography (Catani, Howard, Pajevic, & Jones, 2002; Jones, Horsfield, & Simmons, 1999; Wakana et al., 2007). The estimation of fibre trajectories making up white matter tracts can be realised with deterministic or probabilistic tractography. Both methods consist of three steps: seeding, propagation, and termination. The seeding- step defines the starting point for the fibre trajectories. Frequently, regions of interest (ROIs) are determined, and one or more seeds are placed within every voxel of the ROI. Deterministic and probabilistic tractography differ in the second step, propagation. During propagation the fibre streamlines are gradually defined. Deterministic tractography reconstructs one fibre pathway from the seed by following the principal eigenvector of the diffusion tensor for each voxel. As opposed to following one streamline across different voxels, a distribution of fibre orientations at each voxel is calculated during probabilistic tractography. This process results in maps of a voxel's probability to be part of different fibre tracts and multiple possible fibres stemming from the seed. The tracking procedure is terminated based on different termination criterions like FA or turning angle thresholds (Jones, 2010; Soares et al., 2013).

One limitation of employing the tensor model for tractography lies in the failure of the tensor model to account for fibre orientations that differ from the principal diffusion direction due to crossing, bending, splaying, or twisting fibres (Jones, 2010). This can lead to underrepresentation of the actual brain structure. The use of high angular resolution diffusion imaging (HARDI) together with spherical deconvolution methods can account for different fibre orientations while evading the computational high demand of probabilistic tractography (Hagler et al., 2009). HARDI requires the acquisition of diffusion-weighted images using more than six diffusion-weighted directions as well as a higher b-value and or multiple shells of data. The b-value describes the timing and strength of the diffusion-sensitising gradients (Beaulieu, 2002). Therefore, diffusion-weighted images with a higher b-value are sampled along more diffusion-weighted gradients. This leads to a better representation of diffusion within a

voxel. Consequently, the combination of HARDI acquisition protocols and spherical deconvolution methods during data processing can improve tractography (Dell'Acqua & Tournier, 2018; Le Bihan et al., 2001).

### 1.2.2 Resting-state functional resonance imaging

Describing structural connections via DWI is not the only way to look at intrinsic connectivity patterns of the brain. Analysing functional connectivity at rest, in the absence of any specific task or stimuli, is another method that is proposed to reflect the intrinsic connectivity of the brain's networks (Smitha et al., 2017). Connectivity in functional MRI (fMRI) is expressed by the level of co-activation of brain regions or the correlation between the BOLD timeseries of the voxels comprising different brain regions (Van den Heuvel & Pol, 2010). In their seminal work, Biswal and colleagues asked participants to relax and not think of anything in particular. During this rest period, they acquired fMRI timeseries reflecting spontaneous functional activity. Instead of finding the brain idle or non-specific noise, they found high correlation between fMRI BOLD timeseries of different brain regions, demonstrating that even at rest anatomically distanced regions interact functionally and process information (Biswal, Yetkin, Haughton, & Hyde, 1995; Biswal, Kylen, & Hyde, 1997).

The BOLD (blood oxygen level dependent) contrast in fMRI is based on the oxygenation level in blood and the different magnetic properties of oxyhaemoglobin and deoxyhaemoglobin. An increase in BOLD signal results from a low concentration of deoxyhaemoglobin whereas a high level of deoxyhaemoglobin leads to a decreased BOLD response. Resting-state as opposed to task-based fMRI is based on low frequency fluctuations (<0.1 Hz) in the BOLD signal (Heeger & Ress, 2002; Smitha et al., 2017). There are different methods to analyse resting-state fMRI data. They differ in the assumptions made. There are model-free methods like independent or principal component analysis (ICA/PCA). ICA searches multiple simultaneous voxel-to-voxel interactions for those that best explain the data while maximizing the independence of the sources from each other. Model-based approaches like seed/ROI based analysis, on the contrary, estimate the correlation between BOLD signal in *a priori* defined regions

of the brain. These regions can be anatomically defined or based on task-dependent fMRI signal (Smitha et al., 2017; Van den Heuvel & Pol, 2010).

Networks like the attention network, the default mode network, or the salience network have been shown to display intrinsic connectivity with resting-state fMRI and changes within them have been related to neuropsychiatric disorders (cf., Alonazi et al., 2019). Furthermore, researchers were able to reliably identify participants in the Human Connectome Project based on their functional connectivity profiles (Finn et al., 2015). In the same study, individual variability in functional connectivity at rest could be related to interindividual differences in behaviour.

The previous sections were aimed at providing a short overview of the methods employed in this thesis to investigate interindividual differences in reward-related memory effects. DWI and resting-state fMRI offer the possibility to investigate differences in microstructure and intrinsic connectivity patterns at rest with their relationship to interindividual variability in behaviour like reward-related memory.

## 1.3 Aims of the thesis and overview of experimental chapters

We derive meaning from our past experiences to inform our current and future behaviour. The experience of reward is one way an episodic event obtains motivational relevance and increased probability to be remembered. Sometimes, this can only be adaptive when the fine-grained temporal detail of an event can be remembered, especially if a small difference in an often-encountered event leads to increased motivational value. This thesis aims to investigate how reward influences hippocampus-dependent associative memory, notably temporal order memory; how intentional memorisation for reward is affected by consolidation; and how interindividual differences in reward-related memory formation are related to variability in structural and functional connectivity within brain networks associated with rewarded memory formation.

This thesis consists of five experimental chapters. The first experimental chapter (Chapter 2) is concerned with two experiments investigating the influence of reward on temporal order memory. The period between encoding and memory test was filled with either wakeful rest or a distractor task. Temporal order memory for object pairs with differing numbers of intervening objects and from differently rewarded contexts is investigated. Chapters 3 and 4 investigate the influence of reward on immediate temporal order memory, recollection memory, and source memory and the neural underpinnings of interindividual differences therein. In Chapter 3, multi-shell DWI was employed, and fibre tracts of interest were reconstructed via deterministic tractography. Correlation analyses were performed between microstructure indices and behaviour which was acquired outside the scanner. In Chapter 4, the same participants also underwent resting-state fMRI scanning. Resting-state functional connectivity measures between regions of interest within the reward and the semantic temporal lobe network were investigated for their relationship with microstructure and behaviour. Chapters 5 and 6 investigate the underlying neuronal systems involved in how reward modulates intentional memorisation. Participants were rewarded for accurate memory tested in an immediate and a delayed memory test. This was aimed at potentially dissociating encoding- and consolidation-related effects of reward on memory formation. In Chapter 5, variability in microstructure indices of fibre tracts reconstructed via deterministic tractography from multi-shell DWI data was correlated with behaviour. In Chapter 6, behavioural measures outside the scanner were investigated for their relationship with changes in resting-state functional connectivity in the reward network and the semantic temporal lobe network.

Together, these findings provide a better understanding of how reward-related adaptive memory formation is supported by structural and functional connectivity in different brain networks underlying distinctive aspects of this adaptive behaviour.

# Chapter 2: Reward-related temporal order memory

Many aspects of events influence whether they enter long-term memory and can be consolidated over time. The salience of an event has been shown to influence its probability of being remembered. Salience can be affected by reward which thereby promotes preferential retention via differing encoding (Adcock et al., 2006; Mason, Farrell, Howard-Jones, & Ludwig, 2017; Wimmer & Shohamy, 2012) or post-encoding processes (Gruber et al., 2016; Murty et al., 2017). Sleep promotes better memory for rewarded or rewarding information (Dupret et al., 2010; Igloi et al., 2015; Lansink et al., 2008; Lee & Wilson, 2002; Peyrache et al., 2009). Moreover, memory for low reward information can show a stronger decline from before to after sleep than high reward information (Studte, Bridger, & Mecklinger, 2017). These processes are believed to reflect differing levels of consolidation for high and low reward information (O'Carrol, Martin, Sandin, Frenguelli, & Morris, 2006; McGaugh, 2000). Replay is one process by which post-encoding rest, similar to sleep, can support consolidation because other new input cannot interfere during rest (e.g., Craig, Dewar, Della Sala, Wolbers, 2015; Davidson et al., 2009).

In a study of memory for verbal story material, encoding was followed by either wakeful rest or a perceptual task (Dewar, Alber, Butler, Cowan, & Della Sala, 2012). Memory for material that was followed by wakeful rest was better than memory for material followed by a perceptual task. After a seven-day delay, overall memory for the stories decreased but the difference in memory between information followed by rest versus a perceptual task remained (Dewar et al., 2012). In a different study by Craig and Dewar (2018), rest compared to performing a different task after encoding of images of everyday objects led to better memory as well as more detailed memory. The memory test in that study contained old objects, new objects, and objects that were from the same category as encoded objects but were different depictions (lures). Participants that rested for ten minutes after encoding displayed better ability to recognise these lures as similar than participants that performed a different task for ten minutes after encoding. Participants who rested were less likely to wrongly identify lures as old as

opposed to similar, they had better memory for the details of the encoding material (Craig & Dewar, 2018). Additionally, post-encoding rest has also been shown to increase temporal order memory (Craig et al., 2015).

As discussed in the "General Introduction", the temporal domain as a special form of source memory is an important component of episodic memory (Johnson, Hashtroudi, & Lindsey, 1993; St. Jacques, Rubin, LaBar, & Cabeza, 2008). Deriving meaning from past experiences to inform current decision-making and actions is an essential feature of memory and adaptive behaviour. It has been postulated that to learn from past experiences we will need to be able to reconstruct an event's particular temporal arrangement to discriminate it from an episode with overlapping elements (Clewett & Davachi, 2017; Tubridy & Davachi, 2011). Furthermore, motivation plays an integral part in what information is remembered. Reward as an external motivator has been shown to positively influence memory in a diverse manner including when received or anticipated during encoding, retroactively, and via consolidation processes (e.g., Adcock et al., 2006; Gruber et al., 2016; Igloi et al., 2015; Wimmer & Shohamy, 2012). For one episodic event to be able to guide future behaviour we need to be able to derive meaning from its structure and we need to be motivated to do so. Understanding how the sequential nature of episodic memory is preserved and how that preservation might be improved through motivation is essential to deepen our knowledge of adaptive episodic memory formation. However, studies concerned with temporal order memory in human participants have not investigated how reward affects temporal order memory (DuBrow & Davachi, 2014; Heusser et al., 2016; Heusser et al., 2018). Thereby, two important aspects of episodic memory, its sequential structure and how salience influences retention of such sequential structure, have not been investigated together in humans.

Furthermore, even though both a reward-related memory benefit (Adcock et al., 2006; Gruber et al., 2016; Mason et al., 2017; Studte et al., 2017; Wittmann et al., 2005) and temporal order memory (Craig et al., 2015; Griessenberger et al., 2012) have been shown to improve with post-encoding rest or sleep, their interaction has not been investigated with human subjects. Within a framework of adaptive memory,

understanding of the interaction between reward, post-encoding processes, and temporal order memory is important because it will further the understanding of how we learn from experience. An effect of reward on measures of memory for detailed contextual information like recollection, source memory, and high confidence memory has been demonstrated (e.g., Adcock et al., 2006; Gruber et al., 2016). This lends itself to the prediction of reward-modulation of temporal order memory as an additional type of contextual information that is integral to episodic memory (St. Jacques et al., 2008). Modulation of associative memory measures through reward has also been shown to interact with post-encoding processes and sleep (e.g., Murayama & Kitagami, 2014; Murty et al., 2017). Therefore, an interaction between a potential reward-related temporal order memory benefit and the post-encoding period could be predicted.

The experiments described here are aimed at closing the apparent gap in the literature on how reward influences temporal order memory in human subjects. The experiments will additionally investigate whether the potential effect of reward on temporal order memory depends on the type of post-encoding period. In this between-subjects design, participants encoded object sequences in high versus low reward contexts. One group of participants rested for ten minutes after encoding while the other group of participants completed a distractor during the ten-minute post-encoding period. In the subsequent memory test, participants' temporal order memory for object pairs was tested.

To summarise, I hypothesised that temporal order memory would be better for high than for low reward object pairs. Increased precision of temporal order representations through reward was investigated as well. Memory for object pairs with small and larger numbers of intervening items was compared. I predicted that reward would increase memory precision and thereby increase memory for object pairs with smaller lags, thereby reducing the effect of lag. Furthermore, an interaction between reward-related memory benefits for temporal order and different post-encoding processes (distractor versus wakeful rest) was investigated. Since effects of reward on associative memory processes have been found to increase through consolidation and post-encoding rest can mimic consolidation, I hypothesised that wakeful rest compared

to a distractor task after encoding would increase the potential effect of reward on temporal order memory.

## 2.1 Methods

There were three stages to the experiment in both groups, a reward-motivated encoding-phase that lasted about 50 minutes, a 10-minute post-encoding distractor- or wakeful rest-phase, and a memory-test (Figure 2.1).

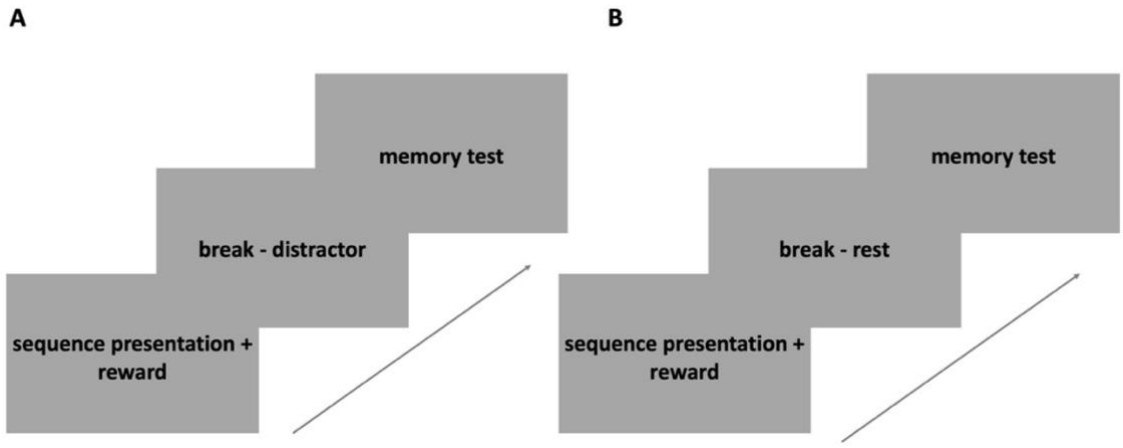


**Figure 2.1. Overall representation of the three stages of the studies. A.** Distractor group where the second stage between encoding and memory test was a 10-minute distractor task. **B.** Wakeful rest group where the second stage between encoding and memory test was a 10-minute wakeful rest period.

During encoding, participants made yes/no- judgments on 320 objects presented in 40 sequences. Sequences were denoted by changing background scenes that semantically matched the judgements. Four semantic questions were posited during the experiment. Participants received high (£2) or low (£0.02) reward for correctly answering these questions within two seconds. After encoding, participants of the first group were given a mathematical distractor task, followed by the memory test. Participants of the second group were given a 10-minute wakeful rest period during which they were presented with a fixation cross on the screen. Participants were instructed to relax and clear their mind, but to stay awake. They were told that the fixation cross was there to support this. Wakeful rest was also followed by a memory test. The memory test comprised three questions testing temporal order memory, object memory, and source memory.

## 2.1.1 Participants

For both experiments, the Ethical Review Board of the School of Psychology at Cardiff University approved the study procedures. Participants were recruited via the Experimental Management System (EMS) and received course credit (4 credits/hour) or payment (£6/hour) for their participation. Monetary rewards were independent of chosen compensation. All participants gave informed written consent. Participants had normal or corrected-to-normal vision. They were only included in the final analysis if they had never been diagnosed with a psychiatric condition, did not take psychiatric medication, and reported that they did not consume alcohol or drugs prior to testing ("healthy" criterion).

### 2.1.1.1 Distractor group

Data were collected from 29 people. Data from 10 participants had to be excluded from the final analysis. Three participants were excluded because they did not meet the criteria of being "healthy". Two other participants did not show any temporal order memory (choosing the "don't know"- option for over 80% of the old-old and old-new test pairs per condition). Five more participants were excluded because they displayed more false alarms than hits for their temporal order memory. The remaining dataset contained data from 19 healthy people (4 male, mean age = 18.95; SD = 0.78, range = 18-20). For one of these participants the dataset of memory test results used for analysis excluded all test pairs taken from the first three encoding blocks due to a break in data collection. This was considered potentially adverse especially for the comparison with wakeful rest.

### 2.1.1.2 Wakeful rest group

Data were collected from 34 participants. Data from 16 participants had to be excluded from the final analysis. Five participants were excluded due to the "healthy"-criterion. Four additional participants reported that they practiced some of the objects or sequences during the 10-minute rest period. Four participants chose the "don't know"- option during the temporal order memory test for more than 80% of the 60 object pairs that were tested per condition (40 old-old pairs, 20 old-new pairs for high

and low reward condition). Three participants had a higher false alarm than hit rate. Data from 18 healthy people (5 male, mean age = 19.56, SD = 1.5, range = 18-24) were analysed.

## 2.1.2 Reward-motivated encoding

Participants answered one semantic question to a sequence of eight objects, a mini-block. A mini-block lasted approximately 25 seconds. Figure 2.2 depicts two exemplary mini-blocks, one with high and one with low reward. One encoding block contained four mini-blocks, each mini-block involved a different semantic judgement. Therefore, each encoding block comprised four different semantic judgements. Within an encoding-block, reward always switched between high and low. The experiment contained 10 encoding-blocks and therefore 40 mini-blocks/sequences.

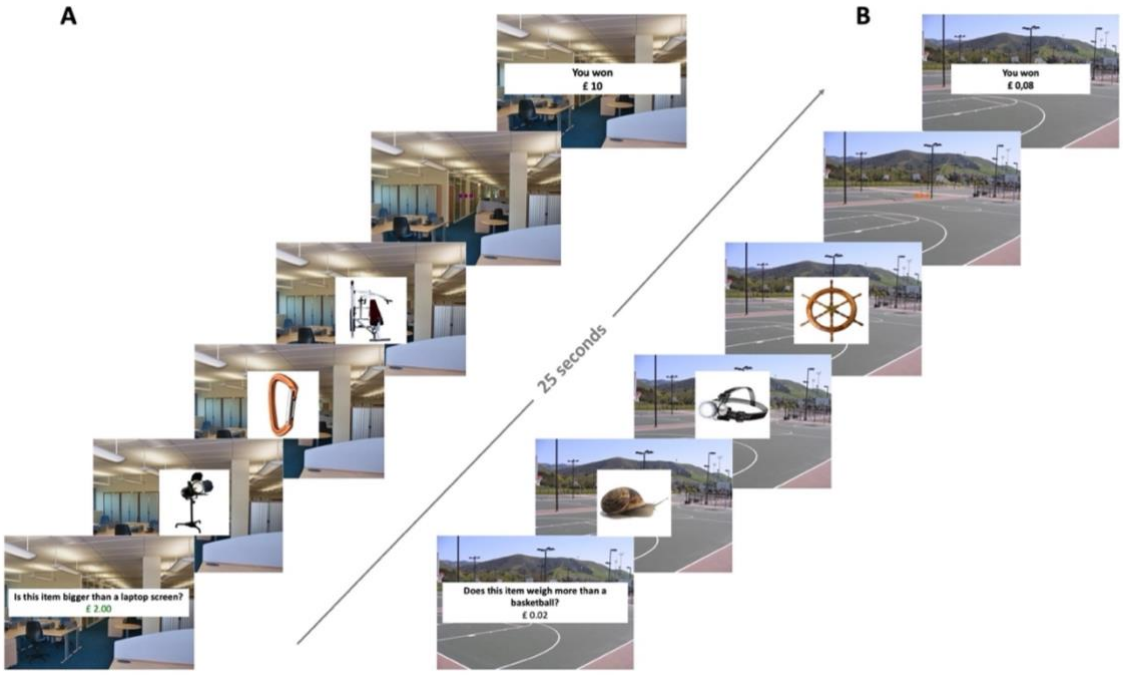


**Figure 2.2. Example of a high and a low reward encoding mini-block. A.** High reward mini-block. The semantic judgement matching the background scene was presented together with the high reward cue. High reward was denoted by the amount in GBP (£2.00) and font colour (green). **B.** Low reward mini-block. The semantic judgement matching the background scene was presented together with the low reward cue. Low reward was denoted by the amount in GBP (£0.02) and font colour (black). Each mini-block contained eight objects, depicted are 3. Each mini-block lasted 25 seconds and ended with reward feedback.

A mini-block started with the presentation of a high or low reward cue (high = £2.00, low = £0.02) and the particular semantic judgement above a semantically

matched background scene for 2 seconds. The background scene remained on the screen and each object of the sequence was presented for 2 seconds in the middle of the screen. Participants responded via button press to the semantic question. The inter-stimulus-interval (ISI) was randomly jittered between 2 and 3 seconds. At the end of a mini-block, participants received feedback about the winnings they made in the preceding mini-block via presentation on the screen for 2 seconds. Winnings were based on participants' performance on the semantic judgement task. Additionally, participants were instructed to relate the objects of one sequence to each other and their background. Ahead of the encoding phase, participants were informed about the memory test but not the type of memory test. They were instructed that making up a story about the objects interacting would be a good strategy to relate the objects within a sequence. Nevertheless, their primary task remained to make the semantic yes/no-judgements. Over the course of the experiment there were four different judgements (cf., Gruber et al., 2016). The background scenes were semantically matched to specific judgements. The scene of an outdoor basketball court corresponded to the judgement "Does this item weigh more than a basketball?" (court scene, basketball judgement). An indoor swimming pool scene was matched to the judgment "Would this item float for a bit?" (pool scene, floating judgement). Participants were asked "Is this item bigger than a laptop screen?" in front of an indoor office scene (office scene, laptop judgement). The semantic judgement "Is it possible to juggle three exemplars of this item?" was to be made in front of a circus tent scene (tent scene, juggling judgement). After making the same judgment on one sequence the background scene and judgement switched.

In the first experiment, encoding was followed by a 10-minute distractor task. The distractor task was a paper pen arithmetic test adding and subtracting up to three-digit numbers. Participants were informed that their performance on this task would not influence their winnings. In the second experiment, participants were given a 10-minute wakeful rest period. They were presented with a fixation cross on the screen and were told to relax and to not think about anything specific, but to avoid falling asleep. After distractor or wakeful rest, participants received instructions for the memory test.

## 2.1.3 Memory test

During the memory test, participants were presented with object pairs on the screen and were instructed to consider both objects together when answering three questions about the pair. The test was self-paced. Participants were instructed to try their best to answer all questions. The object, temporal order, and source memory test were always presented in that order. For each memory test trial, this triplet of questions was aimed at the same pair of objects (Figure 2.3). Object pairs were presented centred in front of a grey background, the memory question above the pair at the top of the screen, and a legend, displaying the keys corresponding to the possible answers, underneath that. Each question of the triplet was displayed until participants gave their response, which was followed by a fixation cross for 1 second. Participants were tested on 120 object pairs (80 old-old, 40 old-new). Testing was self-paced and lasted about 30-45 minutes.


**Figure 2.3. Triplet of questions for memory test.** Participants had to answer three questions about the same pair of objects. Object pairs either contained two objects presented during encoding (old-old) or comprised one old and one new object (old-new). Old-old object pairs were always taken from the same sequence. **A.** Object memory test. A remember-know-new- design (Yonelinas, 2002) was employed to investigate participants' overall memory and ensure temporal order memory responses were based on reliable item memory. Participants had to consider both objects for their response. **B.** Temporal order memory test. Participants indicated their pick for first via keypress. Keys corresponded to side of the screen the object was presented on. Participants could choose "don't know" for old-new object pairs to indicate that the pair contained a new object. **C.** Source memory test. Participants picked the background scene they believed both objects to be presented in front of.

A triplet started with the first question aimed at object memory: "Have you seen both of these images before?" (Figure 2.3 A). Measures of recollection and familiarity were investigated with a remember-know-new design (e.g., Yonelinas, 2002; Yonelinas & Jacoby, 1995). But as opposed to the standard design, participants were instructed to consider a pair and not a single object. Both objects of the object pair had to be deemed "old" by the participant to warrant either a remember- or a know-response. Participants

were instructed to give a remember-response if they remembered both or one of the objects as long as they knew the other object of the pair to be "old". The remember-know-new memory test was employed on the object pairs to ensure that participants displayed reliable item memory before giving a temporal order memory response. Object pairs as opposed to single objects were used to avoid priming of the objects before investigation of temporal order memory.

After they answered the object memory question, the question "Which came first?" appeared on top of the same pair of objects (Figure 2.3 B). Participants had three options for answering, which were displayed with their corresponding keys underneath the object pairs. They could choose whether the object on the right side of the screen came first within a sequence of eight objects encountered during encoding or whether the object on the left side of the screen was the first. The third option was to be picked if participants thought they did not know the answer ("don't know"). They were also instructed to choose that option if they answered "new" to the preceding object memory question.

The temporal order memory task was followed by a similar source memory task as in Gruber et al. (2016) (Figure 2.3 C). Participants were asked: "These images appeared in front of which background?". They were told to pick the "don't know"-option if they responded "new" to the object memory question or if they truly did not know the answer. Participants were instructed to only answer the question with picking one of the four backgrounds if they were sure that both objects had been presented to them in the previous stage, meaning that they were told to answer "don't know" even if they remembered the background for one of the two objects of the pair but did not remember the second object of the pair to be part of the previous stage of the experiment.

### 2.1.4 Stimuli

Grouping and assignment of stimuli to reward-conditions during encoding test was the same in both studies and was adapted from Gruber et al. (2016). The procedure of

choosing object pairs for the temporal order memory test was the same in both groups, distractor and wakeful rest.

#### 2.1.4.1 Reward-motivated encoding

The 320 coloured pictures of objects for encoding, 120 coloured pictures of objects as potential distractors in the memory test, and 4 coloured background scenes (basketball court, swimming pool, office, and circus tent) were sourced via a publicly available database (Brady, Konkle, Alvarez, & Oliva, 2008). Randomisation- and grouping- processes were the same as in Gruber et al. (2016). The four background scenes were matched to the four judgements participants were instructed to make on the 320 objects during encoding (basketball court scene with basketball judgement; pool scene with floating judgement; office scene with laptop judgement; tent scene with juggling judgement). Subsets of 80 pictures were pseudo-randomly assigned to the four different backgrounds. The assignment of subsets to backgrounds was counterbalanced across participants. For one half of participants, two item sets (A and B) were assigned to the basketball court and the swimming pool scenes and the other two item sets (C and D) to the office and circus tent scenes and vice versa in the other half of participants. The 80 objects per background scene, and thereby judgement, were split into 10 sequences of eight. Therefore, participants encoded and were tested on 40 sequences of eight objects each. Across the experiment, scenes and judgements were counterbalanced between high and low reward conditions. The basketball court and swimming pool were always assigned together to either high or low reward conditions whereas the office and circus tent scenes were always used together for the other reward condition. Correct answers to the yes/no- judgements were roughly equally distributed across the subsets. If the “correct” answer was ambiguous, both yes and no responses were rewarded, unbeknownst to the participant. Additionally, only 80% of responses were rewarded overall. This was employed to ensure a level of attention due to some uncertainty about the exact reward participants could expect and thereby increasing attention (Gruber, Gelman, & Ranganath, 2014; Gruber et al., 2016). Participants were informed of that.

### 2.1.4.2 Memory test

Out of the 40 sequences that the participants encoded, two pairs of objects per sequence were chosen for the memory test. Therefore, object memory, temporal order memory, and source memory were tested on 80 pairs (40 high and 40 low reward). The two pairs taken from each sequence differed in their lag, the number of intervening objects within the sequence. Two different lags were chosen, a larger one with three objects between the objects chosen for the memory test (lag 3) and a smaller one with only one intervening object (lag 1). Previous research points towards imprecise temporal order memory for objects encoded closely together (e.g., DuBrow & Davachi, 2014). Nevertheless, lag 1 pairs were included here to investigate a hypothesised increase in precision of temporal order memory through reward.

Figure 2.4 depicts the different options for lag 3 pairs and the resulting possible combinations of lag 1 pairs. Two conditions restricted the possible combinations. First, the lag 3 and the lag 1 pairs of the same sequence should not contain the same objects. Second, the first and last objects of a sequence were not included. Following these restrictions, there were two possible pairs with 3 intervening objects: the 2$^{nd}$ and 6$^{th}$ objects of an 8-object-sequence (Combination A; Figure 2.4 A) as well as the 3$^{rd}$ and 7$^{th}$ objects (Combination B; Figure 2.4 B). Consequently, there remained two options each for lag 1 pairs of the same sequence. For combination A, one lag 1 pair comprised the 3$^{rd}$ and 5$^{th}$ objects of the sequence (Figure 2.4 A.a). The other possible lag 1 pair comprised the 5$^{th}$ and 7$^{th}$ objects of the sequence (Figure 2.4. A.b). For combination B, one lag 1 pair comprised the 2$^{nd}$ and 4$^{th}$ objects of the sequence (Figure 2.4 B.a). The other possible lag 1 pair comprised the 4$^{th}$ and 6$^{th}$ objects of the sequence (Figure 2.4 B.b).

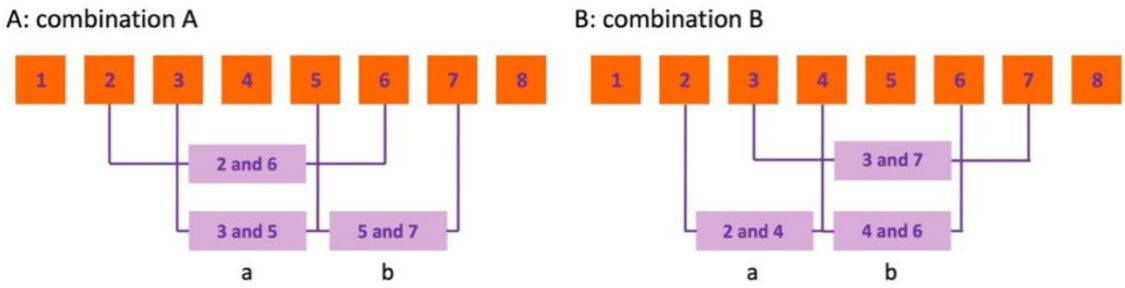


**Figure 2.4. Possible combinations of object pairs with three and one intervening objects. A.** Combination A. Object pair with three intervening objects (lag 3; 2nd and 6th object) and possible lag 1 object pairs. **A.a.** Object pair with one intervening object (lag 1; 3rd and 5th object). Both objects of the pair lie within the lag 3 object pair. **A.b.** Object pair with one intervening object (lag 1; 5th and 7th object). The object pair spans the second object of the lag 3 object pair. **B.** Combination B. Object pair with three intervening objects (lag 3; 3rd and 7th object) and possible lag 1 object pairs. **B.a.** Object pair with one intervening object (lag 1; 2nd and 4th object). The object pair spans the first object of the lag 3 object pair. **B.b.** Object pair with one intervening object (lag 1; 4th and 6th object). Both objects of the pair lie within the lag 3 object pair.

Accordingly, one of the lag 1 pairs was within the lag 3 pair of the sequence, consisting of intervening objects. For combination A this was object pair A.a, for combination B this was object pair B.b. The other possible lag 1 pair went across the last or first object of the corresponding lag 3 pair. For combination A this was object pair A.b, for combination B this was object pair B.a. The four possible combinations of lag 3 and lag 1 test-pairs were equally distributed between high and low reward conditions. The remaining objects (Combination A: 4th object of the sequence; Combination B: 5th) were also used and paired with a randomly chosen new object from the 120 distractor-objects (old-new pair). Across all 40 sequences, two objects from the 1st and two objects from the 8th position of four randomly chosen sequences were paired with a new object. Therefore, two old-new object pairs comprised randomly chosen 1st and two comprised randomly chosen 8th objects of the encoding sequences as the old object. Thus, across the experiment, participants were tested on their memory for the whole sequence. From the 40 sequences that were encoded, 120 pairs were tested, three per sequence (two old-old pairs, one old-new pair). 80 pairs consisted of two objects the participants saw during reward-motivated encoding (40 high reward, 40 low reward; old-old). 40 pairs were made up of one object participants saw during encoding and one new object (20 high reward, 20 low reward; old-new). Old-new pairs were attributed to high versus low reward condition based on the old object's encoding context.

## 2.1.5 Behavioural analysis

Behavioural analyses were carried out in JASP (JASP Team, 2019; version 0.11.1). Behavioural measures were introduced into mixed-effects ANOVAs with *group* (distractor versus wakeful rest) as between-subjects factor. *Lag* (lag 3 versus lag 1) and *reward* (high versus low) served as within-subject factors. Detailed planned and exploratory follow-up analyses are described in the following paragraphs. In the follow-up, high and low reward conditions were compared with one-tailed paired sample t-tests that investigated better memory for object pairs from high as opposed to low reward sequences. Finally, correlation analyses were performed to reveal influences of possible differences during encoding on differences in memory test performance. Only temporal order memory results will be reported here (see Appendix 1 for object and source memory results). Because the object and source memory tests employed object pairs, participants' responses are ambiguous. Even though participants were instructed to only consider the objects as pairs, their thresholds for specific object or source memory responses remain unclear.

### 2.1.5.1 Encoding

Percentages of correct responses and mean reaction times (RTs) for correct responses to the semantic questions during encoding were analysed in a mixed-effects ANOVA with *group* (2 levels between-subjects: distractor versus wakeful rest) and *reward* (2 levels: high versus low). Enhancing effects of reward on decision making (e.g., Adcock et al., 2006; Gruber et al., 2016) were investigated with one-tailed paired sample t-test within each study group. Percentages of correct responses were tested for a positive difference (high > low reward) of more correct responses during high compared to low reward encoding. Mean RTs for correct responses were tested for a negative difference (high < low reward) of faster responses during high compared to low reward encoding.

### 2.1.5.2 Temporal order memory

Accuracy measures were calculated by subtracting the percentage of order responses to old-new pairs (false alarms) from the percentage of correct order

responses to old-old object pairs (hits) (formula 2.1). False alarms were attributed to high and low reward based on the old object's reward condition from the old-new object pairs. For lag 3 and lag 1 accuracies the same false alarms were used.

$$accuracy_{lag\ 3\_high\_reward} = hits_{lag\ 3\_high\_reward} - false\ alarms_{high\_reward}$$

**Formula 2.1. Exemplar of accuracy formula for responses to lag 3 high reward object pairs.**

False alarms to the temporal order memory test were not ambiguous. A false alarm in temporal order was counted if a participant chose left or right first as a response to an old-new-pair. A mixed-effects ANOVA on hits corrected by false alarms (accuracy) was used to investigate the effects of *reward* (2 levels: high versus low) and *lag* (2 levels: lag 3 versus lag 1) of the object pairs on temporal order memory and whether the type of post-encoding phase (*group*, 2 levels between-subjects: distractor versus wakeful rest) interacts with potential reward-enhancements.

#### 2.1.5.3 Correlation analysis

Reward-related benefits were calculated by subtracting the value of the low reward condition from the value of the high reward condition. This was executed for encoding accuracy, encoding RTs, and temporal order accuracy. Reward-modulated encoding performance (high reward encoding accuracy/RTs – low reward encoding accuracy/RTs) was correlated with the reward-related temporal order memory benefit for lag3 and lag 1 object pairs. The correlations were corrected for multiple comparisons with Bonferroni adjusted p-values. The critical value was adjusted from .05 to .0125 (.05/4).

## 2.2. Results

### 2.2.1 Encoding

Overall, encoding accuracy was fairly high in both groups (distractor group: high reward = 90.76%, SE = 0.81; low reward = 88.59%, SE = 0.89; Figure 2.5 A; wakeful rest group: high reward = 90.38%, SE = 1.01; low reward = 89.41%; SE = 1.07; Figure 2.5 B). The mixed-effects ANOVA on percentage correct responses revealed a significant main effect of reward ($F(2,35) = 7.97$, $p = .008$, partial eta squared = 0.19). Neither the

interaction between reward and group ($F$(2,35) = 1.16, $p$ = .289, partial eta squared = 0.03) nor the main effect of group ($F$(2,35) = 0.03, $p$ = .855, partial eta squared = 0) reached significance. A follow-up one-tailed paired sample t-test was performed across post-encoding groups separately. Participants made significantly more correct responses during high reward than low reward encoding ($t$(1,36) = 2.85, $p_{1\text{-}tailed}$ = .004, $d$ = 0.47).

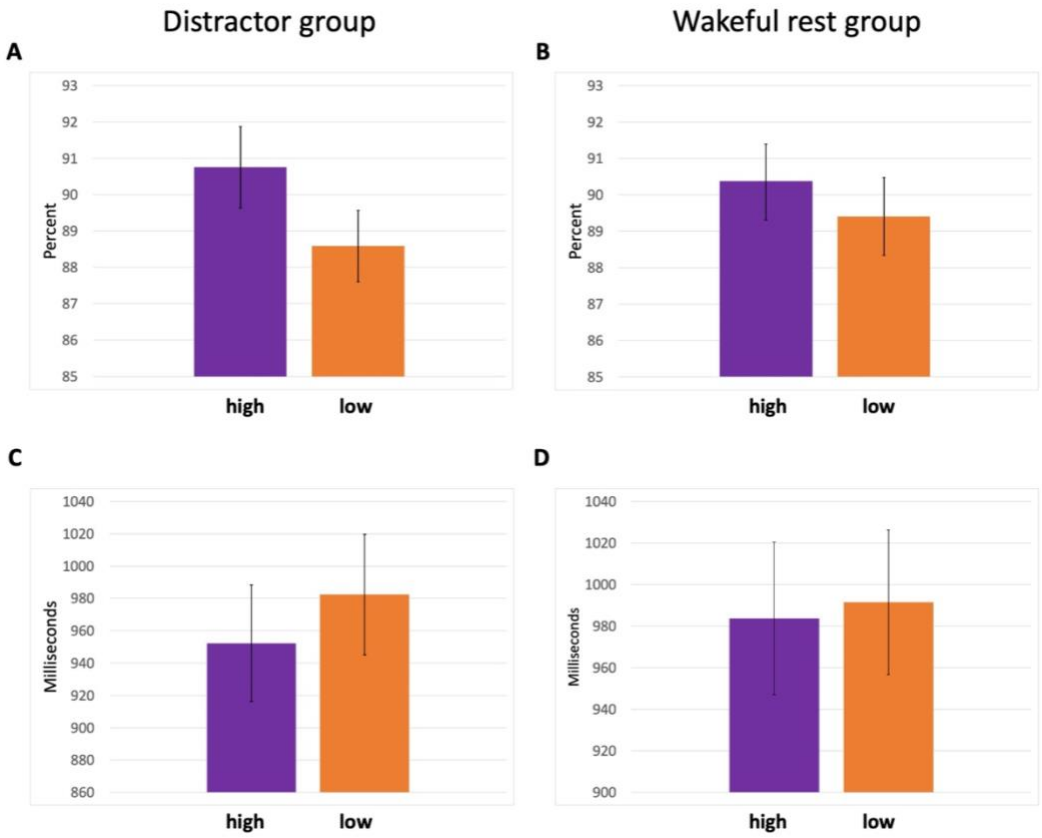


**Figure 2.5. Bar graphs of encoding accuracy and mean reaction times. A.** Encoding accuracy in distractor group. Percentages of correct responses by reward condition (N = 19). **B.** Encoding accuracy in wakeful rest group. Percentages of correct responses by reward condition (N = 18). **C.** Mean reaction times (RTs) during encoding in distractor group. Mean RTs of correct responses in milliseconds by reward condition. **D.** Mean RTs during encoding in wakeful rest group. Mean RTs of correct responses in milliseconds by reward condition. Colours denote reward condition. Purple = high reward, orange = low reward. Standard errors are depicted by a vertical black line.

Mean RTs for correct responses during encoding were analysed in the same manner as encoding accuracy. The mixed-effects ANOVA on reaction times of correct responses showed a significant main effect of reward ($F$(2,35) = 7.37, $p$ = .010, partial eta squared = 0.17). Neither the interaction between reward and group ($F$(2,35) = 2.59, $p$ = .117, partial eta squared = 0.07) nor the main effect of group ($F$(2,35) = 0.16, $p$ =

.692, partial eta squared = 0.00) reached significance. A follow-up one-tailed paired sample t-test was performed across groups. Participants made significantly faster semantic judgments in high than low reward sequences ($t(1,36) = -2.7$, $p_{1\text{-}tailed} = .005$, $d = -0.44$).

## 2.2.2 Temporal order memory

Overall, participants showed a reliably high memory for object pairs with hit rates pooled over recollection and familiarity responses being around 90% for both high and low reward object pairs in both groups (see Appendix 1). Since object and source memories in the distractor as well as the wakeful rest group refer to object pairs as opposed to single objects, the results described in Appendix 1 were mostly referenced to show that effects of temporal order were built on reliable memory overall.

**Table 2.1. Group means and standard deviations (SD) for temporal order accuracy.** Means and SD's are based on percentage accuracies (hits – false alarms). Separated by lag (1 versus 3) and reward (high versus low) conditions. Separate for distractor and wakeful rest groups. SD's in brackets after the means.

| Lag | Reward | Distractor group (SD) | Wakeful rest group (SD) |
|---|---|---|---|
| 1 | high | 32.14 (17.67) | 27.78 (14.37) |
| 1 | low | 26.17 (17.01) | 25.28 (17.36) |
| 3 | high | 36.62 (17.16) | 32.78 (18.08) |
| 3 | low | 24.92 (16.39) | 31.11 (19.75) |

The mixed-effects ANOVA on temporal order memory accuracy (Figure 2.6) showed a significant main effect of reward ($F(2,35) = 6.34$, $p = .017$, partial eta squared = 0.15) as well as a trend towards a main effect of lag ($F(2,35) = 3.52$, $p = .069$, partial eta squared = 0.09). Neither the main effect of group ($F(2,35) = 0.03$, $p = .874$, partial eta squared = 0.00) nor any of the interactions were significant (all $F \leq 2.42$, all $p \geq .129$).

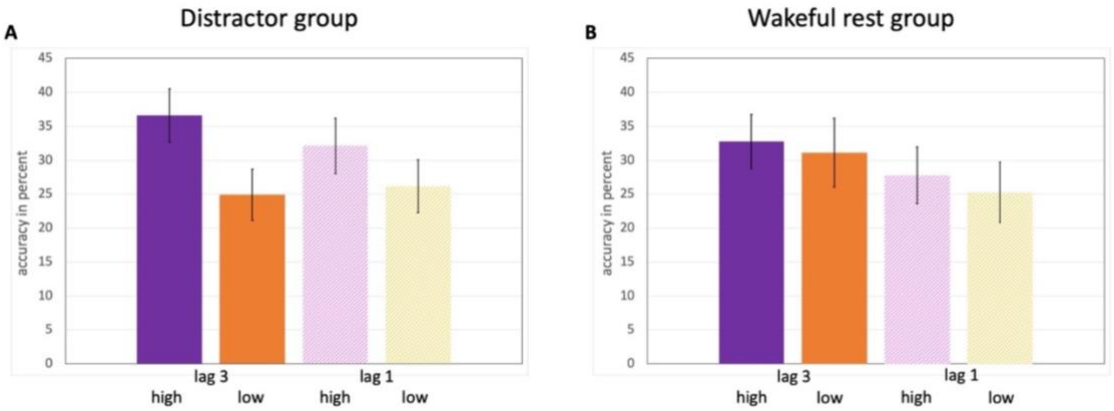


**Figure 2.6. Temporal order accuracy by lag and reward. A.** Temporal order accuracy in the distractor group. Temporal order accuracy (hits – false alarms) by lag (3 versus 1) and reward (high versus low). **B.** Temporal order accuracy in the wakeful rest group. Temporal order accuracy (hits – false alarms) by lag (3 versus 1) and reward (high vs. low). Colourways indicate reward. Purple/pink = high reward. Orange/yellow = low reward. Shading indicates lag. Solid = lag 3. Striped = lag 1.

Follow-up one-tailed paired sample t-test were performed to compare high reward with low reward temporal order accuracy for lag 3 and lag 1 object pairs separately for distractor and wakeful rest group respectively. Better high reward temporal order accuracy was hypothesised. This exploratory follow-up was carried out in the absence of a significant effect of group to inform decisions for the experiment described in Chapters 3 and 4. For the distractor group, high reward lag 3 pairs were significantly better remembered than low reward lag 3 pairs ($t(1,18) = 3.49$, $p_{1\text{-tailed}} = .001$, $d = 0.80$) whereas there was no significant difference for lag 1 pairs ($t(1,18) = 1.26$, $p_{1\text{-tailed}} = .112$, $d = 0.29$). For the wakeful rest group, reward did not significantly influence temporal order accuracy, neither for lag 3 ($t(1,17) = 0.51$, $p_{1\text{-tailed}} = .309$, $d = 0.12$) nor for lag 1 ($t(1,17) = 0.60$, $p_{1\text{-tailed}} = .277$, $d = 0.14$) object pairs.

The lack of reward-related temporal order memory benefit in the wakeful rest group was unexpected. Visual inspection suggested that high reward temporal order memory seemed to not differ between the two groups, while low reward temporal order memory was higher in the wakeful rest than in the distractor group. Exploratory independent samples t-tests were carried out to further investigate this observation. Temporal order memory for lag 3 object pairs did not significantly differ between distractor and wakeful rest group, for neither high nor low reward object pairs (lag 3 high: $t(35) = 0.68$, $p = .500$; lag 3 low: $t(35) = -1.04$, $p = .306$). Temporal order memory

for high and low lag 1 object pairs did not significantly differ between distractor and wakeful rest group (lag 1 high: $t(35) = 0.82$, $p = .417$; lag 1 low: $t(35) = 0.16$, $p = .876$).

## 2.2.3 Correlation analysis

Pearson product moment correlation coefficients were computed to assess whether there was a significant relationship between differences in participants' performance on the semantic judgements during high versus low reward encoding and the reward-related temporal order memory benefits for lag 3 and lag 1 object pairs.

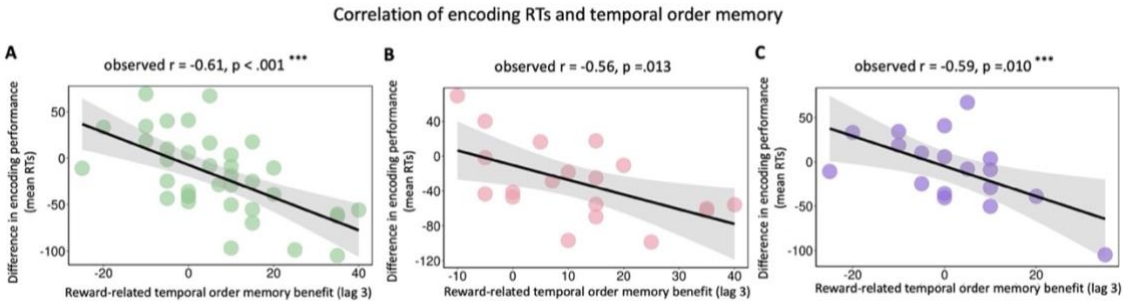


**Figure 2.7. Correlation plot of encoding performance and temporal order accuracy. A.** Significant (FWE-corrected) correlation between the reward-related difference (high – low) in mean RTs and the reward-related temporal accuracy benefit (high – low) for lag 3 object pairs across groups. The line of best fit and 95% confidence interval (CI) is shown with 37 data points. **B.** Correlation between the reward-related difference in mean RTs and the reward-related temporal accuracy benefit (high – low) for lag 3 object pairs in the distractor group. The line of best fit and 95% CI is shown with 19 data points. **C.** Significant (FWE-corrected) correlation between the reward-related difference in mean RTs and the reward-related temporal accuracy benefit (high – low) for lag 3 object pairs in the wakeful rest group. The line of best fit and CI is shown with 18 data points.

Across both groups, there was a significant negative correlation between reward-related reaction time difference of the semantic judgement at encoding and the reward-related temporal order accuracy benefit for lag 3 object pairs ($r(37) = -0.61$, $p < .001 < \alpha_{adjusted} = .0125$; Figure 2.7 A). The correlation between RT difference at encoding and the reward-related temporal order memory benefit for lag 3 object pairs was significant for both the distractor and the wakeful rest group (distractor: $r(18) = -0.56$, $p = .013 > \alpha_{adjusted} = .0125$; Figure 2.7 B; rest: $r(17) = -0.59$, $p = .010 < \alpha_{adjusted} = .0125$; Figure 2.7 C). Faster reaction times during high versus low reward encoding led to a higher reward-related temporal order accuracy benefit for lag 3 object pairs. No other correlations reached significance (all $r \leq -0.25$, all $p \geq .240$)

## 2.3 Discussion

The experiments described above were aimed at investigating the influence of reward on temporal order memory. In a between-subjects design, a mathematical distractor and a wakeful rest post-encoding period were investigated for their influence on potential reward-related temporal order memory benefits. Wakeful rest is proposed to preferentially boost memory for high reward information (e.g., Gruber et al., 2016; Singer & Frank, 2009). Therefore, a distractor- and a rest- filled post-encoding period were compared to investigate whether wakeful rest after encoding leads to increased reward-related temporal order memory benefit.

Temporal order accuracy was higher for object pairs from high than from low reward sequences. Consequently, the experiments show that reward not only enhances object and source memory but also other hippocampus-dependent memory processes like temporal order memory (Adcock et al., 2006; Davachi, 2006; McKenzie et al., 2014; Murty et al., 2017; Shohamy & Adcock, 2010). To my knowledge, the experiments described here appear to be the first demonstrating that reward influences temporal order memory in human subjects.

Temporal order for lag 3 object pairs from high reward sequences was better remembered than for lag 3 object pairs from low reward sequences. This effect was only significant in the distractor group, whereas there was no significant difference in the wakeful rest group. This effect was not in line with the expected increase of reward-related memory benefits through wakeful rest (Gruber et al, 2016; Mercer, 2015; Murty et al., 2017). One possible explanation could lie in an increase in low reward temporal order memory for the wakeful rest group. In a study by Oudiette and colleagues (2013), low value location information was rescued from forgetting through targeted reactivation with an associated sound during a nap. They employed targeted reactivation of low value information that was learned for reward by playing an associated tone during the nap. Thereby, they demonstrated that reactivation of information during sleep and rest subserves the systematic selectivity of memory consolidation. In the absence of their targeted reactivation this consolidation led to

increased memory for high reward information after the nap. However, low reward information could be saved from forgetting by reactivation during sleep. Reactivation during the nap led to memory retention for all low reward information despite only half of the low reward information was targeted for reactivation (Oudiette, Antony, Creery, & Paller, 2013). This exemplifies one manner by which wakeful rest might have led to increased low reward memory. Reactivation of high reward information during wakeful rest could possibly have extended onto low reward information. Reward value has been shown to spread to associated neutral objects through processes of reactivation (Wimmer & Shohamy, 2012). Wakeful rest could support spread from high to low reward sequences by hindering new sensory input and thereby increase sequence memory for low reward. The distractor, introducing interference, leads to the forgetting of less important information, post-encoding wakeful rest can lessen effects of post-encoding interference (Mercer, 2015). However, exploratory follow-up analyses revealed no significant difference in low reward temporal order memory between the groups. Therefore, these considerations are merely speculative.

I did not find an effect of reward on lag 1 object pairs. Here, neither reward nor wakeful rest led to better temporal order memory for object pairs with only 1 intervening object during encoding, even though rest has been suggested to benefit memory for details (Craig & Dewar, 2018). The trend towards a main effect of lag is in line with the literature demonstrating worse temporal order memory performance with decreasing lag between object pairs (Charles et al., 2004; DuBrow & Davachi, 2014; Heusser et al., 2018). While I hypothesised that reward might increase memory precision and thereby memory for lag 1 object pairs, the absence of study-test-cycles, usually employed in the investigation of temporal order memory, might have led to these differences being too small to detect.

It should be noted that the reward-related temporal order memory benefit described above displays a correlation with the reward-related reaction time reduction for encoding judgments in high versus low reward contexts. Participants who were faster in answering the semantic questions to high versus low reward sequences during encoding also displayed a stronger temporal order memory benefit for object pairs from

high as opposed to low reward sequences. This relationship did not hold for encoding accuracy. Furthermore, the correlation between reduced reaction time of encoding judgements in high reward contexts and better temporal order memory was apparent in both distractor and wakeful rest group. Therefore, this correlation cannot explain the absence of a reward-related temporal order memory benefit in the wakeful rest group. Overall, participants who were faster had more time and resources for relational encoding in the form of making up stories to relate objects within a sequence to each other. This effect might be stronger than post-encoding processes.

### 2.3.1 Limitations and future directions

One main limitation lies in the relatively small number of participants retained in the final analysis. A number of participants had to be excluded due to low memory performance. A future study should include pre-screening and a larger number of participants. Although a number of studies investigating temporal order memory report sample sizes that like the present study vary between 20 and 30, the retention within the final sample of those studies is larger (e.g., Ezzyat & Davachi, 2011; Heusser et al., 2018; Jenkins & Ranganath, 2011). Additionally, the employment of object pairs for the investigation of object and source memory made interpretation of results difficult. The experiment described in Chapters 3 and 4 addresses this shortcoming. Furthermore, investigations into temporal order memory in human subjects often rely on study-test cycles (DuBrow & Davachi, 2014; Heusser et al., 2016; Jenkins & Ranganath, 2016). This could increase overall temporal order memory performance but could possibly reduce the influence of reward on memory since reward-related modulation of memory increases with the distance between memory encoding and test (e.g., Adcock et al., 2006; Studte et al., 2017; Wolosin et al., 2012). A future study could test some object pairs in study-test cycles and others after encoding.

## 2.4 Chapter Summary

In conclusion, these experiments suggest that reward can enhance temporal order memory, a form of associative memory, under certain conditions. Strikingly, wakeful rest did not boost these memory benefits. Furthermore, the correlation between

encoding RTs and reward-related temporal order memory benefit that is apparent in both groups points towards the importance of investigating interindividual differences in memory research.

# Chapter 3: Variability in the microstructure of the right ILF is related to variability in reward-related temporal order memory

Although the influence of reward on different types of memory and hippocampus-dependent memory in particular has been studied with a range of experimental designs and stimuli (e.g., Adcock et al., 2006; Cohen, Rissman, Hovhannisyan, Castel, & Knowlton, 2017; Gruber et al., 2016; Mason et al., 2017; Murty et al., 2017; Wittman et al., 2005), there remains little investigation into how reward influences temporal order memory in human subjects. Furthermore, studies have documented a relationship between interindividual variability in memory-modulation through reward and interindividual variability in the BOLD response measured with fMRI during encoding or during post-encoding rest (Adcock et al., 2006; Gruber et al., 2016; Cohen et al., 2014; 2016). However, the neuroanatomical differences underlying these functional and behavioural differences are less well described.

Treating interindividual differences as data, as opposed to noise, and relating microstructural differences in the brain to behavioural differences can reveal specific circuitry associated with brain function (Kanai & Rees, 2011). Diffusion-weighted imaging enables researchers to describe local tissue microstructure, which influences voxel-wise measures of diffusion properties like FA and MD, in-vivo (for review see Assaf, Johansen-Berg, & de Schotten, 2019). These physical characteristics describing white matter have been shown to relate to physiological properties of fibre bundles like conduction time, which can reasonably be assumed to relate to behaviour. Individual differences in behaviour and variation in task-relevant white matter pathways correlate with each other across a wide range of tasks (cf., Assaf et al., 2019). Here, a network-level approach is utilised and differences in the structural make-up of fibres connecting the areas involved in reward-processing and memory are investigated and related to variability in behaviour. Three fibre tracts are investigated for their relationship with reward-based memory enhancements based on the literature: the fornix, the uncinate fasciculus (UF), and the inferior longitudinal fasciculus (ILF) (e.g., Adcock et al., 2006;

Lisman & Grace, 2005; Metzler-Baddeley, Jones, Belaroussi, Aggleton, & O'Sullivan, 2011; Reggente et al., 2018; Hodgetts et al., 2017). A detailed description of some of the regions innervated by these fibre tracts will be given below as well as in Chapter 4.

Modulation between processes in dopaminergic midbrain structures like the VTA, the ventral striatum, which includes the NAcc, and the hippocampus are crucial for motivation-related memory. Consequently, the hippocampus is described as part of the network involved in motivation-modulated memory (e.g., Düzel et al., 2010; Lisman & Grace, 2005; see Miendlarzewska, Bavelier, & Schwartz, 2016 for review). Reward-modulated memory formation has been linked to activation in, and connectivity between, VTA and hippocampus during encoding or post-encoding rest. These processes are proposed to be dopamine-supported (Adcock et al., 2006; Gruber et al., 2016). Long-term declarative memory formation is not only supported by the MTL but also the prefrontal cortex (PFC) (Blumenfeld & Ranganath, 2007; Cabeza & St. Jacques, 2007). Interactions between frontal areas like the medial prefrontal cortex and the MTL support context-dependent memory processing (Dobbins, Foley, Schacter, & Wagner, 2002; Preston & Eichenbaum, 2013; Place, Farovik, Brockmann, & Eichenbaum, 2016; Zeithamova, Dominick, & Preston, 2012). Temporal order memory has been found to relate to increased BOLD response within areas of the PFC during encoding or retrieval (Ezzyat & Davachi, 2011; Tubridy & Davachi, 2011; Jenkins & Ranganath, 2011; St. Jacques et al., 2008). Functional connectivity between PFC and MTL has also been shown to relate to temporal order memory (DuBrow & Davachi, 2016). Additionally, a paradigm of reward- and novelty-modulated memory formation revealed reward-related activation of the medial PFC and the ventral striatum (including NAcc) (Bunzeck, Doeller, Dolan, & Düzel, 2012). The fornix is a major output/input- pathway between the hippocampal formation in the MTL, striatal structures like the NAcc, and the medial PFC (Aggleton & Christiansen, 2015; Aggleton, Wright, Rosene, & Saunders, 2015; Friedman, Aggleton, & Saunders, 2002). Therefore, the present study investigated properties of the fornix for their relationship with reward-modulated memory formation. In a rodent-study, electrical stimulation of the fornix led to significant changes in glucose metabolism (as an indicator of increased activity) in the NAcc and the hippocampus as measured by micro-PET (Shin et al., 2019). Fornix-dissected monkeys have been shown

to be impaired in their judgment of temporal order and this impairment was not related to novelty-detection since that remained intact (Charles et al., 2004). In human participants, reward led to increased BOLD signal within a region in the septum/fornix (Bunzeck et al., 2012). Fornix microstructure has been found to relate to episodic memory performance and the vivid retrieval of contextual detail in autobiographical memory (Hodgetts et al., 2017; Metzler-Baddeley et al., 2011). In another study, fornix microstructure was correlated with recollection memory while not correlating with familiarity (Rudebeck et al., 2009). In line with these findings, the relationship of fornix microstructure with reward-modulated temporal order memory, recollection, and source memory was investigated in this study.

Neither the hippocampus nor the fornix is a unitary structure. Cellular and functional differences delineate the four main components of the hippocampus: the CA1, CA2/3, dentate gyrus, and subiculum (Aggleton & Christiansen, 2015). The fornix can be subdivided into pre- and postcommissural fornix on one end as well as medial and lateral fornix on the other end. Pre- and postcommissural fornix split at the anterior commissure. The precommissural fornix carries projections to the basal forebrain, the ventral striatum (including NAcc), and the PFC while the postcommissural fornix innervates the anterior thalamus and the mammillary bodies (Aggleton, 2012; Christiansen et al., 2016). The medial and lateral fornix are described by their origin within posterior and anterior hippocampus (along its long axis). The medial fornix projections from the posterior hippocampus primarily innervate the mammillary bodies, while the lateral fornix fibres connect anterior hippocampus with PFC, NAcc, and the anteromedial thalamic nucleus (Christiansen et al., 2017; Saunders & Aggleton, 2007). Furthermore, a representational gradient from fine-grained representations within the posterior to more gist-based representations within the anterior hippocampus has been proposed (Ranganath & Ritchey, 2012; Strange, Witter, Lein, & Moser, 2014). Based on these findings and in preparation for functional resting-state connectivity investigations reported in Chapter 4, the anterior hippocampus/lateral fornix and posterior hippocampus/medial fornix subdivisions are well suited for investigation of reward-related memory processes within the present study. Based on the connection between anterior hippocampus and NAcc via the lateral fornix, reward-related memory benefits

were investigated for their relationship to variability in the microstructure of the lateral fornix. Interindividual differences in overall temporal order memory were investigated for their relationship to variability within medial fornix microstructure due to the processing of fine-grained sequential information within the posterior hippocampus (Strange et al., 2014). For a detailed description of this analysis see Appendix 2.

The UF is a fibre bundle that connects the MTL with the frontal cortex, particularly the entorhinal cortex, perirhinal cortex (PrC), and the amygdala with the lateral orbitofrontal cortex in both hemispheres (Catani, Dell'Acqua, & De Schotten, 2013; Catani & De Schotten, 2008; Kondo, Saleem, & Price, 2005). In macaque monkeys, UF disconnection led to the inability to learn sequences leading up to reward while the acquisition of direct reward-item-associations remained intact (Browning & Gaffan, 2008). In humans, UF microstructure was found to be related to individual differences in object-location associative learning (Metzler-Baddeley et al., 2011) as well as face-name and fractal-location associative learning (Alm, Rolheiser, & Olsen, 2016). Critically for this study, UF microstructure was also found to be correlated with free recall of words associated with a high as opposed to a low value (Reggente et al., 2018). In the study by Reggente and colleagues (2018), participants were instructed to remember words from a list. Before each word was presented, participants were informed whether they could gain high or low points for correctly remembering the words in a free recall memory test. Individual differences in UF microstructure correlated with variability in free recall of high value but not low value words, suggesting that the UF might support processing of highly salient information (Reggente et al., 2018). Based on these findings, the relationship of UF microstructure with temporal order memory, recollection, and source memory modulated by reward was investigated in this study.

The ILF is a long-range associative white matter tract within the MTL. It connects the occipital cortex with anterior temporal areas (for review see Herbet, Zemmoura, & Duffau, 2018). The anterior temporal lobe (ATL) has been suggested as a semantic hub (Ralph, Jefferies, Patterson, & Rogers, 2017; Patterson, Nestor, & Rogers, 2007). Strategic engagement of semantic processing has been related to variability in value-based memory (Cohen et al., 2014; Cohen et al., 2017). Patients with semantic dementia

(SD), a neurodegenerative condition associated with the progressive deterioration of knowledge about, and the ability to name, concepts, people, and objects (Patterson et al., 2007), have been shown to possess altered ILF microstructure (Agosta et al., 2009). ILF microstructure differences have also been related with differences in the number of semantic details recalled in an autobiographical interview (Hodgetts et al., 2017). Furthermore, a recent study employed natural language processing tools on Wikipedia articles to create semantic dissimilarity models for famous faces and places stimuli (Morton, Zippi, Noh, & Preston, 2021). These representational semantic models were found to highly correlate with independently established semantic models based on the behaviour of 150 participants in similarity judgement tasks. The Wikipedia-based semantic dissimilarity models were thereby demonstrated to reflect semantic knowledge participants can be presumed to have. A different set of participants then underwent functional MRI scanning while viewing these famous faces and places with their label. During scanning participants fulfilled an unrelated colour-change detection task on dots centred on the images. Neural dissimilarity patterns of activity in regions within a broader semantic network (see Chapter 4) like the fusiform gyrus were explained by the model-based semantic dissimilarity patterns. Semantic dissimilarity models of faces and places were also able to explain unique variance in the activation patterns of the hippocampus (Morton et al., 2021). Thereby Morton and colleagues (2021) demonstrated that semantic knowledge about stimuli is neuronally represented even when semantic knowledge is not required by the task. Additionally, this representation was not limited to regions within a broader semantic network but could also be seen in the hippocampus. Based on these findings, the application of a semantic judgement task during memory encoding can be expected to recruit processing within a semantic network, connected via the ILF. Furthermore, semantic knowledge has also been reflected in hippocampal activation patterns and elaborative processing due to the semantic encoding task might thereby support episodic memory formation. Taken the findings reviewed within this paragraph into account, correlations between interindividual differences in ILF microstructure and interindividual differences in reward-modulated temporal order memory, recollection, and source memory were investigated here.

The present study employed multi-shell diffusion MRI and spherical deconvolution tractography to investigate the relationship between interindividual variability in the microstructure of white matter pathways (fornix, UF, and ILF) and interindividual differences in reward-related memory enhancements. Participants encoded objects in high versus low reward contexts. In a subsequent memory test, participants' temporal order memory for object pairs was tested ("Which came first?"), including a high versus low confidence rating of their temporal order memory. Furthermore, participants were tested for their object and source memory.

Based on the relationship of fornix microstructure with episodic memory (Hodgetts et al., 2017; Metzler-Baddeley et al., 2011), I predicted an association of fornix microstructure with high confidence temporal order and source memory accuracy in this study. Temporal order memory and source memory are proposed to reflect the relationship of episodic events to time and place, leading to the description of temporal memory as episodic-like (Dere et al., 2005). Furthermore, I predicted an association of fornix microstructure with recollection in this study based on the findings by Rudebeck and colleagues (2009). Based on UF microstructure being found to correlate with high value recall (Reggente et al., 2018; Hennessee et al., 2019), I predicted a correlation of UF microstructure with reward-related memory benefits for high confidence temporal order memory, recollection, and source memory. Finally, ILF microstructure has been linked to semantic processing and strategic engagement of semantic processing has been found to be related to value-based recall (Agosta et al., 2009; Cohen et al., 2014; 2016; Herbet et al., 2018; Hodgetts et al., 2017). Variability in ILF microstructure has also been found to correlate with semantic details in autobiographical memory (Hodgetts et al., 2017). Semantic knowledge has been found to be reflected within encoding activity in a functional MRI scanning paradigm in the absence of an explicitly semantic task (Morton et al., 2021). Following these findings, I predicted ILF microstructure to be correlated with reward-related memory benefits for high confidence temporal order memory, recollection, and source memory. Directed tests for correlation analyses of specific microstructure indices were based on the literature (see "3.1.7 Correlation analysis …"). Most of the studies reported here relied on relatively small sample sizes to investigate interindividual differences (e.g., Hodgetts et al., 2017; Reggente et al., 2018;

Rudebeck et al., 2009). This study aims to assess the validity of those findings in a larger sample size. It employs a rewarded semantic judgement task during sequence encoding followed by temporal order as well as object and source memory tests to investigate the relationship between interindividual differences in reward-related associative, specifically temporal order, memory and interindividual differences in white matter microstructure.

# 3.1 Methods

## 3.1.1 General procedure for data collection

Participants took part in data collection over the course of three days. For most participants, the first day consisted of MRI acquisition. High resolution anatomical scans, diffusion-weighted images, and resting-state functional connectivity scans were acquired from all participants. Detailed descriptions of the imaging acquisitions can be found under "3.1.5.1 Imaging- acquisition" and in Chapter 4. The second and third day consisted of behavioural testing. A maximum of three weeks lay between MRI acquisition and the two days of behavioural testing. The two behavioural testing days were always separated by 24 hours. The data collection included a curiosity-related manipulation that is not part of this thesis. On the first day of data collection, participants completed curiosity-motivated encoding as part of a paradigm similar to Gruber et al. (2014). The curiosity-motivated encoding was followed by an intentional memorisation encoding task that will be described in Chapters 5 and 6. Participants were instructed to memorise scenes for reward based on memory test performance. Encoding was followed by an immediate memory test. Participants then returned to the lab approximately 22 hours later. The second day of data collection started with memory tests for material from the curiosity-motivated encoding that is not part of this thesis. This memory test was followed by the delayed memory test for intentionally memorised rewarded scenes (Chapter 5-6). The delayed memory test was followed by the experiment described in this and the following chapter.

## 3.1.2 Participants

Data were collected from 55 people (7 male) with a mean age of 19.31 (SD = 1.78; range = 18-25). Participants were recruited via the Experimental Management System (EMS) at Cardiff University and received course credit (4 credits/hour) and or payment (6 GBP/hour) for their participation. Monetary rewards were independent of chosen compensation. Participants were screened for MRI scanning safety prior to taking part in the study (e.g., pacemakers, electrical/mechanically/magnetically operated devices in the body, stents, epilepsy). Based on self-reports, all participants had normal or corrected to normal vision, had never been diagnosed with a psychiatric or neurological condition, did not take psychiatric medication, and did not consume alcohol or drugs prior to testing. Participants gave written informed consent before the experiment. The Ethical Review Board at the School of Psychology at Cardiff University approved the study procedures.

## 3.1.3 Behavioural procedures

The following paragraphs describe the three stages of the study, adapted from Gruber et al. (2016). The study materials, encoding judgements, and monetary incentives for the reward-motivated encoding-phase were the same as in Gruber et al. (2016) and as described in Chapter 2. The procedure described here differed from Chapter 2 in the way memory was assessed and in the selection of items for the memory tests. Detailed descriptions are given under 3.1.3.2 and 3.1.4.2. The reward-motivated encoding-phase lasted approximately 50 minutes and was followed by a 10-minute post-encoding distractor-phase and a two-phased memory test. The memory test was self-paced and lasted approximately 50 minutes. The participants encoded 320 objects in differently rewarding contexts (high versus low reward). Objects were grouped into sequences of eight denoted by four different background scenes. During encoding, participants made yes/no- judgements on four different semantic questions matching the background scenes. Depending on the reward-condition, they received either high (£2.00) or low (£0.02) reward for correctly answering these semantic questions within two seconds. The memory test comprised three questions, one each to test temporal order memory, object memory, and source memory as described below.

### 3.1.3.1 Reward-motivated encoding

The reward-motivated encoding did not differ from the encoding described in "2.1.2 Reward-motivated encoding". Participants answered one semantic question to a sequence of eight objects, a mini-block. Figure 3.1 depicts two exemplary mini-blocks, one with high and one with low reward. Each mini-block started with the presentation of a high or low reward cue (£2.00 or £0.02) and the particular semantic judgement above the semantically matched background scene for 2 seconds. The background scene remained, and the objects were presented for 2 seconds each in the middle of the screen while participants responded to the semantic question via key press. The inter-stimulus-interval (ISI) was randomly jittered between 2 and 3 seconds. At the end of a mini-block, participants received feedback about the winnings they made in the preceding mini-block via a presentation on the screen for 2 seconds.

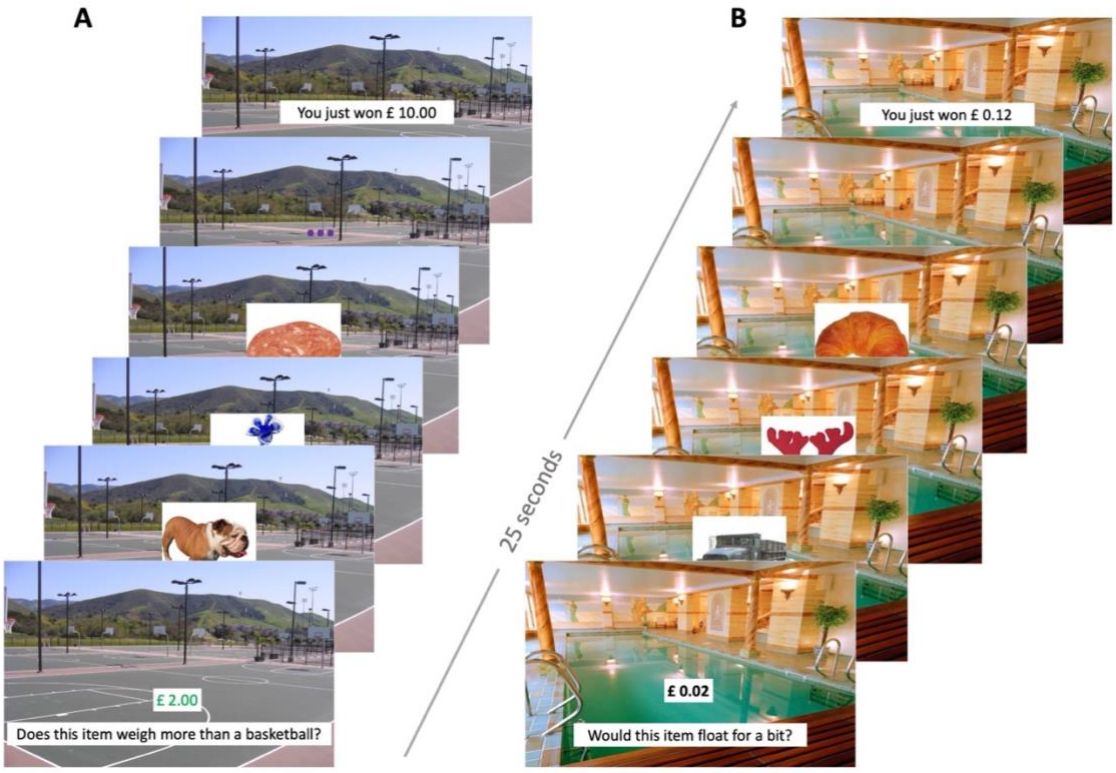


**Figure 3.1. Example of high and low reward encoding sequences. A.** High reward mini-block. The semantic judgement matching the background scene was presented together with the high reward cue. **B.** Low reward mini-block. The semantic judgement matching the background scene was presented together with the low reward cue. Participants received reward for correct responses. The semantic questions were: "Does this item weigh more than a basketball?" (basketball court scene); "Would this item float for a bit?" (swimming pool scene); "Is this item bigger than a laptop screen?" (office scene); "Is it possible to juggle three exemplars of this particular item?" (circus tent scene). A mini-block contained eight objects, depicted are three. Cue and font colour denote reward (high = £2.00 in green font, low = £0.02 in black font). A mini-block ended with reward feedback.

After four mini-blocks containing the four different background scenes and matching judgements, one encoding-block ended with the presentation of a fixation cross on a grey background for 3 seconds. Within an encoding-block reward always switched between high and low. Participants could take self-paced breaks after the fourth and the eighth block. The experiment consisted of 10 encoding-blocks and therefore 40 mini-blocks/sequences. Participants were also instructed to relate the objects of one sequence to each other and their background scene. Before encoding, participants were informed about the later memory test but not the type of memory test.

Encoding was followed by a 10-minute distractor task. Based on the results reported in Chapter 2 "2.2.2 Temporal order memory", a distractor task as opposed to rest was employed to maximise reward-related memory benefits for temporal order specifically in the immediate memory test. Despite the absence of a significant difference between distractor and wakeful rest group, the exploratory analysis conducted in Chapter 2 indicated that the distractor task would lead to effects of reward on temporal order memory. The distractor task was a paper pen arithmetic test involving three-digit additions and subtractions. Participants were informed that their performance on this task would not influence their winnings. Afterwards, participants received instructions for the memory test.

#### 3.1.3.2 Memory test

The memory test procedures described here differed from the procedures described in Chapter 2. Here, the memory test was divided into two phases. The first phase tested participants' temporal order memory by presenting them with object pairs on the screen and asking them "Which came first?" (Figure 3.2). If participants remembered both objects, they were instructed to indicate via key press whether the object presented on the left or the right side of screen came first during encoding.

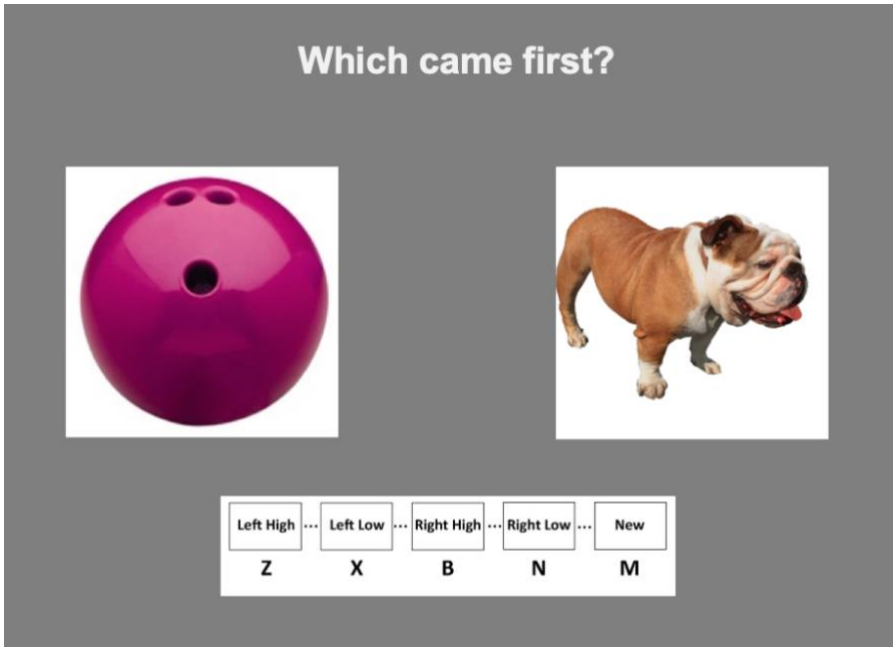


**Figure 3.2**. **Temporal order memory test.** Object pairs either contained two objects presented during encoding (old-old) or comprised one old and one new object (old-new). Old-old object pairs were always taken from the same sequence. When participants remembered both objects as old, they were instructed to judge their confidence in their pick of the first items. Participants were instructed to give a "new" -response if one of the objects feels new to them.

Following Jenkins and Ranganath (2016), participants judged their confidence in their pick as high or low. Whether the object that was presented earlier within a sequence during encoding was presented on the left or right side of the screen during the memory test, was randomised and equally distributed between high and low reward condition. If participants only recognised one of the objects from the encoding phase, they were instructed to give a "new"-response. Participants were tested on 120 object pairs (80 old-old, 40 old-new). Testing was self-paced and lasted approximately 20 minutes. Afterwards, a white text on grey screen informed participants of the end of the first phase and asked them to continue to the second phase via key press.

Based on the limitations reported in Chapter 2, object and source memory were investigated separately from temporal order memory. Furthermore, single objects, as opposed to object pairs, were employed. During the second phase of the memory test, participants were tested on their object and source memory (Figure 3.3). Objects that have not been employed for the temporal order memory test were used for the object and source memory test. Therefore, participants' memory for every object within the sequence was tested across the entirety of the experiment. Recollection and familiarity

measures were examined in a classic remember-know-new design (e.g., Yonelinas, 2002; Yonelinas & Jacoby, 1995). Participants were instructed to give a "remember"-response if they were able to recollect something specific about encountering the object during encoding. Participants should respond "know" if they recognised the object as "old" in the absence of any recollection for the experience of being presented with the object during encoding.

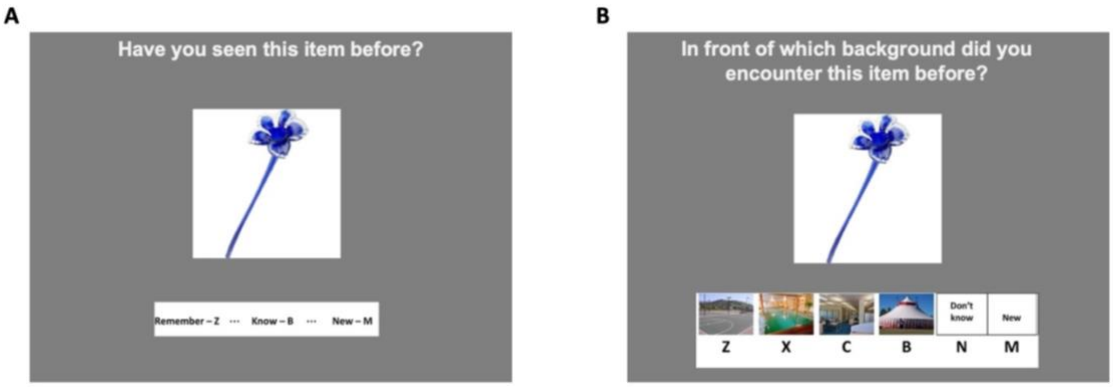


**Figure 3.3. Object and source memory test. A.** Object memory test. Recollection and familiarity were investigated in a classic remember-know-new design. **B.** Source memory test. The same objects were tested. Participants were instructed to pick the background scene they thought the object was presented in front of during encoding. Participants were able to give a "don't know"- response. A "new"- response had to be given for both memory tests.

Next, participants' source memory for the same object was tested by presenting them with the associated encoding contexts (the semantically matched background scenes). Participants picked the scene which they thought the object was presented in front of during encoding. They could give a "don't know"- response if the object was old but they did not remember in front of which background they encountered the object during encoding. "New"- responses were to be given to both object and source memory test questions if participants did not remember encountering the object during encoding. Testing was self-paced. Participants were tested on 160 objects (120 old = 60 per reward condition, 40 new). The memory tests lasted approximately 30 minutes.

### 3.1.4 Stimuli

The 320 coloured pictures of objects for encoding, 120 coloured pictures of objects as distractors in the memory test, and 4 coloured background scenes (basketball court, swimming pool, office, and circus tent) were the same as in Gruber et al. (2016) and

Chapter 2. Gruber et al. (2016) sourced the images via a publicly available database (Brady et al., 2008).

#### 3.1.4.1 Reward-motivated encoding

Randomisation- and grouping- processes for the encoding stimuli set were adapted from Gruber et al. (2016) and the same as described in Chapter 2. The four background scenes were matched to the four judgements that participants were instructed to make on the 320 objects during encoding (basketball court scene, basketball judgement; pool scene, floating judgement; office scene, laptop judgement; and tent scene, juggling judgement). Scenes and judgements were counterbalanced between high and low reward conditions across participants. Correct yes/no- answers were roughly equally distributed across the subsets. If the "correct" answer was ambiguous, both yes and no responses were rewarded, unbeknownst to the participant. Additionally, only 80% of responses were rewarded overall ensuring a level of attention due to some uncertainty about reward (cf., Gruber et al., 2016). Participants were informed of that.

#### 3.1.4.2 Memory test

The procedure of object selection for the memory tests differed from that described in Chapter 2. Out of the 40 sequences that the participants encoded, two pairs of objects per sequence were chosen for the temporal order memory test (80 pairs = 40 high and 40 low reward). Based on the results reported in "2.2.2 Temporal order memory" and previous research (e.g., DuBrow & Davachi, 2014), pairs were chosen to maximise the number of objects that are between the two objects tested while at the same time not using the first and last objects of a sequence in the pair. The maximum number of intervening objects (lag) was three. Accordingly, the 2$^{nd}$ and 6$^{th}$ as well as 3$^{rd}$ and 7$^{th}$ object of each sequence were always used for the temporal order memory test. One additional object of each sequence was chosen to pair with a randomly picked new object to build an old-new object pair (20 old-new pairs per reward-condition). The position the old object from the old-new pair had within a sequence during encoding (1$^{st}$, 4$^{th}$, 5$^{th}$, and 8$^{th}$ position) was counterbalanced across participants and reward condition.

After the objects were assigned to object pairs for the temporal order memory test, three objects per sequence remained (4th, 5th, and 8th; 1st, 5th, and 8th; 1st, 4th, and 8th; or 1st, 4th, and 5th) to be used in the object and source memory test. During the object and source memory test 120 old objects were presented (60 high reward, 60 low reward, three objects per encoding sequence). Each object was tested for object as well as source memory. Together with the remaining objects from the distractor- set these objects were randomly shuffled and constituted the stimulus set for the object and source memory test (160 objects).

## 3.1.5 Imaging

### 3.1.5.1 Imaging- acquisition

Imaging was conducted at CUBRIC, Cardiff University, on a 3 Tesla MRI scanner (Siemens Megnetom Prisma) with a 32-channel head coil. High-resolution anatomical images were obtained with a T1- weighted 3D MPRAGE sequence (TR = 2500ms, TE = 3.06ms, flip angle = 9°, FoV = 256mm$^2$, voxel-size = 1.0 x 1.0 x 1.0 mm, slice thickness = 1mm, 224 sagittal slices, bandwidth = 230 Hz/pixel; total acquisition time = 7 minutes and 36 seconds). Diffusion-weighted data were collected with a multi-shell spin-echo echoplanar imaging (EPI) sequence (TR = 9400ms, TE = 70ms, slice thickness = 2mm, 80 transversal/axial slices along the A-P axis, FoV = 256mm$^2$, voxel size = 2.0 x 2.0 x 2.0 mm). Diffusion gradients were applied in multiple directions (30 isotropic directions with a diffusion-weighted factor *b*=1200sec/mm$^2$; 60 isotropic directions with a diffusion-weighted factor *b*=2400sec/mm$^2$) and a volume without diffusion gradients was obtained (*b*=0sec/mm2) (bandwidth = 1954Hz/pixel; total acquisition time = 15 minutes 51 seconds). Furthermore, a diffusion-weighted image along the same isotropic directions within the two shells but with a reversed phase encoding was obtained (TR = 9400ms, TE = 70ms, slice thickness = 2mm, 80 transversal/axial slices along the P-A axis, FoV = 256mm$^2$, voxel-size = 2.0 x 2.0 x 2.0 mm; bandwidth = 1954Hz/pixel; total acquisition time = 58 seconds).

### 3.1.5.2 Diffusion MRI- pre-processing

Diffusion-weighted images were pre-processed in a multi-step pipeline that was built within CUBRIC. First, data were denoised with a Marchenko-Pastur principal component analysis (MPPCA; Veraart, Novikov, Christiaens, Ades-aron, Sijbers, & Fieremans, 2016). The edge of the Marchenko-Pastur distribution was employed to discriminate principal components that contain noise and those that entail signal. Data were then corrected for distortions introduced through eddy currents and participant movement with FSL's *eddy*- tool (Andersson & Sotiropoulos, 2016). B=0 volumes of the diffusion-weighted images (A-P) and the b=0 volume of the reverse phase-encoded (P-A) acquisition were introduced to a Gaussian estimation of eddy distortions, skull-stripped (FSL' *BET*- tool; fractional intensity threshold set to 0.4; Smith, 2002), and then applied to all volumes of the diffusion-weighted acquisition. Furthermore, ringing-artefact correction was performed with a Full-Fourier transform (MRtrix3; Kellner, Dhital, Kiselev, & Reisert, 2016). DTI indices of white-matter tracts near the ventricles like the fornix are affected by free water like cerebrospinal fluid and correcting for free water contamination will improve white matter reconstruction (Pasternak, Sochen, Gur, Intrator, & Assaf, 2009). Therefore, a Free Water Elimination (FWE) procedure following Pasternak et al. (2009) was applied to the b=1200 data. This resulted in whole-brain FA and MD maps that were voxel-wise corrected for partial volume artefacts from free water. Tractography analysis in the native subject space was carried out on the b=2400 maps. Tract information from this shell was then registered to FA and MD maps in the b=1200 shell to obtain tract-specific FA and MD data.

### 3.1.5.3 Tractography

Whole-brain tractography was conducted on the b=2400 data not b=1200 images for better fibre orientation estimations (Vettel, Cooper, Garcia, Yeh, & Verstynen, 2017). A damped Richardson-Lucy spherical deconvolution (dRL-SD; Dell'Acqua et al., 2010) was employed on the b=2400 images. Peaks in the fibre orientation density functions (fODF) at the centre of each voxel were extracted and then tracts were reconstructed following streamlines along the orientation of the fODF peaks using a seed-point resolution of $2mm^3$ and a step size of 0.5mm. Streamline tracts were estimated within

a fibre length range of 30-500mm and terminated if the direction of the pathway changed at an angle greater than 45° or if the fODF threshold fell below 0.5 (lambda = 0.9, beta = 0.00076).

After whole-brain tractography, manual tractography within the b=2400 shell was carried out in ExploreDTI (Leemans, Jeurissen, Sijbers, & Jones, 2009; version 4.8.6) employing AND, NOT, and SEED gates. SEED gates were used as a starting-point for fibres that passed through the SEED, extracting fibres starting at a SEED and then only included those fibres that also passed through any added AND gates. NOT gates were employed to exclude fibres that passed through them. Manual tractography was carried out by one examiner (VD) on 20 participants. The 20 participants were pseudo-randomly chosen based on the participant number participants were assigned on the first day of data collection (numbers 1-20). Manual tracts were then subjected to an algorithm building a tract model (Parker et al., 2013). The tract model was then used to perform automated tractography on the whole dataset of 55 participants. The model describes the shape and position of the tract by exploiting the consistency with which streamlines belonging to those anatomical features of interest project to distinct sub-regions. To then reconstruct those white matter tracts, streamlines following the modelled projected positions are included in the tract (Parker et al., 2013). After automation, each tract was visually inspected and fibres that did not follow the tract of interest were excluded employing additional NOT gates. The resulting tract masks in the b=2400 space needed to then be registered with the whole-brain free-water corrected FA and MD maps from the b=1200 volumes; this resulted in tract-specific free-water corrected FA and MD maps. Mean FA and MD values were then extracted from the tract-specific b=1200 maps for statistical analysis (via customised MATLAB scripts).

#### *3.1.5.3.1 Fornix tractography*

The landmarks described in Catani and de Shotten (2008) were used to place the ROIs during manual tractography of the whole fornix (Figure 3.4 A; for medial and lateral fornix see Appendix 2). The anterior commissure was found in the mid-sagittal slice of the brain. The coronal crosshair was moved to that landmark and then moved approximately 6 voxels towards the posterior. The fornix bundle was identified in the

coronal plane where the anterior pillars enter the body of the fornix. One AND ROI was drawn around the fornix bundle. Fibres that were not part of the fornix (protruding out or crossing the hemispheres) were excluded by drawing NOT gates.

*3.1.5.3.2 Uncinate fasciculus tractography*

The landmarks described in Catani et al. (2008) and in Wakana et al. (2007) were used to place the ROIs during manual tractography (Figure 3.4 B). Tractography was performed separately in the two hemispheres. One SEED ROI was drawn around the entire right or left hemisphere in the coronal slice just anterior to the corpus callosum, identified in the mid-sagittal view of the brain. In the axial plane, one AND ROI was placed around the region where the fibres of the UF curve around the Sylvian fissure in the left or right hemisphere. This should be found just superior to the pons, visible in the mid-sagittal view. NOT gates were drawn to exclude fibres not consistent with the UF pathway.

*3.1.5.3.3 Inferior longitudinal fasciculus tractography*

The landmarks described in Wakana et al. (2007) were used to place the ROIs during manual tractography (Figure 3.4 C). One SEED ROI was placed around the entire left or right hemisphere in the coronal slice just posterior to the corpus collosum, identified by placing the anterior crosshair in the mid-sagittal view. One AND ROI was drawn around the temporal lobe of that same hemisphere in the last coronal slice where the temporal and frontal lobe were separate. One NOT ROI was drawn in the midline of the hemispheres excluding crossing fibres. Another NOT gate was placed in the midline of the corpus callosum excluding fibres reaching too far superior from the longitudinal axis. Additional NOT gates were placed to exclude any fibres inconsistent with the ILF pathway.

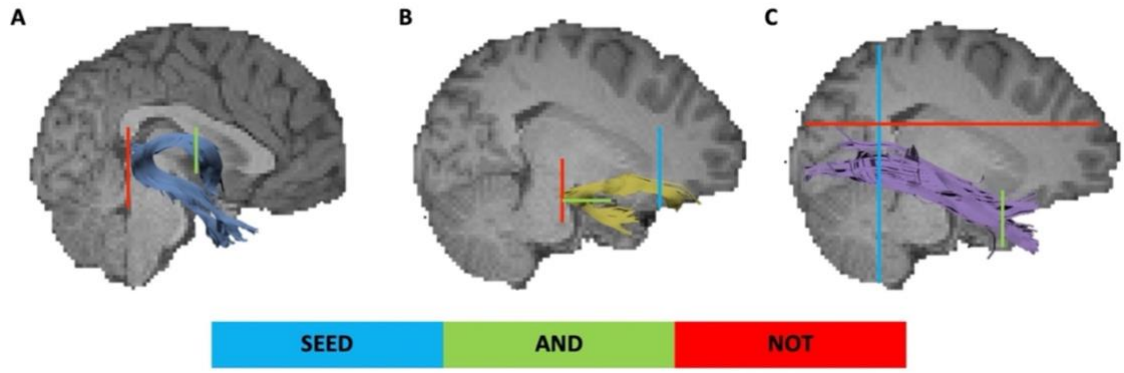


**Figure 3.4**. **Main gates employed by manual tractography for the three tracts of interest. A.** Fornix. AND and main NOT gate employed for fornix tractography. **B.** Uncinate fasciculus (UF). SEED, AND, and NOT gates for manual tractography of the right UF. **C.** Inferior longitudinal fasciculus (ILF). depicts the SEED, AND, and one of the NOT gates employed for manual tractography of the right ILF. Colours denote the type of gate. Blue = SEED, green = AND, red = NOT gate.

## 3.1.6 Behavioural analysis

Behavioural analyses steps for each memory test are described below. Behavioural analyses were carried out in JASP (JASP team, 2019; version 0.11.1). The effect of reward on memory was investigated with uncorrected t-tests. Measures of a reward-related memory benefit (i.e., accuracy for high reward minus accuracy for low reward) and overall memory (mean accuracy across reward conditions) were introduced to correlation analyses to test for associations between the microstructure of the tracts of interest and memory. One participant was excluded from all analyses (behavioural and correlation analyses) due to not making any judgements on over 50% of the trials during encoding. All participants within the analyses displayed over 70% encoding accuracy, on both high and low reward trials. Participants with low memory performance were retained in all analyses. Low memory performance was defined as overall memory accuracy being negative or 0. Because in the study of interindividual differences in memory participants with low or no memory carry information as well (Kanai & Rees, 2011), data from participants with low or no memory were retained for analysis. Only datapoints that were below or above 3 standard deviations (SD) from the mean were replaced by the respective 3SD value. This was only the case in four different participants on different measures. Whether replacements were made or not or whether these participants were excluded from analysis did not change the significant results. The following analyses are based on 54 participants (7 males, mean age = 19.28).

### 3.1.6.1 Encoding

Percentages of correct responses and mean reaction times to correct responses were investigated with one-tailed paired sample t-tests. Based on findings that reward enhances decision making (e.g., Wimmer & Shohamy, 2012; Zhang et al., 2018), percentages of correct responses were tested for a positive difference (high reward > low reward) and mean reaction times were tested for a negative difference (high reward < low reward).

### 3.1.6.2 Temporal order memory

Accuracy measures were calculated by subtracting the percentage of order responses to old-new pairs (false alarms) from the percentage of correct order responses to old-old object pairs (hits) for high and low confidence responses separately (formula 3.1).

$$accuracy_{high\ confidence} = hits_{high\ confidence} - false\ alarms_{high\ confidence}$$

**Formula 3.1**. Example of accuracy formula for responses to high reward object pairs.

Accuracy measures for high confidence temporal order memory were then compared in a one-tailed paired-sample t-test. Accuracy for high confidence responses were tested for a positive difference because, for high confidence, better memory for object pairs from high versus low reward sequences was hypothesised. Low confidence accuracy was investigated in an exploratory analysis and is reported in Appendix 3.

### 3.1.6.3 Object memory

Recollection was calculated following Gruber et al. (2016) by subtracting the proportion of false alarm "remember"- responses to new objects from the proportion of correct "remember"- responses to old objects (*percentage hits "remember" – percentage false alarms "remember"*). While a positive effect of reward on hippocampus-dependent memory like recollection is reliably reported, reward effects on familiarity are less frequent (e.g., Gruber et al., 2016). Therefore, recollection measures were investigated for a reward-related memory advantage with a one-tailed paired-sample t-test testing for a positive difference. Higher recollection of high reward

objects was expected. In an exploratory analysis, reward-related effects on familiarity were investigated with a two-tailed paired-sample t-test and are reported in Appendix 3.

#### 3.1.6.4 Source memory

Source accuracy was calculated by subtracting the percentage of false alarm source- responses to new objects from the percentage of correct source responses to old objects (*percentage hits source – percentage source false alarms*). Based on previous results (e.g., Gruber et al., 2016), the reward-related memory advantage for source memory was investigated with a one-tailed paired-sample t-test. A positive difference was tested because better source memory for high reward than low reward objects was hypothesised.

### 3.1.7 Correlation analysis – relationship between behaviour and fibre tract microstructure

Correlation analyses were performed in JASP (JASP-team, 2019; version 0.11.1). Memory effects were correlated with the different indicators (FA and MD) of microstructure in the different tracts of interest. All variables were z-standardised for each participants' data before correlation analysis (formula 3.2). Overall memory (average of high and low reward responses) and reward-related memory benefits (high – low reward) were calculated for all memory measures (i.e., high confidence temporal order memory accuracy, source memory accuracy, recollection). Directed hypotheses for the correlations between memory measures (overall memory, reward-related memory benefits) and microstructure were based on the literature.

$$z_{high\ reward\ recollection} = \frac{high\ reward\ recollection_{pptx} - mean_{high\ reward\ recollection}}{standard\ deviation_{high\ reward\ recollection}}$$

**Formula 3.2.** Example of z-standardisation for high reward recollection.

Correlations of microstructure with overall memory and reward-related memory benefits for high confidence temporal order accuracy, recollection, and source accuracy were investigated with directed hypotheses. FA of the tracts was predicted to positively

correlate with the memory measures (e.g., Hodgetts et al., 2017; Reggente et al., 2018). For MD, a negative correlation between memory and microstructure was predicted (e.g., Hennessee et al., 2019; Hodgetts et al., 2017).

Pearson's correlation indices were corrected for family-wise error rates (FWE) with the Holm-Bonferroni method (Holm, 1979; formula 3.3). Corrections were performed on the correlations performed within each tract. Correlations were corrected for 12 comparisons that were investigated with a directed hypothesis (2 memory effects [overall memory, reward-related memory benefit] x 3 types of memory [high confidence temporal order accuracy, recollection, source accuracy] x 2 microstructure indices [FA, MD]).

$$corrected\ \alpha_p = \frac{0.05}{N - rank\ number\ of\ p + 1}$$

**Formula 3.3. Holm-Bonferroni correction.** N = number of correlations calculated. p = p-value of correlation.

The following paragraphs describe how Holm-Bonferroni correction was performed. Uncorrected p-values of the correlations calculated within a tract were ordered from smallest to greatest and then the target alpha of .05 was divided by the difference of the rank position of the to be corrected p-value from the number of correlations calculated. For example, to correct the p-values of the correlation analyses between fornix FA and recollection measures, the p-values of the 12 correlations investigated with a directed hypothesis (2 memory effects x 3 types of memory x 2 microstructure indices) within the fornix were sorted by size in an ascending order. In the hypothetical example, the positive correlation between fornix FA and reward-related recollection benefit (high reward recollection – low reward recollection) is the second smallest with a p-value of .003. Therefore, the fornix FA and reward-related recollection benefit correlation has the rank number 2, whereas a total number of 12 correlations were calculated. Formula 3.4 shows the example of calculating the corrected $\alpha$ for the reward-related recollection benefit.

$$corrected \propto = \frac{0.05}{12-2+1} = 0.0045$$

**Formula 3.4. Example for Holm-Bonferroni correction.** Hypothetical correlation between fornix FA and the reward-related recollection benefit.

The p-value of each correlation is then compared to its corrected $\alpha$. In the hypothetical example the correlation between fornix FA and reward-related recollection benefit survives the family-wise error correction (p = .003 < corrected $\alpha$ = .0045).

# 3.2 Results

## 3.2.1 Behavioural results

Encoding accuracy was high for high and low reward sequences (high reward = 90.88%, SE = 0.61; low reward = 89.48%, SE = 0.50). High reward accuracy of one participant was replaced with the value of 3SDs above the mean. This replacement did not change the reported results. High reward accuracy was significantly above low reward accuracy ($t(1,53) = 2.66$, $p_{1\text{-tailed}} = .005$, $d = 0.36$). Participants were also significantly faster in high as opposed to low reward sequences (high reward = 1035msec, SE = 19.59msec; low reward = 1066.2msec, SE = 18.43msec; $t(1,53) = -4.90$, $p_{1\text{-tailed}} < .001$, $d = -0.67$).

**Table 3.1. Group means and standard deviations (SD) of the memory measures.** Means and SDs are based on percentage accuracies (hits – false alarms). Separated by reward (high versus low). SDs in brackets after the means.

| Memory measure | Reward | Mean (SD) |
|---|---|---|
| High confidence temporal order memory | high | 16.34 (19.27) |
| | low | 15.05 (16.69) |
| Recollection | high | 46.31 (24.62) |
| | low | 45.69 (24.57) |
| Source accuracy | high | 40.69 (15.20) |
| | low | 38.87 (15.92) |

Reward did not significantly influence high confidence temporal order memory ($t(1,53) = 0.89$, $p_{1\text{-tailed}} = .189$, $d = 0.12$; Table 3.1), recollection ($t(1,53) = 0.42$, $p_{1\text{-tailed}} = .34$, $d = 0.06$), and source memory ($t(1,53) = 1.21$, $p_{1\text{-tailed}} = .116$, $d = 0.16$) on a group level. Interindividual differences in reward-related memory benefits were investigated with the correlation analyses.

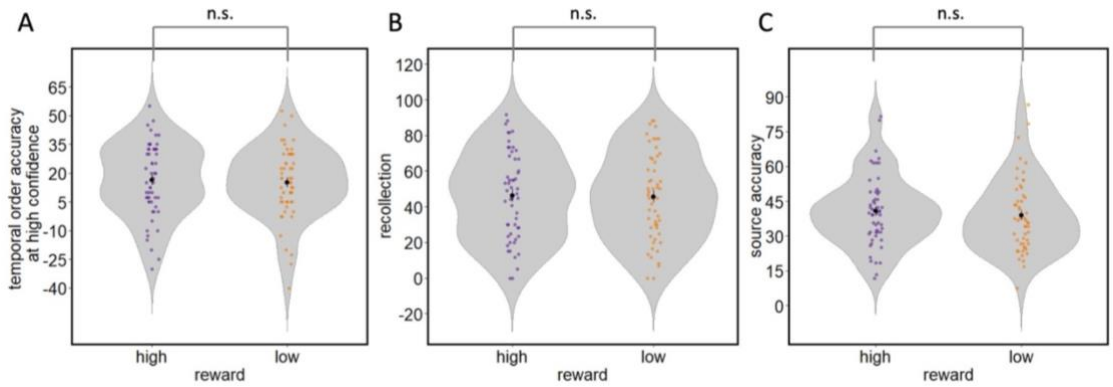


**Figure 3.5. Violin plots for the behavioural measures included in the directed correlation analyses. A.** Temporal order accuracy at high confidence split by high and low reward. **B.** Recollection split by high and low reward. **C.** Source accuracy split by high and low reward. Colours indicate reward condition. Purple = high reward. Orange = low reward. 54 data points are shown on each violin plot. Means +/- 1 SE are displayed on each plot. n.s. = not significant.

## 3.2.2 Fornix microstructure did not relate to memory

Following the hypothesised relationship with fornix microstructure and high confidence temporal order memory, reward-related memory benefit (high reward accuracy – low reward accuracy) and overall temporal order memory performance at high confidence were correlated with fornix microstructure (FA and MD). Fornix microstructure did not significantly correlate with *overall* high confidence temporal order accuracy, recollection, or source accuracy (high confidence temporal order: FA: $r(52) = -0.04$, $p_{1\text{-tailed}} = .609$; MD: $r(52) = -0.001$, $p_{1\text{-tailed}} = .497$; recollection: FA: $r(52) = 0.08$, $p_{1\text{-tailed}} = .272$; MD: $r(52) = 0.08$, $p_{1\text{-tailed}} = .727$; source accuracy: FA: $r(52) = -0.01$, $p_{1\text{-tailed}} = .525$; MD: $r(52) = -0.01$, $p_{1\text{-tailed}} = .474$). The *reward-related memory benefit* for high confidence temporal order accuracy, recollection, or source accuracy did also not significantly correlate with fornix microstructure (high confidence temporal order: FA: $r(52) = -0.05$, $p_{1\text{-tailed}} = .632$; MD: $r(52) = -0.02$, $p_{1\text{-tailed}} = .431$; recollection: FA: $r(52) = -0.14$, $p_{1\text{-tailed}} = .845$; MD: $r(52) = 0.15$, $p_{1\text{-tailed}} = .853$; source accuracy: FA: $r(52) = -0.36$, $p_{1\text{-tailed}} = .996$; MD: $r(52) = 0.21$, $p_{1\text{-tailed}} = .936$).

## 3.2.3 Uncinate fasciculus microstructure did not relate to memory

Following the hypothesised relationship between UF microstructure and reward-related memory benefits, positive correlations between UF FA and reward-related memory benefits for high confidence temporal order accuracy, recollection, as well as source memory accuracy were tested. The same memory measures were tested for negative correlations with MD. Left and right UF were investigated separately due to asymmetry reported in the literature (e.g., Alm et al., 2016; Reggente et al., 2019). One participant's FA value for the left UF was below 3 SDs and therefore replaced with the -3SD value. Removing versus retaining this participant's data from analysis did not change the direction of the reported results.

### 3.2.3.1 Left uncinate fasciculus microstructure and memory

Hypothesis-driven investigation of positive correlations between left UF FA and *overall* memory (high confidence temporal order: $r(52) = 0.10$, $p_{1\text{-tailed}} = .243$; recollection: $r(52) = 0.07$, $p_{1\text{-tailed}} = .315$; source accuracy: $r(52) = 0.05$, $p_{1\text{-tailed}} = .371$) as well as *reward-related memory benefits* for high confidence temporal order accuracy, recollection, and source accuracy (high confidence temporal order: $r(52) = 0.11$, $p_{1\text{-tailed}} = .207$; recollection: $r(52) = 0.14$, $p_{1\text{-tailed}} = .155$; source accuracy: $r(52) = -0.03$, $p_{1\text{-tailed}} = .593$) did not show significant results. Investigation of negative correlations between left UF MD and *overall* memory (high confidence temporal order: $r(52) = 0.13$, $p_{1\text{-tailed}} = .819$; recollection: $r(52) = 0.11$, $p_{1\text{-tailed}} = .786$; source accuracy: $r(52) = -0.10$, $p_{1\text{-tailed}} = .474$) as well as *reward related memory benefits* for high confidence temporal order accuracy, recollection, and source accuracy (high confidence temporal order: $r(52) = -0.09$, $p_{1\text{-tailed}} = .245$; recollection: $r(52) = 0.17$, $p_{1\text{-tailed}} = .887$; source accuracy: $r(52) = 0.07$, $p_{1\text{-tailed}} = .681$) did also not yield significant results.

### 3.2.3.2 Right uncinate fasciculus microstructure and memory

The right UF did not correlate with *overall* high confidence temporal order memory, recollection, or source memory (high confidence temporal order: FA: $r(52) = -0.10$, $p_{1\text{-tailed}} = .768$ ; MD: $r(52) = 0.16$, $p_{1\text{-tailed}} = .881$; recollection: FA: $r(52) = 0.11$, $p_{1\text{-tailed}} = .21$ ; MD: $r(52) = 0.12$, $p_{1\text{-tailed}} = .808$; source accuracy: FA: $r(52) = 0.10$, $p_{1\text{-tailed}} = .228$ ;

MD: $r(52) = -0.06$, $p_{1\text{-tailed}} = .324$). *Reward-related memory benefits* for high confidence temporal order accuracy, recollection, and source accuracy did not correlate with right UF microstructure (high confidence temporal order: FA: $r(52) = 0.06$, $p_{1\text{-tailed}} = .343$ ; MD: $r(52) = -0.02$, $p_{1\text{-tailed}} = .449$; recollection: FA: $r(52) = 0.09$, $p_{1\text{-tailed}} = .271$ ; MD: $r(52) = 0.13$, $p_{1\text{-tailed}} = .823$; source accuracy: FA: $r(52) = 0.07$, $p_{1\text{-tailed}} = .317$ ; MD: $r(52) = -0.07$, $p_{1\text{-tailed}} = .301$).

## 3.2.4 Microstructure of the ILF related to reward-related memory benefits

I hypothesised that, at immediate memory tests, semantic processing, mediated by ILF microstructure, is of importance for overall memory as well as reward-related memory benefits. Left and right ILF were investigated separately due to asymmetry reported in the literature (e.g., Alm et al., 2016; Hodgetts et al., 2017). One participant's FA value for the right ILF was below 3 SDs and therefore replaced with the -3SD value. Removing versus retaining this participant's data from analysis did not change the reported results.

### 3.2.4.1 Left inferior longitudinal fasciculus microstructure and memory

#### *3.2.4.1.1 Overall memory*

Overall high confidence temporal order memory did not significantly correlate with left ILF microstructure (FA: $r(52) = 0.10$, $p_{1\text{-tailed}} = .243$; MD: $r(52) = -0.13$, $p_{1\text{-tailed}} = .168$). Similarly, overall recollection did not significantly correlate with left ILF microstructure (FA: $r(52) = -0.20$, $p_{1\text{-tailed}} = .914$; MD: $r(52) = 0.27$, $p_{1\text{-tailed}} = .973$). Left ILF microstructure did not significantly correlate with overall source accuracy (FA: $r(52) = -0.02$, $p_{1\text{-tailed}} = .555$; MD: $r(52) = -0.002$, $p_{1\text{-tailed}} = .496$).

#### *3.2.4.1.2 Reward-related memory benefit*

*High confidence temporal order memory.* Left ILF microstructure did not significantly correlate with the reward-related memory benefit for high confidence temporal order accuracy (FA: $r(52) = 0.12$, $p_{1\text{-tailed}} = .193$, MD: $r(52) = 0.05$, $p_{1\text{-tailed}} = .637$).

*Recollection memory.* Left ILF microstructure (FA) correlated positively with the reward-related recollection memory benefit (FA: $r(52) = 0.25$, $p_{1\text{-}tailed} = .037$; MD: $r(52) = 0.02$, $p_{1\text{-}tailed} = .546$). This correlation (Figure 3.6 B) did not survive FWE- correction ($p_{1\text{-}tailed} = .037 > \alpha_{corrected} = .004$).

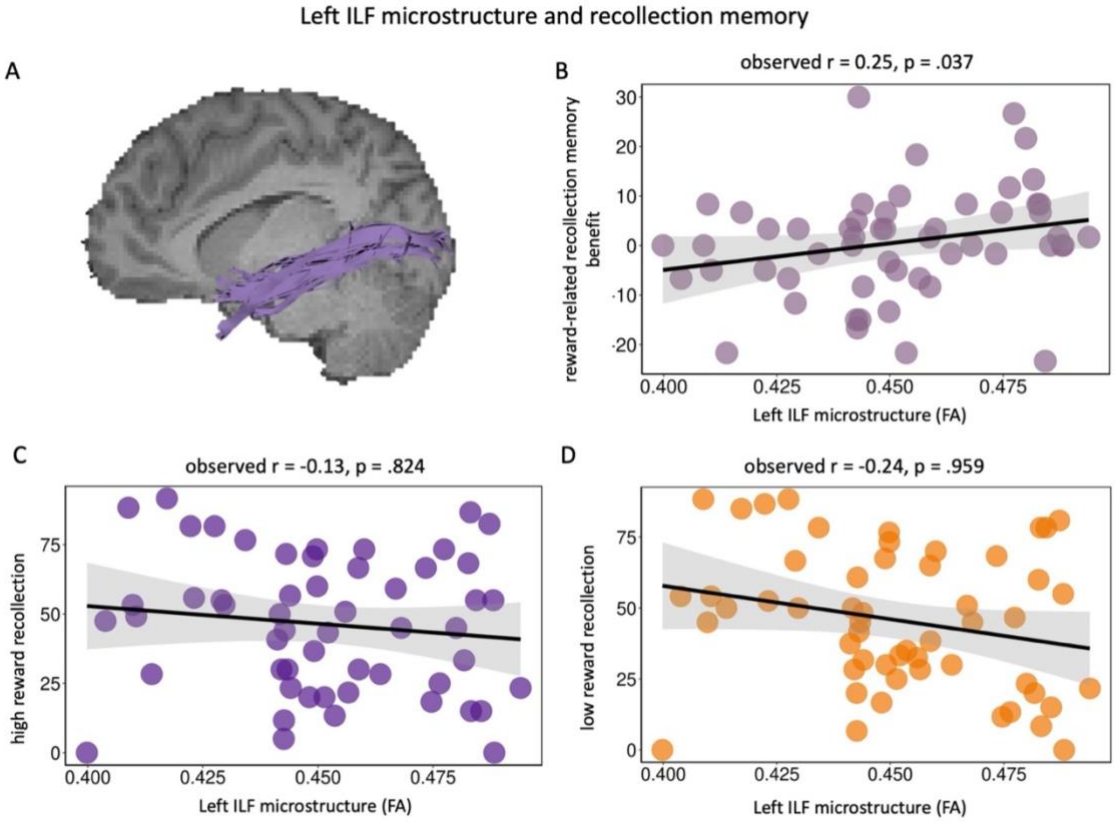


**Figure 3.6. Correlation of left inferior longitudinal fasciculus (ILF) fractional anisotropy (FA) and reward-related recollection memory benefit. A.** Left ILF on brain. **B.** Positive (uncorrected significant) correlation of left ILF FA with reward-related recollection memory benefit. **C.** Correlation of left ILF FA with high reward recollection. **D.** Correlation of left ILF FA with low reward recollection. The line of best fit and 95% confidence interval (CI) is shown on each scatterplot with 54 data points.

Follow-up analyses correlating left ILF FA with high reward ($r(52) = -0.13$, $p_{1\text{-}tailed} = .824$; Figure 3.6 C) and low reward ($r(52) = -0.24$, $p_{1\text{-}tailed} = .959$; Figure 3.6 D) recollection did not reach significance.

*Source accuracy.* There was a trend towards a significant correlation between left ILF microstructure (FA) and the reward-related source memory benefit (FA: $r(52) = 0.19$, $p_{1\text{-}tailed} = .08$; MD: $r(52) = 0.02$, $p_{1\text{-}tailed} = .558$).

### 3.2.4.2 Right inferior longitudinal fasciculus microstructure and memory

#### *3.2.4.2.1 Overall memory*

Overall high confidence temporal order memory did not significantly correlate with right ILF microstructure (FA: $r(52) = 0.02$, $p_{1\text{-}tailed} = .444$; MD: $r(52) = -0.03$, $p_{1\text{-}tailed} = .409$). Similarly, overall recollection did not significantly correlate with right ILF microstructure (FA: $r(52) = -0.16$, $p_{1\text{-}tailed} = .881$; MD: $r(52) = 0.24$, $p_{1\text{-}tailed} = .959$). Right ILF microstructure did not significantly correlate with overall source accuracy (FA: $r(52) = -0.02$, $p_{1\text{-}tailed} = .548$; MD: $r(52) = 0.03$, $p_{1\text{-}tailed} = .573$).

#### *3.2.4.2.2 Reward-related memory benefit*

*High confidence temporal order memory.* Right ILF microstructure (FA) significantly correlated with the reward-related memory benefit for high confidence temporal order accuracy (right ILF: $r(52) = 0.50$, $p_{1\text{-}tailed} < .001 < \alpha_{corrected} = .004$; MD: $r(52) = -0.12$, $p = .194$; Figure 3.7 B). This correlation survived FWE- correction. Follow-up analyses show no correlation with either high reward ($r(52) = 0.16$, $p_{1\text{-}tailed} = .126$; Figure 3.7 C) or low reward temporal order accuracy ($r(52) = -0.13$, $p_{1\text{-}tailed} = .816$; Figure 3.7 D). These results remain unchanged when outliers and participants with low memory performance are removed from the analysis.

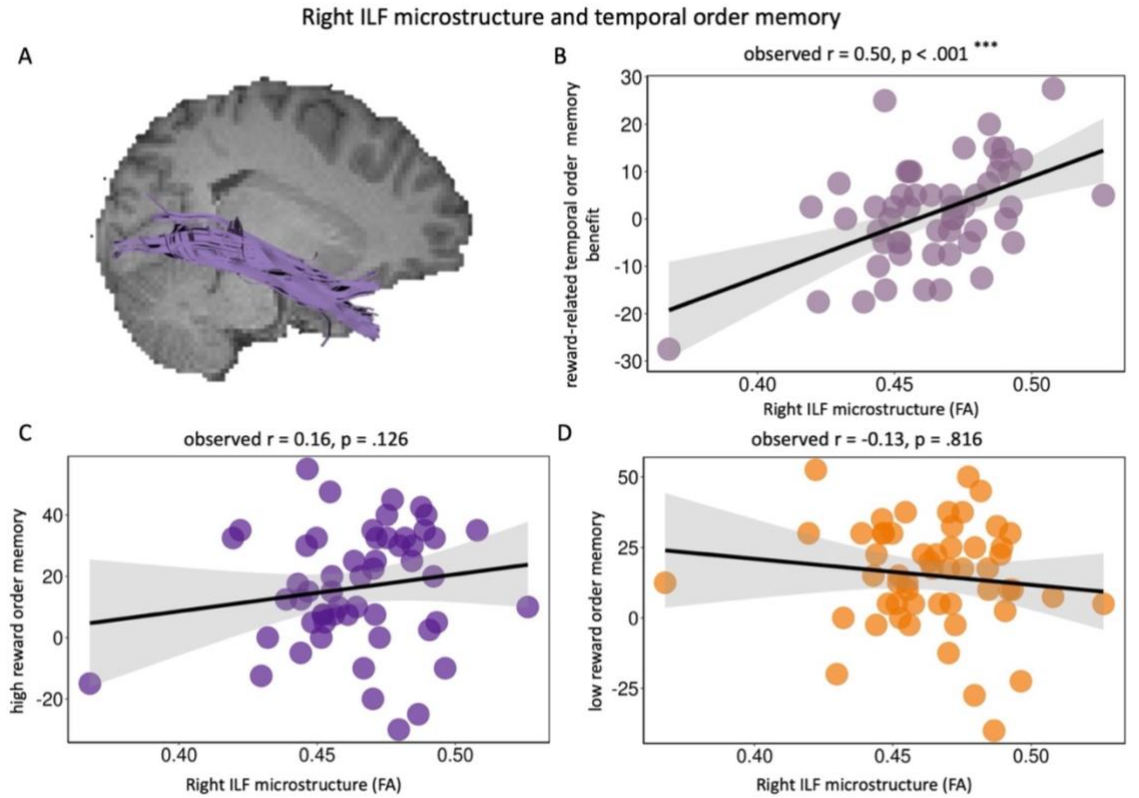


**Figure 3.7 Correlation of right inferior longitudinal fasciculus (ILF) fractional anisotropy (FA) and high confidence temporal order memory. A.** right ILF on brain. **B.** Significant (FWE-corrected) correlation between right ILF FA and the reward-related high confidence temporal order memory benefit. **C.** Correlation of right ILF FA with high reward temporal order accuracy. **D.** Correlation of right ILF FA with low reward temporal order accuracy. The follow-up analyses did not reach significance. The line of best fit and 95% confidence interval (CI) is shown on each scatterplot with 54 data points. *** = significant after FWE-correction.

To further investigate whether the relationship between right ILF microstructure and reward-related memory benefits is independent of overall temporal order memory, right ILF microstructure (FA) and overall memory values were introduced as predictors of reward-related memory benefits in a hierarchical linear regression model via enter method. Overall memory was included into the null model (intercept model). For high confidence temporal order memory, the model of right ILF microstructure and overall memory significantly explained the variance in the reward-related temporal order accuracy benefit ($F(2,51) = 8.711$, $p < .001$). Right ILF microstructure explained 25.1% more variance than the null model containing the intercept and overall temporal order accuracy ($R^2$ change = 0.251; right ILF: beta = 0.502; $t(54) = 4.148$, $p < .001$; overall memory: beta = 0.046; $t(54) = 0.384$, $p = .703$).

*Recollection.* Right ILF microstructure (FA) significantly correlated with the reward-related recollection memory benefit (FA: $r(52) = 0.36$, $p_{1\text{-}tailed} = .004$; MD: $r(52) = -0.03$, $p_{1\text{-}tailed} = .413$; Figure 3.8 A). This correlation survived FWE- correction ($p_{1\text{-}tailed} = .004 < \alpha_{corrected} = .0045$). Follow-up analyses correlating right ILF FA with high reward ($r(52) = -0.08$, $p_{1\text{-}tailed} = .716$; Figure 3.8 B) reward and low reward recollection did not reach significance ($r(52) = -0.24$, $p_{1\text{-}tailed} = .959$; Figure 3.8 C).

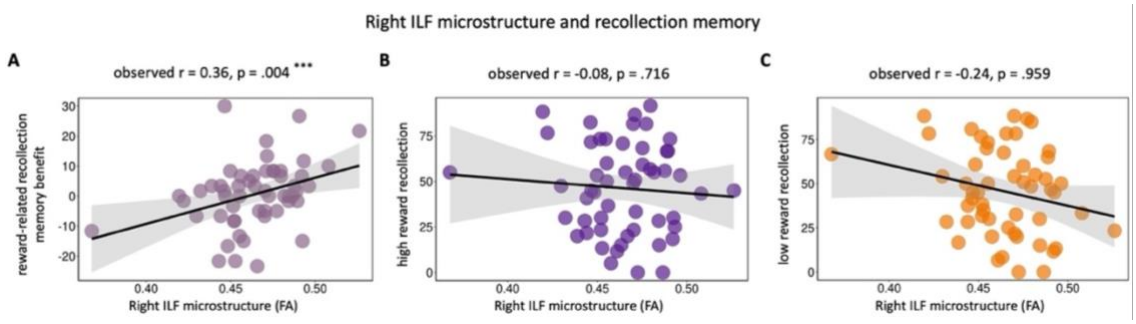


**Figure 3.8. Correlation of right Inferior Longitudinal Fasciculus (ILF) fractional anisotropy (FA) and reward-related recollection memory benefit. A.** Significant (FWE-corrected) positive correlation of right ILF FA with reward-related recollection memory benefit. **B.** Correlation of right ILF FA with high reward recollection. **C.** Correlation of right ILF FA with low reward recollection. The line of best fit and 95% confidence interval (CI) is shown on each scatterplot with 54 data points. *** = significant after FWE-correction.

To further investigate whether the relationship between right ILF microstructure and reward-related memory benefits is independent overall recollection memory, right ILF microstructure (FA) and overall recollection memory values were introduced as predictors of reward-related memory benefits in a hierarchical linear regression model via enter method. Overall memory was included into the null model (intercept model). For recollection, the model of right ILF microstructure and overall memory significantly explained the variance in the reward-related recollection benefit ($F(2,51) = 3.878$, $p = .027$). Right ILF microstructure explained 13.2% more variance than the null model containing the intercept and overall recollection ($R^2$ change = 0.132; right ILF: beta = 0.368; $t(54) = 2.785$, $p = .007$; overall memory: beta = 0.065; $t(54) = 0.493$, $p = .624$)

*Source accuracy.* There was a positive relationship between right ILF microstructure (FA) and the reward-related memory benefit for source accuracy which did not survive FWE- correction ($r(52) = 0.31$, $p_{1\text{-}tailed} = .011 > \alpha_{corrected} = .005$; MD: $r(52) = -0.11$, $p_{1\text{-}tailed} = .209$; Figure 3.9 A).

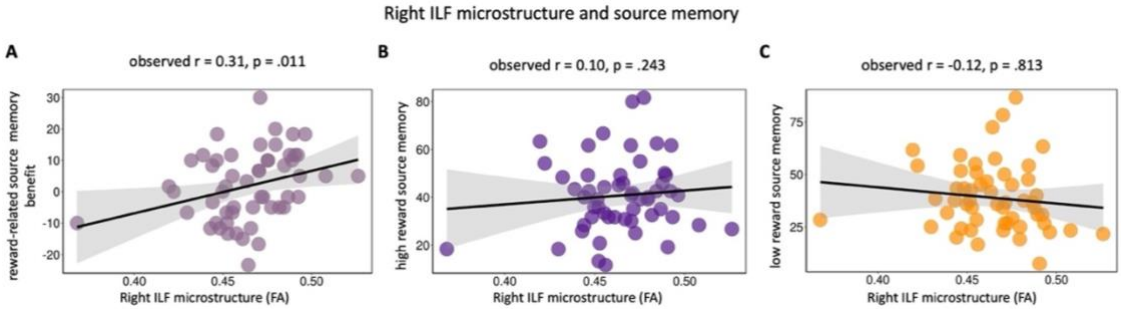


**Figure 3.9. Correlation of right inferior longitudinal fasciculus (ILF) fractional anisotropy (FA) and reward-related source memory benefit. A.** Significant (uncorrected) correlation of right ILF FA with the reward-related source accuracy benefit. **B.** Correlation of right ILF FA with high reward source accuracy **C.** Correlation of right ILF FA with low reward source accuracy. The follow-up analyses did not reach significance. The line of best fit and 95% confidence interval (CI) is shown on each scatterplot with 54 data points.

Follow-up analyses revealed a non-significant positive correlation between right ILF FA and high reward source accuracy and a non-significant negative correlation between right ILF FA and low reward source accuracy (high reward: $r(52) = 0.10$, $p_{1\text{-tailed}} = .243$; Figure 3.9 B; low reward: $r(52) = -0.12$, $p_{2\text{-tailed}} = .813$; Figure 3.9 C).

## 3.3 Discussion

Episodic memory, the ability to recall events of one's own past, requires the ability to specifically recall the spatiotemporal context of an event. For me to be able to distinguish a specific meeting with a friend whom I am meeting often at the same spot, I have to be able to recall fine-grained temporal information of that specific event. Therefore, independent of participants' difficulty in recalling temporal order in comparison to object memory within the laboratory context (e.g., Clewett & Davachi, 2017; DuBrow & Davachi, 2014; Heusser et al., 2016), temporal order memory is a defining characteristic of episodic memory (Eichenbaum, 2013; Dere et al., 2005; Manns et al., 2007; St. Jacques et al., 2008; Tulving, 2002). Furthermore, within a framework of adaptive memory, an event's probability of being remembered is related to its salience and motivational context (Cohen et al., 2017; Mason at al., 2017; Miendlarzewska et al., 2016; Shohamy & Adcock, 2010). Here, spherical deconvolution tractography was employed to investigate the relationship between interindividual variability in white matter pathways and variability in reward-modulated memory. Participants encoded sequences of objects in differently rewarding contexts (high versus low reward). Next,

their memory was tested in a two-phased memory test. Participants were tested on their temporal order memory, object, and source memory. Indicators of overall memory and reward-related memory benefits were correlated with indicators of fibre tract microstructure.

### 3.3.1 Fornix microstructure and reward-modulated memory

Here, no associations between fornix microstructure and reward-modulated memory were found. This was unexpected. One possible explanation lies in the immediate memory test employed in this study. Dopamine-driven hippocampus-dependent memory is often more pronounced after a delay (Murayama & Kitagami, 2014; Spaniol, Schain, & Bowen, 2014). Additionally, the main encoding task (semantic questions) as well as the additional encoding task (associating objects of a sequence with each other and their background) might have interfered with dopamine-driven memory processes. Even though fornix microstructure has been found to be related to associative memory (Metzler-Baddeley et al., 2011) and the temporal order and source memory tests employed here are believed to reflect associative memory processes, fornix microstructure was also not related to overall memory performance on either measure. A study that investigated the relationship between microstructure indices of fornix subdivisions and different memory measures in healthy aging participants also did not find a reliable relationship between fornix microstructure and memory test performance (Coad et al., 2020). Coad and colleagues were only able to demonstrate the microstructure of the postcommissural fornix to be related to associative memory test performance. However, they could not demonstrate clear dissociations in the relationship with memory between the two subdivisions. This led them to argue that fornix subdivisions might both contribute to a particular cognitive task but in a different manner. The present study also did not find a relationship between fornix microstructure and memory test performance. This was neither the case for the whole fornix nor for fornix subdivisions based on hippocampal gradient (see Appendix 2). As discussed above, variability in performance in the task at hand might not relate to variability in fornix microstructure due to the immediate memory test.

### 3.3.2 Uncinate microstructure and reward-modulated memory

Here, no associations between UF microstructure and reward-modulated memory were found. This was unexpected as relationships between UF microstructure and associative memory (Metzler-Baddeley et al., 2011) as well as memory for rewarding information (Reggente et al., 2018) have been reported. In the study by Reggente et al. (2018), participants' free recall for word lists was tested in study test cycles with feedback. It has been suggested that UF microstructure relates to memory especially under conditions of competing memory representations at retrieval (Alm et al., 2016). This might be due to the UF connecting temporal and frontal lobes (Browning & Gaffan, 2008; Catani et al., 2013). Frontal involvement in studies of temporal order memory has been demonstrated (Ezzyat & Davachi, 2014; Jenkins & Ranganath, 2010). Additionally, functional connectivity between PFC and MTL during encoding correlated with temporal order memory performance (DuBrow & Davachi, 2016). Despite these reports, variability in microstructure of the UF subserving frontal and temporal lobe was not be related to variability in memory performance here.

### 3.3.3 ILF microstructure and reward-related memory benefits

Participants made semantic judgements on the objects within the sequences based on their context (background scene) during encoding. This might have increased the reliance on semantic processing in this task. This would lend itself to finding a relationship between reward-modulated memory here and *left* ILF microstructure specifically because semantic processing via verbal information is described as left lateralised (Herbet et al., 2018; Ralph et al., 2017). But it has been suggested that the occipital-amygdala pathway is stronger within the right ILF and contributes to emotional (face) processing (Herbet et al., 2018). Furthermore, processing of visually complex stimuli has been reported to be more reliant on the right hemispheric semantic processing system (Ralph et al., 2017). Right hemispheric connections between amygdala and visual processing in the occipital lobe supported by the ILF might support reward-related benefits on memory in this study.

In line with these considerations, right ILF microstructure was found to be particularly associated with reward-related memory benefits for high confidence temporal order memory and recollection. In the follow-up analyses, although not significant, right ILF microstructure negatively correlated with low reward memory and positively with high reward memory. Participants with higher fractional anisotropy had more accurate high reward temporal order memory and less accurate low reward temporal order memory. The non-significant negative correlation between right ILF microstructure and low reward memory performance was found consistently across the memory measures. Cohen et al. (2014; 2017) describe that strategic ignoring and thereby disengaging of semantic processing of low value items more strongly correlated with optimal performance than the strategic remembering of high value items. Here, ILF microstructure, as part of a semantic processing system, correlated with reward-related memory benefits by enhancing communication between the semantic processing areas strategically disengaging during low reward stimuli, marking them as to be forgotten.

### 3.3.4 Limitations and future directions

Strong reward-related memory effects in other studies involve shorter encoding sequences (Gruber et al., 2016) or study-test cycles (Cohen et al., 2014; Cohen et al., 2017; Reggente et al., 2018). Studies concerned with temporal order memory also involve study-test cycles and do not include reward in human subjects (DuBrow & Davachi, 2014; Heusser et al., 2016; Heusser et al., 2018). In a future study, a balance will need to be struck between reliable temporal order representation and reward-modulated incidental memory. When temporal order memory is investigated in study-test cycles, memory is high and manipulations like event borders can influence temporal memory (Ezzyat & Davachi, 2014; Heusser et al., 2018); this might also include reward-related influences. A new study can investigate this by testing temporal order memory for high versus low reward sequences in study-test cycles. Then, object and source memory for objects not tested during temporal order memory tests can be tested separately and more removed from the temporal order memory test. The temporal order memory test possibly relies more on strategic semantic encoding, partly induced by the encoding task. Separating the memory test for temporal order from the memory test for objects and sources could potentially increase the influence of dopaminergic

hippocampus-dependent memory processes on recollection and source memory. Furthermore, repeated memory tests could lead to participants learning how to invest their strategic resources best. Thereby, memory performance might then be influenced more by dopamine-driven processes.

## 3.4 Chapter Summary

In this study, partially encouraged by the semantic task during encoding, reward-related memory enhancements are more reliant on semantic processing supported by the ILF as opposed to the involvement of the dopaminergic circuitry supported by the fornix. Interindividual variations in microstructure of the inferior longitudinal fasciculus but not the fornix or the UF were associated with interindividual differences in reward-related memory benefits. These findings build a basis to further investigate the dissociable involvement of semantic processing and incidental modulation of memory processing via dopamine expression and salience-based memory processes.

# Chapter 4: Resting-state functional connectivity within the semantic temporal lobe network underlying reward-related temporal order memory

Despite the fact that there is striking variability in reward-induced brain activity and reward-related memory modulation (e.g., Adcock et al., 2006; Berridge, 2007; Cohen et al., 2005; Cohen et al., 2014; 2016; Gruber et al., 2016), the interindividual variability in behaviour and brain activation is often treated as noise in neurocognitive studies. However, when individual differences in brain activation are treated as inherent features of individuals then meaningful variation between individuals can be utilised to describe function. Psychological and neurobiological factors like different strategies participants utilise, different states participants are in, and differing degrees in underlying brain structure and function can contribute to variability in behaviour (Seghir & Price, 2018; Tavor et al., 2016). With data from the Human Connectome Project, Tavor and colleagues (2016) were able to successfully predict task-based activity on a variety of tasks based on a single functional MRI resting-state scan. Regression models that were trained on functional connectivity during rest were able to predict interindividual differences in shape, size, and topography of task activation (Tavor et al., 2016). Here, a network-level approach is employed to investigate the relationship between interindividual differences in reward-related temporal order memory specifically and variability in resting-state functional connectivity. Previously, variability in reward-modulated memory formation has been related to variability in task-based functional activation as well as connectivity between brain areas during encoding or post-encoding rest measured in functional MRI designs (e.g., Adcock et al., 2006; Cohen et al., 2014; 2016; Gruber et al., 2016). Based on those reports and the results reported in Chapter 3, two networks will be investigated here: the hippocampal-VTA loop and the semantic temporal lobe network.

The VTA, NAcc, and hippocampus form a functional loop (Lisman & Grace, 2005). In an investigation of resting-state functional connectivity within a large sample, these three regions have been shown to be intrinsically connected at rest (Kahn & Shohamy,

2013). Additionally, interindividual variability in this intrinsic connectivity between VTA, NAcc, and hippocampus was found. This variability between subjects could not be explained by gender and only partly (statistical trend) by age (Kahn & Shohamy, 2013). Accordingly, between-subject variability in the intrinsic connectivity between VTA, NAcc, and hippocampus reflects meaningful variation that can be related to variability in behaviour. In a study of reward-motivated memorisation, increased connectivity between VTA and hippocampus after a high reward cue during encoding was predictive of memory formation (Adcock et al., 2006). Furthermore, changes of resting-state functional connectivity between VTA and hippocampus from pre- to post-encoding rest correlated with the reward-related memory benefit in a study of incidental memory (Gruber et al., 2016). The studies reviewed above illustrate that functional connectivity between VTA, NAcc, and hippocampus is intrinsic, can vary between individuals, and can be related to. Interindividual differences in memory performance. However, despite previous literature indicating that processing of temporal order relies on the hippocampus (e.g., DuBrow & Davachi, 2014; Eichenbaum, 2013; Jenkins & Ranganath, 2016; Tubridy & Davachi, 2011), it remains elusive how resting-state functional connectivity within this network relates to reward-modulated memory for temporal order.

Associative memory processes are not supported solely by the hippocampus. Within the temporal lobe, the anterior temporal lobes (ATL) are proposed to serve as “hubs” within a distributed network for semantic processing (Ralph et al., 2017; Patterson et al., 2007). During memory formation of salient information, associative processing combines object representations in the visual system with salience/reward representations from frontal and midbrain regions into a coherent representation. This can be supported by connectivity along the temporal lobe, from extrastriatal regions within the occipital cortex towards the anterior temporal lobe (Bajada et al., 2017; Ralph et al., 2017). Value-based recall is also sustained by the systematic engagement or disengagement of elaborative semantic processing (Cohen et al., 2014). The graded hub framework of the ATL proposes gradually different semantic representation along the temporal lobe (Ralph et al., 2017). This is based on a varying pattern of connectivity to the different representational modes. Within this framework, the anterior inferior

temporal gyrus (ITG) and anterior middle temporal gyrus (MTG) are understood as an amodal semantic hub because of converging connectivity from all modalities (Ralph et al., 2017). Additionally, semantic processing in the ventral ATL, encompassing ITG and MTG, has been shown to differ between individuals (Chen et al., 2016). Electrocorticograms (ECoG) of ventral and lateral ATL from pre-operative patients were acquired during a semantic task. Local-field potentials (LFP) of the ventral ATL correlated with modelled responses based on semantic feature representation. There was interindividual variability in the onset of when, after the presentation of the item in the semantic task, the semantic feature model and the LFPs of the ventral ATL significantly correlated with each other (Chen et al., 2016). Activation in the superior temporal gyrus (STG) has been found to be related to semantic as well as autobiographical temporal order memory (Rekkas et al., 2005). In another study, variability in activity in the MTG and the perirhinal cortex (PrC) within the ventromedial temporal lobe during encoding was correlated with variability in temporal order memory (Ezzyat & Davachi, 2011). Furthermore, the PrC supports associative memory processes along the ventral visual pathway and codes familiarity as well as recency (e.g., Miyashita, 2019; Xiang & Brown, 1998). In summary, although processing within the semantic temporal lobe network has been related to value-based memory modulation (Cohen et al., 2014; 2016; Cohen et al., 2019) and activation of regions within this network has been found to relate to temporal order memory (Ezzyat & Davachi, 2014; Miyashita, 2019; Rekkas et al., 2005), the literature concerning the effect of reward on temporal order memory and processing within the semantic temporal lobe network is lacking. Here, changes in resting-state functional connectivity of the anterior ITG, the PrC, and a region within the occipital cortex to other regions within the semantic temporal lobe network were investigated for their relationship to reward-related memory.

The studies reviewed above indicate a relationship between reward-based memory modulation and activation in, as well as functional connectivity between, regions within the mesolimbic pathway (NAcc, VTA) and the hippocampus (e.g., Adcock et al., 2006; Bunzeck et al., 2012; Gruber et al., 2016). Additionally, temporal order memory processing has been shown to rely on the hippocampus (e.g., DuBrow & Davachi, 2014; Jenkins & Ranganath, 2016). Based on these findings, I predicted an

association between interindividual differences in reward-related memory benefits and interindividual differences in functional connectivity within the hippocampal-VTA loop network at rest. Furthermore, activation within the semantic temporal lobe network has been shown to relate to temporal order memory and variability in value-modulated memory as well (Cohen et al., 2014; Cohen et al., 2019; Ezzyat & Davachi, 2014; Rekkas et al., 2005). Based on these findings, I predicted that interindividual differences in the reward-related temporal order memory benefit specifically are related to interindividual differences in resting-state functional connectivity within the semantic temporal lobe network.

As discussed in the previous chapter, the fornix constitutes a major pathway between the hippocampus, the ventral striatum encompassing the NAcc, and the frontal cortex (Aggleton, 2012; Aggleton et al., 2015). Investigations within the animal model demonstrated that deep brain stimulation (DBS) of the fornix resulted in increased activity (in BOLD, in glucose metabolism) within the hippocampus, VTA, and NAcc (Ross et al., 2016; Shin et al., 2019). Furthermore, a long and latent increase in dopamine efflux within NAcc was measured after fornix stimulation via DBS (Ross et al., 2016). The specific mechanism by which this efflux resulted from fornix stimulation was not determined in the study by Ross and colleagues (2016) but neurotransmitter release in the hippocampal-VTA-loop could account for this finding. As described in Chapter 1, the excitatory (glutamatergic) connections from the hippocampus to NAcc are carried via the fornix (Lisman & Grace, 2005). The resulting inhibitory GABAergic input from the NAcc to the ventral pallidum in turn releases the VTA from GABAerbic inhibition via the ventral pallidum. The release from inhibition leads to dopamine release within the VTA and the VTA then projects dopamine back to the NAcc and the hippocampus thereby promoting LTP and learning (Lisman & Grace, 2005; see Figure 1.1; green line representing glutamatergic hippocampus-NAcc pathway is carried via the fornix). Additionally, the semantic processing network along the length of the temporal lobe from extrastriatal regions within the occipital cortex towards the anterior temporal lobe discussed above has been demonstrated to be innervated by the ILF (Bajada et al., 2017; Catani, Jones, Donato, & Ffytche, 2003; Ralph et al., 2017). Functionality within the hippocampal-VTA-loop has been shown to support reward-related memory formation

(Adcock et al., 2006; Gruber et al., 2016). The fornix is part of this pathway (Lisman & Grace, 2005; Ross et al., 2016; Shin et al., 2019). Modulation of recall memory through reward has been related to elaborative processing supported by the semantic network (Cohen et al., 2014; 2017). Connectivity along the temporal lobe between regions involved in semantic processing is provided by the ILF and its microstructure has been found to relate to memory (Bajada et al., 2017; Catani et al., 2003; Hodgetts et al., 2017). Therefore, indices of fornix and ILF microstructure based on DWI were included in this analysis to investigate the relationship between variability in structural and variability in functional connectivity subserving memory.

# 4.1 Methods

## 4.1.1 Participants

Collection of resting-state fMRI data was conducted in the same participant pool as described in 3.1.2 (N = 55). The Ethical Review Board at the School of Psychology at Cardiff University approved the study procedures. For the resting-state fMRI analyses described here, six participants were excluded. One participant was excluded due to not answering over 50% of encoding trials, five participants could not be included due to the low quality of the resting-state fMRI data. Details about quality assurance variables and exclusion criteria are described under "4.1.4.2 Resting-state functional MRI pre-processing". Data analyses are based on 49 participants (6 males, mean age = 19.25, SE = 0.26).

## 4.1.2 Behavioural procedures

The study procedure was described under 3.1.3 in Chapter 3 and adapted from Gruber at al. (2016). The experiment was conducted in three phases, a reward-motivated encoding (Figure 4.1 A), a distractor, and a memory test phase (Figure 4.1 B through D).

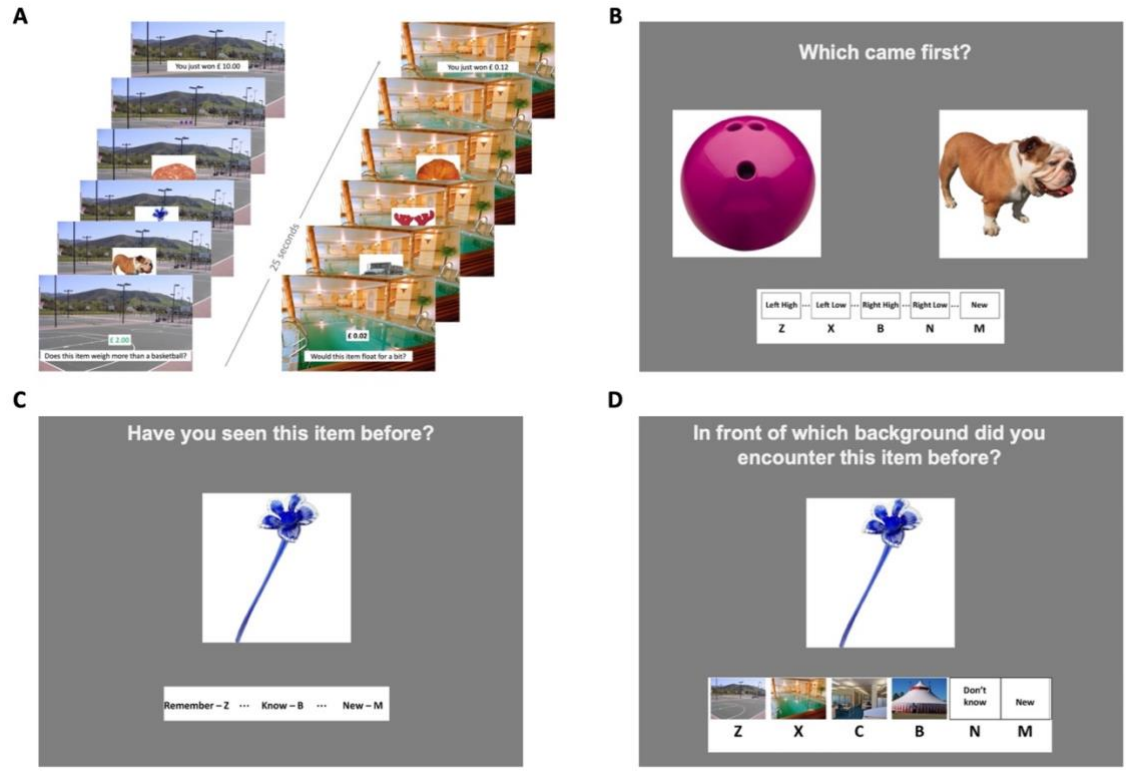


**Figure 4.1. Three-stages of study. A.** Encoding. Participants made yes/no- judgements on questions that semantically matched the background scene. They received high (£2.00) or low (£0.02) reward for correct responses. The semantic questions were: "Does this item weigh more than a basketball?" (scene of a basketball court); "Would this item float for a bit?" (scene of an indoor swimming pool); "Is this item bigger than a laptop screen?" (scene of an office); "Is it possible to juggle three exemplars of this particular item?" (scene of a circus tent). **B.** Temporal order memory test. Old-old or old-new object pairs were presented. Participants indicated their confidence in their choice of which object came first. **C.** Object memory test. Participants made a classic remember-know-new judgement on objects not used during B. **D.** Source memory test. Participants chose the matching background scene for the same objects as in C.

During encoding, participants made yes/no- judgements on 320 objects presented in 40 sequences. Sequences were denoted by changing background scenes that semantically matched the questions. Four semantic questions were posited during the experiment. Depending on the reward-condition, participants received high (£2.00) or low (£0.02) reward for correctly answering these semantic questions within two seconds. Participants' main task was answering the semantic questions, but they were additionally instructed to relate the objects within a sequence to each other and their background. They were informed of the memory test but not the type of memory test.

Encoding was followed by a 10-minute paper pen arithmetic distractor task before the memory test. Based on the results reported in Chapter 2, a distractor as opposed to rest was employed in this immediate memory test to maximise reward-related memory

benefits for temporal order specifically. The memory test comprised three questions aimed at the investigation of temporal order memory, object memory, and source memory. Temporal order memory was tested on 120 object pairs (80 old-old pairs; 40 high reward pairs, 40 low reward pairs). Additionally, 40 object pairs encompassed one old and one new object (old-new pairs; 20 high reward pairs, 20 low reward pairs). If participants remembered both objects as old, they were to indicate which object they believed to have encountered first during encoding and judge their confidence in this. The 120 (60 high reward, 60 low reward) remaining objects from encoding and 40 new objects were used for the object and source memory test. A classic remember-know-new-judgement (e.g., Yonelinas, 2002) was employed to investigate participants' recollection and familiarity memory for the object. Then, the associated background scenes were presented, and participants picked the scene they thought served as background for the object during encoding.

## 4.1.3 Stimuli

Randomization- and grouping-processes for the encoding were adapted from Gruber et al. (2016) and are described under 3.1.4 in Chapter 3. Images were sourced from a publicly available database (Brady et al., 2008). Positions of objects within the encoding sequences chosen as object pairs for the temporal order memory test were based on previous experiments (see Chapter 2) and previous research (e.g., DuBrow & Davachi, 2014).

## 4.1.4 Imaging

### 4.1.4.1 Imaging- acquisition

Imaging was conducted at CUBRIC, Cardiff University, on a 3 Tesla MRI scanner (Siemens Megnetom Prisma) with a 32-channel head coil. High-resolution anatomical images were obtained with a T1- weighted 3D MPRAGE sequence (TR = 2500ms, TE = 3.06ms, flip angle = 9°, FoV = 256mm$^2$, voxel-size = 1.0 x 1.0 x 1.0 mm, slice thickness = 1mm, 224 sagittal slices, bandwidth = 230 Hz/pixel; total acquisition time = 7 minutes and 36 seconds). An echoplanar imaging (EPI) sequence was used to acquire the resting-state functional MRI images. Fifty transversal slices were taken along the A-P axis (TR =

3000ms, TE = 30ms, flip angle = 89°, FoV = 192mm$^2$, voxel-size = 2mm$^3$, slice thickness = 2mm, bandwidth = 2170Hz/pixel; total acquisition time = 10 minutes and 11 seconds). During resting-state image acquisition, a black fixation cross centred on a grey background was presented to participants. Participants were instructed to keep their eyes open, fixate on the cross, and clear their mind to the best of their ability. They were told not to linger on things that came to their mind during the resting-state scan. This introduction was given to ensure that functional connectivity measures based on this resting-state scan reflect variability in intrinsic, rather than task-based, connectivity (Biswal et al., 1997).

#### 4.1.4.2 Resting-state functional MRI pre-processing

Pre-processing and connectivity analyses were conducted in the CONN toolbox (Whitfield-Gabrieli & Nieto-Castanon, 2012; version 18.b), which employs SPM12 (Statistical Parametric Mapping; Wellcome Trust Centre for Neuroimaging, London) functions using Matlab (The MathWorks Inc; version r2015a). During pre-processing, CONN employs SPM12's "realign and unwarp" function (Andersson, Hutton, Ashburner, Turner, & Friston, 2001). All functional scans were realigned and resampled to a reference image, the first scan of the acquisition. Furthermore, Andersson et al.'s (2001) method also takes inhomogeneities and distortions introduced by movement into account to unwarp the images. Then, each subject's functional run was centred at [0,0,0] and slice-time corrected following Henson and colleagues (Henson, Buechel, Josephs, & Friston, 1999). Slice-time correction adjusts for differences in acquisition times in the inter-leaved scans ("interleaved Siemens") by time-shifting and resampling to the middle of each TA through sinc-interpolation. CONN uses ART (Artifact Detection Tool)-based identification of outlier scans (www.nitrc.org/projects/artifact_detect/). Here, acquisitions with a frame-wise displacement >0.5mm and a global BOLD signal change >3SD of the subject-specific means were flagged as potential outliers. Then, structural and functional images were normalised to standard MNI space. Simultaneously, the images were segmented into CSF, grey matter, and white matter as well as normalised. Functional direct segmentation and normalisation was conducted via SPM12 following Ashburner and Friston (2005). Based on the intensity values of the reference image, non-linear spatial transformations of the posterior tissue probability maps (TPM) are

iteratively estimated for tissue classification until they best approximate the posterior and prior TPMs. The mean BOLD-image serves as the reference for the functional data segmentation and normalisation, whereas the reference-image for the structural data is the raw T1-weighted volume. For both, estimation is based on a 180x216x180mm bounding box with 2mm isotropic voxels for the functional images and 1mm voxels for the structural images. After segmentation and normalisation to MNI space, functional images were spatially smoothed with a 6mm full-width-half-maximum (FWHM) Gaussian kernel.

These pre-processing steps were followed by denoising steps to remove unwanted effects of movement, as well as physiological and other artefacts before computing functional connectivity. CONN employs an anatomical component-based noise correction procedure (aCompCor; Behzadi, Restom, Liau, & Liu, 2007) using five potential noise components above a threshold in the BOLD signal (Chai, Castañón, Öngür, & Whitfield-Gabrieli, 2012) from cerebral white matter and CSF masks to identify and remove confounds to the BOLD signal introduced by white matter and CSF. 12 potential noise components (3 translation, 3 rotation parameters, and their respective first-order derivatives) originated from the estimated subject-motion parameters (Friston, Williams, Howard, Frackowiak, & Turner, 1996) and were used to reduce variability in the BOLD signal due to motion. Outlier scans identified by ART were included as confounds and scrubbed during denoising. A linear detrending term was introduced to remove slow trends in the signal and initial magnetisation transients from the BOLD response. White matter and CSF confounds, the 12 noise components due to motion, ART-identified outliers, and the detrending term were removed from the BOLD signal within each voxel for each subject during the one resting-state functional run with an Ordinary Least Squares (OLS) linear regression retaining the BOLD timeseries orthogonal to the confounds (first level nuisance variables). The resulting signal was temporally band-pass filtered between 0.008Hz and 0.09Hz to minimise the influence of noise.

Five quality assurance variables were used to identify participants to be excluded from further analyses: number of invalid scans identified by ART, maximum and mean

motion, and maximum and mean global signal change. Participants whose resting-state data were 1.5 above or below the 3rd quartile on three or more quality assurance variables or whose number of invalid scans was above 20% of the total number of scans were excluded from the functional connectivity analyses (e.g., Power et al., 2014). This exclusion affected five participants.

## 4.1.5 Behavioural and microstructure analyses

Behavioural and DTI analyses were the same as described under 3.1.6 and 3.1.7 in Chapter 3 and were merely repeated in the smaller sample (N = 49 here vs. N = 54 in Chapter 3) to ensure that the removal of 5 participants due to quality of the resting-state fMRI data did not change the reported results. Neither the behavioural results nor the correlations between behaviour and microstructure were different or differed in a way that would change interpretation from the results reported in Chapter 3 (see Appendix 4).

## 4.1.6 Functional resting-state analyses

### 4.1.6.1 Regions of interest

Regions of interests (ROIs) that were not available from the Harvard-Oxford cortical atlas (Grabner et al., 2006) implemented in CONN were added to the analysis. This included probabilistic masks of the left and right VTA (Murty et al., 2014), anatomical masks of the left and right perirhinal cortex (Gruber et al., 2016), and a 2mm isotropic sphere within the left and right occipital cortex.

#### *4.1.6.1.1 Regions of interest within the hippocampal-VTA loop*

The hippocampus forms a functional loop with the NAcc and the VTA, which directly innervates the hippocampus, to support memory formation through novelty and salience (Lisman & Grace, 2005). There was no strong hypothesis regarding lateralisation of the investigated effects and both left and right ROIs were included in the ROI-to-ROI connectivity model. The following ROIs were investigated (Figure 4.2): left and right hippocampus (Harvard-Oxford; Figure 4.2 A and B), left and right NAcc (Harvard-Oxford; Figure 4.2 C), as well as left and right VTA (Murty et al., 2014; Figure 4.2 D).

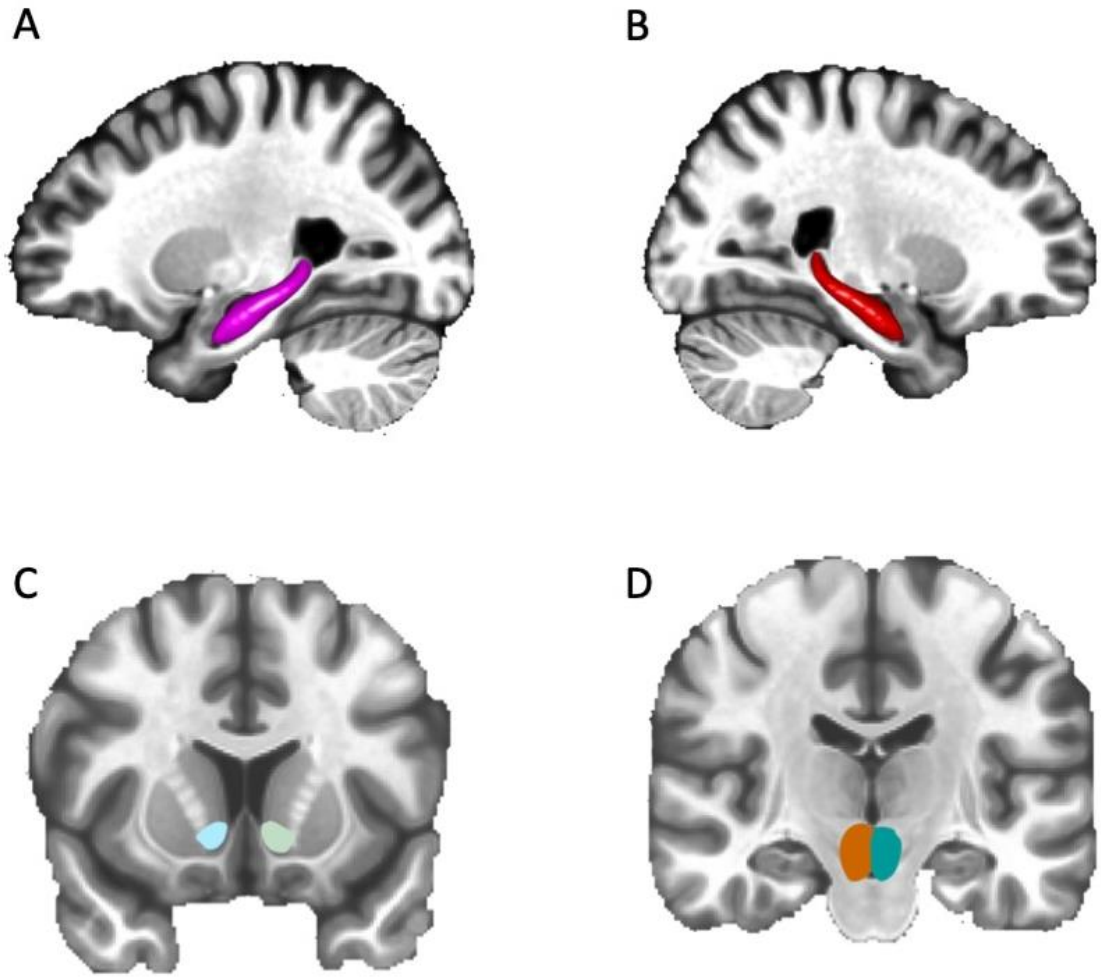


**Figure 4.2. Regions of interest of the hippocampal-VTA loop included in resting-state functional connectivity (RSFC) analysis.** ROIs are displayed on a standard 2mm MNI brain mask (MNI ICBM152 non-linear; Grabner et al., 2006). **A.** Left hippocampus (pink): x = -26, y = -18, z = -16. **B.** Right hippocampus (red): x = 24, y = -14, z = -16. **C.** Left (light blue) and right (sage) nucleus accumbens (NAcc): x = -8, y = 12, z = -6. **D.** Left (mustard) and right (teal) ventral tegmental area (VTA): x = -2, y = -18, z = -16.

The probabilistic VTA maps from Murty et al. (2014) were co-registered to a T1 2mm MNI standard brain mask employing FSL's FLIRT and then binarized.

*4.1.6.1.2 Regions of interest within the semantic temporal lobe network*

Regions of interest that were included in the model were based on Bajada et al. (2017). They employed a 2mm isotropic seed region within the occipital cortex ("OCC-seed") to reconstruct fibres originating from this seed within fibre termination maps of the temporal lobe. The resulting OCC fibre complex comprised fibres terminating along the whole surface of the temporal lobe and was described to include fibres from the ILF as well as the IFOF (inferior fronto-occipital fascisulus). They then divided the occipital termination map into three sub-sections containing two anatomical regions each and

described these as terminations of the ILF (Bajada et al., 2017). Most of the anatomical regions along the occipital termination map described by Bajada et al. (2017) were available in CONN (Harvard-Oxford).

Bajada et al. (2017) placed the "OCC-seed" at the apex of the posterior horn of the lateral ventricle within the left and right occipital lobe. Here, this ROI was reconstructed by creating a 2mm isotropic sphere around the MNI coordinates for the centroid of the OCC-seed as reported by Bajada et al. (2017). The PrC region was added since associations between the BOLD-response of the PrC and ILF microstructure have been reported previously (Hodgetts et al., 2015). The PrC has also been reported to support temporal order memory (Ezzyat & Davachi, 2011). The PrC region of interest was hand-drawn based on anatomical landmarks along the group-averaged brain (using DARTEL) from the Gruber et al. (2016) dataset. Before being added to the CONN analyses, the left and right PrC ROIs were co-registered to the same T1 2mm MNI template employed by CONN (via FLIRT) and binarised.

The regions of interest were based on the anatomical ROIs within the OCC fibre complex as described by Bajada et al. (2017) and included the OCC-seed as well as the PrC (Figure 4.3). The regions of interest in the semantic temporal lobe network investigated here were the anterior ITG (Figure 4.3 A, blue), the posterior ITG (Figure 4.3 A, cyan), the anterior MTG (Figure 4.3 B, teal), the anterior STG (Figure 4.3 B, lilac), the anterior temporal fusiform cortex (TFC; Figure 4.3 C, purple), and the posterior TFC (Figure 4.3 C, red) via CONN (Harvard-Oxford), the reconstructed OCC-seed region (Figure 4.3 C, orange) as well as the PrC (Figure 4.3 D, green).

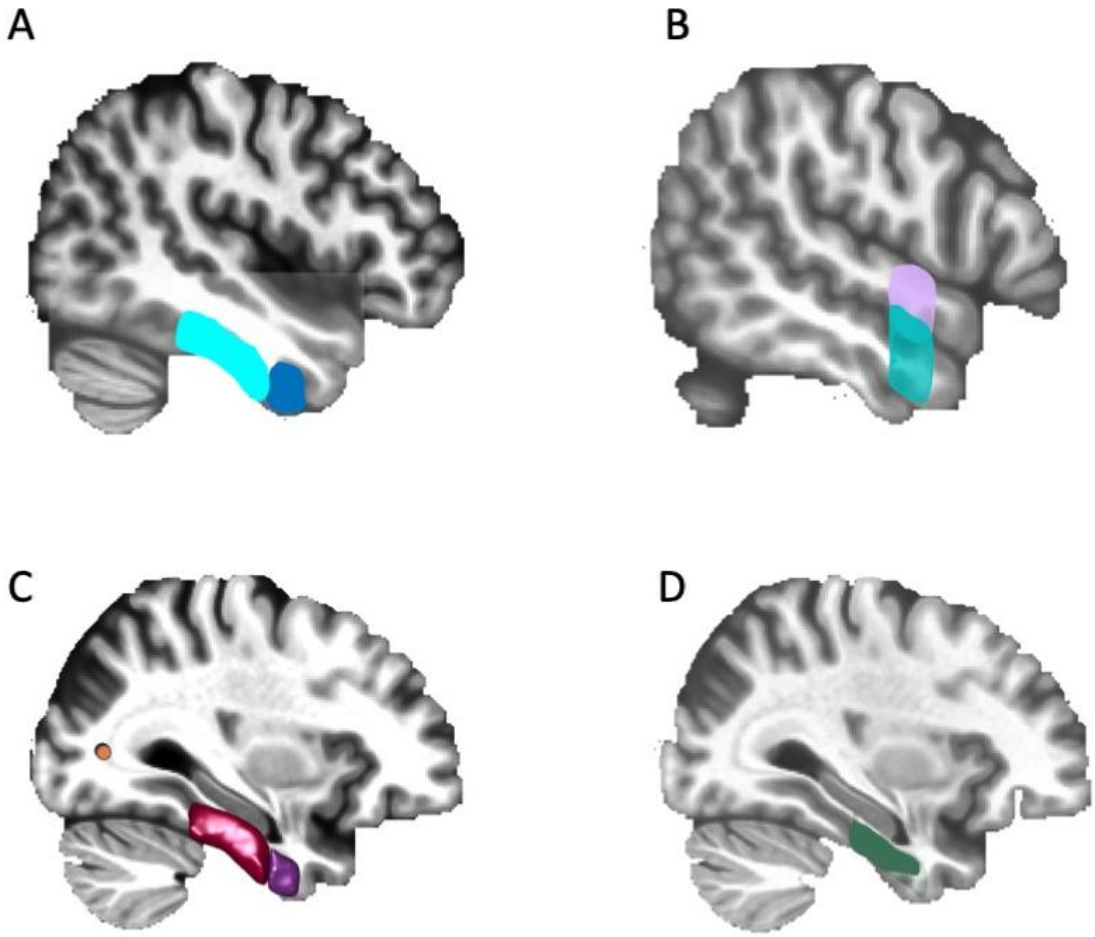


**Figure 4.3. Regions of interest within the semantic temporal lobe network included in the RSFC analysis.** Exemplary for the right hemisphere. ROIs are displayed on a standard 2mm MNI brain (MNI ICBM152 non-linear; Grabner et al., 2006). **A.** Right anterior ITG (blue) and right posterior ITG (cyan): x = 54, y = 0, z = -38. **B.** Right anterior STG (lilac) and right anterior MTG (teal): x = 52, y = -4, z = -38. **C.** Right OCC-seed (orange), right posterior TFC (red) and right anterior TFC (purple): x = 32, y = -72, z = 6. **D.** Right PrC (green): x = 46, y = -4, z = -38.

Based on the hemispheric differences in the relationship of right versus left ILF with behaviour reported under 3.2.4 in Chapter 3, models including the eight ROIs were calculated for the right and left hemispheres separately. Furthermore, the ATL hub is described as primarily bilateral but with graded hemispheric differences based on differing white matter connectivity to the input and output systems. Whereas the left hemisphere shows stronger effects for speech, the right hemispheric ATL supports fine-grained visual features like face recognition (Ralph et al., 2017).

#### 4.1.6.2 ROI-to-ROI connectivity

Separate models were analysed for the six ROIs of the hippocampal-VTA loop (three left hemispheric, three right hemispheric), the eight ROIs of the semantic temporal lobe network within the right, and within the left hemisphere in CONN. Fischer-transformed bivariate Pearson correlation coefficients between the averaged BOLD timeseries across the voxels within each ROI and the averaged BOLD timeseries across the voxels within the other ROIs of the model were calculated. A weighted least squares linear model with a boxcar timeseries for the rest-condition convolved with a canonical hemodynamic response function was employed to calculate the bivariate correlation coefficients (Nieto-Castanon, 2020).

#### 4.1.6.3 Independent measures of interest

Accuracy measures for temporal order and source memory accuracy as well as recollection were calculated and z-standardised (see formula 3.2 in Chapter 3). Furthermore, based on the correlations between right ILF microstructure and behaviour reported under 3.2.4.2 in Chapter 3, interaction-terms were calculated between right ILF FA and the reward-related memory benefit (high – low reward) for high confidence temporal order accuracy, between right ILF FA and reward-related recollection memory benefit, as well as between right ILF FA and the reward-related source memory benefit. Interaction-terms were calculated by multiplying the z-standardised ILF FA with each z-standardised behavioural measure for each participant. Z-standardised fornix, right, and left ILF microstructure indices (FA, MD), as well as the reward-related memory benefit (high – low reward), overall memory (average of high and low reward) of high confidence temporal order accuracy, recollection, and source accuracy values as well as the interaction terms were introduced into CONN. Overall memory measures were merely included to follow-up on effects of reward-related memory benefits on resting-state ROI-to-ROI connectivity by correcting the linear regression model by overall memory effects. Microstructure indices of fornix and ILF were included to explore the relationship between variability in fornix/ILF microstructure and variability in resting-state functional connectivity within the hippocampal-VTA loop/semantic temporal lobe network.

Consequently, five GLMs were investigated within the hippocampal-VTA loop (2 microstructure measures [FA and MD of the fornix], and 3 behavioural measures [(1) reward-related memory benefit for high confidence temporal order memory, (2) reward-related recollection memory benefit, (3) reward-related source memory benefit]), eight GLMs were investigated in the right semantic temporal lobe network (2 microstructure measures [FA and MD of the right ILF], 3 behavioural measures [(1) reward-related memory benefit for high confidence temporal order memory, (2) reward-related recollection memory benefit, (3) reward-related source memory benefit], and 3 interaction terms between microstructure and behaviour [(1) right ILF FA x reward-related high confidence temporal order memory benefit, (2) right ILF FA x reward-related recollection memory benefit, (3) right ILF FA x reward-related source memory benefit]), and five GLMs were investigated in the left semantic temporal lobe network (2 microstructure measures [FA and MD of the left ILF], and 3 behavioural measures [(1) reward-related memory benefit for high confidence temporal order memory, (2) reward-related recollection memory benefit, (3) reward-related source memory benefit]).

#### 4.1.6.4 Functional connectivity analysis

In CONN, separate GLMs, employing an ordinary least squares (OLS) solution, were used to define linear associations between an independent measure of interest (i.e., behaviour or microstructure) and functional connectivity between the ROIs of interest (six [three left, three right] hippocampal-VTA loop ROIs, eight right, or eight left semantic temporal lobe network ROIs) as dependent measures. For example, to investigate whether variability between subjects in the reward-related recollection memory benefit was related to changes in functional connectivity between the ROIs of the hippocampal-VTA loop at rest, an OLS GLM is employed to express a linear regression of ROI-to-ROI connectivity (measured by a bivariate correlation) onto the reward-related recollection memory benefit as between-subjects effect.

For the regions of interest within the hippocampal-VTA loop, the NAcc and hippocampus (HC) were selected as seeds to investigate their connectivity to all the other ROIs within the network. (VTA in both hemispheres, NAcc and HC in the other

hemisphere, e.g., left NAcc and left HC = seed, then their connectivity to right NAcc and right HC included in the model). The significant interactions between connectivity within the hippocampal-VTA loop and reward-related memory were reported mostly between VTA and hippocampus (e.g., Adcock et al., 2006; Gruber et al., 2016). If they are to be found in the study at hand, they will be captured by employing only one of those ROIs as seed in the functional connectivity analysis. Here, the hippocampus was chosen. Brain activation during reward-anticipation has been found not only in the VTA but also the NAcc (Adcock et al., 2006). The NAcc is chosen as a seed region in this analysis to investigate the relationship between differences in the intrinsic resting-state functional connectivity within the hippocampal-VTA loop and reward-related memory. NAcc and hippocampus seed ROIs were investigated in separate GLMs for each hemisphere (left/right NAcc and left/right hippocampus together) while target ROIs included both hemispheres. Connection-level corrections of individual ROI-to-ROI connections (t-statistic) were FDR-corrected in three different ways. Firstly, analysis-level FDR-correction corrected across all 15 possible connections (across the entire connectivity matrix). Secondly, seed-level correction was applied across all connections of a certain seed (e.g., five connections of the right NAcc seed to the other ROIs within the network). Connection-level statistics could also be uncorrected. Uncorrected and seed-level FDR-correction on the connection level were combined with an appropriate seed-level correction (F-statistic) for selecting more than one seed-ROI. FDR-corrections were calculated following Benjamini and Hochberg (1995).

Based on the results reported in 3.2.4, separate models within the left and right hemisphere were calculated for the regions of interest in the semantic temporal lobe network. In each hemisphere, the anterior ITG, the OCC-seed, and the PrC were investigated as seeds for their connectivity with the other ROIs within the model. The anterior ITG was chosen due to its position as a semantic hub (Ralph et al., 2017) on one endpoint of the temporal termination map, whereas the OCC-seed region served as the other endpoint of the temporal termination map (Bajada et al., 2017). The PrC was investigated as a seed due to its reported relationship with ILF microstructure (Hodgetts et al., 2015) and temporal order memory (Ezzyat & Davachi, 2011). Connection-level corrections of individual ROI-to-ROI connections (t-statistic) were FDR-corrected at the

analysis-level across all 28 possible connections (across the entire connectivity matrix). Seed-level correction was applied across all connections of a certain seed (e.g., seven connections of the right ITG seed to the other ROIs within the network). Connection-level statistics could also be uncorrected. Uncorrected and seed-level FDR-correction on the connection level were combined with an appropriate seed-level correction (F-statistic) for selecting more than one seed-ROI. FDR-corrections were calculated following Benjamini and Hochberg (1995).

No directed hypotheses were made about whether variability in behaviour or microstructure would be explained by an increase or decrease in functional connectivity at rest. Consequently, all tests were two-tailed. Only follow-up tests were directed based on the effect to be followed up on.

# 4.2 Results

## 4.2.1 Resting-state functional connectivity within the hippocampal-VTA loop

### 4.2.1.1 Reward-related memory benefit

*High confidence temporal order memory.* The reward-related temporal order memory benefit at high confidence was not related to any changes in resting-state functional connectivity within the hippocampal-VTA loop (all $F \leq 0.93$, all p-FDR $\geq .502$).

*Recollection.* Between-subject variability of the reward-related recollection memory benefit was associated with significant variability in resting-state functional connectivity of the right NAcc ($F(6,43) = 2.89$, $p = .024$, *p-FDR* = .049; Figure 4.4 A), which includes uncorrected decreased connectivity to right VTA ($t(47) = -2.24$, $p = .030$, *p-FDR-seed* = .075; Figure 4.4 B) and uncorrected increased connectivity to left NAcc ($t(47) = 2.28$, $p = .027$, *p-FDR-seed* = .075; Figure 4.4 C).

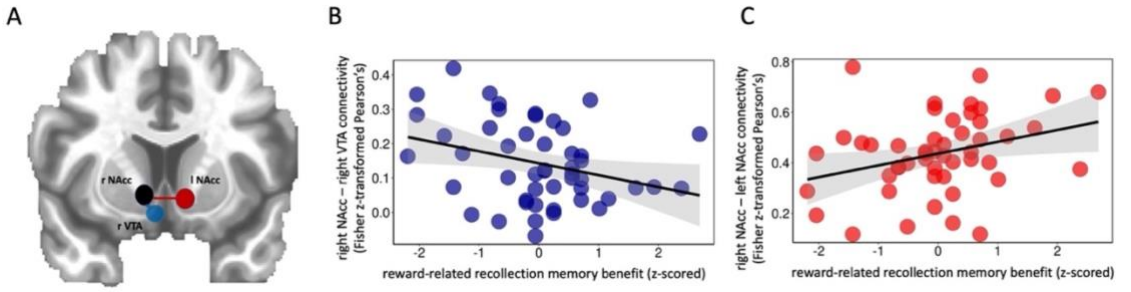


**Figure 4.4. Connectivity of right NAcc at rest and reward-related recollection memory benefit. A.** RSFC between right NAcc and right VTA as well as between right NAcc and left NAcc in relation to the reward-related recollection memory benefit. ROIs are displayed on reference slice at [9.37/10.20/-6.53]. Dots denote ROIs. Lines denote connectivity. Colours denote direction of connectivity. Blue = decrease in RSFC, red = increase in RSFC. Black = seed ROI. **B.** Scatterplot of ROI-to-ROI connectivity between right NAcc and right VTA onto the reward-related recollection memory benefit. Decreased connectivity related to higher reward-related recollection memory benefit. **C.** Scatterplot of ROI-to-ROI connectivity between right NAcc and left NAcc onto the reward-related recollection memory benefit. Increased connectivity related to higher reward-related recollection memory benefit. ROI-to-ROI connectivity measured by Pearson's correlation and Fisher z-transformed. Reward-related recollection memory benefit was z-scored. The line of best fit and 95% confidence interval is shown on each scatterplot with 49 data points.

To follow these results up, ROI-to-ROI connectivity within the hippocampal-VTA loop was regressed onto the reward-related recollection memory benefit while overall recollection was held constant. In the follow-up, changes in resting-state functional connectivity were investigated for a decrease between right NAcc and right VTA and an increase between right NAcc and left NAcc based on the results in the relationship between resting-state functional connectivity and the reward-related recollection memory benefit. When corrected for overall recollection, functional connectivity of the right NAcc displayed merely a trend towards a significant relationship with the reward-related recollection memory benefit ($F(6,42) = 2.84$, $p = .027$, $p\text{-}FDR = .053$). Uncorrected, between-subject variability in increased RSFC between right NAcc and left NAcc was related to between-subject variability in the reward-related recollection memory benefit ($t(47) = 2.25$, $p_{1\text{-}tailed} = .015$, $p\text{-}FDR\text{-}seed_{1\text{-}tailed} = .074$). Uncorrected, decreased functional connectivity between right NAcc and right VTA at rest was related to between-subject variability in reward-related recollection memory benefit when overall recollection was held constant ($t(47) = -2.21$, $p_{1\text{-}tailed} = .016$, $p\text{-}FDR\text{-}seed_{1\text{-}tailed} = .061$). The relationship between reward-related memory benefit and *decreased* functional connectivity between NAcc and VTA at rest was surprising based on the literature (e.g., Adcock et al., 2006; Reggente et al., 2018). The relationship of interindividual differences in RSFC between NAcc and VTA with high reward recollection

as well as low reward recollection was explored to follow up on this surprising effect. Only right NAcc and right VTA were included in the model. Neither variability in high reward recollection ($t$(47) = -1.48, $p$ = .146) nor variability in low reward recollection ($t$(47) = -0.44, $p$ = .659) significantly related to variability in functional connectivity between right NAcc and right VTA at rest.

*Source accuracy.* Decreased connectivity between right NAcc and right VTA at rest was also found to be related to interindividual differences in reward-related source memory benefit ($t$(47) = -3.97, $p$ < .001, *p-FDR-analys*is = .002; Figure 4.5 B).

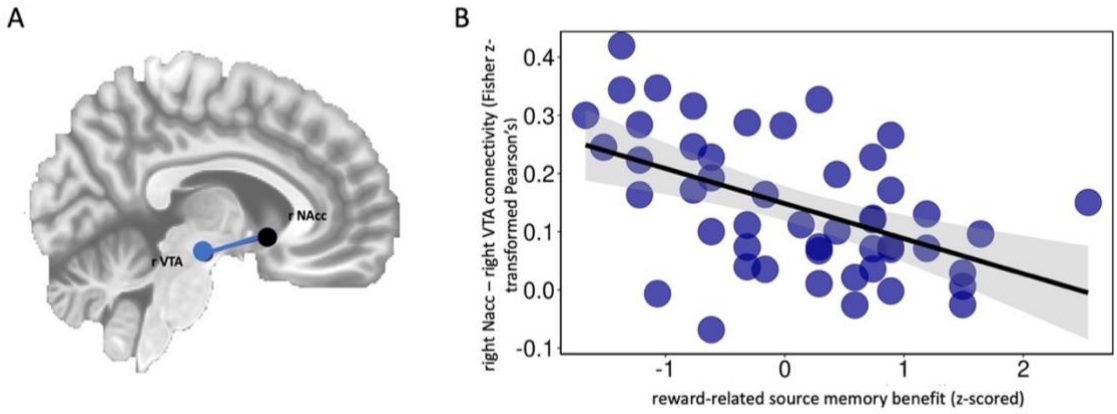


**Figure 4.5. Reward-related source memory benefit and resting-state functional connectivity within the hippocampal-VTA loop. A.** RSFC between right NAcc and right VTA in relation to the reward-related source memory benefit. ROIs are displayed on reference slice at [6.37/12.20/-6.53]. Dots denote ROIs. Lines denote connectivity. Colours denote direction of connectivity. Blue = decrease in RSFC. Black = seed ROI. **B.** Scatterplot of ROI-to-ROI connectivity between right NAcc and right VTA onto reward-related source memory benefit. Decreased connectivity of right NAcc with right VTA related to increase in reward-related source memory benefit. ROI-to-ROI connectivity measured by Pearson's correlation and Fisher z-transformed. Reward-related source memory benefit was z-scored. The line of best fit and 95% confidence interval is shown on each scatterplot with 49 data points.

In the follow-up, this significant decrease in resting-state connectivity between right NAcc and right VTA remains when the reward-related source memory benefit is corrected for overall source memory ($t$(46) = -3.96, $p_{1\text{-}tailed}$ = .0001, *p-FDR-analysis*$_{1\text{-}tailed}$ = .0013). The relationship between reward-related memory benefit and *decreased* functional connectivity between NAcc and VTA at rest was surprising based on the literature (e.g., Adcock et al., 2006; Reggente et al., 2018). The relationship of interindividual differences in RSFC between NAcc and VTA with high reward source accuracy as well as low reward source accuracy was explored to follow up on this surprising effect. Only right NAcc and right VTA were included in the model. Neither

variability in high reward source accuracy ($t(47) = -1.16$, $p = .251$) nor variability in low reward source accuracy ($t(47) = 1.49$, $p = .144$) significantly related to variability in functional connectivity between right NAcc and right VTA at rest.

#### 4.2.1.2 Fornix microstructure

Fornix microstructure measured by FA was not significantly related to variability in resting state functional connectivity within the hippocampal-VTA loop (all $F \leq 1.65$, all p-FDR $\geq .335$). Changes in functional connectivity within the hippocampal-VTA loop at rest were not related to between-subject variability of fornix microstructure measured by MD (all $F \leq 2.20$, all p-FDR $\geq .143$).

### 4.2.2 Resting-state functional connectivity within the semantic temporal lobe network

#### 4.2.2.1 Left hemisphere and reward-related memory benefits

*High confidence temporal order memory.* Interindividual differences in the reward-related temporal order memory benefit at high confidence were not related to changes in resting-state functional connectivity of the investigated regions with other regions within the semantic temporal lobe network in the left hemisphere (all $F \leq 1.66$, all p-FDR $\geq .314$).

*Recollection.* Changes in functional connectivity within the left hemispheric semantic temporal lobe network were not significantly related to interindividual differences in the reward-related recollection memory benefit (all $F \leq 2.00$, all p-FDR $\geq .237$).

*Source accuracy.* Between-subject variability in the reward-related source memory benefit was not related to changes in functional connectivity within the left hemispheric semantic temporal lobe network (all $F \leq 1.15$, all p-FDR $\geq .869$).

#### 4.2.2.2 Left ILF microstructure

Interindividual differences in left ILF microstructure measured by FA were not significantly related to changes in resting-state functional connectivity of the regions

within the semantic temporal lobe network of the left hemisphere (all F ≤ 0.92, all p-FDR ≥ .556). Variability in functional connectivity within the left hemispheric semantic temporal network was not significantly related to between-subject variability of left ILF microstructure measured by MD (all F ≤ 2.14, all p ≥ .181).

### 4.2.2.3 Right hemisphere and reward-related memory benefits

*High confidence temporal order memory. OCC-seed analysis.* Variability in resting-state functional connectivity of the right OCC-seed to the other ROIs within the right hemispheric semantic temporal lobe network was significantly associated with variability in the reward-related temporal order memory benefit ($F(7,41) = 2.56$, $p = .028$, *p-FDR* = .041; Figure 4.6 A). Uncorrected, this variability included decreased RSFC between the right OCC-seed region and the right anterior temporal fusiform cortex (TFC) ($t(47) = -2.16$, $p = .036$, *p-FDR-seed* = .183; Figure 4.6 B).

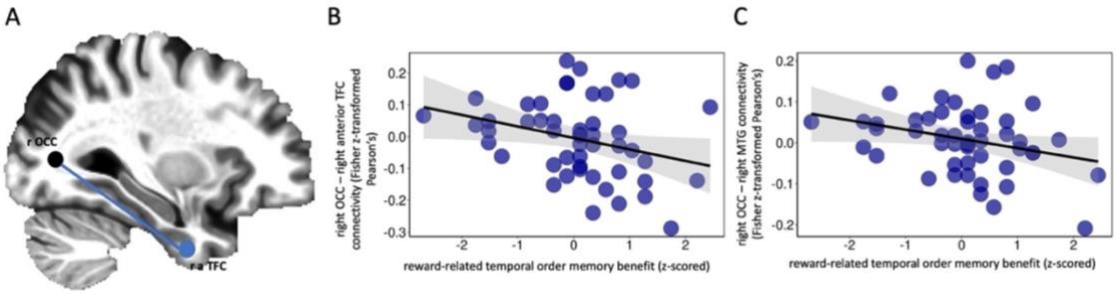


**Figure 4.6. High confidence temporal order memory benefit and resting-state functional connectivity (RSFC) of the OCC-seed within the semantic temporal lobe network. A.** RSFC between right OCC-seed and right anterior temporal fusiform cortex (TFC) in relation to the reward-related temporal order memory benefit. ROIs are displayed on reference slice at [31.06/-2.81/-42.34]. Dots denote ROIs. Lines denote connectivity. Colours denote direction of connectivity. Blue = decrease in RSFC. Black = seed ROI. **B.** Scatterplot of ROI-to-ROI connectivity of right OCC-seed with right anterior TFC onto the reward-related temporal order memory benefit. **C.** Scatterplot of ROI-to-ROI connectivity of right OCC-seed with right anterior MTG onto the reward-related temporal order memory benefit. The line of best fit and 95% confidence interval is shown on each scatterplot with 49 data points.

To follow these results up, ROI-to-ROI connectivity within the right semantic temporal lobe network at rest was regressed onto between-subject variability in the reward-related temporal order memory benefit while holding the effect of overall temporal order memory constant. Changes in connectivity of the right OCC-seed region remained significant ($F(7,40) = 2.57$, $p = .027$, *p-FDR* = .041). Based on the results for the reward-related temporal order memory benefit at high confidence, changes in connectivity of the right OCC-seed region were tested for a decrease in connectivity.

There was a trend towards significantly decreased resting-state functional connectivity between the right OCC-seed and the right anterior TFC ($t(46) = -2.14$, $p_{1\text{-}tailed} = .019$, $p\text{-}FDR\text{-}seed_{1\text{-}tailed} = .079$) as well as between the right OCC-seed and the right anterior MTG ($t(46)$ -2.06, $p_{1\text{-}sided} = .023$, $p\text{-}FDR\text{-}seed_{1\text{-}sided} = .079$; Figure 4.6 C) at rest to be related to between-subject variability in the reward-related temporal order memory benefit when controlled for overall temporal order memory.

*High confidence temporal order memory. PrC-seed analysis.* Interindividual differences in reward-related temporal order memory benefit were related to a significant change in connectivity of the right PrC to other regions within the right semantic temporal lobe network ($F(7,41) = 2.81$, $p = .017$, $p\text{-}FDR = .041$; Figure 4.7 A). Uncorrected, this included an increase of connectivity between the right PrC and the right posterior TFC ($t(47) = 2.21$, $p = .032$, $p\text{-}FDR = .216$; Figure 4.6 B).

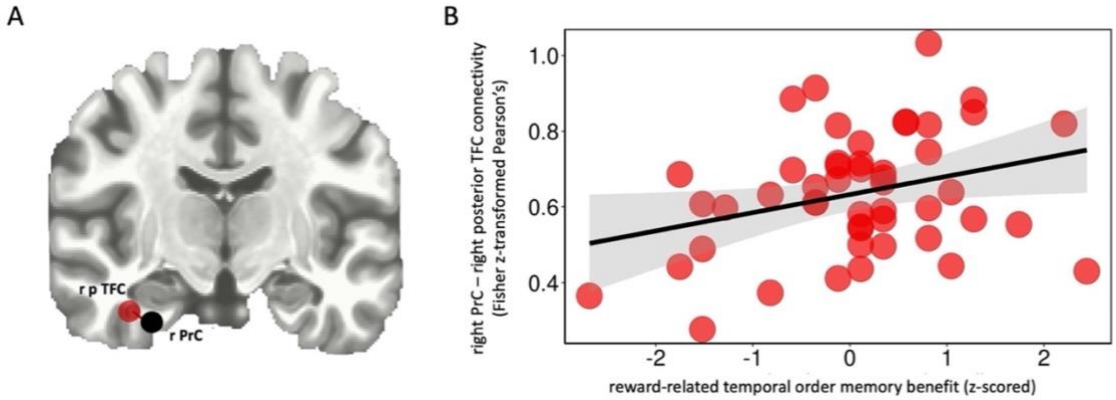


**Figure 4.7. High confidence temporal order memory benefit and resting-state functional connectivity (RSFC) of right PrC within the semantic temporal lobe network. A.** RSFC between right PrC and right posterior temporal fusiform cortex (TFC) in relation to the reward-related temporal order memory benefit. ROIs are displayed on reference slice at [33.80/13.14/-27.83]. Dots denote ROIs. Lines denote connectivity. Colours denote direction of connectivity. Red = increase in RSFC. Black = seed ROI. **B.** Scatterplot of ROI-to-ROI connectivity of right PrC with right posterior TFC onto the reward-related temporal order memory benefit. The line of best fit and 95% confidence interval (CI) is shown on the scatterplot with 49 data points.

To follow these results up, ROI-to-ROI connectivity within the right semantic temporal lobe network at rest was regressed onto between-subject variability in the reward-related temporal order memory benefit while holding the effect of overall temporal order memory constant. The relationship between changes in resting-state functional connectivity of the right PrC and between-subject variability of the reward-

related temporal order memory benefit remained significant when controlled for overall temporal order memory ($F(7,40) = 2.79$, $p = .018$, *p-FDR* = .041). Based on the previous results, changes of the right PrC in functional connectivity at rest were tested for an increase in connectivity. Increased functional connectivity of right PrC and right posterior TFC related to interindividual differences of the reward-related temporal order memory benefit when corrected for overall temporal order memory only on an uncorrected level ($t(46) = 2.16$, $p_{1\text{-}tailed} = .018$, $p\text{-}FDR\text{-}seed_{1\text{-}tailed} = .126$).

*Recollection.* Interindividual differences in the reward-related recollection memory benefit were not related to changes in functional connectivity within the right hemispheric semantic temporal lobe network at rest (all F ≤ 0.95, all p-FDR ≥ .744).

*Source accuracy.* Interindividual differences in the reward-related source memory benefit were not related to changes in functional connectivity within the right hemispheric semantic temporal lobe network at rest (all F ≤ 1.07, all p-FDR ≥ .763).

#### 4.2.2.4 Right ILF microstructure

Interindividual differences in right ILF microstructure measured by FA were not related to significant changes in functional connectivity at rest within the semantic temporal lobe network (all F ≤ 1.26, all p-FDR ≥ .739). Between-subject variability of right ILF microstructure measured by MD was not significantly related to variability in resting-state functional connectivity between the investigated seeds and other regions within the right hemispheric semantic temporal lobe network (all F ≤ 1.86, all p-FDR ≥ .298).

#### 4.2.2.5 Interaction between microstructure and reward-related memory in the right hemisphere

To follow up on the significant correlations between right ILF FA and reward-related memory benefits for high confidence temporal order memory, recollection, and source memory described in 3.2.4.2, the interaction terms of right ILF FA and reward-related memory benefits were investigated for their relationship to variability in resting-state functional connectivity between regions within the right semantic temporal lobe network.

*Interaction of high confidence temporal order memory benefit and ILF FA.* The interaction-term of right ILF microstructure and the reward-related temporal order memory benefit did not significantly relate to variability in the resting-state functional connectivity between the investigated seeds and other regions within the semantic temporal lobe network of the right hemisphere (all $F \leq 2.61$, all p-FDR $\geq .076$)

*Interaction of recollection memory benefit and right ILF FA.* Interindividual differences in the interaction-term did not significantly relate to changes in resting-state functional connectivity of the investigated seed regions to other regions within the right semantic temporal lobe network (all $F \leq 1.76$, all p-FDR $\geq .364$).

*Interaction of source memory benefit and right ILF FA.* There was no significant relationship between the interindividual differences in the interaction-term and interindividual differences in resting-state functional connectivity of the investigated seed regions to other regions within the right semantic temporal lobe network (all $F \leq 1.45$, all p-FDR $\geq .475$).

## 4.3 Discussion

This study investigated interindividual differences in functional connections underlying memory modulation through reward. The analyses were concentrated on two networks, the salience hippocampus network and the semantic temporal lobe network. Functional connectivity was investigated at rest, in the absence of a task, and examined for a relationship with interindividual differences in reward-related memory benefits. Participants encoded sequences of objects in high versus low rewarding contexts. Participants' memory for the temporal order of object pairs was subsequently tested in an immediate memory test. Participants' object and source memory was tested in a second phase of that memory test. This study found that decreased resting-state functional connectivity between the nucleus accumbens and the ventral tegmental area was related to the reward-related memory benefit for recollection and source memory. Additionally, differences in functional connectivity along the representational gradient along the temporal lobe were found to be related to interindividual differences

in the reward-related temporal order memory benefit. The following paragraphs will discuss the results in this study in more detail.

### 4.3.1 Resting-state functional connectivity within the hippocampal-VTA loop was related to reward-related memory benefit

Increased memory for rewarding information had been linked to activation in and connectivity between areas in the mesolimbic pathway (NAcc, VTA) and the hippocampus (Adcock et al., 2006; Gruber et al., 2016; Murty et al., 2017; van der Meer et al., 2010). Processing within the hippocampus had been connected with memory for temporal order (Charles, et al., 2004; DuBrow & Davachi, 2014; Eichenbaum, 2013; Jenkins & Ranganath, 2016). Nevertheless, modulation of temporal order memory through reward has yet to be described in humans. Additionally, the functional processes underlying reward-modulated temporal order memory have yet to be investigated in humans. Here, resting-state fMRI was employed to investigate the relationship between variability in resting-state functional connectivity within the salience-hippocampal network and variability in reward-related memory benefits. Between-subject variability and resting-state functional connectivity were employed to explore the relationship between function and behaviour.

This study found decreased resting-state functional connectivity between the NAcc and the VTA to be associated with variability in the reward-related recollection memory and source memory benefit. For the source memory benefit, this relationship survived FDR-correction across the entire connectivity matrix and remained significant when the model controlled for overall memory. In this study, only changes of intrinsic connectivity between the reward-processing mesolimbic structures (i.e., NAcc and VTA) but not resting-state functional connectivity of the hippocampus were related to interindividual differences in memory modulation by reward. Adcock et al. (2006) found activity in the NAcc and the VTA during high reward anticipation to be increased for subsequently remembered versus forgotten stimuli. In a study of free recall by Reggente et al. (2018), participants' structural connectivity (based on probabilistic tractography) between NAcc and VTA correlated with their high value recall as well as their sensitivity

to value (how their recall performance is influenced by value). Here, decreased functional connectivity between NAcc and VTA was related to the reward-related recollection and source accuracy memory benefit. This was surprising. Neither high nor low reward memory alone was related to variability in RSFC between NAcc and VTA. The effect was specific to the difference between high and low reward memory.

The absence of hippocampal involvement in the relationship between resting-state functional connectivity and reward-related memory benefits can potentially be explained by the immediate memory test employed in this study. Dopamine-driven hippocampus-dependent memory processes are often most pronounced after a longer delay (e.g., Adcock et al., 2006; Bunzeck et al., 2010; Murty et al., 2017). In an immediate memory test, the modulation of memory through reward via dopamine-driven processing might not be pronounced enough to be reliably related to variability in resting-state functional connectivity. Even though resting-state connectivity can be predictive of task-based activity (Tavor et al., 2016), the immediate memory test in combination with the way temporal order, object, and source memory was tested in this study could impede the detection of a relationship between variability in hippocampus-midbrain functional connectivity and variability in reward-related memory. When a temporal order memory test precedes an object memory test, objects that intervene the object pairs tested during the temporal order memory test can be primed (DuBrow & Davachi, 2014). This could possibly interfere with modulation of memory by reward.

### 4.3.2 Resting-state functional connectivity within the semantic temporal lobe network was related to reward-related memory benefit for temporal order

Systematic engagement of processing within a semantic network had been associated to memory for high value information in immediate memory tests (Cohen et al., 2014; 2016). Strategic prioritisation of high reward information through semantic processing had also been shown to be separable from reward-related activation within a reward-network (Cohen et al., 2019). Furthermore, brain activation along the MTL, including the PrC, had been connected to temporal order memory, associative memory, and memory strength (Ezzyat & Davachi, 2011; Jenkins & Ranganath, 2016; Tompary et

al., 2016). However, how strategic engagement of semantic processing influences reward-modulated memory for temporal order specifically has not been explored. Here, resting-state fMRI was employed to investigate the relationship of variability in functional connectivity within a semantic temporal lobe network and between-subject variability in reward-related memory benefits.

In this study, *decreased* functional connectivity at rest between the right OCC-seed and the right anterior temporal fusiform cortex was significantly associated with interindividual variability in the reward-related high confidence temporal order memory benefit. This relationship remained when the reward-related memory benefit was corrected by overall temporal order memory. In contrast, *increased* functional connectivity at rest between right PrC and right posterior temporal fusiform cortex was related to interindividual variability in reward-related high confidence temporal order memory benefit. Likewise, this relationship remained when the reward-related memory benefit was corrected by overall temporal order memory. This pattern is in accordance with the proposed representational gradient along the temporal cortex from more unimodal processing in the posterior cortex and amodal "hub-like" processing in the anterior cortex (Freches et al., 2020; Ralph et al., 2017; Rice, Miller, & Ralph, 2015). Decreased resting-state functional connectivity between the OCC-seed and the anterior temporal fusiform cortex might reflect the relationship between the ability of these regions to disengage and the modulation of temporal order memory through reward. The ability to disengage input from the unimodal end (Bajada et al., 2017) from the more amodal "hub-like" part of the processing pathway (Ralph et al., 2017) might support the strategic prioritisation of high value information. Insofar in that cognitive processes that require the integration of information from multiple different subsystems can occur without interference from ongoing new input. On the other hand, increased functional connectivity at rest between right PrC and right posterior temporal fusiform cortex reflects more similar processes along the MTL pathway (e.g. Bajada et al., 2017; Davachi, 2006). Between subject variability in reward-related memory benefits for high confidence temporal order memory in this study was related to variability in the ability to systematically disengage between task-general and task-specific processing as well

as to systematically engage overlapping processing along a representational gradient within the semantic temporal lobe network.

Though less unexpected based on the results reported in Chapter 3, the absence of a relationship between functional connectivity at rest in the left hemispheric semantic temporal lobe network and reward-related memory benefits was surprising. Especially since the task of relating objects within a sequence to each other and their background via a story during encoding would encourage verbal semantic processing. If the semantic processing in the verbal domain encouraged by the secondary encoding task had led to reward-related memory benefits in this study, then variability in resting-state functional connectivity within the left hemispheric semantic temporal lobe network could have been expected (e.g., Binder, Desai, Graves, & Conant, 2009). Nevertheless, vision-related processing is found to be more pronounced in the right hemisphere, especially in relation to social processing and the analysis of complex visual cues like facial expressions (e.g., Freches et al., 2020; Bajada et al., 2017; Ralph et al., 2017).

### 4.3.3 Limitations and future directions

The limitations to the behavioural paradigm discussed under 3.3.4 in Chapter 3 apply here as well. Limitations to ROI-based resting-state functional connectivity analyses employed here will be discussed in detail in Chapter 7. Furthermore, although the regions of interest were in part chosen to correspond to regions connected via the fibre tracts investigated in this thesis, I could not find a significant relationship between variability in microstructure indices and variability in resting-state functional connectivity of the seed-ROIs investigated. Follow-up studies could investigate the whole connectivity matrix. This would however increase the number of corrections that will have to be applied and lower the sensitivity of the model. Nevertheless, microstructure and resting-state functional connectivity analyses did display converging relationships to variability in the behaviour investigated in this chapter and Chapter 3. This will be discussed in more detail in Chapter 7.

## 4.4 Chapter Summary

Here, decreased functional connectivity between NAcc and VTA at rest was related to the reward-related memory benefit in recollection and source memory. For source memory, this effect was driven by a not significant association of increased resting-state functional connectivity between NAcc and VTA with interindividual differences in low reward memory. Furthermore, participants' reward-related temporal order memory benefit was related to the ability to systematically engage as well as disengage processing along a representational gradient within the semantic temporal lobe network of the visually dominant right hemisphere.

# Chapter 5: Neuroanatomical substrates of long-term memory for intentionally memorised rewarded information

Episodic memory is influenced by varying processes during encoding (Tulving, 2002). We do not remember everything we experience and, aside from aspects pointing to an event's salience, our own intention to remember the event can influence memory. Intentional memorisation can be initiated by contextual information, an event's perceived value, goal-oriented memorisation to inform later behaviours/decision-making, or a combination of these. Reward is one way to mark information for intentional memorisation and introduce salience. The first three experimental chapters of this thesis were aimed at memory for objects encoded during differently rewarding contexts. The following two chapters were aimed at investigating the effect of reward on intentional memorisation specifically to increase memory test performance.

Reward or rewarding contexts have been shown to enhance memory for objects (Gruber et al., 2016; Shohamy & Adcock, 2010; Wimmer & Shohamy, 2012) as well as associative memory measures of object-context memory (Gruber et al., 2016) or object-label memory (Murty et al., 2017). Reward has also been demonstrated to bias decision-making (Wimmer & Shohamy, 2012) and increase memory through intentional memorisation (Adcock et al., 2006; Kuhl, Shah, DuBrow, & Wagner, 2010). During investigation of episodic-like memory in animals, hippocampal replay of encoding activity for a path leading up to reward during wakeful rest (Davidson et al., 2009; Karlsson & Frank, 2009; Singer & Frank, 2009) or sleep (Dupret et al., 2010; Lansink et al., 2008; Lee & Wilson, 2002; Peyrache et al., 2009) has been found to be related to successful memory and memory benefits for rewarded information. Consistent with these studies in animals, human imaging studies reveal, that processes during post-encoding rest (Gruber et al., 2016; Murty et al., 2017) as well as preferential replay during sleep (Igloi et al., 2015) lead to enhanced memory for high reward compared to low reward information. Memory for low reward information shows a greater decline from before to after sleep than high reward information (Studte et al., 2017; for alternative findings, Oudiette et al., 2013). The studies reviewed above demonstrate

that consolidation processes during sleep can positively impact memory for rewarded/rewarding information. The intention to remember certain information can influence these processes (e.g., Adcock et al., 2006).

The hippocampus and other regions of the MTL have long been investigated in their relation to episodic and other memory processes (e.g., Tulving et al., 1991; Levine et al., 1998). The hippocampus is described as part of the network involved in reward-modulated memory (see Miendlarzewska et al., 2016 for review). Hippocampus-dependent recollection is especially influenced by reward (Wittman et al., 2005). Reward can enhance memory formation via dopaminergic connections between the midbrain and hippocampus (Adcock et al., 2006; Gruber et al., 2016; Murty & Adcock, 2014; Shohamy & Adcock, 2010; Wolosin et al., 2012). Another mechanism through which reward can modulate memory involves the systematic engagement of semantic encoding (Cohen et al., 2014; 2016). Based on circumstance or task, these two mechanisms can separately or simultaneously lead to enhanced memory for rewarded information (Cohen et al., 2017). Furthermore, there is interindividual variability in how much a certain reward incentivises (e.g., Berridge, 2007; Cohen et al., 2005). Thus, modulation of memory through reward is similarly variable. This variability in behaviour has been found to be related to interindividual variability in the reward-processing as well as the semantic neural system (e.g., Adcock et al., 2006; Gruber et al., 2016; Cohen et al., 2014; 2016; Morris & Dolan, 2001). However, the effect of intentional memorisation on immediate versus consolidated memory in relation to variability within the hippocampal-VTA loop and the semantic system have not been investigated in detail. Intentional memorisation in anticipation of upcoming reward is an important aspect of episodic memory in relation to adaptive memory formation. Based on this understanding, it is adaptive that more than one neuronal system supports long-term memory formation for valuable information because different parts of an event can become important. Nonetheless, the conditions under which these systems, memory formation via dopaminergic connections and elaborative semantic processing, display converging or separate contributions to reward-modulated memory formation have not been investigated in detail.

This study employs multi-shell diffusion MRI and spherical deconvolution tractography to investigate the relationship between interindividual variability in the microstructure of white matter pathways and interindividual differences in reward-related memory enhancements. Participants intentionally memorised scenes that were associated with high or low reward for correctly remembering the scenes. Recollection and familiarity were investigated in an immediate and a delayed memory test. Variability in white matter fibre bundles, which facilitate communication between processing in distal brain regions, has been argued to contribute to variability in behaviour (Assaf et al., 2019; Kanai & Rees, 2011). Based on the literature investigating the modulation of memory through reward, three fibre tracts were of interest for their relationship to reward-related memory performance in this study: the fornix, the UF, and the ILF.

Reward-related memory benefits have been found to be associated with hippocampal memory formation, modulated by processes in dopaminergic midbrain structures like the VTA, and the ventral striatum, which includes the NAcc (Adcock et al., 2006; Gruber et al., 2016; Murty et al., 2017; Wittmann et al., 2005). Interindividual variability in sustained connectivity between VTA and MTL subregions during encoding was found to be related to variability in reward-modulation in intentional memorisation tasks (Adcock et al., 2006; Wolosin et al., 2012). The fornix is the major afferent/efferent- pathway between the hippocampal formation in the MTL and structures within the dopaminergic system like the NAcc (Aggleton et al., 2015; Friedman et al., 2002). Therefore, this study examined the relationship between interindividual differences in fornix microstructure and interindividual differences in reward-related memory. Microstructural variability of the whole fornix has been found to relate to episodic memory performance and the vivid retrieval of contextual detail in autobiographical memory (Hodgetts et al., 2017; Metzler-Baddeley et al., 2011) and recollection (Rudebeck et al., 2009). Based on these findings, the study described here investigated the relationship between fornix microstructure and recollection memory specifically. Furthermore, hippocampus-dependent and dopamine-driven memory is thought to be more pronounced after a longer delay, after early consolidation processes (Adcock et al., 2006; Murty et al., 2017). Following these findings, the relationship of

fornix microstructure to changes in recollection memory from immediate to delayed memory test were investigated. Additionally, the relationship between fornix microstructure and memory was hypothesised to be more pronounced in the delayed memory test. As discussed in Chapter 3, the fornix is not a unitary structure. Again, the lateral and medial fornix subdivisions, that carry anterior hippocampus–PFC/NAcc and posterior hippocampus–mammillary body projections respectively, have been chosen for investigation of the relationship between recollection memory and microstructure properties (Christiansen et al., 2017). This analysis and its results are reported in Appendix 6.

The UF connects the anterior MTL and the prefrontal cortex (PFC) in both hemispheres (Catani et al., 2013; Catani & De Schotten, 2008; Kondo et al., 2005). The PFC is involved in the disambiguation of different memory traces (Botvinick, Braver, Barch, Carter, & Cohen, 2001; Eichenbaum, 2013). In the context of the intentional memorisation of rewarding information, communication between the PFC and the MTL might facilitate memory by distinguishing rewarding, to-be-remembered information from less rewarding, to-be-forgotten information occurring at the same time. UF microstructure was found to be related to individual differences in participants' ability to learn associations (Alm et al., 2016). Furthermore, participants' error rates in an associative learning task were related to UF microstructure (Metzler-Baddeley et al., 2011). In a study by Reggente and colleagues (2018), participants were instructed to memorise lists of words. Each word of the list was preceded by a high or low reward cue that indicated the number of points participants could earn for correctly recalling the word. Points were converted into monetary rewards. Microstructure of the UF correlated with recall of high value but not low value words (Reggente et al., 2018). Based on the described relationship between UF microstructure and associative memory, a relationship with recollection memory was investigated in this study. Positive associations with UF microstructure and reward-related memory were hypothesised. The relationship between UF microstructure and the difference in reward-related memory between the immediate and the delayed memory test were also investigated. Memory performance in the immediate memory test was analysed given that the

reported effects were based on immediate memory tests (Alm et al., 2016; Metzler-Baddeley et al., 2011; Reggente et al., 2018).

The ILF is a long-range associative white matter tract within the MTL, connecting occipital lobe with the semantic "hub" in the ATL (Ralph et al., 2017; Patterson et al., 2007; for review see Herbet et al., 2018). Variability in value-based recall has been related to systematic engagement of semantic processing, especially in an immediate memory test (Cohen et al., 2014; 2016). ILF microstructure differences have also been related to differences in the number of semantic details recalled in an autobiographical interview (Hodgetts et al., 2017). Based on these findings and the results reported in Chapter 3, correlations between interindividual differences in ILF microstructure and reward-related differences in recollection memory were investigated in the current study. Changes in recollection memory from immediate to delayed memory test were also investigated for their relationship with ILF microstructure. Furthermore, variability of reward-related recollection at the immediate memory test was hypothesised to display a more pronounced relationship with ILF microstructure.

In conclusion, a relationship between fornix microstructure and reward-related recollection memory differences between the immediate and the delayed memory test was hypothesised. In particular, the relationship between fornix microstructure and reward-related recollection memory was hypothesised to be more prevalent for delayed memory test performance. I also hypothesised a relationship between UF microstructure and reward-related recollection memory differences between the immediate and the delayed memory test. This relationship was hypothesised to be more prevalent for interindividual differences in immediate memory test performance. For ILF microstructure, the same hypotheses as for UF microstructure were made. Directed correlation analyses for specific microstructure indices were based on the literature (see 5.1.6 "Correlation analyses").

# 5.1 Methods

## 5.1.1 Participants

Data were collected from the same participant pool as described in Chapter 3 (N = 55). The Ethical Review Board at the School of Psychology at Cardiff University approved the study procedures. For the analyses described here, eight participants were excluded from the analysis due to an error during data collection. These eight participants only encoded 10 scenes overall. Data analyses were based on 47 participants (7 males, mean age = 19.13, SD = 1.62, range = 18-25).

## 5.1.2 Behavioural procedures

The following paragraphs describe the three stages of the study, an encoding-phase that lasted approximately 5 minutes, a 2-minute post-encoding distractor-phase, and a two-phased memory test (immediate versus 24-hour delay). The memory tests were self-paced and lasted approximately 3 minutes each. The participants encoded 40 scenes and were differently rewarded for correctly remembering the scenes in the subsequent memory tests (high versus low reward). During encoding, participants made yes/no- judgements on the perceived pleasantness of the scene. Depending on the reward-condition, they received high (£1.00) or low (£0.01) reward for correctly remembering the scenes in the subsequent memory tests.

### 5.1.2.1 Encoding – Intentional memorisation

Participants encoded 40 scenes, 20 scenes each for the high (£1.00) and low (£0.01) reward conditions. Figure 5.1 depicts an exemplary high reward encoding trial. Each encoding trial started with a white fixation cross in the middle of a grey screen for 1 second. The fixation period was followed by a high or low reward cue presented for 1 second. Reward was indicated by the amount in GBP (high = £1.00, low = £0.01) and the font colour (high = green, low = white). The to-be-remembered scenes were centred on the screen for 2 seconds during which participants were instructed to make a yes/no-pleasantness judgement on the scene via key press.

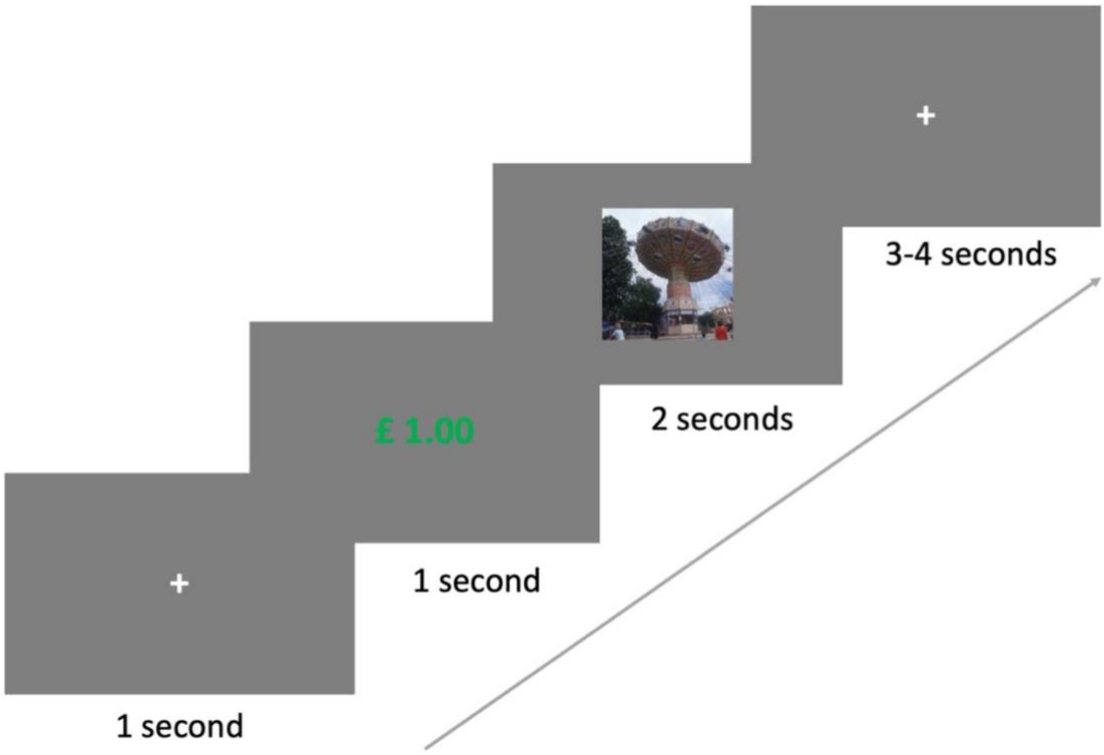


**Figure 5.1. High reward encoding trial.** A trial started with a fixation, followed by a reward cue (high reward = £1.00 in green font, low reward = £0.01 in white font). The cue indicated the amount of reward for correctly remembering the scene presented afterwards. A trial ended with an inter-trial-interval (ITI) jittered between 3 and 4 seconds.

Participants were instructed to use the inter-trial-interval (ITI) of 3-4 seconds to finish pleasantness judgments they were unable to make during scene presentation and the remainder of the time to memorise the scenes for the memory tests. The ITI consisted of a white fixation cross on a grey background. High and low reward trials were randomised.

Encoding lasted approximately 5 minutes and was followed by a 2-minute distractor task. The distractor task was a paper pen arithmetic test involving three-digit addition and subtraction. Participants were informed that their performance on this task would not influence their winnings. Next, participants received instructions for the memory test.

### 5.1.2.2 Memory test

The memory test was divided into two parts, an immediate and a 24-hour delayed memory test. Each memory test contained 30 items. Participants were asked “Have you

seen this item before?" and participants gave remember, know, or new responses (Figure 5.2). A memory test comprised 10 items each from high and low reward conditions as well as 10 new distractors. Item presentation was randomised.


**Figure 5.2**. **Scene memory test.** Participants were tested on 30 items (10 old high reward, 10 old low reward, 10 new) each in an immediate and a 24-hour delayed memory test. A classic remember-know-new design was employed to investigate participants' recollection and familiarity memory. After each response the next item in the test was presented.

Recollection and familiarity measures for the scenes were examined in a remember-know-new-design (Yonelinas, 2002). Participants were instructed to give a "remember"- response if they were able to recollect something specific about encountering the scenes during encoding. Participants should respond "know" if they recognised the scene as "old" in the absence of any recollection for the experience of being presented with the scene during encoding. If they felt that they had not seen the scene before, participants gave a "new"- response. The memory test was self-paced. Participants were instructed that for every scene they correctly label as "old" they would receive the amount of reward (high = £1.00, low = £0.01) that preceded the scene during encoding. They were also informed that they would receive a penalty of £0.25 for every new scene they incorrectly label as "old". Participants were told that the penalty was included to encourage them to make use of their memory and discourage them to simply give an "old"- response to every test-stimulus. Participants returned to the lab after 24 hours for another memory test consisting of 30 items, 20 old (10 high reward,

10 low reward) and 10 new scenes. A percentage of the theoretical winnings of £20.20 was capped at £3.00 and added to participants' compensation for study participation.

### 5.1.3 Stimuli

The 60 coloured scenes were taken from Konkle, Brady, Alvarez, and Oliva (2010). Scenes were pseudo-randomly selected from the categories provided in the database. No scenes depicting the same setting were included. Scenes were organised into six sets consisting of 10 images each. Each set contained an equal number of natural and manmade landscapes. Manmade scenes were equally distributed between interiors and exteriors. Most scenes did not include people or animals.

A set of scenes was assigned to either reward (high versus low) or memory test (immediate versus delayed) condition. Two sets of scenes served as distractor-sets for the immediate or delayed memory test. 20 scenes were tested immediately (10 high versus 10 low reward), 20 scenes were tested after a 24-hour delay (10 high versus 10 low reward). Each memory test contained 10 distractors. Across participants, the assignment of item-set to reward condition, memory test condition, or distractor-set was counterbalanced. Item-presentation during the memory tests was randomised.

### 5.1.4 Imaging acquisition and preprocessing

Imaging acquisition and pre-processing procedures were the same as in Chapter 3. High-resolution anatomical and diffusion-weighted images were obtained with a 3 Tesla MRI scanner (Siemens Magnetom Prisma). The diffusion-weighted images along the A-P axis were registered to the image along the P-A axis and free water corrected. The tractography of the fornix, UF, and ILF was the same as in Chapter 3. Manual tractography on the b=2400 diffusion-weighted images was carried out on a subset of participants. Manual tracts were then introduced to a model building algorithm. Models were then applied to the whole data set, resulting in tract masks in the b=2400 space. These were then registered to the b=1200 images, resulting in tract-specific free-water corrected FA and MD maps. Mean FA and MD values of the tracts were extracted for statistical analysis.

## 5.1.5 Behavioural analysis

Behavioural analyses were carried out in JASP (JASP Team, 2019; version 0.11.1). Participants with low memory performance were retained in all analyses. Low memory performance was defined as overall memory accuracy being negative or 0. In the study of interindividual differences in memory, participants with low or no memory carry information as well (Kanai & Rees, 2011). Datapoints of participants that were below or above 3 SDs from the mean were replaced by the respective 3SD value. This was the case in five different participants on different measures. Replacements versus exclusion of the participants in question did not change the direction of the reported results.

### 5.1.5.1 Encoding

Percentages of pleasantness ratings during encoding were investigated with a two-tailed paired sample t-test. No directed hypotheses were made for a difference in ratings during high versus low reward trials.

### 5.1.5.2 Recollection and familiarity

Recollection and familiarity measures were calculated as described in Chapter 3 and Appendix 3. Only recollection measures were analysed further since modulation of recollection through reward was expected to be stronger than that of familiarity (see Appendix 5 for familiarity). The effects of *reward* (high versus low) and *testing timepoint* (immediate versus delayed) on recollection were investigated with a 2x2 repeated-measures ANOVA. Follow-up analyses on recollection were conducted with one-tailed paired sample t-tests testing for a positive difference. Higher recollection for high reward scenes was expected. In the follow-up on timepoint, higher recollection memory was expected in the immediate versus the delayed memory test.

## 5.1.6 Correlation analysis – relationship between behaviour and fibre tract microstructure

Correlation analyses were carried out in JASP (JASP Team, 2019; version 0.11.1). Correlation analyses between memory measures and microstructure were only carried out for recollection memory. Memory effects were correlated with the different indicators (FA and MD) of microstructure in the different tracts of interest. All variables

were z-standardised for each participants' data before correlation analysis (see formula 3.2 in 3.1.7). Reward-related recollection memory benefits (high reward – low reward) and overall recollection (mean across high and low reward) were investigated for their relationship to fibre microstructure. Indicators of changes of reward-related memory from immediate to delayed memory test were calculated for recollection. Two different indicators of memory change were calculated based on the hypothesised direction of change in relation to the fibre tract of interest. If it was hypothesised that better memory in delayed memory test was related to microstructure of the tract then performance at immediate was subtracted from performance at delayed memory test (reward-related memory benefit/overall memory at delayed memory test – reward-related memory benefit/overall memory at immediate). If it was hypothesised that better memory in immediate memory test was related to microstructure of the tract then performance at delayed was subtracted from performance at immediate memory test (reward-related memory benefit/overall memory at immediate memory test – reward-related memory benefit/overall memory at delayed). Directed hypotheses for the correlations between recollection measures and microstructure were based on the literature.

For FA, a positive correlation between fornix, UF, and ILF microstructure and memory performance was predicted (e.g., Hodgetts et al., 2017; Reggente et al., 2018). For MD, a negative correlation between memory and microstructure was predicted (e.g., Hennessee et al., 2019; Hodgetts et al., 2017).

Pearson's correlation indices were corrected for family-wise error rates (FWE) with the Holm-Bonferroni method which is described in detail in Chapter 3 under "3.1.7 Correlation analysis" (Holm, 1979). Corrections were performed on the correlations performed within each tract.

For example, to correct the p-values of the correlation analyses between fornix FA and recollection measures, the p-values of the 8 correlations investigated with a directed hypothesis (4 memory measures [(1) difference in overall memory between memory tests, (2) difference in reward-related memory benefit between memory tests,

(3) overall memory at delayed memory test, (4) reward-related memory difference at delayed memory test] x 2 microstructure measures [FA, MD]) within the fornix were sorted by size in an ascending order. In the hypothetical example, the positive correlation between fornix FA and reward-related recollection benefit (high reward recollection – low reward recollection) is the second smallest with a p-value of .003. Therefore, the fornix FA and reward-related recollection benefit correlation has the rank number 2, whereas a total number of 8 correlations were calculated. Formula 5.1 shows the example of calculating the corrected $\alpha$ for the reward-related recollection benefit.

$$corrected \ \propto = \frac{0.05}{8-2+1} = 0.007$$

**Formula 5.1.** Holm-Bonferroni correction for a hypothetical correlation between fornix FA and the reward-related recollection benefit.

The p-value of each correlation is then compared to its corrected $\alpha$. In the hypothetical example the correlation between fornix FA and reward-related recollection benefit survives the FWE-correction (.003 < .007).

# 5.2 Results

## 5.2.1 Behavioural results

Overall, participants judged more scenes as pleasant (high reward = 66.28%, SE = 2.38; low reward = 60.74%, SE = 2.11) as opposed to not pleasant (high reward = 29.47%, SE = 2.27; low reward = 34.47%, SE = 2.02). Participants judged significantly more scenes as pleasant in high reward trials than in low reward trials ($t(46) = 2.42$, $p = .02$, $d = 0.35$). Participants did not make a pleasantness judgment on 4.52% of trials; this did not differ between high and low reward trials ($t(46) = -0.62$, $p = .54$, $d = -0.09$).

**Table 5.1. Group means and standard deviations (SD) for the behavioural measures.** Means and SDs are based on percentage accuracies (hits – false alarms). Separated by reward (high versus low) and memory test (immediate versus delayed). SDs in brackets behind means.

| Memory measure | Reward | Mean (SD) |
|---|---|---|
| Immediate recollection | high | 74.89 (25.78) |
| | low | 69.15 (27.01) |
| Delayed recollection | high | 62.34 (28.68) |
| | low | 59.57 (27.66) |

Two participants only made "know"- responses in the immediate memory test, removing them from the analysis did not change the reported results. Therefore, all participants were retained for all analyses. A 2x2 repeated-measures ANOVA of the effects of *timepoint* (immediate versus delayed) and *reward* (high versus low) on recollection revealed a significant main effect of *timepoint* ($F(1,46) = 9.6$, $p = .003$, *partial eta squared* = 0.17) and a trend towards a significant effect of *reward* ($F(1,46) = 3.42$, $p = .07$, *partial eta squared* = 0.07). The interaction of timepoint and reward was not significant ($F(1,46) = 0.86$, $p = .36$, *partial eta squared* = 0.02).

## 5.2.2 Correlation results – relationship between behaviour and fibre tract microstructure

### 5.2.2.1 Fornix microstructure related to overall recollection at delayed memory test

For the relationship between fornix microstructure and behaviour, a stronger influence of interindividual variability in fornix microstructure on interindividual differences in delayed memory test performance was hypothesised. Therefore, the index of change that was correlated with fornix microstructure was calculated by subtracting immediate memory test performance from delayed memory test performance.

*5.2.2.1.1 Overall recollection*

Fornix microstructure did not correlate with the difference of overall recollection between immediate and delayed (delayed – immediate) memory test (FA: $r(45) = 0.13$, $p_{1\text{-tailed}} = .19$; MD: $r(45) = 0.02$, $p_{1\text{-tailed}} = .55$). Based on the hypothesised relationship between fornix microstructure and reward-related memory performance in the delayed memory test specifically, delayed memory test performance was investigated for a correlation with fornix microstructure. Before FWE-correction, variability in overall recollection at delayed memory test correlated with variability in fornix microstructure (FA: $r(45) = 0.27$, $p_{1\text{-tailed}} = .03 > \alpha_{\text{corrected}} = .007$; Figure 5.3 B; MD: $r(45) = 0.06$, $p_{1\text{-tailed}} = .65$).

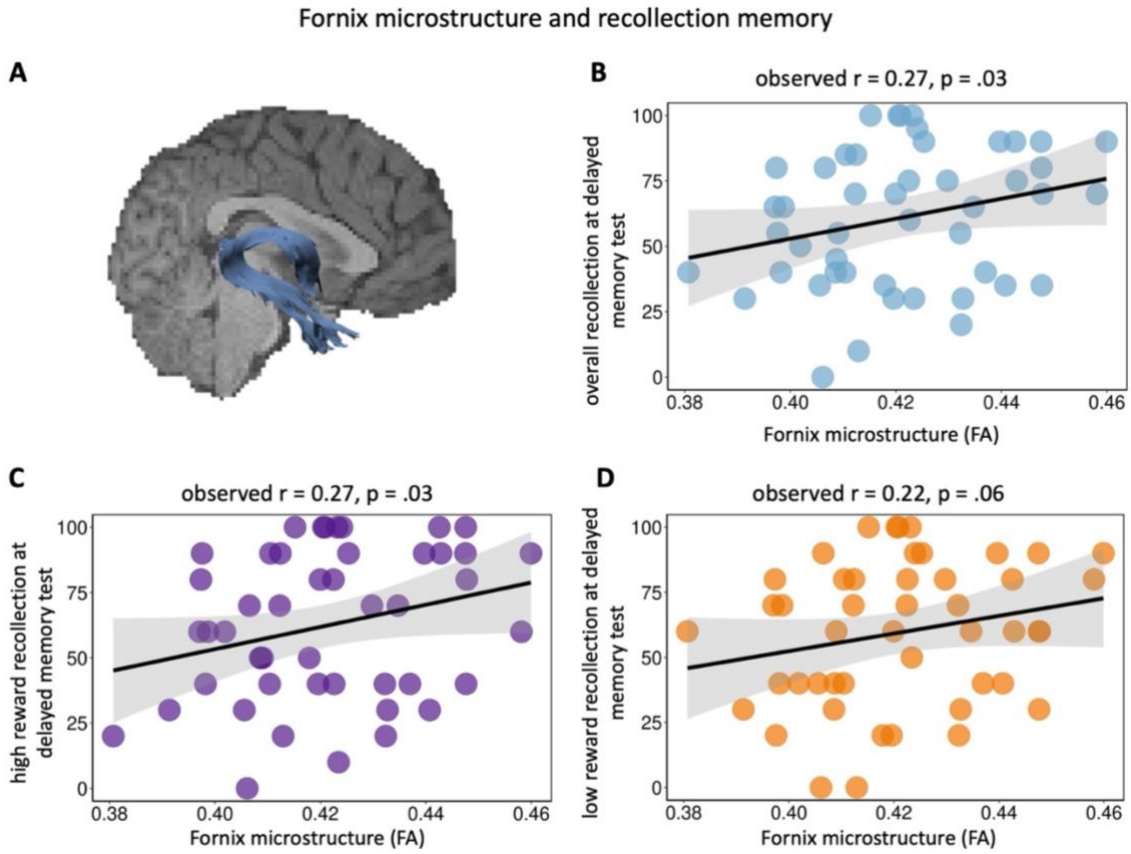


**Figure 5.3. Correlation of fornix fractional anisotropy (FA) with overall recollection at delayed memory test. A.** Fornix on brain slice. **B.** Uncorrected significant positive correlation of fornix FA with overall recollection at delayed memory test. **C.** Significant (uncorrected) correlation of fornix FA with high reward recollection at delayed memory test. **D.** Correlation of fornix FA with low reward recollection at delayed memory test. The line of best fit and 95% confidence interval (CI) is shown on each scatterplot with 47 data points.

The correlation between fornix microstructure (FA) and overall recollection at delayed memory test was followed up on. High and low reward recollection at the delayed memory test were investigated for a positive correlation with fornix microstructure. Interindividual differences of high reward recollection at delayed memory correlated with fornix FA ($r(45) = 0.27$, $p_{1\text{-tailed}} = .03$; Figure 5.3 C). The correlation between interindividual differences in low reward recollection and fornix FA displayed a trend ($r(45) = 0.22$, $p_{1\text{-tailed}} = .06$; Figure 5.3 D).

An exploratory analysis of overall recollection at immediate memory test showed no significant correlation between behaviour and fornix microstructure (FA: $r(45) = 0.17$, $p_{1\text{-tailed}} = .125$; MD: $r(45) = 0.04$, $p_{1\text{-tailed}} = .608$).

#### *5.2.2.1.2 Reward-related recollection memory benefit*

Fornix microstructure did not correlate with the difference of the reward-related recollection memory benefit between immediate and delayed (delayed – immediate) memory test (FA: $r(45) = 0.13$, $p_{1\text{-tailed}} = .2$; MD: $r(45) = 0.07$, $p_{1\text{-tailed}} = .69$). Based on the hypothesised relationship between fornix microstructure and reward-related memory performance in the delayed memory test specifically, delayed memory test performance was investigated for a correlation with fornix microstructure. At delayed memory test, variability in fornix microstructure did not significantly correlate with the reward-related recollection memory benefit (FA: $r(45) = 0.09$, $p_{1\text{-tailed}} = .27$; MD: $r(45) = 0.02$ , $p_{1\text{-tailed}} = .56$).

An exploratory analysis of immediate memory test performance showed no significant correlation between the reward-related recollection memory benefit and fornix microstructure (FA: $r(45) = -0.06$, $p_{1\text{-tailed}} = .652$; MD: $r(45) = -0.07$, $p_{1\text{-tailed}} = .325$).

### 5.2.2.2 Left uncinate microstructure related to overall recollection at immediate memory test

For the relationship between UF microstructure and behaviour, a stronger influence of interindividual variability in UF microstructure on interindividual differences in immediate memory test performance was hypothesised. Therefore, the index of change that was correlated with UF microstructure was calculated by subtracting

delayed memory test performance from immediate memory test performance. UF microstructure was not averaged across hemispheres since hemispheric differences in the relationship between UF microstructure and memory have been reported (Alm et al., 2016; Reggente et al., 2018). Results for the correlation analyses between left UF microstructure and behaviour are reported first.

*5.2.2.2.1 Overall recollection*

Before FWE-correction, interindividual differences in left UF microstructure significantly correlated with variability in the difference of overall recollection between immediate and delayed (immediate – delayed) memory test (FA: $r(45) = 0.26$, $p_{1\text{-}tailed} = .04 > \alpha_{corrected} = .007$; Figure 5.4 B; MD: $r(45) = -0.10$, $p_{1\text{-}tailed} = .25$). Based on the hypothesised relationship between UF microstructure and reward-related memory performance in the immediate memory test specifically, immediate memory test performance was investigated for a correlation with left UF microstructure. Before FWE-correction, variability in overall recollection at immediate memory test significantly correlated with variability in left UF microstructure (FA: $r(45) = 0.31$, $p_{1\text{-}tailed} = .02 > \alpha_{corrected} = .007$; Figure 5.4 C). These correlations changed strength after outlier removal such that they displayed the same direction but did not reach (uncorrected) significance.

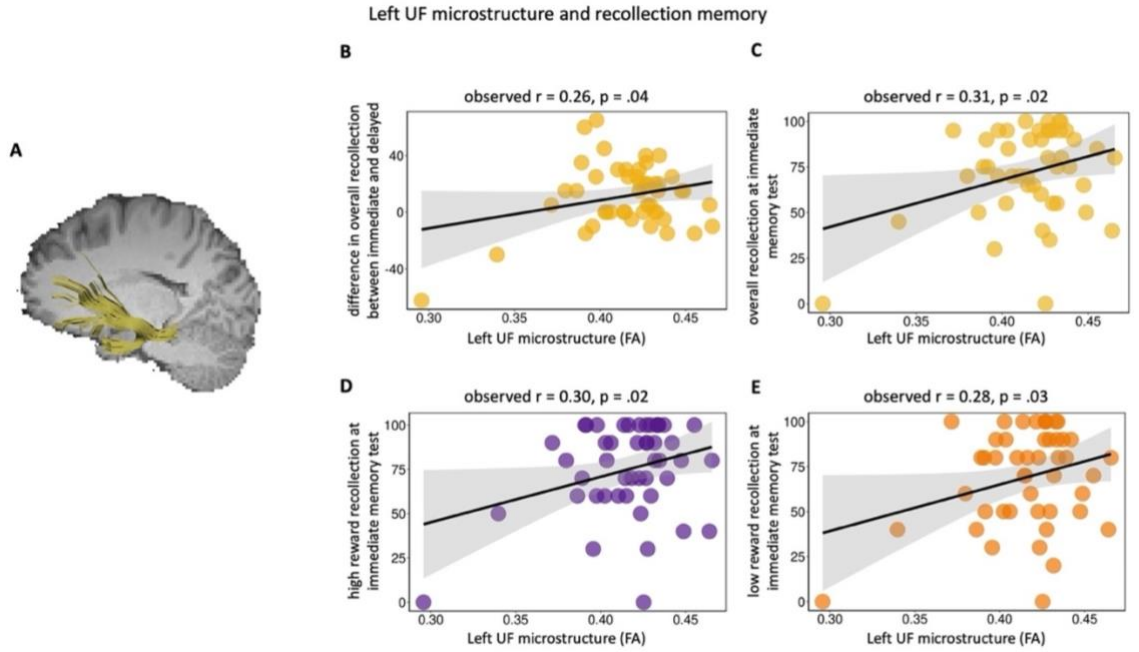


**Figure 5.4. Correlation of left uncinate fasciulus (UF) microstructure and overall recollection. A:** Left UF on brain slice. **B.** Uncorrected significant positive correlation of left UF fractional anisotropy (FA) with the difference (immediate – delayed) in overall recollection between immediate and delayed memory test. **C.** Uncorrected significant positive correlation of left UF FA with overall recollection at immediate memory test. **D.** Uncorrected significant positive correlation of left UF FA with high reward recollection at immediate memory test. **E.** Uncorrected significant positive correlation of left UF FA with low reward recollection at immediate memory test. The line of best fit and 95% confidence interval (CI) is shown on each scatterplot with 47 data points.

In the follow-up analysis within the immediate memory test, interindividual differences in both high ($r(45) = 0.30$, $p_{1\text{-tailed}} = .02$; Figure 5.3 D) and low reward recollection ($r(45) = 0.28$, $p_{1\text{-tailed}} = .03$; Figure 5.3 E) positively correlated with left UF FA.

An exploratory analysis of delayed memory test performance showed no significant correlation between overall recollection and left UF microstructure (FA: $r(45) = -0.01$, $p_{1\text{-tailed}} = .518$; MD: $r(45) = 0.10$, $p_{1\text{-tailed}} = .749$).

*5.2.2.2.2 Reward-related recollection memory benefit*

Left UF microstructure did not correlate with the difference of the reward-related memory benefit between immediate and delayed (immediate – delayed) memory test (FA: $r(45) = 0.08$, $p_{1\text{-tailed}} = .7$; MD: $r(45) = 0.16$, $p_{1\text{-tailed}} = .85$). Based on the hypothesised relationship between UF microstructure and reward-related memory performance in the immediate memory test specifically, immediate memory test performance was investigated for a correlation with left UF microstructure. At immediate memory test,

variability in left UF microstructure did not correlate with variability in the reward-related recollection memory benefit (FA: $r(45) = -0.01$, $p_{1\text{-}tailed} = .52$; MD: $r(45) = 0.29$, $p_{1\text{-}tailed} = .98$).

An exploratory analysis of delayed memory test performance showed no significant correlation between the reward-related recollection memory benefit and left UF microstructure (FA: $r(45) = 0.08$, $p_{1\text{-}tailed} = .288$; MD: $r(45) = 0.09$, $p_{1\text{-}tailed} = .722$).

### 5.2.2.3 Right uncinate microstructure did not relate to memory

#### *5.2.2.3.1 Overall recollection*

The correlation between right UF microstructure and interindividual variability in the difference (immediate – delayed) in overall recollection between immediate and delayed memory test did not reach significance (FA: $r(45) = 0.08$, $p_{1\text{-}tailed} = .28$; MD: $r(45) = -0.05$, $p_{1\text{-}tailed} = .37$). Based on the hypothesised relationship between UF microstructure and reward-related memory performance in the immediate memory test specifically, immediate memory test performance was investigated for a correlation with right UF microstructure. At immediate memory test, variability in overall recollection did not correlate with variability in right UF microstructure (FA: $r(45) = 0.02$, $p_{1\text{-}tailed} = .43$; MD: $r(45) = 0.06$, $p_{1\text{-}tailed} = .66$).

An exploratory analysis of delayed memory test performance showed no significant correlation between overall recollection and right UF microstructure (FA: $r(45) = -0.08$, $p_{1\text{-}tailed} = .696$; MD: $r(45) = 0.10$, $p_{1\text{-}tailed} = .751$).

#### *5.2.2.3.2 Reward-related recollection memory benefit*

Right UF microstructure did not correlate with the difference (immediate – delayed) in reward-related recollection memory benefit between immediate and delayed memory test (FA: $r(45) = -0.15$, $p_{1\text{-}tailed} = .85$; MD: $r(45) = 0.01$, $p_{1\text{-}tailed} = .52$). Based on the hypothesised relationship between UF microstructure and reward-related memory performance in the immediate memory test specifically, immediate memory test performance was investigated for a correlation with right UF microstructure. At immediate memory test, variability in right UF microstructure did not correlate with

variability in the reward-related recollection memory benefit (FA: $r(45) = -0.04$, $p_{1\text{-tailed}} = .61$; MD: $r(45) = 0.15$, $p_{1\text{-tailed}} = .84$).

An exploratory analysis of delayed memory test performance showed no significant correlation between the reward-related recollection memory benefit and right UF microstructure (FA: $r(45) = 0.14$, $p_{1\text{-tailed}} = .178$; MD: $r(45) = 0.12$, $p_{1\text{-tailed}} = .796$).

#### 5.2.2.4 Left inferior longitudinal fasciculus microstructure did not relate to memory

For the relationship between ILF microstructure and behaviour, a stronger influence of interindividual variability in ILF microstructure on interindividual differences in immediate memory test performance was hypothesised. Therefore, the index of change that was correlated with ILF microstructure was calculated by subtracting delayed memory test performance from immediate memory test performance. ILF microstructure was not averaged across hemispheres since hemispheric differences in the relationship between ILF microstructure and memory have been reported (Hodgetts et al., 2017). Furthermore, the results reported in Chapter 3 display hemispheric differences in the correlations between ILF microstructure and immediate memory test performance.

##### *5.2.2.4.1 Overall recollection*

Interindividual variability in left ILF microstructure did not correlate with the difference (immediate – delayed) in overall recollection between immediate and delayed memory test (FA: $r(45) = 0.16$, $p_{1\text{-tailed}} = .14$; MD: $r(45) = -0.22$, $p_{1\text{-tailed}} = .07$). Based on the hypothesised relationship between ILF microstructure and reward-related memory performance in the immediate memory test specifically, immediate memory test performance was investigated for a correlation with left ILF microstructure. Variability in overall recollection at immediate memory test did not correlate with left ILF microstructure (FA: $r(45) = -0.14$, $p_{1\text{-tailed}} = .82$; MD: $r(45) = -0.001$, $p_{1\text{-tailed}} = .50$).

An exploratory analysis of delayed memory test performance showed no significant correlation between overall recollection and left ILF microstructure (FA: $r(45) = -0.30$, $p_{1\text{-tailed}} = .979$; MD: $r(45) = 0.20$, $p_{1\text{-tailed}} = .906$).

#### *5.2.2.4.2 Reward-related recollection memory benefit*

Left ILF microstructure did not correlate with the difference (immediate – delayed) in reward-related recollection memory benefit between immediate and delayed memory test (FA: $r(45) = 0.05$, $p_{1\text{-tailed}} = .38$; MD: $r(45) = -0.10$, $p_{1\text{-tailed}} = .25$). Based on the hypothesised relationship between ILF microstructure and reward-related memory performance in the immediate memory test specifically, immediate memory test performance was investigated for a correlation with left ILF microstructure. The reward-related recollection memory benefit at immediate memory test did not significantly correlate with left ILF microstructure (FA: $r(45) = 0.21$, $p_{1\text{-tailed}} = .08$; MD: $r(45) = -0.07$, $p_{1\text{-tailed}} = .31$).

An exploratory analysis of delayed memory test performance showed no significant correlation between the reward-related recollection memory benefit and left ILF microstructure (FA: $r(45) = 0.14$, $p_{1\text{-tailed}} = .175$; MD: $r(45) = 0.05$, $p_{1.\text{-tailed}} = .617$).

### 5.2.2.5 Right ILF microstructure related to reward-related memory benefits

#### *5.2.2.5.1 Overall recollection*

There was no significant correlation between right ILF microstructure and interindividual variability in the difference (immediate – delayed) in overall recollection between immediate and delayed memory test (FA: $r(45) = 0.06$, $p_{1\text{-tailed}} = .35$; MD: $r(45) = -0.08$, $p_{1\text{-tailed}} = .30$). Based on the hypothesised relationship between ILF microstructure and reward-related memory performance in the immediate memory test specifically, immediate memory test performance was investigated for a correlation with right ILF microstructure. Interindividual differences in right ILF microstructure did not significantly correlate with interindividual differences in overall recollection at immediate memory test (FA: $r(45) = -0.26$, $p_{1\text{-tailed}} = .96$; MD: $r(45) = 0.11$, $p_{1\text{-tailed}} = .77$).

An exploratory analysis of delayed memory test performance showed no significant correlation between overall recollection and right ILF microstructure (FA: $r(45) = -0.30$, $p_{1\text{-tailed}} = .976$; MD: $r(45) = 0.17$, $p_{1\text{-tailed}} = .869$).

#### *5.2.2.5.2 Reward-related recollection memory benefit*

Before FWE-correction, right ILF microstructure significantly correlated with the difference (immediate – delayed) in reward-related recollection memory benefit between immediate and delayed memory test (FA: $r(45) = 0.24$, $p_{1\text{-tailed}} = .05$; Figure 5.5 B; after outlier removal: same direction but not significant; MD: $r(45) = -0.26$, $p_{1\text{-tailed}} = .04 > \alpha_{\text{corrected}} = .007$). Based on the hypothesised relationship between ILF microstructure and reward-related memory performance in the immediate memory test specifically, immediate memory test performance was investigated for a correlation with right ILF microstructure. Before FWE-correction, there was a trend towards an uncorrected significant correlation between interindividual differences in right ILF microstructure and interindividual differences in the reward-related recollection memory benefit at immediate memory test (FA: $r(45) = 0.20$, $p_{1\text{-tailed}} = .09$; Figure 5.5 C; MD: $r(45) = -0.08$, $p_{1\text{-tailed}} = .30$).

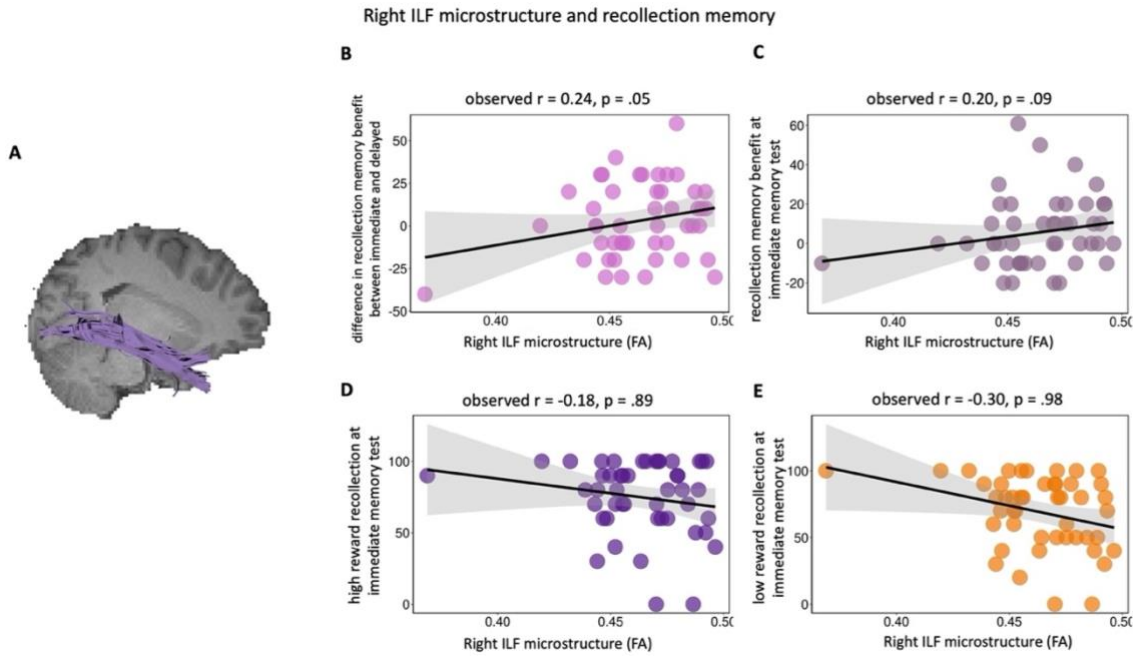


**Figure 5.5. Correlation of right inferior longitudinal (ILF) fractional anisotropy (FA) and recollection memory. A:** Right ILF on brain slice. **B.** Uncorrected significant positive correlation of right ILF FA with the difference (immediate – delayed) in reward-related recollection memory benefit between immediate and delayed memory test. **C.** Positive correlation of right ILF FA with reward-related recollection memory benefit at immediate memory test. **D.** Negative correlation of right ILF FA with high reward recollection at immediate memory test. **E.** Negative correlation of right ILF FA with low reward recollection at immediate memory test. The line of best fit and 95% confidence interval (CI) is shown on each scatterplot with 47 data points.

The follow-up showed neither interindividual differences in high reward (FA: $r(45) = -0.18$, $p_{1\text{-tailed}} = .89$) nor low reward (FA: $r(45) = -0.30$, $p_{1\text{-tailed}} = .98$) recollection at immediate memory test significantly correlated with right ILF microstructure (FA). Since the correlation between right ILF microstructure measured with FA was investigated for a positive correlation and both high and low reward recollection negatively correlated with right ILF FA, the follow-up was not significant. When tests were undirected, the correlation between right ILF FA and low reward recollection at immediate memory test was significant ($p_{2\text{-tailed}} = .04$) while the correlation with high reward recollection was not ($p_{2\text{-tailed}} = .22$).

An exploratory analysis of delayed memory test performance showed no significant correlation between the reward-related recollection memory benefit and right ILF microstructure (FA: $r(45) = -0.09$, $p_{1\text{-tailed}} = .719$; MD: $r(45) = 0.22$, $p_{1\text{-tailed}} = .933$).

## 5.3 Discussion

What is remembered during episodic memory formation is influenced by salience (e.g., Cohen et al., 2017; Mason at al., 2017; Miendlarzewska et al., 2016; Shohamy & Adcock, 2010), consolidation processes during sleep, and their interaction (Igloi et al., 2015; Studte et al., 2017). Here, I employed spherical deconvolution tractography to investigate the relationship between interindividual variability in white matter pathways and variability in reward-related recollection memory for intentionally memorised items. Participants encoded pictures of scenes and were differently rewarded (high versus low reward) for remembering the scenes in the memory tests that followed. During encoding, participants were informed whether a scene will gain them high or low reward for correctly remembering it. Their memory was tested in an immediate and a delayed memory test. Scene memory was investigated in a standard remember-know-new design (Yonelinas, 2002). Indicators of overall memory and reward-related memory benefits were correlated with indicators of fibre tract microstructure.

Overall, recollection memory performance was high, but reward only displayed a trend towards a significant influence on recollection memory. This was not expected but could be attributed to the overall small number of memoranda (20 items per condition). Thusly, the number of to-be-forgotten items might be reduced in a manner that selective memory formation and consolidation becomes unnecessary. Furthermore, it has to be noted that none of the reported correlations survived FWE-correction and should therefore be interpreted with caution. The following paragraphs summarise the findings and provide cautious interpretations.

### 5.3.1 Delayed memory test performance and fornix microstructure

I expected fornix microstructure to be correlated with reward-related memory benefits in the delayed memory test specifically, since dopamine-driven memory formation in the hippocampal-VTA loop (Lisman & Grace, 2005) leads to reward-related memory benefits reliably after a longer delay (Adcock et al., 2006; Murty et al., 2017). I did not find a relationship between fornix microstructure and the reward-related recollection memory benefit at delayed memory test. However, variability in fornix

microstructure did correlate with variability in overall recollection at delayed memory test. This is in line with other findings that show the ability of reward to spread enhancement onto items encoded in proximity to reward (Cohen et al., 2017; Murayama & Kitagami, 2014; Wimmer & Shohamy, 2012). In the study by Murayama and Kitagami (2014), encoding was followed by an unrelated rewarded task or not. Memory for objects followed by reward on an unrelated task was increased. This was apparent only after a delay. This effect was interpreted as being related to dopaminergic memory consolidation processes (Murayama & Kitagami, 2014). Here, overall recollection at delayed memory test, independent of reward, was related to fornix microstructure. Furthermore, high and low reward recollection memory did not significantly differ. Both of these results point to the possibility that reward in this study might have also increased memory for low reward items that were encoded in temporal proximity to high reward items. This was possibly supported by dopaminergic consolidation processes exemplified by the relation of overall delayed memory performance to fornix microstructure.

### 5.3.2 Immediate memory test performance and uncinate fasciculus microstructure

I found left UF microstructure to be correlated with the difference in overall recollection between immediate and delayed memory test. As hypothesised, UF microstructure positively correlated with recollection memory at immediate but not at delayed memory test. The reward-related recollection benefit did not correlate with left UF microstructure. The associative memory processes that have been found to relate to UF microstructure (Alm et al., 2016; Metzler-Baddeley et al., 2011) support my findings with overall recollection. Like with fornix microstructure, I did not find a correlation between left UF microstructure and reward-related recollection benefit. However, based on the study by Reggente and colleagues (2018), I expected a correlation between left UF microstructure and the reward-related recollection memory benefit at immediate memory test. Here, both high and low reward recollection at immediate memory test correlated with left UF microstructure. In the study by Reggente and colleagues (2018) participants freely recalled word lists in a study-test design. Words were assigned high or low value for correct recall. After participants' recall they received

feedback on their performance and a new list started (Reggente et al., 2018). In both the study at hand and Reggente et al.'s (2018) study, participants intentionally encoded items for memory tests. Here, all items were encoded before the memory test and no feedback on performance was given, so participants might encode less systematically. Furthermore, low reward recollection was higher in the study at hand than low value recall in the Reggente et al. (2018) study. Consequently, reward-related memory benefits in this study might be too small and not variable enough to be reflected in interindividual differences of white matter microstructure. Furthermore, Alm and colleagues (2016) proposed UF microstructure to be related to associative memory especially under conditions of competing memory representations at retrieval. With overall memory performance being fairly high in both reward conditions in the present study, memory representations might be stable and therefore non-competing.

### 5.3.3 Reward-related memory benefit at immediate memory test and ILF microstructure

In the present study, variability in microstructure of the right ILF was related to variability in the change of the reward-related recollection memory benefit from immediate to delayed memory test. As hypothesised, the reward-related recollection memory benefit at immediate memory test related to right ILF microstructure while the reward-related recollection memory benefit at delayed memory test did not. The relationship between right ILF microstructure and the reward-related memory benefit at immediate memory test seems to have been driven by participants' low reward memory performance. Variability in low reward recollection at immediate memory test correlated *negatively* with right ILF microstructure where participants with higher microstructure indices displayed lower memory for low reward scenes. Participants' strategic engagement of semantic encoding during intentional memorisation of high or low value items has been shown to influence memory in an immediate memory test (Cohen et al., 2017). In a study by Cohen and colleagues (2017), participants displayed varying degrees in reward-sensitivity. While participants that reported to not be sensitive to the value assigned to the stimulus during encoding showed no difference in memory for high versus low value items, participants with moderate to strong sensitivity showed better memory for high than low value items. Participants with strong value

sensitivity described trying to ignore low value items to increase their points (Cohen et al., 2017). In another study, participants' selectivity index, their ability to optimise encoding for high value items, correlated negatively with low value recall and just mildly with high value recall (Cohen et al., 2014). Furthermore, the selectivity index of participants that reported ignoring low value items was higher than that of participants reporting to have tried harder to memorise the high value items. Selectivity indices related to task-based activation of areas along the temporal lobe during the encoding period of the item (Cohen et al., 2014). Those areas are described to be innervated via the ILF (Bajada et al., 2017). All these results support the findings in the present study. Participants with higher ILF microstructure displayed higher reward-related recollection memory benefits at immediate memory test. This was driven by the negative correlation between ILF microstructure and low reward recollection. Participants with higher microstructure of the ILF, the tract connecting semantic processing areas along the temporal lobe, showed reduced memory for low reward scenes. This might reflect these participants' ability to systematically disengage semantic encoding and thereby successfully disregard low reward information.

### 5.3.4 Limitations and future directions

Consistent with earlier findings (Adcock et al., 2006; Murayama & Kitagami, 2014; Spaniol et al., 2014), I expected the reward-related recollection memory benefit to increase at delayed memory test, but it did not differ from the reward-related recollection memory benefit at immediate memory test in the present study. Furthermore, high and low reward recollection did not significantly differ from each other. Here, a low number of scenes were presented for memorisation overall (40 items) and participants were encouraged to continuously memorise the scenes during encoding. This led to high memory performance on both memory tests. Other studies employed distractor tasks to discourage participants from practicing items in the inter-trial-interval (Adcock et al., 2006). A future study could include more items overall as well as a filler/distractor task during encoding to potentially increase the reward-related memory benefit at delayed memory test. A future study could also include a control group without reward manipulation to determine the to be expected baseline memory performance in immediate and delayed memory test. The proposed increase in low

reward memory due to temporal proximity with high reward items during encoding supported by dopaminergic consolidation can then be interrogated further. Additionally, it has to be noted that none of the reported correlations survived FWE-correction, so all interpretations should be taken with caution.

## 5.4 Chapter Summary

Although none of the reported correlations survived FWE-correction, this study contributes to the body of research relating fornix microstructure with recollection memory. As with details in autobiographical memory (e.g., Hodgetts et al., 2017), recall that is further removed from encoding (delayed memory test) correlated with fornix microstructure. Additionally, the reward-related recollection memory benefit at immediate memory test displayed a relationship with right ILF microstructure. This adds to the literature showing that strategic engagement of semantic processing during value-based encoding is driven by strategic ignoring of low value information (Cohen et al., 2014; Cohen et al., 2017).

# Chapter 6: Resting-state functional connectivity within the hippocampal-VTA loop underlying delayed memory

During an average day, we encounter a large amount of information, but we do not remember everything. For memory formation to be adaptive, salient information needs to be remembered selectively. Different ways that salience has been introduced to information for the investigation of selective memory formation include reward (Adcock et al., 2006; Murty et al., 2017; Wolosin et al., 2012), point values that represent rewards (Castel, 2007; Cohen et al., 2014; 2016; Cohen et al., 2019), novelty (Bunzeck et al., 2010; Bunzeck et al., 2012; Düzel et al., 2010; Lisman & Grace, 2005), and curiosity (Gruber, Gelman, & Ranganath, 2014). One underlying mechanism common to these different studies of memory formation for important information lies in the interaction between parts of the mesolimbic system (i.e., NAcc and VTA) and the hippocampus via dopamine (Adcock et al., 2006; Gruber et al., 2014; Lisman, Grace, & Düzel, 2011; O'Carrol et al., 2006). Cohen and colleagues (Cohen et al., 2014; 2016; Cohen et al., 2017) suggest that another mechanism lies in the selective engagement of semantic encoding. They argue that these two mechanisms, dopamine-driven enhancement and selective semantic encoding, are distinct and contribute more or less to selective memory for rewarding information depending on task structure and demands (Cohen et al., 2017; Cohen et al., 2019). Additionally, dopamine-driven enhancement for high reward information is often more pronounced after a delay, pointing towards the importance of consolidation and post-encoding processes (Adcock et al., 2006; Murty et al., 2017; Studte et al., 2017). Therefore, memory enhancements for rewarding information can be supported by mesolimbic-MTL interactions (e.g., Gruber et al., 2016; Wittman et al., 2005), but might similarly rely on selective semantic encoding (e.g., Cohen et al., 2017).

Memory-modulation, as well as functional activation through reward, display a high level of between-subject variability (e.g., Adcock et al., 2006; Berridge, 2007; Cohen et al., 2005; Cohen et al., 2014; 2016; Gruber et al., 2016). When data is investigated for central tendency (most common = average), interindividual variability in behaviour and

brain activation are treated as noise as opposed to inherent features of individuals contributing to function (Seghir & Price, 2018; Tavor et al., 2016). With data from the Human Connectome Project, Finn and colleagues (2015) were able to show that functional connectivity profiles can act like a fingerprint. Based on an individual's connectivity profile at rest or during a task acquired one day, that same individual could be reliably identified from a large sample of connectivity profiles at rest or during different tasks acquired on a different day. This identification was reliable not only across sessions (different days) but also across rest and task (identifying an individual's task-based connectivity from their connectivity at rest) (Finn et al., 2015). In a different study by Tavor and colleagues (2016), resting-state functional connectivity profiles were able to predict interindividual differences in properties of task activation (Tavor et al., 2016). In the present study, a network-level approach is employed to investigate interindividual differences in the effects of intentional memorisation on immediate versus delayed memory for rewarding information and their relationship to variability in resting-state functional connectivity. Based on the literature and the results reported in Chapter 5, two networks were investigated here: the hippocampal-VTA loop and the semantic temporal lobe network.

In a large sample, Kahn and Shohamy (2013) found the regions within the hippocampal-VTA loop (HC, Nacc, VTA) to be intrinsically connected at rest. They also showed that this intrinsic connectivity varies between subjects. In a study of intentional memorisation by Adcock and colleagues (2006), participants received high or low reward cues preceding to-be-remembered scenes. Participants were informed of the memory test procedures. After 20 to 26 hours, their memory for the scenes was tested. Participants remembered more high than low reward scenes. Activation of the VTA, NAcc, and hippocampus during high reward cue presentation was higher for remembered as opposed to forgotten scenes that followed. Furthermore, increased connectivity between VTA and hippocampus after a high reward cue was predictive of memory formation. Interindividual differences in the activation of VTA during the cue-period of high value remembered versus forgotten trials correlated with interindividual differences in high confidence memory performance (Adcock et al., 2006). Since resting-state functional connectivity profiles can predict task-based activation (Tavor et al.,

2016) and resting-state activity within the MTL has been found to be positively correlated with memory ability (Wig et al., 2008), this study investigated interindividual differences in resting-state functional connectivity between VTA, NAcc, and hippocampus and related those to differences in memory performance in an intentional reward-motivated memorisation task (cf., Adcock et al., 2006).

Memory for high value information is also supported by a more systematic and selective engagement of the semantic processing system (Cohen et al., 2014; 2016; Cohen et al., 2017; Cohen et al., 2019). The ATL is proposed to serve as an amodal "hub" within a distributed network for semantic processing (Ralph et al., 2017; Patterson et al., 2007). Object representations in the visual system and valence representations from frontal and midbrain regions are associated and these associations are upheld by connectivity along the temporal lobe (Bajada et al., 2017; Ralph et al., 2017). In particular, the anterior ITG and the anterior MTG are proposed as amodal semantic hubs because of converging connectivity from all modalities (Ralph et al., 2017). Semantic processing within this hub has been shown to differ between individuals (Chen et al., 2016). Cohen and colleagues (2019) investigated the relationship between successful memory and encoding activity in reward processing as well as in semantic processing regions. They employed study-test cycles with feedback aimed at encouraging strategic processing (Cohen et al., 2017). In Cohen et al. (2019), two stimuli were presented at the same time. One was arbitrarily assigned high value for correctly remembering it in the subsequent memory test, the other one was assigned low value. Encoding-related activation of VTA and NAcc, as well as connectivity between VTA and MTL regions, was increased for successful memory, independent of reward. Contrarily, activation within the semantic processing system displayed more systematic effects. Increased connectivity between a cortical region and the MTG, ITG, as well as the fusiform cortex was correlated with selective memory (high > low value memory). Participants with increased connectivity to regions within the semantic temporal lobe system (MTG, ITG, fusiform) displayed higher selective memory (Cohen et al., 2019). In a different study, participants' selectivity in memory for high versus low value items was correlated with higher task-based activation in posterior parts of the MTG and ITG during encoding of high rather than low value items (Cohen et al., 2014). In the present study, changes in

resting-state connectivity of the anterior ITG, the PrC, and a region within the occipital cortex to other regions within the semantic temporal lobe network are investigated for their relationship to intentional memorisation of rewarding information for an immediate and a delayed memory test.

Some studies report a relationship between functional connectivity within the salience-hippocampal network during encoding and intentional memorisation of high value information (Adcock et al., 2006; Cohen et al., 2014). Other studies point towards the relationship between functional connectivity within the salience-hippocampal network during post-encoding rest and incidental memory for high value information (Gruber et al., 2016). There is a gap in the literature considering the relationship between the intrinsic connectivity of this network (measured at rest independent of a task) and intentional memorisation of rewarding information for an immediate versus delayed memory test. Furthermore, although processing within the semantic temporal lobe network has been related to memory modulation through reward and selective encoding (Cohen et al., 2014; 2016), the literature concerning the effect of reward on intentional memorisation without feedback and processing within the semantic temporal lobe network is lacking. Here, a network level approach and between-subject variance is employed to explore and better understand function-behaviour associations related to interindividual differences in reward-based memory.

In this study, a relationship between resting-state functional connectivity (RSFC) within the hippocampal-VTA loop and reward-related recollection memory differences between immediate and delayed memory test was hypothesised. In particular, the relationship between RSFC and reward-related recollection memory was hypothesised to be more prevalent for delayed memory test performance. Within the semantic temporal lobe network, a relationship between RSCF and reward-related recollection memory differences between immediate and delayed memory test was hypothesised. This relationship was hypothesised to be more prevalent for interindividual differences in immediate memory test performance.

# 6.1 Methods

## 6.1.1 Participants

Resting-state functional MRI data collection was conducted in the same participant pool as described in Chapter 3 (N = 55). The Ethical Review Board of the School of Psychology at Cardiff University approved the study procedures. For the experiment described here, eight participants had to be excluded from the analysis due to an error during behavioural data collection. Five additional participants were excluded due to low quality of the resting-state fMRI data (for quality assurance variables and exclusion criteria see "6.1.4.1 Imaging- acquisition and resting-state fMRI pre-processing"). Data analyses are based on 42 participants (6 males, mean age = 19.07, SE = 0.25, range = 18-25).

## 6.1.2 Behavioural procedures

The study procedure was described in Chapter 5 (see Figure 6.1 for overview). The participants encoded 40 scenes and were differently rewarded for correctly remembering the scenes in the subsequent memory tests (high versus low reward).

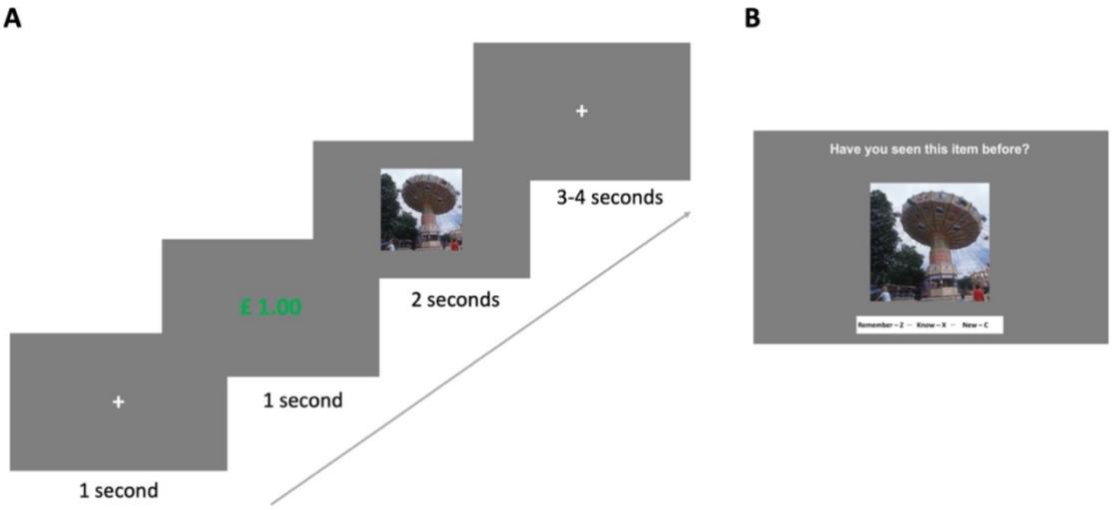


**Figure 6.1. Study procedure. A.** Exemplary high reward encoding trial. Participants made yes/no-pleasantness judgements and were informed of the reward they would receive for correctly remembering the scenes in the subsequent memory tests (high reward = £1.00 in green font; low reward = £0.01 in white font). **B.** Memory test. Measuring recollection and familiarity through a classic remember-know-new judgement (Yonelinas et al., 2002). Participants' memory for half of the encoded scenes was tested in an immediate memory test after a 2-minute distractor, memory for the other half of the scenes was tested after a 24-hour delay.

During encoding, participants made yes/no- judgements on the perceived pleasantness of the scene. Depending on the reward-condition, they received high (£1.00) or low (£0.01) reward for correctly remembering the scenes in the subsequent memory tests. Participants were instructed to use the inter-trial-interval (ITI) of 3-4 seconds to finish pleasantness judgements they were unable to make during scene presentation and the remainder of the time to memorise the scenes for the memory tests. The ITI consisted of a white fixation cross on a grey background. High and low reward trials were randomised. Encoding was followed by a 2-minute paper pen arithmetic test as a distractor task. Participants' memory for the scenes was tested in an immediate and a 24-hour delayed memory test. Participants were informed that accurate memory would lead to reward corresponding to cue during encoding (high reward = £1; low reward = £0.01) and that "false alarms" ("old"-response to new item) were penalised (£0.25). Each memory test comprised 10 items from high and 10 items from low reward conditions as well as 10 new distractors. Item presentation was randomised. Recollection and familiarity measures for the scenes were examined in a classic remember-know-new-design (e.g., Yonelinas et al., 2002).

## 6.1.3 Stimuli

The 60 coloured scenes were taken from Konkle et al. (2010). Details of the selection and randomisation procedure are described under 5.1.3 in Chapter 5. Scenes were pseudo-randomly selected from the categories provided in the database. No scenes depicting the same setting were included. Most images did not depict humans or animals.

## 6.1.4 Imaging

### 6.1.4.1 Imaging- acquisition and resting-state fMRI pre-processing

Resting-state functional imaging acquisition and pre-processing were the same as in Chapter 4. High-resolution anatomical and functional images were obtained with a 3 Tesla MRI scanner (Siemens Magnetom Prisma). Pre-processing and connectivity analyses were conducted using the CONN toolbox (version 18.b, Whitfield-Gabrieli & Nieto-Castanon, 2012), which employs SPM12 functions (Wellcome Trust Centre for

Neuroimaging, London). All functional scans were realigned and unwarped following Andersson et al. (2001). Then, each subject's functional run was centred at [0,0,0] and slice-time corrected following Henson et al. (1999). Outlier scans were identified in CONN with ART (frame-wise displacement >0.5mm, global BOLD signal change >3SD; www.nitrc.org/projects/artifact_detect/). Simultaneously, the images were segmented into CSF, grey matter, and white matter and normalised (Ashburner & Friston, 2005). After segmentation and normalisation to MNI space, functional images were spatially smoothed with a 6mm full-width-half-maximum (FWHM) Gaussian kernel. Then, functional images were denoised. During denoising, white matter and CSF confounds identified via aCompCor (Behzadi et al., 2007), the 12 noise components due to motion, ART-identified outliers, and the detrending term were removed from the BOLD signal within each voxel for each subject during the one resting-state functional run with an Ordinary Least Squares (OLS) linear regression. The OLS linear regression retains the BOLD timeseries orthogonal to the confounds because confounds are included as nuisance regressors. The resulting signal was temporally band-pass filtered between 0.008Hz and 0.09Hz to minimise the influence of noise.

Five quality assurance variables were used to identify participants to be excluded from further analyses: number of invalid scans identified by ART, maximum and mean motion, and maximum and mean global signal change. Participants whose resting-state data were 1.5 above or below the 3$^{rd}$ quartile on three or more variables and or whose number of invalid scans was above 20% of the total number of scans were excluded from the functional connectivity analyses (Power et al., 2014).

### 6.1.5 Behavioural and microstructure analyses

Behavioural and DTI analyses were the same as described in Chapter 5 and were merely repeated in the smaller sample (N = 42 here vs. N = 47 in Chapter 5) to ensure that the removal of five participants due to quality of the resting-state data did not change the reported results. Neither the behavioural results nor the correlation results between behaviour and microstructure were different or differed in a way that would change interpretation from the results reported in Chapter 5 (see Appendix 7).

### 6.1.6 Functional resting-state analyses

Functional resting-state analyses and regions of interest (ROIs) included in the analyses were the same as described in Chapter 4. The ROIs investigated within the hippocampal-VTA loop were left and right hippocampus (Harvard-Oxford; Grabner et al., 2006), left and right NAcc (Harvard-Oxford; Grabner et al., 2006), as well as left and right VTA (Murty et al., 2014; non-thresholded binarised probabilistic map). There were no strong hypotheses regarding lateralisation within the hippocampal-VTA loop. Therefore, ROIs from both hemispheres were included in the model.

The ROIs within the semantic temporal lobe network modelled in the resting-state analysis were the anterior ITG, the anterior temporal fusiform cortex (TFC), the anterior MTG, the anterior STG, the posterior ITG, and the posterior TFC via CONN (Harvard-Oxford; Grabner et al., 2006), the reconstructed OCC-seed region (2mm isotropic sphere reconstructed around MNI coordinates reported in Bajada et al., 2017), as well as the PrC (hand-drawn with anatomical landmarks from averaged brain via DARTEL from Gruber et al., 2016). Separate models within left and right hemispheres were investigated in the resting-state analyses.

Within CONN, Fischer-transformed bivariate Pearson correlation coefficients between the averaged BOLD timeseries across the voxels within each ROI and the averaged BOLD timeseries across the voxels within the other ROIs of the model were calculated. The behavioural measures of interest that were introduced into CONN were the same as described in Chapter 5 under “5.1.6 Correlation analysis”. Only recollection memory was investigated for its relationship to changes in functional connectivity at rest because reward-modulation was believed to be stronger in recollection than familiarity (Cohen et al., 2017; Gruber et al., 2016). Furthermore, due to high memory performance and a small number of items (40 items) overall, familiarity measures were based on very few trial numbers. Recollection at immediate and delayed memory test was calculated and z-standardised (see formula 3.2. in Chapter 3). Reward-related recollection memory benefits (high – low reward) and overall recollection (average of high and low reward) at immediate and delayed memory test were introduced into

CONN. Indicators of changes of reward-related memory from immediate to delayed memory test were calculated for recollection. Two different indicators of memory change were calculated based on the hypothesised relationship between the network of interest and the timepoint of the memory test. For the hippocampal-VTA loop, the relationship between memory performance and variability in functional connectivity at rest was hypothesised to be more pronounced for performance in the delayed as opposed to immediate memory test. Therefore, the index of change was calculated by subtracting immediate memory test performance from delayed memory test performance (reward-related recollection memory benefit/overall recollection at delayed – reward-related recollection memory benefit/overall recollection at immediate memory test). For the semantic temporal lobe network, the relationship between memory performance and variability in functional connectivity at rest was hypothesised to be more pronounced for immediate as opposed to delayed memory test performance. Therefore, the index of change was calculated by subtracting delayed memory test performance from immediate memory test performance (reward-related recollection memory benefit/overall recollection at immediate – reward-related recollection memory benefit/overall recollection at delayed memory test). Z-standardised values of the behavioural measures of interest and z-standardised microstructure indices were introduced into CONN. Microstructure indices were also included to investigate whether microstructure was related to resting-state functional connectivity. The relationship between microstructure of the fornix and RSFC within the hippocampal-VTA loop was examined. The relationship between microstructure of the ILF and RSFC within the semantic temporal network was examined.

#### 6.1.6.1 Functional connectivity analysis

Details of the functional connectivity analysis are described in Chapter 4 under 4.1.6.4. In CONN, separate GLMs, employing an OLS solution, were used to define linear associations between an independent measure of interest (i.e., microstructure or behaviour) and functional connectivity between the ROIs (six hippocampal-VTA loop network ROIs [three right, three left], eight right, or eight left semantic temporal lobe network ROIs) as dependent measures. For example, to investigate whether variability between subjects in the change of the reward-related recollection memory benefit from

immediate to delayed memory test was related to changes in functional connectivity between the ROIs of the hippocampal-VTA loop at rest, an OLS GLM is employed to express a linear regression of ROI-to-ROI connectivity (measured by a bivariate correlation) on to the behavioural effect. Six GLMs were investigated within the hippocampal-VTA loop (4 behavioural measures [(1) index of the difference between delayed and immediate (delayed – immediate) memory test in the reward-related recollection memory benefit, (2) index of the difference between delayed and immediate memory test in overall recollection, (3) reward-related recollection memory benefit at delayed memory test, (4) overall recollection at delayed memory test] and 2 microstructure measures [FA and MD of fornix]). Six GLMs each were investigated within the left and right semantic temporal lobe network (4 behavioural measures [(1) index of the difference between delayed and immediate (immediate – delayed) memory test in the reward-related recollection memory benefit, (2) index of the difference between delayed and immediate memory test in overall recollection, (3) reward-related recollection memory benefit at immediate memory test,(4) overall recollection at immediate memory test] and 2 microstructure measures [FA and MD of fornix]). These GLMs represent the planned analyses; exploratory follow up analyses are reported separately when applicable.

Within each GLM, connection-level corrections of individual ROI-to-ROI connections (t-statistic) were FDR-corrected in three different ways. Analysis-level FDR-correction corrects across the entire connectivity matrix, across all possible connections within the network. Within the hippocampal-VTA loop, analysis-level correction corrects across all 15 possible connections on the connection level. Within the temporal lobe network, analysis-level correction corrects across 28 possible connections. Another connection-level correction is seed-level correction. Seed-level correction was applied across all connections of a certain seed (e.g., five connections of the right NAcc seed to the other ROIs within the hippocampal-VTA loop, seven connections of the right ITG seed to the other ROIs within the semantic temporal lobe network). Connection-level statistics could also be uncorrected. Uncorrected and seed-level FDR-correction on the connection level were combined with an appropriate seed-level correction (F-statistic)

for selecting more than one seed-ROI. FDR-corrections were calculated following Benjamini and Hochberg (1995).

No directed hypotheses were made about whether variability in behaviour or microstructure would be explained by an increase or decrease in functional connectivity at rest. Consequently, all tests were two-tailed. Only follow-up tests were directed based on the effect to be followed up on.

# 6.2 Results

## 6.2.1 Resting-state functional connectivity within the hippocampal-VTA loop

### 6.2.1.1 Overall recollection

The difference of overall recollection between immediate and delayed memory test (delayed – immediate) was not related to resting-state functional connectivity (all F ≤ 1.32, all p-FDR ≥ .554). Interindividual differences in overall recollection memory at delayed memory test did not significantly relate to interindividual differences in functional connectivity within the hippocampal-VTA loop at rest (all F ≤ 1.61, all p-FDR ≥ .356).

In the exploratory analysis of the relationship between functional connectivity at rest and overall recollection memory at immediate memory test, interindividual differences in overall recollection were significantly associated with increased resting-state functional connectivity of the left NAcc ($F(5,36) = 2.69$, $p = .037$, *p-FDR* = .048). This included increased RSFC of left NAcc with left hippocampus ($t(40) = 3.26$, $p = .002$, *p-FDR-analysis* = .011; Figure 6.2 B; outlier removal did not change the results), of left NAcc with right hippocampus ($t(40) = 2.46$, $p = .018$, *p-FDR-seed* = .039; Figure 6.2 C; outlier removal did not change the results), as well as of left NAcc with right NAcc ($t(40) = 2.36$, $p = .024$, *p-FDR-seed* = .039; Figure 6.2 D; outlier removal did not change the results).

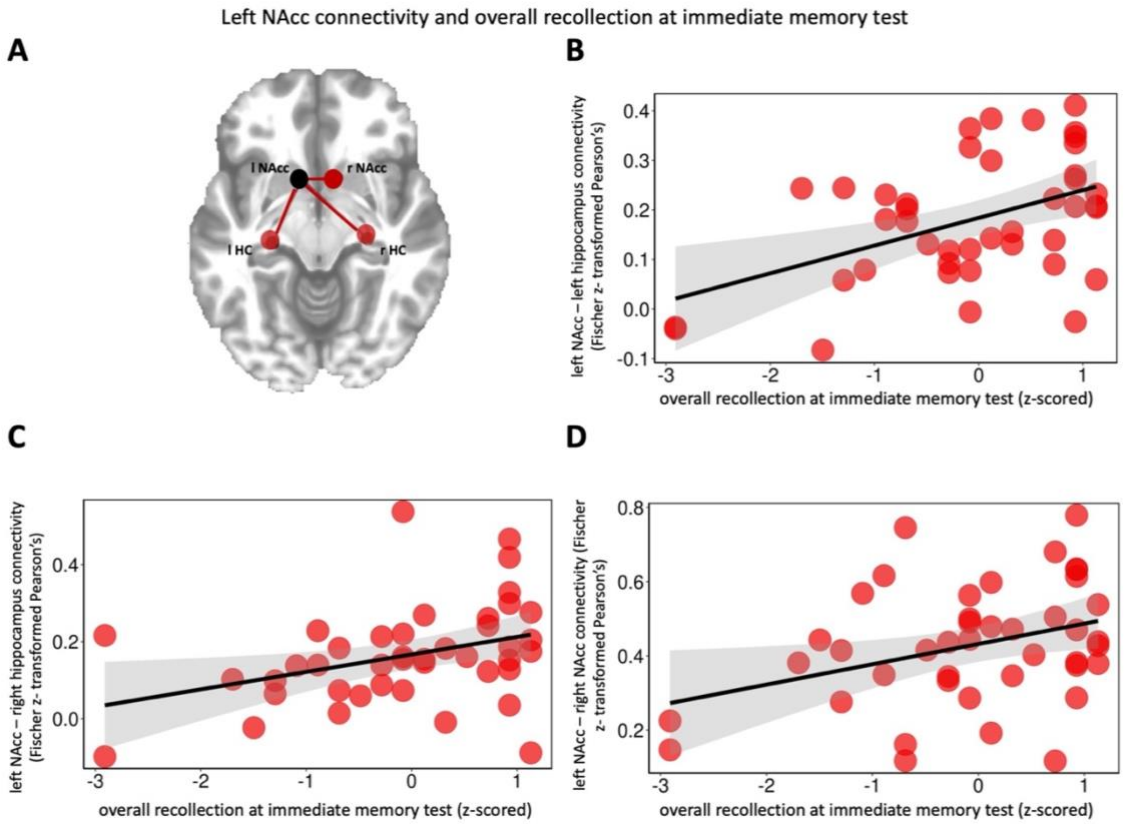


**Figure 6.2. Overall recollection memory at immediate memory test and resting-state functional connectivity within the hippocampal-VTA loop. A.** Connectivity profile of the left NAcc in relation to overall recollection at immediate memory test. ROIs are displayed on reference slice at [9.37/10.20/-8.53]. Dots denote ROIs. Lines denote connectivity. Colours denote direction of connectivity. Red = increase in RSFC. Black = seed ROI. **B.** Scatterplot of ROI-to-ROI connectivity of left NAcc with left hippocampus onto overall recollection at immediate memory test. **C.** Scatterplot of ROI-to-ROI connectivity of left NAcc with right hippocampus onto overall recollection at immediate memory test. **D.** Scatterplot of ROI-to-ROI connectivity of left NAcc with right NAcc onto overall recollection at immediate memory test. Increased connectivity relates to higher overall recollection at immediate memory test. ROI-to-ROI connectivity measured by Pearson's correlation and Fisher z-transformed. Overall recollection was z-scored. The line of best fit and 95% confidence interval is shown on each scatterplot with 42 data points.

### 6.2.1.2 Reward-related recollection memory benefit

The difference in reward-related recollection memory benefit between immediate and delayed memory test (delayed – immediate) was not related to changes in resting-state functional connectivity (all $F \leq 1.74$, all p-FDR $\geq .299$). An exploratory analysis of the relationship between functional connectivity at rest and the reward-related recollection memory benefit at immediate memory test showed no significant effects (all $F \leq 1.76$, all p-FDR $\geq .172$). However, in the analysis of the relationship between interindividual differences in reward-related recollection memory benefit at delayed memory test and functional connectivity at rest, decreased resting-state functional connectivity of the right NAcc was significantly associated with differences in memory

(*F*(5,36) = 2.5, *p* = .048, p-*FDR* = .048). This included decreased RSFC of right NAcc with right hippocampus (*t*(40) = -2.43, *p* = .020, *p-FDR-seed* = .036; Figure 6.3 B), right NAcc with left hippocampus (*t*(40) = -2.41, *p* = .021, *p-FDR-seed* = .036; Figure 6.3 C), as well as right with left NAcc (*t*(40) = -2.39, *p* = .022, *p-FDR-seed* = .037; Figure 6.3 D).

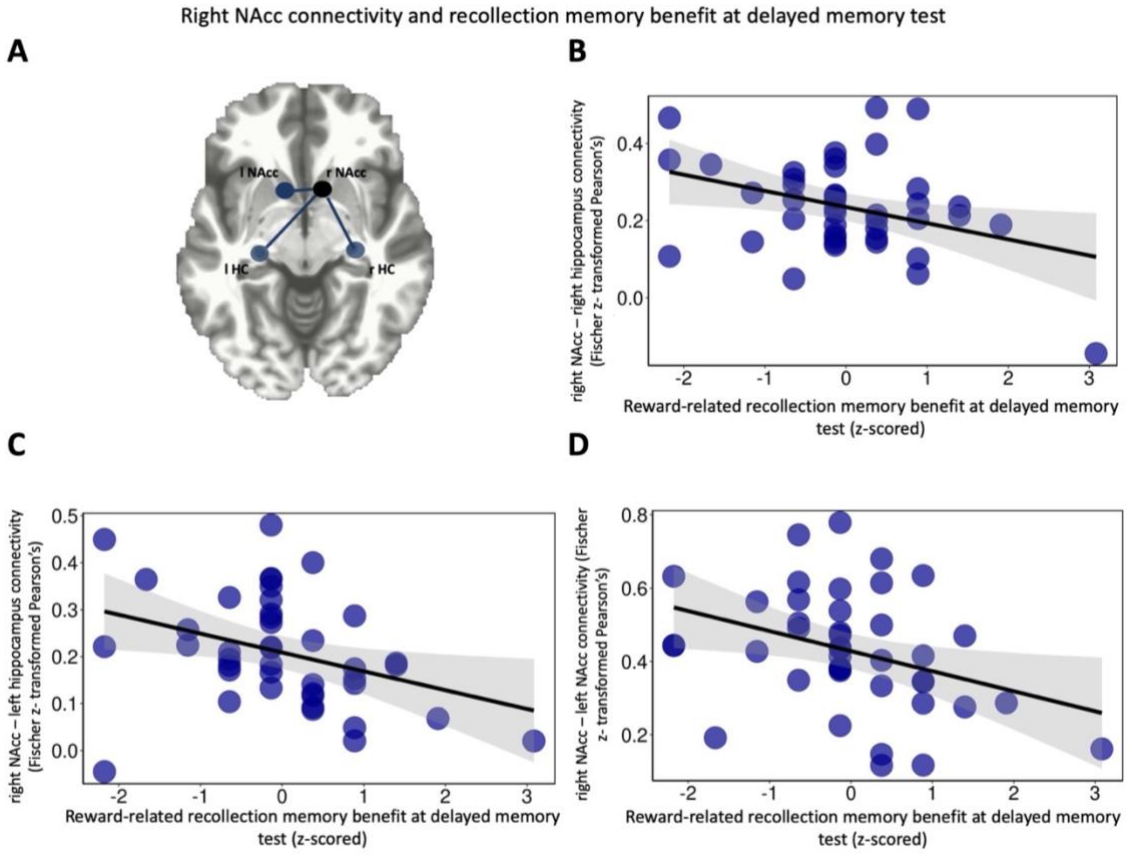


**Figure 6.3. Reward-related recollection memory benefit and resting-state functional connectivity within the hippocampal-VTA loop. A.** Connectivity profile of the right NAcc in relation to reward-related recollection memory benefit at delayed memory test. ROIs are displayed on reference slice at [9.37/12.20/-6.53]. Dots denote ROIs. Lines denote connectivity. Colours denote direction of connectivity. Blue = decrease in RSFC. Black = seed ROI. **B.** Scatterplot of ROI-to-ROI connectivity of right NAcc with right hippocampus onto the reward-related recollection memory benefit at delayed memory test. **C.** Scatterplot of ROI-to-ROI connectivity of right NAcc with left hippocampus onto the reward-related recollection memory benefit at delayed memory test. **D.** Scatterplot of ROI-to-ROI connectivity of right NAcc with left NAcc onto the reward-related recollection memory benefit at delayed memory test. Decreased connectivity relates to higher reward-related recollection memory benefit at delayed memory test. ROI-to-ROI connectivity measured by Pearson's correlation and Fisher z-transformed. Reward-related recollection memory benefit was z-scored. The line of best fit and 95% confidence interval is shown on each scatterplot with 42 data points.

To follow these results up, ROI-to-ROI connectivity within the hippocampal-VTA loop was regressed onto the reward-related recollection memory benefit at delayed memory test while overall recollection at delayed memory test was held constant. In the follow-up, changes in resting-state functional connectivity were investigated for a

decrease based on the results in the relationship between resting-state and the reward-related recollection memory benefit at delayed memory test. Between-subject variability of the behaviour remained significantly related to a decreased resting-state functional connectivity of right NAcc ($F(5,35) = 2.99$, $p = .024$, *p-FDR* = .048). This included decreased RSFC between right NAcc and left NAcc ($t(39) = -2.52$, $p_{1\text{-}tailed} = .008$, $p\text{-}FDR\text{-}analysis_{1\text{-}tailed} = .024$), right NAcc and left hippocampus ($t(39) = -2.51$, $p_{1\text{-}tailed} = .008$, $p\text{-}FDR\text{-}analysis_{1\text{-}tailed} = .024$), as well as right NAcc and right hippocampus ($t(39) = -2.44$, $p_{1\text{-}tailed} = .010$, $p\text{-}FDR\text{-}analysis_{1\text{-}tailed} = .024$).

The relationship between the reward-related recollection memory benefit at delayed memory test and *decreased* functional connectivity between NAcc and hippocampus was unexpected. To further elucidate this relationship, exploratory analyses with high and low reward recollection at delayed memory test were conducted. Only NAcc and hippocampus ROIs were included in each GLM. Interindividual differences in high reward recollection at delayed memory test did not significantly explain changes in resting-state functional connectivity of right NAcc ($F(38) = 0.36$, *p-FDR* = .811). Interindividual differences in low reward recollection at delayed memory test were significantly associated with increased resting-state functional connectivity of right NAcc ($F(3,38) = 3.16$, *p-FDR* = .035). This included increased RSFC between right NAcc and left NAcc ($t(40) = 2.43$, $p = .019$, *p-FDR-analysis* = .042) as well as between right NAcc and left hippocampus ($t(40) = 2.29$, $p = .028$, *p-FDR-analysis* = .042).

#### 6.2.1.3 Fornix microstructure

Interindividual differences in fornix microstructure measure by FA were not significantly related to interindividual differences in resting-state functional connectivity within the hippocampal-VTA loop (all $F \leq 1.32$, all p-FDR $\geq .453$). Between-subject variability of fornix microstructure measured by MD was not related to changes in resting-state functional connectivity within the salience hippocampus network (all $F \leq 1.68$, all p-FDR $\geq .330$).

## 6.2.2 Resting-state functional connectivity within the semantic temporal lobe network

### 6.2.2.1 Right hemisphere and overall recollection

Interindividual variability in the difference of overall recollection between immediate and delayed memory test (immediate – delayed) was not related to resting-state functional connectivity within the semantic temporal lobe network in the right hemisphere (all F ≤ 1.2, all p-FDR ≥ .464). In the analysis of the relationship between interindividual differences in overall recollection at immediate memory test and functional connectivity at rest, none of the investigated seeds displayed a significant effect (all F ≤ 0.82, all p-FDR ≥ .938).

### 6.2.2.2 Right hemisphere and reward-related recollection memory benefit

Between-subject variability in the difference of the reward-related recollection memory benefit between immediate and delayed memory test (immediate – delayed) was not significantly explained by changes in functional resting state connectivity of any of the seeds tested (all F ≤ 0.83, all p-FDR ≥ .848). In the analysis of the relationship between interindividual differences in reward-related recollection memory benefit at immediate memory test and functional connectivity at rest, none of the investigated seeds displayed a significant effect (all F ≤ 0.68, all p-FDR ≥ .257).

### 6.2.2.3 Right ILF microstructure

There was a trend towards a significant relationship between right ILF microstructure measured by FA and an increase in functional connectivity of right PRC with right posterior ITG at rest ($t(40) = 2.77$, $p = .008$, *p-FDR* = .059). Furthermore, there was a trend towards a significant relationship between interindividual differences in right ILF microstructure measured by MD and an increase in functional connectivity of right anterior ITG with the right OCC-seed region at rest ($t(40) = 2.82$, $p = .007$, *p-FDR* = .052).

#### 6.2.2.4 Left hemisphere and overall recollection

Changes in resting-state functional connectivity within the left hemispheric semantic temporal lobe network were not related to between-subject variability in the difference of overall recollection between immediate and delayed memory test (all F ≤ 1.62, all p-FDR ≥ .481). In the analysis of the relationship between interindividual differences in overall recollection at immediate memory test and functional connectivity at rest, none of the investigated seeds displayed a significant effect (all F ≤ 1.67, all p-FDR ≥ .461).

#### 6.2.2.5 Left hemisphere and reward-related recollection memory benefit

Changes in resting-state functional connectivity within the left hemispheric semantic temporal lobe network were not related to between-subject variability in the difference of the reward-related recollection memory benefit between immediate and delayed memory test (all F ≤ 0.96, all p-FDR ≥ .796). In the analysis of the relationship between interindividual differences in reward-related recollection memory benefit at immediate memory test and functional connectivity at rest, none of the investigated seeds displayed a significant effect (all F ≤ 1.07, all p-FDR ≥ .829).

#### 6.2.2.6 Left ILF microstructure

Interindividual differences in left ILF microstructure measured by FA were not related to any changes in resting-state functional connectivity between the regions investigated (all F ≤ 1.05, p-FDR ≥ .270). Interindividual differences in left ILF microstructure measured by MD were significantly related to an increase in resting-state functional connectivity of the left PrC with left posterior ITG ($t(40) = 2.96$, $p = .005$, $p\text{-}FDR = .037$).

## 6.3 Discussion

This study aimed to examine the relationship between interindividual differences in reward-related memory performance in an intentional memorisation task and interindividual differences in resting-state functional connectivity. Two networks were investigated due to their involvement in modulation of memory through reward: the

hippocampal-VTA loop and the semantic temporal lobe network. Only a relationship between interindividual differences in memory performance and variability in resting-state functional connectivity within the hippocampal-VTA loop was found when reward was aimed at memory test as opposed to encoding performance.

### 6.3.1 Resting-state functional connectivity between nucleus accumbens and hippocampus was related to memory

Activation in, or connectivity between, hippocampus and reward-processing areas in the midbrain (VTA) and the ventral striatum (NAcc) during encoding or post-encoding rest had been related to increased memory for rewarding information (Adcock et al., 2006; Gruber et al., 2016; Murty et al., 2017; van der Meer et al., 2010). These studies involved intentional memorisation (Adcock et al., 2006; Murty et al., 2017), incidental memory formation (Gruber et al., 2016), and delayed or immediate memory tests. However, those reports are mostly based on task-based activations and interindividual differences in the intrinsic (resting-state acquired independently of encoding) connectivity between these regions and reward-modulated memory formation need more exploration. Here, resting-state fMRI was employed to investigate the relationship between variability in resting-state functional connectivity within the salience-hippocampal network and variability in reward-related memory formation for immediate versus delayed memory test. Between-subject variability and resting-state functional connectivity is employed to explore the relationship between function and behaviour.

Here, *decreased* functional connectivity between NAcc and hippocampus at rest was related to the reward-related recollection memory benefit at delayed memory test and *increased* functional connectivity between NAcc and hippocampus at rest was related to overall recollection at immediate memory test. Both of these effects seem to be driven by a stronger relationship between *low* reward recollection and variability in the increase of RSFC between NAcc and hippocampus at immediate as well as delayed memory test. Interindividual differences in low reward recollection for both memory test timepoints were related to increased functional connectivity at rest between NAcc and hippocampus. This finding was comparable to other studies finding enhancements

for items not directly paired with reward but encoded before a separate rewarded task or strongly associated with a rewarded item (e.g., Murayama & Kitagami, 2014; Wimmer & Shohamy, 2012). In the study by Wimmer and Shohamy (2012), stimuli were in a first phase consistently paired with each other. Then, in a second phase, one of the associates was paired with reward, the other was not. In a third phase, participants were instructed to pick out of two items, the one they felt was luckier. One of those items was associated with an item that was subsequently rewarded, while not being rewarded itself. Behaviourally, participants were biased towards choosing the neutral item that was associated with a rewarded item. This bias towards items associated with a rewarded item but never rewarded themselves correlated with increased connectivity between hippocampus and striatum, which encompasses the NAcc, during reward processing (Wimmer & Shohamy, 2012). Furthermore, increased encoding activity in NAcc has been found to be related to successful memory, independent of high or low value (Cohen et al., 2019). Here, participants with increased resting-state functional connectivity between NAcc and hippocampus might display a stronger susceptibility to the influence of reward, independent of its size.

### 6.3.2 Resting-state functional connectivity within the semantic temporal lobe network was not related to intentional memorisation

Systematic engagement of processing within a semantic network had been associated to memory for high value information in immediate memory tests (Cohen et al., 2014; 2016). Strategic prioritisation of high reward information through semantic processing had been shown to be separable from reward-related activation within a reward-network (Cohen et al., 2019). However, how strategic engagement of semantic processing influences intentional memorisation in an immediate versus delayed memory test specifically needs further exploration. Here, resting-state fMRI was employed to investigate the relationship of variability in functional connectivity within a semantic temporal lobe network at rest and between-subject variability in intentional memorisation for immediate and delayed memory tests.

Interindividual differences in resting-state functional connectivity in neither the left nor the right hemispheric semantic temporal lobe network were related to recollection memory in this study. The absence of a relationship between recollection memory and resting-state functional connectivity within the semantic temporal lobe network can be explained by the reduced need for strategic semantic encoding for high reward memorisation. In the study at hand, overall memory performance was fairly high. Furthermore, the task that was employed here might not encourage strategic semantic encoding. Cohen and colleagues (2017) demonstrated that study-test cycles with feedback regarding memory performance led to higher reliance of participants on strategic semantic encoding of high versus low reward information than when memory tests were administered at the end of encoding (Cohen et al., 2017). Here, only a small number of scenes (40 items) needed to be encoded overall and no study-test cycles with feedback were provided. Participants might not have needed to rely on strategic elaborative encoding based on semantic processing to ensure good memory performance. Strategic semantic encoding and more dopamine-driven encoding have been proposed to be distinct but also complementary for adaptive memory formation of salient information (e.g., Cohen et al., 2014; Cohen et al., 2017; Cohen et al., 2019). Here, it might have been adaptive to rely on dopamine-driven encoding supported by the hippocampal-VTA loop as opposed to strategic semantic encoding.

### 6.3.3 Limitations and future directions

Only a low number of scenes were encoded overall, and participants were encouraged to utilise ITIs to memorise scenes. Other studies of the relationship between intentional memorisation and functioning within the hippocampal-VTA loop had participants encode a much larger number of items (e.g., Adcock et al., 2006). Additionally, distractor tasks were included to discourage prolonged practice (Adcock et al., 2006). Here, participants might have not seen the need to rely on strategic semantic encoding to successfully remember the scenes. Strategic semantic encoding has been shown to rely on feedback and develop over the course of an experiment (e.g., Cohen et al., 2017). A potential future study could include a larger number of items to be remembered to increase the number of forgotten items and therefore be more sensitive to subtle differences.

## 6.4 Chapter Summary

In conclusion, this study employed resting-state fMRI and an intentional memorisation paradigm to investigate the relationship between reward-modulated memory at immediate versus delayed memory test and functional connectivity within the hippocampal-VTA loop as well as the semantic temporal lobe network at rest. Variability in increased functional connectivity between NAcc and hippocampus at rest was related to recollection for especially low reward information in immediate as well as delayed memory test.

# Chapter 7: General Discussion

This thesis set out to examine the neuroanatomical and neurofunctional underpinnings of reward-modulated memory. Reward designates information as important and important information is more likely to be remembered successfully. This process strongly contributes to adaptive behaviour. Therefore, it seems likely that more than one mechanism contributes to the modulation of memory via reward. This thesis investigated two proposed processes of reward-modulated memory formation, one more dopamine-driven process and one of elaborative semantic encoding (Cohen et al., 2016; Cohen et al., 2019; Miendlarzewska et al., 2016; Shohamy & Adcock, 2010). Additionally, reward has been known to differently affect immediate versus consolidated memory (Murayama & Kuhbandner; 2011; Spaniol et al., 2014; Wittmann et al., 2005). This thesis investigated the different contributions of the networks of interest on immediate and delayed reward-modulated memory. This thesis also examined the influence of reward on hippocampus-dependent associative memory like recollection and temporal order memory. Reward influences memory, but there is striking variability between individuals in reward-modulated memory formation (e.g., Cohen et al., 2005; Gruber et al., 2016; Wolosin et al., 2012). This thesis set out to investigate the relationship between variability in reward-modulated memory and interindividual differences in the anatomical and functional connections in the dopamine-driven and the semantic processing networks. Chapter 2 examined the influence of reward on temporal order memory and whether this depends on the type of post-encoding period, i.e., wakeful rest versus a distractor task. Chapters 3 and 4 examined the anatomical and functional connections within different brain networks and their relationship to reward-modulated temporal order memory specifically. Chapters 5 and 6 examined the anatomical and functional connections within different brain networks and their relationship to modulation of immediate versus consolidated memory through reward. Figure 7.1 provides an overview of the main results from each chapter.

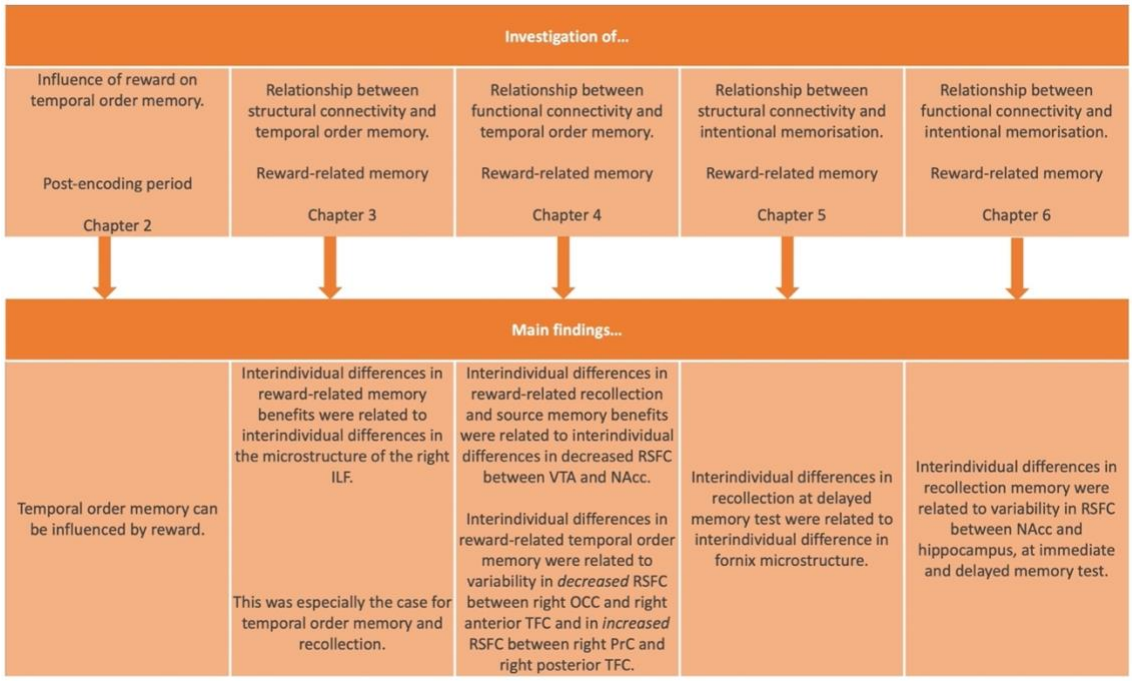


**Figure 7.1. Thesis summary and main findings.** ILF = inferior longitudinal fasciculus, RSFC = resting-state functional connectivity, TFC = temporal fusiform cortex.

In this thesis, reward-modulated temporal order memory and memory consolidation were shown to display different structural and functional correlates. In line with previous research, high versus low reward intentional memorisation led to memory enhancements for high reward memoranda. Furthermore, reward did not explicitly influence temporal order memory on a group level, but interindividual differences in reward-modulated temporal order memory were related to variability in the microstructure of white matter and functional connectivity at rest. In this general discussion I will discuss the main findings of this thesis, the methodology I employed and its associated limitations. I will propose future directions to further build on the findings of this thesis.

## 7.1 Temporal order memory and the semantic network

Chapters 2, 3, and 4 set out to investigate the influence of reward on temporal order memory as well as its neuroanatomical and neurofunctional underpinnings. Diffusion-weighted imaging (DWI) was employed in Chapter 3 to investigate the relationship between interindividual differences in reward-modulated temporal memory and interindividual differences in the microstructure of white matter pathways

connecting regions understood to support reward-related memory formation as well as associative memory processes. In Chapter 4, ROI-based resting-state functional connectivity analysis was employed to investigate the relationship between interindividual differences in reward-modulated memory and interindividual differences in resting-state functional connectivity of regions within the hippocampal-VTA loop and the semantic temporal lobe network. To date, little data has been reported on the influence of reward on temporal order memory in human subjects. In Chapter 2, a trend towards better memory for the temporal order of object pairs from high as opposed to low reward encoding sequences was found. This trend could not be bolstered across the larger sample investigated in Chapters 3 and 4. Despite the lack of a robust behavioural effect on a group level, variability in reward-related temporal order memory benefit was found to be related to variability of a white matter pathway connecting areas along the length of the temporal lobe, the ILF (Chapter 3). Moreover, interindividual differences in resting-state functional connectivity between regions along the temporal lobe, regions that constitute parts of the semantic temporal lobe network, were found to be related to interindividual differences in the reward-related temporal order memory benefit (Chapter 4).

In Chapter 3, interindividual differences in microstructure of the right ILF were found to be related to interindividual differences in the reward-related temporal order memory benefit. In Chapter 4, the regions of interest were chosen due to their relationship to (value-based) semantic processing (Cohen et al., 2019; Ralph et al., 2017) as well as to microstructural (including ILF) termination maps along the temporal lobe (Bajada et al., 2017). Interindividual differences in resting-state functional connectivity between a seed region in the right occipital cortex (right OCC-seed) and the right anterior temporal fusiform cortex were found to be related to interindividual differences in the reward-related temporal order memory benefit. Additionally, interindividual differences in resting-state functional connectivity between the right perirhinal cortex and the right posterior temporal fusiform cortex were also found to be related to interindividual differences in the reward-related temporal order memory benefit. Consequently, both chapters (3 and 4) signify the importance of systematic engagement and disengagement of elaborative semantic processing for temporal order

memory. Thus, the literature on systematic engagement of semantic processing during value-based encoding is extended onto temporal order memory. Furthermore, the studies concerned with the relationship between value-based memory enhancements and systematic semantic encoding employed study-test cycles and feedback to induce strategic behaviour (Cohen et al., 2014; 2016; Cohen et al., 2017). Here, one long encoding block was followed by the memory test. Yet, participants' ability to systematically engage or disengage their semantic processing was found to be related to reward-modulated associative memory for temporal order specifically. This was reflected in the relationship of memory performance to between-subject variability in the microstructure of the ILF as well as to resting-state functional connectivity within the semantic temporal lobe network.

The absence of a strong relationship between variability in temporal order memory and variability in structural and functional connectivity of the hippocampus was surprising based on the known involvement of the hippocampus in temporal order memory processing (e.g., DuBrow & Davachi, 2014; Fortin et al., 2002; Jenkins & Ranganath, 2016; Tubridy & Davachi, 2011). Most of these studies reported this relationship between activation patterns within the hippocampus and temporal order memory based on functional MR imaging during encoding. Furthermore, temporal order memory was primarily assessed within study-test cycles in those studies. This could increase the fidelity of hippocampal representations for temporal order. In contrast, the studies reported within this thesis investigated temporal order memory for object pairs after one long encoding block and an intervening distractor task. Furthermore, the relationship between variability in behaviour and variability in the structural as well as functional resting-state connectivity as opposed to task-based activity was investigated in this thesis. The temporal order memory representations participants rely on in the studies presented in this thesis could simply not be fine-grained and detailed enough to be reflected in variability within a hippocampal network. In a study that investigated temporal order memory for autobiographical scenes, participants incidentally encoded indoor and outdoor scenes by taking part in a guided photo taking session around a university campus (St. Jacques et al., 2008). Next, participants were presented with pairs of photos they had taken the previous day and had to make an order discrimination

judgement while functional MR imaging was conducted. Retrieval activity within the right fusiform gyrus was increased during temporal order judgements for scene pairs with a long lag, i.e., with more intervening scenes during encoding (St. Jacques et al., 2008). The results presented in Chapter 4 demonstrated that participants with a distinct pattern of functional resting-state connectivity with the temporal fusiform cortex that follows the representational gradient within the semantic processing network, displayed better high confidence temporal order memory.

## 7.2 Reward-modulated memory and the hippocampal-VTA loop

Chapters 5 and 6 set out to investigate the neuroanatomical and neurofunctional underpinnings of consolidation of intentionally memorised rewarded information. DWI was employed in Chapter 5 to investigate the relationship between interindividual differences in reward-modulated memory and interindividual differences in the microstructure of white matter pathways connecting regions understood to support reward-related memory formation as well as associative memory processes. In Chapter 6, ROI-based resting-state functional connectivity analysis was employed to investigate the relationship between interindividual differences in consolidated reward-modulated memory and interindividual differences in connectivity of the hippocampal-VTA loop and the semantic temporal lobe network. Behaviourally, intentional memorisation for memory tests led to a trend in increased recollection memory for high reward memoranda over low reward items, independent of the timepoint of the memory test. The absence of a reward-related memory benefit in the delayed memory test especially went against the hypothesised increase of reward-related dopamine-driven memory after a delay as based on the literature (e.g., Bunzeck et al., 2010; Murayama & Kitagami, 2014; Murayama & Kuhbandner; 2011; Wittmann et al., 2005). Contrastingly, the relationship between delayed memory test performance and microstructure as well as resting-state functional connectivity within the dopaminergic reward-processing system indicated its involvement, even in the absence of a behaviourally significant effect.

In Chapter 5, interindividual differences in fornix microstructure were related to interindividual differences in overall recollection at delayed memory test. Both high and low reward recollection was positively correlated with fornix microstructure. The fornix comprises the primary output/input pathway between the hippocampus and subcortical regions, including the NAcc (Aggleton et al., 2015; Benear, Ngo, & Olson, 2020). In the animal model, fornix stimulation had been shown to lead to increased dopamine release in the NAcc as well as increased activation in the hippocampus and NAcc (Ross et al., 2016; Shin et al., 2019). Stimulation of the fornix had also been found to improve animals' performance on hippocampus-dependent memory tasks, while fornix-dissected animals showed deficits in certain memory tasks (Charles et al., 2014; Zhang, Hu, Wu, Zhang, & Zhang, 2015). In humans, fornix microstructure had been found to relate to memory performance (Hodgetts et al., 2017; Metzler-Baddeley et al., 2011). The results described in Chapter 5 add to those findings by indicating a relationship between fornix microstructure and delayed memory test performance in an intentional memorisation paradigm. Furthermore, in Chapter 6, interindividual differences in the reward-related recollection memory benefit at delayed memory test were found to be associated with variability in resting-state functional connectivity of the NAcc with the hippocampus. This was driven by the relationship between interindividual differences in recollection memory for *low* reward scenes at the delayed memory test with variability in increased resting-state functional connectivity between the NAcc and the hippocampus. The results of Chapters 5 and 6, in accordance with the literature, indicated that participants with increased intrinsic functional connectivity between the NAcc and the hippocampus display increased recollection at delayed memory test in a rewarded intentional memorisation paradigm. This was possibly supported by their fornix microstructure, reflected in the positive correlation between fornix microstructure and delayed recollection memory. In contrast to the hypothesis, this effect was especially related to participants' recollection memory for scenes they received low reward for remembering. While this was unexpected, other studies have shown that reward can affect memory for items not directly highly rewarded themselves, but encoded in relation to reward (e.g., Murayama & Kitagami, 2014; Wimmer & Shohamy, 2012). For the sample described in this thesis, participants with increased intrinsic functional connectivity between the NAcc and the hippocampus,

possibly supported by their fornix microstructure, exhibit a higher tendency of their recollection memory to be affected by reward, independently of the size of the reward.

## 7.3 Relationship between the semantic temporal lobe network and the hippocampal-VTA loop

The semantic temporal lobe network and the reward-related system in the hippocampal-VTA loop have been found to support different aspects of reward-modulated memory in this thesis. Information can become important for later behaviour through different factors. Hence, more than one mechanism is likely to contribute to the formation of memory for motivationally important information for this process to be adaptive. This thesis found a relationship between processing within the semantic temporal lobe and the modulation of associative memory processes like temporal order memory through reward. This was reflected in the relationship between interindividual differences in reward-related memory benefits and interindividual differences in ILF microstructure as well as differences in resting-state functional connectivity within the semantic temporal lobe network. Between-subject variability in modulation of memory through reward displayed a relationship to between-subject variability in structural connectivity, supported by the ILF, and resting-state functional connectivity within the semantic temporal lobe network specifically at immediate memory test. Variability in delayed memory test performance in a rewarded intentional memorisation paradigm, however, was found to be related to variability within the hippocampal-VTA loop. Interindividual differences within fornix microstructure as well as within resting-state functional connectivity between the NAcc and the hippocampus were found to relate to interindividual differences in reward-related memory.

Remarkably, the relationship between reward-related memory performance and variability within both the semantic network and the hippocampal-VTA loop seems to have displayed a more robust than expected relationship to memory for low reward information specifically. The relationship between ILF microstructure and reward-related memory benefits was driven by the specific interaction of a negative correlation between low reward memory and ILF microstructure and a positive or no correlation

between high reward memory and ILF microstructure. Participants with a higher microstructure index could possibly display better ability to systematically engage as well as disengage semantic processing during encoding of differently rewarding information. This was also reflected in their variability in resting-state functional connectivity along the semantic processing gradient within the temporal lobe (decreased RSFC between OCC and anterior TFC that are far apart in processing, increased RSFC between the PrC and the posterior TFC that are close together in processing). Additionally, the relationship between interindividual differences in participants' memory for *low* reward information at the delayed memory test and structural as well as resting-state functional connectivity within the hippocampal-VTA loop underpins the relationship between reward-related delayed memory and structure as well as function. Participants with increased resting-state functional and structural connectivity displayed increased memory for low reward information. They might have been more susceptible to the effect of reward on rewarded as well as associated information via their increased connectivity within the reward-processing system.

## 7.4 Relationship between structural and functional connections

This thesis set out to examine the neuroanatomical and neurofunctional bases of reward-related memory formation. The fornix constitutes a major pathway between hippocampus and Nacc (Aggleton et al., 2015; Ross et al., 2016; Shin et al., 2019). The hippocampus, the NAcc, and the VTA form a functional loop (Düzel et al., 2010; Lisman & Grace, 2005). The regions of interest within the semantic temporal lobe network investigated in Chapters 4 and 6 were chosen based on their relationship with ILF microstructure (Bajada et al., 2017; Hodgetts et al., 2017). To my knowledge, there is no literature directly examining the relationship between structural connectivity via white matter, functional connectivity at rest, and reward-related memory modulation within these networks. In this thesis, indices of microstructure of the tract of interest (fornix in the hippocampal-VTA loop, ILF in the semantic temporal lobe network) were investigated for their relationship to variability in resting-state functional connectivity. Furthermore, based on the results in Chapter 3, interaction-terms between ILF

microstructure and reward-related memory benefits for temporal order memory, recollection, and source memory were examined for their relationship to interindividual differences in resting-state functional connectivity within the semantic temporal lobe network in Chapter 4. In this thesis, neither microstructure indices nor interaction-terms significantly related to variability in resting-state functional connectivity of the regions of interest investigated as seeds. However, both networks display converging relationships of microstructure and resting-state functional connectivity with behaviour.

Interindividual differences in right ILF microstructure as well as functional connectivity within the right hemispheric semantic temporal lobe network at rest were associated with reward-related temporal order memory benefits (Chapters 3 and 4). Interindividual differences in fornix microstructure as well as resting-state functional connectivity between the NAcc and the hippocampus displayed a relationship with reward-modulated delayed memory in an intentional memorisation paradigm (Chapters 5 and 6). Furthermore, variability in reward-related recollection and source memory benefits for objects encoded in high versus low reward contexts was related to variability in resting-state functional connectivity between the NAcc and the VTA, but not the hippocampus, in Chapter 4. This was in line with previous research by Reggente and colleagues (2018) and might explain the absence of a relationship between reward-related memory benefits and fornix microstructure in Chapter 3. Taken together, these results show structural as well as functional connectivity within the same networks to be similarly involved in reward-related memory formation, while a direct relationship between them was absent here. This might be due to the seeds chosen during the resting-state functional connectivity analysis. While this thesis represents a first step, future research should investigate the possibly complementary contributions of structural and functional connections within the hippocampal-VTA loop and the semantic temporal lobe network to reward-related memory formation in a larger sample.

## 7.5 Methodological considerations and limitations

### 7.5.1 Administration

As outlined in "3.1.1 General procedure for data collection", data for most of the studies described in this thesis were acquired as part of a larger data collection that included a curiosity-related manipulation that is not part of this thesis. Data collection took place over the course of three days. One day was dedicated to MRI acquisition of DWI and resting-state functional images. Data for the behavioural components of the studies described in Chapters 3-6 were collected on two consecutive days. Both days included data collection within curiosity as well as reward manipulations. On the first day of behavioural data collection, participants performed a curiosity-motivated encoding task. This was followed by encoding for the intentional scene memorisation study reported in Chapters 5-6 as well as the immediate scene memory test. During the second day, participants were tested for their memory of the material of the curiosity paradigm. This was followed by the delayed memory test of the intentional scene memorisation study. Finally, participants took part in the temporal order memory study reported (Chapters 3-4). This data collection resulted from a balance between efficiency and reasonable expectations about participants' endurance. It did result in the necessity of keeping participants in a heighted state of motivation (either through reward or curiosity) for a prolonged period over the course of two testing days. That this introduces the possibility of reduced reward-related memory differences is a realistic assumption. Participants might have fatigued from the different curiosity- and reward-conditions. Furthermore, the possible interactions between different reward-motivations (rewarded encoding versus memory test) as well as curiosity are unknown. Nevertheless, participants displayed reliable memory performance overall. The reward-manipulation (monetary difference between high and low reward) might have simply been too small within the context of the different motivational manipulations to yield strong behavioural effects. A follow-up study should ensure that motivational manipulations concentrate on reward or that reward and curiosity motivations are separated further from one another.

## 7.5.2 The applicability of monetary rewards for memory research

Episodic memory formation supports adaptive behaviour by guiding decision-making based on previous experience. Episodic memory formation is important for this process because, occasionally, just one episodic event needs to be able to inform future behaviour due to its highly important context or outcome (Wimmer & Büchel, 2016). Motivational factors during encoding influence the probability of an event's long-term memory formation. These factors include reward (Adcock et sl., 2006) but also curiosity (Gruber et al., 2014) and novelty (Bunzeck et al., 2010). The application of monetary reward during laboratory investigations of adaptive memory formation might not be exceptionally representative of real-life motivated memory formation but extrinsic monetary reward has been shown to reliably influence memory across a variety of reward applications (during incidental encoding, in anticipation of future reward based on memory test performance etc.) and memory tests (e.g., Gruber et al., 2016; Murty et al., 2017; Wittmann et al., 2005; Wolosin et al., 2012). Importantly, long-term memory formation due to novelty, curiosity, and reward is proposed to be subserved by functioning within the dopaminergic system for all of these (e.g., Bunzeck et al., 2010; Gruber et al., 2014; Wolosin et al., 2012). Investigations of curiosity-, novelty-, and reward-related memory benefits demonstrate that these motivators share neural circuitry and processing (e.g., Bunzeck et al., 2010; Düzel et al., 2010; Gruber et al., 2014; Murty et al., 2017).

Reward has also been found to increase memory for novel rewarded items over novel unrewarded items (Bunzeck et al., 2012). A significant relationship between increased fMRI activation for novel rewarded over novel unrewarded items and the memory benefit was demonstrated in the anterior MTL, the striatum, and the VTA (Bunzeck et al., 2012). Curiosity as well as novelty might seem like the more likely candidates to motivate real-life long-term adaptive memory formation. However, in light of their shared circuitry with reward, the reliably demonstrated effect of reward in a variety of memory tasks, and the undetermined relationship between temporal order memory and motivational memory in human subjects, a monetary reward manipulation was a preferable first step in the research of adaptive temporal order memory formation within this thesis. Furthermore, humans do make decisions based on anticipated

monetary reward; we gamble, we decide not to buy something because we anticipate the reward from savings to be higher, we prepare for our annual review in anticipation of a raise. These decisions are adaptive, and they are based on memory induced by rewarded experiences.

### 7.5.3 Measuring structural and functional markers for adaptive memory formation

Palombo, Sheldon et al. (2018) liken variability in autobiographical memory to a "trait" that is maladaptive at the extremes and reflects normal trait-like variability like other cognitive abilities along its spectrum. They propose that the study of people with highly superior autobiographical memory and those with severely deficient autobiographical memory highlights the adaptive importance of detailed remembering but also forgetting. Palombo and colleagues suggest that the investigation of individual differences should specifically be able to elucidate the components that underly adaptive memory formation (Palombo, Sheldon et al., 2018). Therefore, the investigations within this thesis can be seen as part of a broader reframing of the investigation of episodic memory formation for adaptive behaviour. In line with this, it remains of importance to understand how stable the interindividual differences are. Recent work of repeated MRI acquisition within a small sample has demonstrated that microstructural properties based on DWI can display a high degree of repeatability across five acquisitions over the course of two weeks (Koller et al., 2021). Microstructural indices like FA and MD of the fornix for example displayed a test-retest intra-class correlation larger than 0.90 in the study by Koller and colleagues. In another study, Chou, Panych, Dickey, Petrella, and Chen (2012) repeatedly acquired functional resting-state MRI in a small sample over the course of over a year. They were able to demonstrate that whole-brain functional connectivity matrices showed test-retest reproducibility within subjects of around 0.90. Test-retest reproducibility for a specific network was high as well, averaging at 0.80 (Chou et al., 2012). These studies show that interindividual differences in structural and functional connectivity are accompanied by relative stability of these measures within individuals (Chou et al., 2012; Koller et al., 2021); at least within the timeframe of data collection for the studies in this thesis. This, together with the results presented in this thesis, establishes an exciting starting point

for the investigation of variability in adaptive memory formation. A future study could investigate the relationships between specific brain networks and specific reward-modulated memory processes further by establishing whether the trait-like stability of these underlies a certain stability in motivated adaptive memory formation. A next step would then be to explore how stable these structure-function-behaviour relationships remain over a longer timeframe.

### 7.5.4 Participants

A limiting factor for the interpretation of the presented results lies in the gender distribution of the sample. In a recent study by Warthen et al. (2020), a large sample of young women and men was investigated for sex differences in a variety of measures related to reward responsiveness. Their findings were in line with a proposed sexual dimorphism in the reward system. The participants in Warthen et al.'s (2020) study performed a monetary incentive task (MID) that modulated reward salience as well as valence. On each trial, participants had either a certain or uncertain (low or high salience) probability of incurring losses (negative valance) or gaining wins (positive valence), or both components were neutral. On low salience trials win or loss of $1 was independent of participants' performance. During high salience trials participants were able to win $1 or avoid a $1 loss with accurate performance. Neutral trials led to neither wins nor losses. Skin conductance measures during task performance were taken from all participants. A subgroup of participants underwent functional MR imaging during the MID task. When comparing high versus low salience trials, men displayed higher ratings of subjective arousal, higher behavioural accuracy, higher skin conductance, and higher neuronal responsiveness within the NAcc on trials with high versus low behavioural relevance (Warthen et al., 2020). The sample within the studies reported on in this thesis consisted of mostly women. Thereby, the monetary reward-manipulation might not have modulated memory reliably in a predominantly female sample. However, behavioural salience within the present studies did not vary in the same way as during Warthen et al.'s (2020) MID task. It could be argued that mainly reward valence (high versus low reward compares to win versus loss; see Madan & Spetch, 2012) varied within the present studies. Men and women did not vary in their behavioural, autonomic (skin conductance), and neural responsiveness to valance in Warthen et al. (2020).

Furthermore, most of the studies I reviewed in relation to memory modulation through reward comprised very asymmetric, predominantly female samples while demonstrating reward-related memory benefits as well as neural responses (e.g., Cohen et al., 2017; Cohen et al., 2019; Murty et al., 2017). Nevertheless, a future study should aim for a more balanced sample based on gender to be able to include it as a covariate for example.

Additionally, findings in young adults could be specific to them and might not extend towards an expectation of comparable results in older adults. Castel (2007) suggests that the reliance of older adults on processing of high value information at the expense of memory for detail is adaptive in that it reflects efficient use of changing resources across the adult lifespan. This loss in memory for detail could therefore be of great relevance to the investigation of reward-modulated temporal order memory in the study reported on in Chapters 3-4. However, older adults have been demonstrated to remain sensitive to reward in an intentional memorisation paradigm and display reward-related memory benefits like younger adults (Spaniol et al., 2014). In contrast, Bowen, Gallant, and Moon (2020) demonstrated in a study of the influence of reward-motivation on directed remembering and forgetting that the introduction of reward led to better memory for to-be-remembered as well as to-be-forgotten stimuli in older adults but not in younger adults. This was interpreted as a deficit to selectively control their encoding processing (Bowan et al., 2020). This is of interest in light of the reported relationship between elaborative processing within the semantic network and reward-related temporal order memory benefits in Chapters 3-4. Despite the proposal that the relationship between structural/functional connectivity within the networks investigated here and memory reflects a trait-like ability in episodic memory formation, I do not propose this ability to remain stable over the course of a lifetime. A future study could investigate this relationship in various samples to examine how structure-function-behaviour relationships arise, stabilise, and change.

### 7.5.5 Statistics and multiple comparisons

This thesis employed Holm-Bonferroni correction on Pearson's bivariate correlation coefficients between fibre tract microstructure and behaviour to control for

family-wise error rates (Holm, 1979). FWE-correction is employed to reduce the probability of finding a false positive (Type-I error) in a family of tests (Genovese, Lazar, & Nichols, 2001). Here, the planned comparisons within each tract were defined as a family, while the comparisons across the tracts were considered as separate. This meant that the maximum number of comparisons corrected for was 16 within each fibre tract for the behavioural effects in the intentional memorisation study (Chapter 5). This was intended to counteract a bias towards the observation of only more extreme relationships as well as Type-II errors (false negatives) when strong FWE-correction methods are applied (Lieberman & Cunningham, 2009). For the study at hand, the strongest correlation between right ILF FA and temporal order memory benefit survives even the highest level of correction across all planned comparisons in all the fibre tracts. However, despite this attempt to balance Type-I and Type-II errors within the comparisons in this thesis, correlation coefficients greater than 0.30 did not survive correction. Within the resting-state analysis, although ROI-to-ROI connectivity measures that were reported in Chapters 4 and 6 were corrected across the connections that were investigated within each GLM, no correction across the number of GLMs that were investigated within each network was made. Consequently, each behavioural measure that was investigated within a network was treated as a family of comparisons. This could have potentially increased the possibility of Type-I errors in this thesis. Whereas the networks investigated were based on the literature, this thesis was mostly exploratory due to the unknown contributions of said networks to reward-related modulation of memory for temporal order specifically. A future study could build upon the results presented here and investigate fewer behavioural measures. Regardless, Lieberman and Cunningham (2009) suggested that neuroimaging studies should rely more on replication studies and meta-analysis than to endeavour to strictly correct for Type-I errors since false positives simply do not replicate. Teipel and colleagues (2010) demonstrated a relationship between functional connectivity measured at rest and structural white-matter connectivity of the underlying pathways in a theory-driven and ROI-based analysis of RSFC and DTI. They then employed PCA and a purely data-driven approach to replicate those theory-driven findings (Teipel et al., 2010). The studies reported in Chapters 3-6 employed theory-driven and ROI-based correlational analysis to investigate the relationship between structural connectivity underlying functional

connectivity and behavioural variability. Even though the direct investigation of a relationship between variability in resting-state functional connectivity and variability in the microstructure of fibre tracts proposed to subserve connectivity between these regions did not yield significant results in this thesis, variability in structural and functional connectivity displayed converging relationships with behaviour. A future study could employ a more data-driven approach like PCA to investigate the structure-function relationship underlying this convergence in relationship to behaviour.

### 7.5.6 Limitations of diffusion imaging and resting-state functional connectivity

This thesis applied multi-shell diffusion imaging and spherical deconvolution to reduce the diffusion tensor model's difficulty in accounting for crossing, bending, or twisting fibres. This led to better representation of diffusion within a voxel and can thusly improve tractography (Dell'Acqua & Tournier, 2018; Jones, 2010; Le Bihan et al., 2001). Nevertheless, scalar measures (FA and MD) were employed to describe structural connectivity via the fibre tracts of interest. FA and MD have been found to relate to myelination, axonal coherence, and physiological properties of fibre bundles like conduction time (Assaf et al., 2017; Beaulieu, 2002; Le Bihan, 2003). Typically, an inverse relationship between FA and MD measures has been described (e.g., Hodgetts et al., 2017; Vettel et al., 2017). Correspondingly, it has been suggested to examine more than one diffusion measure to describe tissue properties reliably (Alexander et al., 2007). This was pursued here and directed hypotheses of the correlation between behaviour and FA as well as MD were based on the literature. Yet mostly FA displayed significant correlations with the behavioural measures in this thesis. In general, MD displayed only mildly negative or positive correlations with the behavioural measures of interest. While it is usually the case, lower MD and higher FA do not always reflect higher myelination since DTI does not allow for the specification of the factor mostly influencing the resulting FA or MD value (Alexander et al., 2007). Therefore, a future investigation could employ more advanced DTI models like NODDI (neurite orientation dispersion and density imaging) which evaluates the bending and fanning of axons (orientation dispersion index) as well as their density (density index) (Zhang, Schneider, Wheeler-Kingshott, & Alexander, 2012). Or other more sensitive measures of white matter

properties like the hindrance modulated orientational anisotropy (HMOA) index, which is capable of detecting even small microstructural changes, could be utilised in a future investigation (Dell'Acqua, Simmons, Williams, & Catani, 2013). These improvements to the description of the microstructural architecture notwithstanding, the analyses of the relationship between microstructure and behavioural variability remain correlational. Experience and training in motor, but also cognitive, tasks have been shown to change white matter microstructure and activity-dependent changes in myelination have been suggested to underpin learning (e.g., Nichols et al., 2020; Sampaio-Baptista & Johansen-Berg, 2017; Scholz, Klein, Behrens, & Johansen-Berg, 2009). Longitudinal approaches could investigate the manner in which variability in white matter and variability in reward-sensitivity influence each other to further elucidate the relationship between structure and behaviour.

The methods employed in this thesis to investigate resting-state functional connectivity are also limited by their correlational nature. It has been argued that the measured level of co-activation between brain regions does not reflect genuine connectivity since it does not reflect the causal influence of processing in one area on processing in another (Friston, Moran, & Seth, 2013; Stephan & Friston, 2010). While the former describes undirected connectivity in that it searches for mutual information between different regions of interest, the latter seeks to describe directed connectivity in that it describes the underlying dynamic/causal dependencies between these regions. Granger Causality Analysis and Dynamic Causal Modelling are two methods to evaluate directed connectivity. Whereas their application to fMRI data remains debated due to the latency of the haemodynamic response, their ability to directly model and test the underlying causal functions of brain network makes them advantageous over correlational models of functional connectivity (Friston et al., 2013). In this study, the directed connectivity within the hippocampal-VTA loop (Düzel et al., 2010; Lisman & Grace, 2005) for example, could be directly modelled and tested. A future study could investigate directed connectivity within this loop based on task-based activation during a reward-motivated task, like the monetary incentive delay task (Knutson, Adams, Fong, & Hommer, 2011). Between-subject variability within this directed connectivity could

then be related to variability in reward-related memory benefits acquired independently.

## 7.6 Conclusions and future directions

This thesis set out to investigate the relationship between interindividual differences in reward-modulated memory and interindividual differences in neuroanatomical and functional connectivity in a larger sample size than commonly reported. Here, variability in hippocampus-dependent memory like associative memory, recollection, temporal order memory and consolidation was related to variability within different networks that are often investigated in value-modulated memory research. This thesis is the first to my knowledge to examine the influence of reward on temporal order memory in human subjects. Chapter 2 found that participants had better memory for the temporal order of object pairs from high reward as opposed to low reward encoding contexts. Chapter 2 also showed that this effect was not increased by a post-encoding wakeful rest period. This behavioural effect could not be replicated in the larger sample investigated in Chapters 3 and 4. However, variability within the reward-related temporal order memory benefit was shown to be related to variability within the semantic temporal lobe network. This was reflected in the association between temporal order memory benefit and ILF microstructure in Chapter 3. The relationship between the temporal order memory benefit and resting-state functional connectivity within the semantic temporal lobe network reported in Chapter 4 demonstrated this as well. Participants with higher ILF FA displayed a higher reward-related temporal order memory benefit, high as opposed to low reward led to better memory for temporal order. This might have been supported by their increased ability to systematically engage semantic processing for high reward sequences and disengage semantic processing for low reward sequences, supported by the ILF. The relationship between variability in the reward-related temporal order memory benefit and variability in resting-state functional connectivity within the semantic temporal lobe network displayed an analogous pattern. Participants with better ability to systematically disengage semantic processing between distal areas along the semantic processing gradient within the temporal lobe, reflected in their decreased RSFC between the OCC-

seed and the anterior temporal fusiform cortex, displayed a higher reward-related temporal order memory benefit. Additionally, participants with better ability to systematically engage semantic processing between areas close together along the semantic processing gradient, reflected in their increased RSFC between PrC and posterior temporal fusiform cortex, also displayed a higher reward-related temporal order memory benefit. The results described in Chapters 3 and 4 signify the importance of the interaction between the systematic engagement or disengagement of semantic processing and remembering high reward information or forgetting low reward information. Thus, this thesis extends the literature on value-based systematic (dis)engagement of the semantic processing system onto memory for temporal order, an important aspect of episodic memory. Future studies should be aimed at increasing temporal order memory overall, by employing study-test cycles for example, to further elucidate the relationship between reward-related temporal order memory and the semantic processing system within the temporal lobe reported here.

Consolidation of reward-modulated recollection memory was found to rely on the hippocampal-VTA loop in Chapters 5 and 6. Participants with higher fornix FA displayed higher recollection memory at delayed memory test, independent of reward. Furthermore, participants with increased resting-state functional connectivity between NAcc and hippocampus, possibly supported by the fornix, displayed better memory for low reward memoranda in the delayed memory test. The results described in both chapters indicate that participants with increased structural and functional connectivity within the hippocampal-VTA loop were possibly more susceptible to reward during the intentional memorisation paradigm in that reward increased their delayed memory for low reward items encoded in temporal proximity to high reward items. Hence, while memory for high reward items was better than memory for low reward items in the immediate memory test, memory did not differ between reward conditions in the delayed memory test. This could have been due to unspecific consolidation for all scenes encoded during rewarded memorisation by participants with increased structural and functional connectivity within the hippocampal-VTA loop. A future study could increase the number of to-be-remembered items and include distractor-tasks during encoding to

investigate whether the findings presented here persist when memory is more competitive.

This thesis took first steps to investigate the relationship between structure and function and their contribution to reward-modulated memory. Indices of the microstructural architecture of fibre tracts, that have been proposed to connect the areas within the networks of interest (e.g., Aggleton et al., 2015; Bajada et al., 2017) were investigated for their relationship to interindividual differences in resting-state functional connectivity within the hippocampal-VTA loop and the semantic temporal lobe network (Chapters 4 and 6). Here, no significant relationships were found. However, both structural and functional connectivity display converging associations with the behaviour investigated in this thesis. The absence of a relationship between microstructure and resting-state functional connectivity itself could have been due to the choice of regions investigated as seeds. Although regions of interests were chosen based on the literature and aimed to reflect connectivity along the extent of the network, choice of seed and target ROIs can induce bias (Damoiseaux & Greicius, 2009). Furthermore, as discussed above, there exist more sensitive measures of microstructural architecture than FA and MD. While the results reported in this thesis indicate that structural as well as functional connections within the hippocampal-VTA loop and the semantic network support modulation of memory through reward, a future study could employ more sensitive measures of microstructure as well as a larger sample size, which would increase statistical power, to further illuminate the structure-function relationship that underlies reward-related memory formation.

This thesis examined the structural and functional connections within the brain underpinning interindividual differences in reward-modulated memory formation. This thesis found that the semantic temporal lobe network and the hippocampal-VTA loop contribute differently to temporal order memory and consolidated intentional memory respectively. The utilisation of different neuroimaging methods in this thesis has provided a promising foundation upon which to further investigate the relationship between structural and functional networks and their association with different aspects of reward-related memory. The investigation of the influence of reward on temporal

order in human subjects within this thesis reflects an important contribution to the research on episodic memory formation.

# Appendices

## Appendix 1

**Means and standard deviations (SD) for the object and source memory tests not reported in Chapter 2.** Means and SDs are based on percentages of hits (correct remember, know, source response). Hits were not corrected by false alarms since participants might have made their response based on the old object of an old-new pair. SDs reported in brackets after the means.

| Memory test | Measure | Reward | Distractor group (SD) | Wakeful rest group (SD) |
|---|---|---|---|---|
| Object memory | recollection | high | 69.68 (13.03) | 66.67 (10.98) |
| | | low | 69.08 (13.67) | 65.83 (10.25) |
| | familiarity | high | 22.68 (12.65) | 24.31 (12.74) |
| | | low | 22.23 (12.61) | 23.19 (10.94) |
| | overall | high | 92.37 (04.75) | 90.97 (06.25) |
| | | low | 91.32 (06.37) | 89.03 (05.82) |
| Source memory | | high | 61.99 (14.48) | 57.22 (17.88) |
| | | low | 57.73 (13.87) | 53.47 (14.35) |
| Old-new pairs | Correct reject | | 84.47 (12.49) | 85.00 (12.37) |

# Appendix 2

Medial and lateral fornix reconstructions were based on the method described by Christiansen and colleagues (2017). AND and NOT gates that were set during tractography of the whole fornix were employed for the extraction of these fornical subdivisions. Some NOT gates were changed to better extract the streamlines of the medial (**A**) and lateral fornix (**B**). Following Poppenk, Evensmoen, Moscovitch, and Nadel (2013, the uncal apex was taken as a landmark for the anterior-posterior hippocampal boundary. The uncal apax is small grey matter bundle that outlines the most anterior extent of the parahippocampal gyrus (Poppenk et al., 2013). Manual tractography of the medial and lateral fornix was carried out for 20 participants by identifying this landmark for each hemisphere separately. The most anterior part of the uncal apax was localised and then traced to its posterior boundary. The landmark for the anterior-posterior hippocampal boundary was set in the first coronal slice, in which the uncal apex was not visible anymore. Landmarks were identified within the left and right hemispheres. Then, at each hemisphere's landmark, one NOT gate was drawn around the hippocampus to set boundaries for the medial fornix. Fibres passing through these NOT gates were removed (**C**). The NOT gates that were employed to identify the medial fornix where then replaced with one AND gate each for the left (**D**) and right lateral fornix (**E**). After manual tractography was performed on 20 participants, automated tractography was carried as described in Chapter 3.

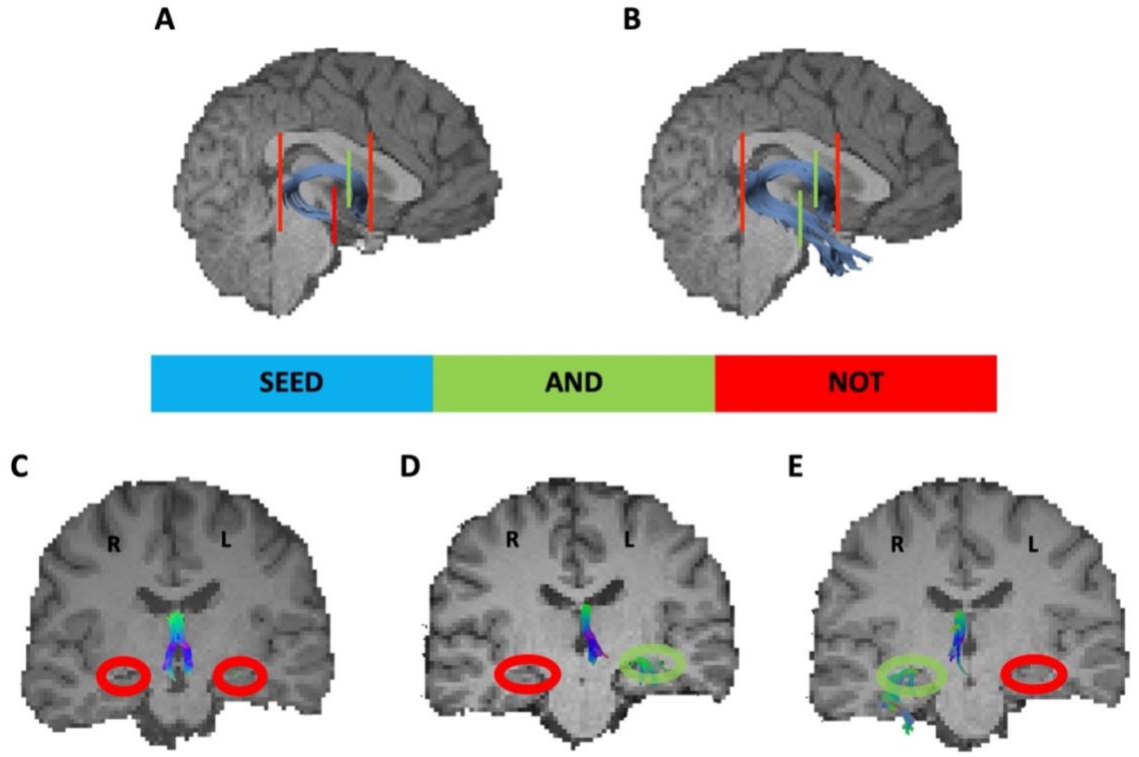


**Figure Appendix 2.** Medial and lateral fornix. Main gates employed by manual tractography for the three tracts of interest. **A.** medial fornix. **B.** Right lateral fornix. **C.** medial fornix at [66|64|40]. **D.** Left lateral fornix at [69|64|40]. **E.** Right lateral fornix at [68|64|40].

Correlation analyses were performed in JASP (JASP-team, 2019; version 0.11.1). Memory effects were correlated with the different indicators (FA and MD) of microstructure in medial, left, and right lateral fornix. All variables were z-standardised for each participants' data before correlation analysis (formula 3.2). Overall memory (average of high and low reward responses) and reward-related memory benefits (high – low reward) were calculated for all memory measures (i.e., high confidence temporal order memory accuracy, source memory accuracy, recollection). Directed hypotheses for the correlations between memory measures (overall memory, reward-related memory benefits) and microstructure were based on the literature. The results of this correlation analysis are reported in the table below.

**Correlations between microstructure indices of medial, left, and right lateral fornix and behavioural measures reported in Chapter 3.**

| Microstructure | Memory measure | | | | | |
|---|---|---|---|---|---|---|
| | High confidence temporal order memory | | Recollection | | Source accuracy | |
| | Overall memory | Reward-related memory benefit | Overall memory | Reward-related memory benefit | Overall memory | Reward-related memory benefit |
| Medial fornix FA | | | | | | |
| Pearson's r | -0.06 | -0.15 | 0.09 | -0.10 | 0.01 | -0.34 |
| *p-value* | .668 | .867 | .267 | .765 | .745 | .994 |
| Medial fornix MD | | | | | | |
| Pearson's r | 0.09 | -0.02 | 0.06 | 0.17 | 0.09 | 0.16 |
| *p-value* | .751 | .447 | .679 | .887 | .735 | .873 |
| Left lateral fornix FA | | | | | | |
| Pearson's r | 0.01 | -0.20 | 0.08 | -0.08 | -0.01 | -0.29 |
| *p-value* | .476 | .925 | .280 | .713 | .527 | .985 |
| Left lateral fornix MD | | | | | | |
| Pearson's r | -0.05 | -0.04 | 0.13 | 0.26 | -0.06 | 0.25 |
| *p-value* | .347 | .376 | .834 | .970 | .343 | .968 |
| Right lateral fornix FA | | | | | | |
| Pearson's | -0.01 | 0.09 | 0.06 | -0.10 | 0.05 | -0.30 |
| *p-value* | .540 | .252 | .342 | .769 | .348 | .985 |
| Right lateral fornix MD | | | | | | |
| Pearson's | 0.01 | -0.06 | 0.03 | 0.02 | -0.08 | 0.05 |
| *p-value* | .523 | .326 | .579 | .565 | .291 | .631 |

Microstructure indices for none of the fornix subdivisions significantly correlated with none of the behavioural measures. Based on these results, RSFC analysis in Chapter 4 was based on the whole hippocampus to increase signal-to-noise-ratio.

# Appendix 3

Familiarity measures were calculated following Libby, Yonelinas, Ranganath, and Ragland (2013). Familiarity was corrected not only by the proportion of false alarm "know"- responses to new objects but also by the proportion of trials where participants did not make a "remember"- response to an old object and therefore a "know"-response could have been made. Therefore, familiarity was calculated for old and for new objects and then the familiarity value for new objects was subtracted from the familiarity value for old objects (formula).

$$familiarity_{old} = \frac{proportion\ know_{old}}{(1 - proportion\ remember_{old})}$$

$$familiarity_{new} = \frac{proportion\ know_{new}}{(1 - \ proportion\ remember_{new})}$$

$$familiarity = \ familiarity_{old} - familiarity_{new}$$

**Formula.** Familiarity corrected for non-independence.

**Means and standard deviations (SD) for low confidence temporal order memory and familiarity not reported in Chapter 3.** Means and SDs for temporal order are based on accuracy (hits – false alarms). Familiarity was calculated based on Libby et al. (2013). SDs reported in brackets after the means.

| Memory measure | Reward | Mean (SD) |
|---|---|---|
| Low confidence temporal order memory | high | 15.99 (17.30) |
| | low | 17.36 (20.83) |
| Familiarity | high | 0.56 (0.22) |
| | low | 0.56 (0.22) |

Two-tailed paired sample t-test on low confidence temporal order accuracy and familiarity did not yield significant results (low confidence temporal order: $t(53) = -0.78$, $p = .439$, $d = 0.11$; familiarity: $t(53) = -0.20$, $p = .840$, $d = 0.03$).

# Appendix 4

One-tailed paired-sample t-tests were employed to investigate the influence of reward on memory performance. Better memory for high reward items was hypothesised. The analyses were repeated in the smaller sample described in Chapter 4 to confirm that exclusion of five participants due to quality of resting-state data did not change the reported results of Chapter 3 (N = 54 in Chapter 3 and N = 49 in Chapter 4).

**Means and standard deviations (SDs) for the memory measures reported in Chapter 3 in the smaller sample (N = 49) of Chapter 4.** Means and SDs are based on percentage accuracies (hits – false alarms). Separated by reward (high versus low). SDs in brackets after the means.

| Memory measure | Reward | Mean (SD) |
|---|---|---|
| High confidence temporal order memory | high | 16.02 (19.55) |
| | low | 13.93 (18.63) |
| Recollection | high | 43.91 (24.12) |
| | low | 43.23 (23.84) |
| Source accuracy | high | 39.56 (14.69) |
| | low | 36.73 (13.97) |

Reward did not significantly influence high confidence temporal order memory ($t(1,48) = 1.34$, $p_{1\text{-tailed}} = .092$, $d = 0.19$) and recollection ($t(1,48) = 0.42$, $p_{1\text{-tailed}} = .34$, $d = 0.06$). High reward source memory was better than low reward source memory in the smaller sample ($t(1,48) = 1.83$, $p_{1\text{-tailed}} = .03$, $d = 0.26$).

**Correlations between microstructure indices and behavioural measures reported in Chapter 3 in the smaller sample (N = 49) reported in Chapter 4.**

| Microstructure | Memory measure | | | | | |
|---|---|---|---|---|---|---|
| | High confidence temporal order memory | | Recollection | | Source accuracy | |
| | Overall memory | Reward-related memory benefit | Overall memory | Reward-related memory benefit | Overall memory | Reward-related memory benefit |
| Fornix FA | | | | | | |
| Pearson's r | -0.09 | -0.04 | 0.10 | -0.16 | -0.10 | -0.34 |
| *p-value* | .725 | .609 | .252 | .866 | .745 | .992 |
| Fornix MD | | | | | | |
| Pearson's r | 0.03 | -0.01 | 0.10 | 0.15 | 0.04 | 0.20 |
| *p-value* | .582 | .469 | .759 | .856 | .600 | .915 |
| Left UF FA | | | | | | |
| Pearson's r | 0.01 | -0.03 | 0.11 | 0.13 | 0.05 | -0.04 |
| *p-value* | .482 | .554 | .221 | .184 | .371 | .593 |
| Left UF MD | | | | | | |
| Pearson's r | 0.19 | -0.06 | 0.08 | 0.16 | -0.01 | 0.07 |
| *p-value* | .829 | .391 | .711 | .869 | .474 | .681 |
| Right UF FA | | | | | | |
| Pearson's | -0.12 | -0.09 | 0.13 | 0.08 | 0.10 | 0.07 |
| *p-value* | .726 | .668 | .184 | .289 | .228 | .317 |
| Right UF MD | | | | | | |
| Pearson's | 0.19 | 0.13 | 0.15 | 0.12 | -0.06 | -0.07 |
| *p-value* | .833 | .735 | .849 | .793 | .324 | .301 |
| Left ILF FA | | | | | | |
| Pearson's | 0.12 | 0.12 | -0.21 | 0.24 | 0.03 | 0.22 |
| *p-value* | .206 | .206 | .930 | .046 | .415 | .062 |
| Left ILF MD | | | | | | |
| Pearson's | -0.13 | 0.03 | 0.31 | 0.01 | -0.02 | 0.06 |
| *p-value* | .192 | .577 | .986 | .536 | .433 | .671 |
| Right ILF FA | | | | | | |
| Pearson's | 0.01 | 0.50 | -0.16 | 0.37 | -0.03 | 0.32 |
| *p-value* | .468 | < .000 | .868 | .004 | .591 | .012 |
| Right ILF MD | | | | | | |
| Pearson's | -0.01 | -0.13 | 0.24 | -0.04 | -0.00 | -0.05 |
| *p-value* | .458 | .187 | .950 | .394 | .496 | .359 |

# Appendix 5

**Means and standard deviations (SD) for familiarity not reported in Chapter 5.** Familiarity was calculated based on Libby et al. (2013). SDs reported in brackets after the means.

| Memory measure | Reward | Mean (SD) |
|---|---|---|
| Immediate familiarity | high | 0.65 (0.45) |
| | low | 0.63 (0.44) |
| Delayed familiarity | high | 0.63 (0.38) |
| | low | 0.60 (0.35) |

A 2x2 repeated-measures ANOVA of the effects of *timepoint* (immediate versus delayed) and *reward* (high versus low) on familiarity was performed. Neither main effects nor the interaction was significant (timepoint: ($F$(1,46) = 0.24, $p$ = .673, *partial eta squared* = 0.01; reward: $F$(1,46) = 0.29, $p$ = .595, *partial eta squared* = 0.01; interaction: $F$(1,46) = 0.04, $p$ = .834, *partial eta squared* = 0.001).

# Appendix 6

All variables were z-standardised for each participants' data before correlation analysis (formula 3.2). Directed hypotheses for the correlations between memory measures (overall memory, reward-related memory benefits) and microstructure were based on the literature. The results of this correlation analysis are reported in the table below.

**Correlations between microstructure indices of medial, left, and right lateral fornix and behavioural measures reported in Chapter 5.**

| Microstructure | Memory measure | | | | | |
|---|---|---|---|---|---|---|
| | Difference between immediate and delayed memory test | | Immediate memory test | | Delayed memory test | |
| | Overall memory | Reward-related memory benefit | Overall memory | Reward-related memory benefit | Overall memory | Reward-related memory benefit |
| Medial fornix FA | | | | | | |
| Pearson's r | 0.10 | -0.00 | 0.16 | 0.06 | 0.23 | 0.05 |
| *p-value* | .250 | .509 | .149 | .346 | .064 | .369 |
| Medial fornix MD | | | | | | |
| Pearson's r | 0.00 | 0.04 | 0.04 | -0.01 | 0.05 | 0.05 |
| *p-value* | .505 | .617 | .614 | .486 | .636 | .619 |
| Left lateral fornix FA | | | | | | |
| Pearson's r | 0.13 | 0.18 | 0.17 | -0.08 | 0.26* | 0.12 |
| *p-value* | .200 | .119 | .120 | .706 | .041 | .203 |
| Left lateral fornix MD | | | | | | |
| Pearson's r | 0.15 | 0.04 | -0.12 | -0.09 | 0.04 | -0.04 |
| *p-value* | .844 | .602 | .214 | .275 | .611 | .401 |
| Right lateral fornix FA | | | | | | |
| Pearson's | 0.13 | 0.11 | 0.14 | -0.13 | 0.24 | 0.01 |
| *p-value* | .193 | .234 | .174 | .799 | .050 | .477 |
| Right lateral fornix MD | | | | | | |
| Pearson's | -0.04 | 0.29 | 0.22 | -0.24 | 0.17 | 0.11 |
| *p-value* | .402 | .977 | .936 | .054 | .873 | .779 |

Only the correlation between left lateral fornix (anterior hippocampal) FA and overall recollection memory at delayed memory test reached significance ($r(54) = 0.26$, $p = .041$). However, the correlation between overall recollection at delayed memory test and medial (posterior hippocampal) fornix FA as well as right lateral fornix FA displayed a trend towards significance. Following this absence of specific dissociations between the fornix subdivisions in their relationship to memory, all analyses remained based on the whole fornix and the whole hippocampus.

# Appendix 7

The analyses were repeated in the smaller sample described in Chapter 6 to confirm that exclusion of five participants due to quality of resting-state data did not change the reported results of Chapter 5 (N = 47 in Chapter 5 and N = 42 in Chapter 6).

**Group means and standard deviations (SD) for the behavioural measures.** Means and SDs are based on percentage accuracies (hits – false alarms). Separated by reward (high versus low) and memory test (immediate versus delayed). SDs in brackets behind means.

| Memory measure | Reward | Mean (SD) |
|---|---|---|
| Immediate recollection | high | 72.38 (26.02) |
| | low | 68.57 (28.16) |
| Delayed recollection | high | 61.43 (27.99) |
| | low | 58.81 (27.25) |

A 2x2 repeated-measures ANOVA of the effects of *timepoint* (immediate versus delayed) and *reward* (high versus low) on recollection revealed a significant main effect of *timepoint* ($F(1,41) = 9.05$, $p = .004$, *partial eta squared* = 0.18). The main effect of *reward* and the interaction between timepoint and reward did not reach significance (reward: $F(1,41) = 1.73$, $p = .20$, *partial eta squared* = 0.04; interaction: $F(1,41) = 0.12$, $p = .731$, *partial eta squared* = 0.002). One-tailed paired sample t-tests were employed to follow up on the main effect. Comparing immediate versus delayed memory test showed that high reward ($t(41) = 2.92$, $p_{1\text{-tailed}} = .003$, $d = 0.45$) as well as low reward ($t(41) = 2.47$, $p_{1\text{-tailed}} = .009$, $d = 0.38$) recollection was higher in the immediate as opposed to the delayed memory test.

**Correlations between microstructure indices and behavioural measures reported in Chapter 5 in the smaller sample (N = 42) reported in Chapter 6.**

| Microstructure | Memory measure | | | | | |
|---|---|---|---|---|---|---|
| | Difference between immediate and delayed memory test | | Immediate memory test | | Delayed memory test | |
| | Overall memory | Reward-related memory benefit | Overall memory | Reward-related memory benefit | Overall memory | Reward-related memory benefit |
| Fornix FA | | | | | | |
| Pearson's r | 0.07 | 0.15 | 0.19 | -0.11 | 0.24 | 0.07 |
| *p-value* | .326 | .174 | .111 | .760 | .063 | .330 |
| Fornix MD | | | | | | |
| Pearson's r | 0.08 | 0.06 | 0.04 | -0.03 | 0.10 | 0.04 |
| *p-value* | .688 | .646 | .589 | .426 | .739 | .601 |
| Left UF FA | | | | | | |
| Pearson's r | 0.48 | -0.08 | 0.34 | 0.03 | -0.13 | 0.11 |
| *p-value* | < .001 | .692 | .013 | .425 | .785 | .239 |
| Left UF MD | | | | | | |
| Pearson's r | -0.04 | 0.10 | 0.01 | 0.20 | 0.05 | 0.05 |
| *p-value* | .394 | .737 | .537 | .90 | .615 | .634 |
| Right UF FA | | | | | | |
| Pearson's | 0.16 | -0.17 | 0.01 | -0.02 | -0.14 | 0.17 |
| *p-value* | .162 | .853 | .482 | .549 | .816 | .147 |
| Right UF MD | | | | | | |
| Pearson's | 0.06 | -0.03 | 0.10 | 0.06 | 0.06 | 0.08 |
| *p-value* | .650 | .415 | .746 | .643 | .638 | .700 |
| Left ILF FA | | | | | | |
| Pearson's | 0.31 | 0.02 | -0.13 | 0.21 | -0.41 | 0.15 |
| *p-value* | .023 | .445 | .800 | .090 | .997 | 174 |
| Left ILF MD | | | | | | |
| Pearson's | -0.29 | -0.12 | 0.03 | -0.16 | 0.25 | 0.00 |
| *p-value* | .048 | .220 | .584 | .156 | .945 | .505 |
| Right ILF FA | | | | | | |
| Pearson's | 0.02 | 0.28 | -0.26 | 0.26 | -0.27 | -0.09 |
| *p-value* | .454 | .036 | .953 | .049 | .959 | .724 |
| Right ILF MD | | | | | | |
| Pearson's | -0.05 | -0.34 | 0.13 | -0.21 | 0.17 | 0.20 |
| *p-value* | .382 | .015 | .799 | .091 | .852 | .893 |

# References

Adcock, R. A., Thangavel, A., Whitfield-Gabrieli, S., Knutson, B., & Gabrieli, J. D. (2006). Reward-motivated learning: mesolimbic activation precedes memory formation. *Neuron, 50*(3), 507-517. https://doi.org/10.1016/j.neuron.2006.03.036

Aggleton, J. P., & Brown, M. W. (1999). Episodic memory, amnesia and the hippocampal-anterior thalamic axis. Behavioral and brain sciences, 22(3), 425-444.

Aggleton, J. P., & Christiansen, K. (2015). The subiculum: the heart of the extended hippocampal system. In *Progress in brain research* (Vol. 219, pp. 65-82). Elsevier. https://doi.org/10.1016/bs.pbr.2015.03.003

Aggleton, J. P., Dumont, J. R., & Warburton, E. C. (2011). Unraveling the contributions of the diencephalon to recognition memory: a review. Learning & memory (Cold Spring Harbor, N.Y.), 18(6), 384–400. https://doi.org/10.1101/lm.1884611

Aggleton, J. P., Wright, N. F., Rosene, D. L., & Saunders, R. C. (2015). Complementary patterns of direct amygdala and hippocampal projections to the macaque prefrontal cortex. *Cerebral Cortex, 25*(11), 4351-4373. https://doi.org/10.1093/cercor/bhv019

Agosta, F., Henry, R. G., Migliaccio, R., Neuhaus, J., Miller, B. L., Dronkers, N. F., ... & Gorno-Tempini, M. L. (2010). Language networks in semantic dementia. *Brain, 133*(1), 286-299. DOI: 10.1093/brain/awp233

Alexander, A. L., Lee, J. E., Lazar, M., & Field, A. S. (2007). Diffusion tensor imaging of the brain. *Neurotherapeutics*, *4*(3), 316-329. DOI: 10.1016/j.nurt.2007.05.011

Alm, K. H., Rolheiser, T., & Olson, I. R. (2016). Inter-individual variation in fronto-temporal connectivity predicts the ability to learn different types of associations. *Neuroimage*, *132*, 213-224. https://doi.org/10.1016/j.neuroimage.2016.02.038

Alonazi, B. K., Keller, S. S., Fallon, N., Adams, V., Das, K., Marson, A. G., & Sluming, V. (2019). Resting-state functional brain networks in adults with a new diagnosis of focal epilepsy. *Brain and behavior*, *9*(1), e01168. DOI: 10.1002/brb3.1168

Andersson, J. L., & Sotiropoulos, S. N. (2016). An integrated approach to correction for off-resonance effects and subject movement in diffusion MR imaging. *Neuroimage*, *125*, 1063-1078. DOI: 10.1016/j.neuroimage.2015.10.019

Andersson, J. L., Hutton, C., Ashburner, J., Turner, R., & Friston, K. (2001). Modeling geometric deformations in EPI time series. *Neuroimage*, *13*(5), 903-919. DOI: 10.1006/nimg.2001.0746

Ashburner, J., & Friston, K. J. (2005). Unified segmentation. *Neuroimage*, *26*(3), 839-851. DOI: 10.1016/j.neuroimage.2005.02.018

Assaf, Y., & Pasternak, O. (2008). Diffusion tensor imaging (DTI)-based white matter mapping in brain research: a review. *Journal of molecular neuroscience*, *34*(1), 51-61. DOI: 10.1007/s12031-007-0029-0

Assaf, Y., Johansen-Berg, H., & Thiebaut de Schotten, M. (2019). The role of diffusion MRI in neuroscience. *NMR in Biomedicine*, *32*(4), e3762. https://doi.org/10.1002/nbm.3762

Bajada, C. J., Haroon, H. A., Azadbakht, H., Parker, G. J., Ralph, M. A. L., & Cloutman, L. L. (2017). The tract terminations in the temporal lobe: Their location and associated functions. *cortex*, *97*, 277-290. DOI: 10.1016/j.cortex.2016.03.013

Basser, P. J., Mattiello, J., & LeBihan, D. (1994). MR diffusion tensor spectroscopy and imaging. *Biophysical journal*, *66*(1), 259-267. DOI: 10.1016/S0006-3495(94)80775-1

Beaulieu, C. (2002). The basis of anisotropic water diffusion in the nervous system–a technical review. *NMR in Biomedicine*, *15*(7-8), 435-455. DOI: 10.1002/nbm.782

Behzadi, Y., Restom, K., Liau, J., & Liu, T. T. (2007). A component based noise correction method (CompCor) for BOLD and perfusion based fMRI. *Neuroimage*, *37*(1), 90-101. DOI: 10.1016/j.neuroimage.2007.04.042

Benear, S. L., Ngo, C. T., & Olson, I. R. (2020). Dissecting the fornix in basic memory processes and neuropsychiatric disease: A review. *Brain Connectivity*, *10*(7), 331-354. DOI: 10.1089/brain.2020.0749

Benjamini, Y., & Hochberg, Y. (1995). Controlling the false discovery rate: a practical and powerful approach to multiple testing. *Journal of the Royal statistical society: series B (Methodological)*, *57*(1), 289-300. https://doi.org/10.1111/j.2517-6161.1995.tb02031.x

Berridge, K. C. (2007). The debate over dopamine's role in reward: the case for incentive salience. *Psychopharmacology*, *191*(3), 391-431. DOI: 10.1007/s00213-006-0578-x

Binder, J. R., Desai, R. H., Graves, W. W., & Conant, L. L. (2009). Where is the semantic system? A critical review and meta-analysis of 120 functional neuroimaging studies. *Cerebral cortex*, *19*(12), 2767-2796. https://doi.org/10.1093/cercor/bhp055

Biswal, B. B., Kylen, J. V., & Hyde, J. S. (1997). Simultaneous assessment of flow and BOLD signals in resting-state functional connectivity maps. *NMR in Biomedicine*, *10*(4-5), 165-170. DOI: 10.1002/(sici)1099-1492(199706/08)10:4/5<165::aid-nbm454>3.0.co;2-7

Biswal, B., Zerrin Yetkin, F., Haughton, V. M., & Hyde, J. S. (1995). Functional connectivity in the motor cortex of resting human brain using echo-planar MRI. *Magnetic resonance in medicine*, *34*(4), 537-541. DOI: 10.1002/mrm.1910340409

Blumenfeld, R. S., & Ranganath, C. (2007). Prefrontal cortex and long-term memory encoding: an integrative review of findings from neuropsychology and neuroimaging. *The Neuroscientist*, *13*(3), 280-291. DOI: 10.1177/1073858407299290

Botvinick, M. M., Braver, T. S., Barch, D. M., Carter, C. S., & Cohen, J. D. (2001). Conflict monitoring and cognitive control. *Psychological review*, *108*(3), 624. https://doi.org/10.1037/0033-295X.108.3.624

Bowen, H. J., Gallant, S. N., & Moon, D. H. (2020). Influence of Reward Motivation on Directed Forgetting in Younger and Older Adults. Frontiers in psychology, 11, 1764. https://doi.org/10.3389/fpsyg.2020.01764

Brady, T. F., Konkle, T., Alvarez, G. A., & Oliva, A. (2008). Visual long-term memory has a massive storage capacity for object details. *Proceedings of the National Academy of Sciences*, *105*(38), 14325-14329. https://doi.org/10.1073/pnas.0803390105

Brasted, P. J., Bussey, T. J., Murray, E. A., & Wise, S. P. (2003). Role of the hippocampal system in associative learning beyond the spatial domain. *Brain*, *126*(5), 1202-1223. https://doi.org/10.1093/brain/awg103

Brown, M. W., & Aggleton, J. P. (2001). Recognition memory: what are the roles of the perirhinal cortex and hippocampus?. *Nature Reviews Neuroscience*, *2*(1), 51-61. DOI: 10.1038/35049064

Browning, P. G., & Gaffan, D. (2008). Prefrontal cortex function in the representation of temporally complex events. *Journal of Neuroscience*, *28*(15), 3934-3940. https://doi.org/10.1523/JNEUROSCI.0633-08.2008

Bunzeck, N., Dayan, P., Dolan, R. J., & Düzel, E. (2010). A common mechanism for adaptive scaling of reward and novelty. *Human brain mapping*, *31*(9), 1380-1394. DOI: 10.1002/hbm.20939

Bunzeck, N., Doeller, C. F., Dolan, R. J., & Düzel, E. (2012). Contextual interaction between novelty and reward processing within the mesolimbic system. *Human brain mapping*, *33*(6), 1309-1324. DOI: 10.1002/hbm.21288

Cabeza, R., & St Jacques, P. (2007). Functional neuroimaging of autobiographical memory. Trends in cognitive sciences, 11(5), 219-227. DOI: 10.1016/j.tics.2007.02.005

Castel, A. D. (2007). The adaptive and strategic use of memory by older adults: Evaluative processing and value-directed remembering. *Psychology of learning and motivation*, *48*, 225-270. https://doi.org/10.1016/S0079-7421(07)48006-9

Catani, M., & De Schotten, M. T. (2008). A diffusion tensor imaging tractography atlas for virtual in vivo dissections. *cortex*, *44*(8), 1105-1132. DOI: 10.1016/j.cortex.2008.05.004

Catani, M., Dell'Acqua, F., & De Schotten, M. T. (2013). A revised limbic system model for memory, emotion and behaviour. *Neuroscience & Biobehavioral Reviews*, *37*(8), 1724-1737. DOI: 10.1016/j.neubiorev.2013.07.001

Catani, M., Howard, R. J., Pajevic, S., & Jones, D. K. (2002). Virtual in vivo interactive dissection of white matter fasciculi in the human brain. *Neuroimage*, *17*(1), 77-94. DOI: 10.1006/nimg.2002.1136

Catani, M., Jones, D. K., Donato, R., & Ffytche, D. H. (2003). Occipito-temporal connections in the human brain. Brain, 126(9), 2093-2107.

Chai, X. J., Castañón, A. N., Öngür, D., & Whitfield-Gabrieli, S. (2012). Anticorrelations in resting state networks without global signal regression. *Neuroimage*, *59*(2), 1420-1428. DOI: 10.1016/j.neuroimage.2011.08.048

Charles, D. P., Gaffan, D., & Buckley, M. J. (2004). Impaired recency judgments and intact novelty judgments after fornix transection in monkeys. *Journal of Neuroscience*, *24*(8), 2037-2044. https://doi.org/10.1523/JNEUROSCI.3796-03.2004

Chen, Y., Shimotake, A., Matsumoto, R., Kunieda, T., Kikuchi, T., Miyamoto, S., ... & Ralph, M. L. (2016). The 'when'and 'where'of semantic coding in the anterior temporal lobe: Temporal representational similarity analysis of electrocorticogram data. *Cortex*, *79*, 1-13. DOI: 10.1016/j.cortex.2016.02.015

Chou, Y. H., Panych, L. P., Dickey, C. C., Petrella, J. R., & Chen, N. K. (2012). Investigation of long-term reproducibility of intrinsic connectivity network mapping: a resting-state fMRI study. American Journal of Neuroradiology, 33(5), 833-838.

Christiansen, K., Dillingham, C. M., Wright, N. F., Saunders, R. C., Vann, S. D., & Aggleton, J. P. (2016). Complementary subicular pathways to the anterior thalamic nuclei and mammillary bodies in the rat and macaque monkey brain. European Journal of Neuroscience, 43(8), 1044-1061.

Christiansen, K., Metzler-Baddeley, C., Parker, G. D., Muhlert, N., Jones, D. K., Aggleton, J. P., & Vann, S. D. (2017). Topographic separation of fornical fibers associated with the anterior and posterior hippocampus in the human brain: An MRI-diffusion study. Brain and behavior, 7(1), e00604. https://doi.org/10.1002/brb3.604

Clewett D, Davachi L. The Ebb and Flow of Experience Determines the Temporal Structure of Memory. Curr Opin Behav Sci. 2017 Oct;17:186-193. doi: 10.1016/j.cobeha.2017.08.013.

Cohen, M. S., Cheng, L. Y., Paller, K. A., & Reber, P. J. (2019). Separate memory-enhancing effects of reward and strategic encoding. *Journal of cognitive neuroscience*, *31*(11), 1658-1673. https://doi.org/10.1162/jocn_a_01438

Cohen, M. S., Rissman, J., Hovhannisyan, M., Castel, A. D., & Knowlton, B. J. (2017). Free recall test experience potentiates strategy-driven effects of value on memory. *Journal of Experimental Psychology: Learning, Memory, and Cognition*, *43*(10), 1581. https://doi.org/10.1037/xlm0000395

Cohen, M. S., Rissman, J., Suthana, N. A., Castel, A. D., & Knowlton, B. J. (2014). Value-based modulation of memory encoding involves strategic engagement of fronto-temporal semantic processing regions. *Cognitive, Affective, & Behavioral Neuroscience*, *14*(2), 578-592. https://doi.org/10.3758/s13415-014-0275-x

Cohen, M. S., Rissman, J., Suthana, N. A., Castel, A. D., & Knowlton, B. J. (2016). Effects of aging on value-directed modulation of semantic network activity during verbal learning. *Neuroimage*, *125*, 1046-1062. https://doi.org/10.1016/j.neuroimage.2015.07.079

Cohen, M. X., Young, J., Baek, J. M., Kessler, C., & Ranganath, C. (2005). Individual differences in extraversion and dopamine genetics predict neural reward responses. *Cognitive brain research*, *25*(3), 851-861. DOI: 10.1016/j.cogbrainres.2005.09.018

Cohen, N. J., & Squire, L. R. (1980). Preserved learning and retention of pattern-analyzing skill in amnesia: Dissociation of knowing how and knowing that. *Science*, *210*(4466), 207-210. DOI: 10.1126/science.7414331

Craig, M., & Dewar, M. (2018). Rest-related consolidation protects the fine detail of new memories. *Scientific reports*, *8*(1), 1-9. DOI: 10.1038/s41598-018-25313-y

Craig, M., Dewar, M., Della Sala, S., & Wolbers, T. (2015). Rest boosts the long-term retention of spatial associative and temporal order information. *Hippocampus*, *25*(9), 1017-1027. DOI: 10.1002/hipo.22424

Damoiseaux, J. S., & Greicius, M. D. (2009). Greater than the sum of its parts: a review of studies combining structural connectivity and resting-state functional connectivity. *Brain Structure and Function*, *213*(6), 525-533. DOI: 10.1007/s00429-009-0208-6

Davachi, L. (2006). Item, context and relational episodic encoding in humans. *Current opinion in neurobiology*, *16*(6), 693-700. DOI: 10.1016/j.conb.2006.10.012

Davachi, L., & DuBrow, S. (2015). How the hippocampus preserves order: the role of prediction and context. *Trends in cognitive sciences*, *19*(2), 92-99. DOI: 10.1016/j.tics.2014.12.004

Davidson, T. J., Kloosterman, F., & Wilson, M. A. (2009). Hippocampal replay of extended experience. *Neuron*, *63*(4), 497-507. DOI: 10.1016/j.neuron.2009.07.027

Dell'Acqua, F., & Tournier, J. D. (2019). Modelling white matter with spherical deconvolution: How and why?. *NMR in Biomedicine*, *32*(4), e3945. 10.1002/nbm.3945

Dell'Acqua, F., Scifo, P., Rizzo, G., Catani, M., Simmons, A., Scotti, G., & Fazio, F. (2010). A modified damped Richardson–Lucy algorithm to reduce isotropic background effects in spherical deconvolution. *Neuroimage*, *49*(2), 1446-1458. DOI: 10.1016/j.neuroimage.2009.09.033

Dell'Acqua, F., Simmons, A., Williams, S. C., & Catani, M. (2013). Can spherical deconvolution provide more information than fiber orientations? Hindrance modulated orientational anisotropy, a true-tract specific index to characterize white matter diffusion. *Human brain mapping*, *34*(10), 2464-2483. DOI: 10.1002/hbm.22080

Dere, E., Huston, J. P., & Silva, M. A. D. S. (2005). Episodic-like memory in mice: simultaneous assessment of object, place and temporal order memory. *Brain research protocols*, *16*(1-3), 10-19. DOI: 10.1016/j.brainresprot.2005.08.001

Dewar, M., Alber, J., Butler, C., Cowan, N., & Della Sala, S. (2012). Brief wakeful resting boosts new memories over the long term. *Psychological science*, *23*(9), 955-960. https://doi.org/10.1177/0956797612441220

Dimsdale-Zucker, H. R., Ritchey, M., Ekstrom, A. D., Yonelinas, A. P., & Ranganath, C. (2018). CA1 and CA3 differentially support spontaneous retrieval of episodic contexts within human hippocampal subfields. *Nature communications*, *9*(1), 1-8. 10.1038/s41467-017-02752-1

Dobbins, I. G., Foley, H., Schacter, D. L., & Wagner, A. D. (2002). Executive control during episodic retrieval: multiple prefrontal processes subserve source memory. *Neuron*, *35*(5), 989-996. 10.1016/s0896-6273(02)00858-9

Downes, J. J., Mayes, A. R., MacDonald, C., & Hunkin, N. M. (2002). Temporal order memory in patients with Korsakoff's syndrome and medial temporal amnesia. Neuropsychologia, 40(7), 853-861.

DuBrow, S., & Davachi, L. (2014). Temporal memory is shaped by encoding stability and intervening item reactivation. *Journal of Neuroscience*, *34*(42), 13998-14005. https://doi.org/10.1523/JNEUROSCI.2535-14.2014

Dupret, D., O'neill, J., Pleydell-Bouverie, B., & Csicsvari, J. (2010). The reorganization and reactivation of hippocampal maps predict spatial memory performance. *Nature neuroscience*, *13*(8), 995. DOI: 10.1038/nn.2599

Düzel, E., Bunzeck, N., Guitart-Masip, M., & Düzel, S. (2010). NOvelty-related motivation of anticipation and exploration by dopamine (NOMAD): implications for healthy aging. *Neuroscience & Biobehavioral Reviews*, *34*(5), 660-669. DOI: 10.1016/j.neubiorev.2009.08.006

Eichenbaum, H. (2013). Memory on time. *Trends in cognitive sciences*, *17*(2), 81-88. DOI: 10.1016/j.tics.2012.12.007

Eichenbaum, H., Sauvage, M., Fortin, N., Komorowski, R., & Lipton, P. (2012). Towards a functional organization of episodic memory in the medial temporal lobe. *Neuroscience & Biobehavioral Reviews*, *36*(7), 1597-1608. DOI: 10.1016/j.neubiorev.2011.07.006

Eichenbaum, H., Yonelinas, A. P., & Ranganath, C. (2007). The medial temporal lobe and recognition memory. *Annu. Rev. Neurosci.*, *30*, 123-152. DOI: 10.1146/annurev.neuro.30.051606.094328

Ezzyat, Y., & Davachi, L. (2011). What constitutes an episode in episodic memory?. *Psychological science*, *22*(2), 243-252. DOI: 10.1177/0956797610393742

Ezzyat, Y., & Davachi, L. (2014). Similarity breeds proximity: pattern similarity within and across contexts is related to later mnemonic judgments of temporal proximity. *Neuron*, *81*(5), 1179-1189. DOI: 10.1016/j.neuron.2014.01.042

Finn, E. S., Shen, X., Scheinost, D., Rosenberg, M. D., Huang, J., Chun, M. M., ... & Constable, R. T. (2015). Functional connectome fingerprinting: identifying individuals using patterns of brain connectivity. *Nature neuroscience*, *18*(11), 1664-1671. DOI: 10.1038/nn.4135

Fortin, N. J., Agster, K. L., & Eichenbaum, H. B. (2002). Critical role of the hippocampus in memory for sequences of events. *Nature neuroscience*, *5*(5), 458-462. DOI: 10.1038/nn834

Freches, G. B., Haak, K. V., Bryant, K. L., Schurz, M., Beckmann, C. F., & Mars, R. B. (2020). Principles of temporal association cortex organisation as revealed by connectivity gradients. *Brain Structure and Function*, 1-16. DOI: 10.1007/s00429-020-02047-0

Friedman, D. P., Aggleton, J. P., & Saunders, R. C. (2002). Comparison of hippocampal, amygdala, and perirhinal projections to the nucleus accumbens: combined anterograde and retrograde tracing study in the Macaque brain. *Journal of Comparative Neurology*, *450*(4), 345-365. DOI: 10.1002/cne.10336

Friston, K. J., Williams, S., Howard, R., Frackowiak, R. S., & Turner, R. (1996). Movement-related effects in fMRI time-series. *Magnetic resonance in medicine*, *35*(3), 346-355. DOI: 10.1002/mrm.1910350312

Friston, K., Moran, R., & Seth, A. K. (2013). Analysing connectivity with Granger causality and dynamic causal modelling. *Current opinion in neurobiology*, *23*(2), 172-178. DOI: 10.1016/j.conb.2012.11.010

Genovese, C. R., Lazar, N. A., & Nichols, T. (2002). Thresholding of statistical maps in functional neuroimaging using the false discovery rate. *Neuroimage*, *15*(4), 870-878. DOI: 10.1006/nimg.2001.1037

Grabner, G., Janke, A. L., Budge, M. M., Smith, D., Pruessner, J., & Collins, D. L. (2006, October). Symmetric atlasing and model based segmentation: an application to the hippocampus in older adults. In *International Conference on Medical Image Computing and Computer-Assisted Intervention* (pp. 58-66). Springer, Berlin, Heidelberg. DOI: 10.1007/11866763_8

Griessenberger, H., Hoedlmoser, K., Heib, D. P. J., Lechinger, J., Klimesch, W., & Schabus, M. (2012). Consolidation of temporal order in episodic memories. Biological psychology, 91(1), 150-155.

Gruber, M. J., Gelman, B. D., & Ranganath, C. (2014). States of curiosity modulate hippocampus-dependent learning via the dopaminergic circuit. *Neuron*, *84*(2), 486-496. https://doi.org/10.1016/j.neuron.2014.08.060

Gruber, M. J., Ritchey, M., Wang, S. F., Doss, M. K., & Ranganath, C. (2016). Post-learning hippocampal dynamics promote preferential retention of rewarding events. *Neuron*, *89*(5), 1110-1120. DOI: 10.1016/j.neuron.2016.01.017

Hagler Jr, D. J., Ahmadi, M. E., Kuperman, J., Holland, D., McDonald, C. R., Halgren, E., & Dale, A. M. (2009). Automated white-matter tractography using a probabilistic diffusion tensor atlas: Application to temporal lobe epilepsy. *Human brain mapping*, *30*(5), 1535-1547. DOI: 10.1002/hbm.20619

Hayman, C. A., Macdonald, C. A., & Tulving, E. (1993). The role of repetition and associative interference in new semantic learning in amnesia: A case experiment. *Journal of Cognitive Neuroscience*, *5*(4), 375-389. DOI: 10.1162/jocn.1993.5.4.375

Heeger, D. J., & Ress, D. (2002). What does fMRI tell us about neuronal activity?. *Nature Reviews Neuroscience*, *3*(2), 142-151. DOI: 10.1038/nrn730

Hennessee, J. P., Reggente, N., Cohen, M. S., Rissman, J., Castel, A. D., & Knowlton, B. J. (2019). White matter integrity in brain structures supporting semantic processing is associated with value-directed remembering in older adults. *Neuropsychologia*, *129*, 246-254. DOI: 10.1016/j.neuropsychologia.2019.04.003

Henson, R. N. A., Buechel, C., Josephs, O., & Friston, K. J. (1999). The slice-timing problem in event-related fMRI. *Neuroimage*, *9*, 125.

Herbet, G., Zemmoura, I., & Duffau, H. (2018). Functional anatomy of the inferior longitudinal fasciculus: from historical reports to current hypotheses. *Frontiers in neuroanatomy*, 12, 77. https://doi.org/10.3389/fnana.2018.00077

Heusser, A. C., Ezzyat, Y., Shiff, I., & Davachi, L. (2018). Perceptual boundaries cause mnemonic trade-offs between local boundary processing and across-trial associative binding. *Journal of Experimental Psychology: Learning, Memory, and Cognition*, *44*(7), 1075. DOI: 10.1037/xlm0000503

Heusser, A. C., Poeppel, D., Ezzyat, Y., & Davachi, L. (2016). Episodic sequence memory is supported by a theta–gamma phase code. *Nature neuroscience*, *19*(10), 1374-1380. https://doi.org/10.1038/nn.4374

Hodgetts, C. J., Postans, M., Warne, N., Varnava, A., Lawrence, A. D., & Graham, K. S. (2017). Distinct contributions of the fornix and inferior longitudinal fasciculus to episodic and semantic autobiographical memory. *cortex*, *94*, 1-14. DOI: 10.1016/j.cortex.2017.05.010

Holm, S. (1979). A simple sequentially rejective multiple test procedure. *Scandinavian journal of statistics*, 65-70. DOI: 10.2307/4615733

Hsieh, L. T., Gruber, M. J., Jenkins, L. J., & Ranganath, C. (2014). Hippocampal activity patterns carry information about objects in temporal context. *Neuron*, *81*(5), 1165-1178. DOI: 10.1016/j.neuron.2014.01.015

Huisman, T. A. (2010). Diffusion-weighted and diffusion tensor imaging of the brain, made easy. *Cancer Imaging*, *10*(1A), S163. DOI: 10.1102/1470-7330.2010.9023

Igloi, K., Gaggioni, G., Sterpenich, V., & Schwartz, S. (2015). A nap to recap or how reward regulates hippocampal-prefrontal memory networks during daytime sleep in humans. *Elife*, *4*, e07903. DOI: 10.7554/eLife.07903

JASP Team (2019). JASP (Version 0.11.1) [Computer software].

Jenkins, L. J., & Ranganath, C. (2010). Prefrontal and medial temporal lobe activity at encoding predicts temporal context memory. *Journal of Neuroscience*, *30*(46), 15558-15565. https://doi.org/10.1523/JNEUROSCI.1337-10.2010

Jenkins, L. J., & Ranganath, C. (2016). Distinct neural mechanisms for remembering when an event occurred. *Hippocampus*, *26*(5), 554-559. DOI: 10.1002/hipo.22571

Jones, D. K. (2008). Studying connections in the living human brain with diffusion MRI. *cortex*, *44*(8), 936-952. DOI: 10.1016/j.cortex.2008.05.002

Jones, D. K. (2010). Challenges and limitations of quantifying brain connectivity in vivo with diffusion MRI. *Imaging in Medicine*, *2*(3), 341-355. DOI: 10.2217/iim.10.21

Johnson, M. K., Hashtroudi, S., & Lindsay, D. S. (1993). Source monitoring. Psychological bulletin, 114(1), 3.

Jones, D. K., Horsfield, M. A., & Simmons, A. (1999). Optimal strategies for measuring diffusion in anisotropic systems by magnetic resonance imaging. *Magnetic Resonance in Medicine: An Official Journal of the International Society for Magnetic Resonance in Medicine*, *42*(3), 515-525. https://doi.org/10.1002/(SICI)1522-2594(199909)42:3<515::AID-MRM14>3.0.CO;2-Q

Kahn, I., & Shohamy, D. (2013). Intrinsic connectivity between the hippocampus, nucleus accumbens, and ventral tegmental area in humans. *Hippocampus*, *23*(3), 187-192. DOI: 10.1002/hipo.22077

Kanai, R., & Rees, G. (2011). The structural basis of inter-individual differences in human behaviour and cognition. *Nature Reviews Neuroscience*, *12*(4), 231-242. DOI: 10.1038/nrn3000

Karlsson, M. P., & Frank, L. M. (2009). Awake replay of remote experiences in the hippocampus. *Nature neuroscience*, *12*(7), 913-918. DOI: 10.1038/nn.2344

Kellner, E., Dhital, B., Kiselev, V. G., & Reisert, M. (2016). Gibbs-ringing artifact removal based on local subvoxel-shifts. *Magnetic resonance in medicine*, *76*(5), 1574-1581. DOI: 10.1002/mrm.26054

Kirwan, C. B., Wixted, J. T., & Squire, L. R. (2008). Activity in the medial temporal lobe predicts memory strength, whereas activity in the prefrontal cortex predicts recollection. *Journal of Neuroscience*, *28*(42), 10541-10548. https://doi.org/10.1523/JNEUROSCI.3456-08.2008

Knutson, B., Adams, C. M., Fong, G. W., & Hommer, D. (2001). Anticipation of increasing monetary reward selectively recruits nucleus accumbens. *Journal of Neuroscience*, *21*(16), RC159-RC159. https://doi.org/10.1523/JNEUROSCI.21-16-j0002.2001

Koller, K., Rudrapatna, U., Chamberland, M., Raven, E. P., Parker, G. D., Tax, C. M., ... & Jones, D. K. (2021). Micra: Microstructural image compilation with repeated acquisitions. NeuroImage, 225, 117406.

Kondo, H., Saleem, K. S., & Price, J. L. (2005). Differential connections of the perirhinal and parahippocampal cortex with the orbital and medial prefrontal networks in macaque monkeys. *Journal of Comparative Neurology*, *493*(4), 479-509. DOI: 10.1002/cne.20796

Konkle, T., Brady, T. F., Alvarez, G. A., & Oliva, A. (2010). Scene memory is more detailed than you think: The role of categories in visual long-term memory. *Psychological science*, *21*(11), 1551-1556. DOI: 10.1177/0956797610385359

Kuhl, B. A., Shah, A. T., DuBrow, S., & Wagner, A. D. (2010). Resistance to forgetting associated with hippocampus-mediated reactivation during new learning. *Nature neuroscience*, *13*(4), 501-506. DOI: 10.1038/nn.2498

Kurby, C. A., & Zacks, J. M. (2008). Segmentation in the perception and memory of events. *Trends in cognitive sciences*, *12*(2), 72-79. DOI: 10.1016/j.tics.2007.11.004

Lansink, C. S., Goltstein, P. M., Lankelma, J. V., Joosten, R. N., McNaughton, B. L., & Pennartz, C. M. (2008). Preferential reactivation of motivationally relevant information in the ventral striatum. *Journal of Neuroscience*, *28*(25), 6372-6382. DOI: 10.1523/JNEUROSCI.1054-08.2008

Le Bihan, D. (2003). Looking into the functional architecture of the brain with diffusion MRI. *Nature reviews neuroscience*, *4*(6), 469-480. DOI: 10.1038/nrn1119

Le Bihan, D., & Iima, M. (2015). Diffusion magnetic resonance imaging: what water tells us about biological tissues. *PLoS biology*, *13*(7), e1002203. https://doi.org/10.1371/journal.pbio.1002203

Le Bihan, D., Mangin, J. F., Poupon, C., Clark, C. A., Pappata, S., Molko, N., & Chabriat, H. (2001). Diffusion tensor imaging: concepts and applications. *Journal of Magnetic Resonance Imaging: An Official Journal of the International Society for Magnetic Resonance in Medicine*, *13*(4), 534-546. DOI: 10.1002/jmri.1076

Lee, A. K., & Wilson, M. A. (2002). Memory of sequential experience in the hippocampus during slow wave sleep. *Neuron*, *36*(6), 1183-1194. DOI: 10.1016/s0896-6273(02)01096-6

Leemans, A. J. B. S. J. J. D. K., Jeurissen, B., Sijbers, J., & Jones, D. K. (2009, April). ExploreDTI: a graphical toolbox for processing, analyzing, and visualizing diffusion MR data. In Proc Intl Soc Mag Reson Med (Vol. 17, No. 1).

Lerner, A., Mogensen, M. A., Kim, P. E., Shiroishi, M. S., Hwang, D. H., & Law, M. (2014). Clinical applications of diffusion tensor imaging. *World neurosurgery*, *82*(1-2), 96-109. DOI: 10.1016/j.wneu.2013.07.083

Levine, B., Black, S. E., Cabeza, R., Sinden, M., McIntosh, A. R., Toth, J. P., ... & Stuss, D. T. (1998). Episodic memory and the self in a case of isolated retrograde amnesia. *Brain: a journal of neurology*, *121*(10), 1951-1973. DOI: 10.1093/brain/121.10.1951

Libby, L. A., Yonelinas, A. P., Ranganath, C., & Ragland, J. D. (2013). Recollection and familiarity in schizophrenia: a quantitative review. *Biological psychiatry*, *73*(10), 944-950. https://doi.org/10.1016/j.biopsych.2012.10.027

Lieberman, M. D., & Cunningham, W. A. (2009). Type I and Type II error concerns in fMRI research: re-balancing the scale. *Social cognitive and affective neuroscience*, *4*(4), 423-428. DOI: 10.1093/scan/nsp052

Lisman, J. E., & Grace, A. A. (2005). The hippocampal-VTA loop: controlling the entry of information into long-term memory. *Neuron*, *46*(5), 703-713. DOI: 10.1016/j.neuron.2005.05.002

Lisman, J., Grace, A. A., & Düzel, E. (2011). A neoHebbian framework for episodic memory; role of dopamine-dependent late LTP. *Trends in neurosciences*, *34*(10), 536-547. DOI: 10.1016/j.tins.2011.07.006

MacDonald, C. J., Lepage, K. Q., Eden, U. T., & Eichenbaum, H. (2011). Hippocampal "time cells" bridge the gap in memory for discontiguous events. *Neuron*, *71*(4), 737-749. DOI: 10.1016/j.neuron.2011.07.012

Madan, C. R., & Spetch, M. L. (2012). Is the enhancement of memory due to reward driven by value or salience?. Acta psychologica, 139(2), 343-349. https://doi.org/10.1016/j.actpsy.2011.12.010.

Manns, J. R., Howard, M. W., & Eichenbaum, H. (2007). Gradual changes in hippocampal activity support remembering the order of events. *Neuron*, *56*(3), 530-540. DOI: 10.1016/j.neuron.2007.08.017

Mason, A., Farrell, S., Howard-Jones, P., & Ludwig, C. J. (2017). The role of reward and reward uncertainty in episodic memory. *Journal of memory and language*, *96*, 62-77. DOI: 10.1016/j.jml.2017.05.003

MATLAB. (2015). 8.5.1.281278 (R2015a). Natick, Massachusetts: The MathWorks Inc.

Mayes, A. R., Isaac, C. L., Holdstock, J. S., Hunkin, N. M., Montaldi, D., Downes, J. J., ... & Roberts, J. N. (2001). Memory for single items, word pairs, and temporal order of different kinds in a patient with selective hippocampal lesions. Cognitive neuropsychology, 18(2), 97-123.

McGaugh, J. L. (2000). Memory--a century of consolidation. *Science*, *287*(5451), 248-251. DOI: 10.1126/science.287.5451.248

McKenzie, S., Frank, A. J., Kinsky, N. R., Porter, B., Rivière, P. D., & Eichenbaum, H. (2014). Hippocampal representation of related and opposing memories develop within distinct, hierarchically organized neural schemas. *Neuron*, *83*(1), 202-215. DOI: 10.1016/j.neuron.2014.05.019

Mercer, T. (2015). Wakeful rest alleviates interference-based forgetting. *Memory*, *23*(2), 127-137. DOI: 10.1080/09658211.2013.872279

Metzler-Baddeley, C., Jones, D. K., Belaroussi, B., Aggleton, J. P., & O'Sullivan, M. J. (2011). Frontotemporal connections in episodic memory and aging: a diffusion MRI tractography study. *Journal of Neuroscience*, *31*(37), 13236-13245. https://doi.org/10.1523/JNEUROSCI.2317-11.2011

Miendlarzewska, E. A., Bavelier, D., & Schwartz, S. (2016). Influence of reward motivation on human declarative memory. *Neuroscience & Biobehavioral Reviews*, *61*, 156-176. DOI: 10.1016/j.neubiorev.2015.11.015

Miyashita, Y. (2019). Perirhinal circuits for memory processing. *Nature Reviews Neuroscience*, *20*(10), 577-592. https://doi.org/10.1038/s41583-019-0213-6

Mori, S., & Zhang, J. (2006). Principles of diffusion tensor imaging and its applications to basic neuroscience research. *Neuron*, *51*(5), 527-539. DOI: 10.1016/j.neuron.2006.08.012

Morris, J. S., & Dolan, R. J. (2001). Involvement of human amygdala and orbitofrontal cortex in hunger-enhanced memory for food stimuli. *Journal of*

*Neuroscience*, *21*(14), 5304-5310. https://doi.org/10.1523/JNEUROSCI.21-14-05304.2001

Moss, M., Mahut, H., & Zola-Morgan, S. (1981). Concurrent discrimination learning of monkeys after hippocampal, entorhinal, or fornix lesions. *Journal of Neuroscience*, *1*(3), 227-240. https://doi.org/10.1523/JNEUROSCI.01-03-00227.1981

Murayama, K., & Kitagami, S. (2014). Consolidation power of extrinsic rewards: Reward cues enhance long-term memory for irrelevant past events. *Journal of Experimental Psychology: General*, *143*(1), 15. https://doi.org/10.1037/a0031992

Murayama, K., & Kuhbandner, C. (2011). Money enhances memory consolidation–But only for boring material. *Cognition*, *119*(1), 120-124. DOI: 10.1016/j.cognition.2011.01.001

Murray, E. A., Wise, S. P., & Graham, K. S. (2018). Representational specializations of the hippocampus in phylogenetic perspective. *Neuroscience letters*, *680*, 4-12. https://doi.org/10.1016/j.neulet.2017.04.065

Murty, V. P., & Adcock, R. A. (2014). Enriched encoding: reward motivation organizes cortical networks for hippocampal detection of unexpected events. Cerebral *Cortex*, *24*(8), 2160-2168. DOI: 10.1093/cercor/bht063

Murty, V. P., Shermohammed, M., Smith, D. V., Carter, R. M., Huettel, S. A., & Adcock, R. A. (2014). Resting state networks distinguish human ventral tegmental area from substantia nigra. *Neuroimage*, *100*, 580-589. 10.1016/j.neuroimage.2014.06.047

Murty, V. P., Tompary, A., Adcock, R. A., & Davachi, L. (2017). Selectivity in postencoding connectivity with high-level visual cortex is associated with reward-motivated memory. *Journal of Neuroscience*, *37*(3), 537-545. https://doi.org/10.1523/JNEUROSCI.4032-15.2016

Nichols, E. S., Erez, J., Stojanoski, B., Lyons, K. M., Witt, S. T., Mace, C. A., ... & Owen, A. M. (2020). Longitudinal white matter changes associated with cognitive training. *bioRxiv*. https://doi.org/10.1101/2020.11.24.396119

Nieto-Castanon, Alfonso. (2020). Handbook of functional connectivity Magnetic Resonance Imaging methods in CONN.

O'Keefe, J., & Nadel, L. (1978). The hippocampus as a cognitive map. Oxford: Clarendon Press.

O'Carroll, C. M., Martin, S. J., Sandin, J., Frenguelli, B., & Morris, R. G. (2006). Dopaminergic modulation of the persistence of one-trial hippocampus-dependent memory. *Learning & memory*, *13*(6), 760-769. DOI: 10.1101/lm.321006

O'Donnell, L. J., & Westin, C. F. (2011). An introduction to diffusion tensor image analysis. *Neurosurgery Clinics*, *22*(2), 185-196. DOI: 10.1016/j.nec.2010.12.004

Oudiette, D., Antony, J. W., Creery, J. D., & Paller, K. A. (2013). The role of memory reactivation during wakefulness and sleep in determining which memories endure. *Journal of Neuroscience*, *33*(15), 6672-6678. https://doi.org/10.1523/JNEUROSCI.5497-12.2013

Palombo, D. J., Di Lascio, J. M., Howard, M. W., & Verfaellie, M. (2019). Medial temporal lobe amnesia is associated with a deficit in recovering temporal context. Journal of cognitive neuroscience, 31(2), 236-248.

Palombo, D. J., Sheldon, S., & Levine, B. (2018). Individual differences in autobiographical memory. Trends in Cognitive Sciences, 22(7), 583-597.

Parker, G. D., Marshall, D., Rosin, P. L., Drage, N., Richmond, S., & Jones, D. K. (2013). Fast and fully automated clustering of whole brain tractography results using shape-space analysis. *Proceedings of the International Society for Magnetic Resonance in Medicine*. Salt Lake City, USA, 778.

Pasternak, O., Sochen, N., Gur, Y., Intrator, N., & Assaf, Y. (2009). Free water elimination and mapping from diffusion MRI. *Magnetic Resonance in Medicine: An Official Journal of the International Society for Magnetic Resonance in Medicine*, *62*(3), 717-730. DOI: 10.1002/mrm.22055

Patterson, K., Nestor, P. J., & Rogers, T. T. (2007). Where do you know what you know? The representation of semantic knowledge in the human brain. *Nature reviews neuroscience*, *8*(12), 976-987. DOI: 10.1038/nrn2277

Peyrache, A., Khamassi, M., Benchenane, K., Wiener, S. I., & Battaglia, F. P. (2009). Replay of rule-learning related neural patterns in the prefrontal cortex during sleep. *Nature neuroscience*, *12*(7), 919-926. DOI: 10.1038/nn.2337

Place, R., Farovik, A., Brockmann, M., & Eichenbaum, H. (2016). Bidirectional prefrontal-hippocampal interactions support context-guided memory. *Nature neuroscience*, *19*(8), 992-994. DOI: 10.1038/nn.4327

Polster, M. R., Nadel, L., & Schacter, D. L. (1991). Cognitive neuroscience analyses of memory: A historical perspective. *Journal of Cognitive Neuroscience*, *3*(2), 95-116. DOI: https://doi.org/10.1162/jocn.1991.3.2.95

Poppenk, J., Evensmoen, H. R., Moscovitch, M., & Nadel, L. (2013). Long-axis specialization of the human hippocampus. Trends in cognitive sciences, 17(5), 230-240.

Postma, A., Van Asselen, M., Keuper, O., Wester, A. J., & Kessels, R. P. (2006). Spatial and temporal order memory in Korsakoff patients. Journal of the International Neuropsychological Society: JINS, 12(3), 327.

Power, J. D., Mitra, A., Laumann, T. O., Snyder, A. Z., Schlaggar, B. L., & Petersen, S. E. (2014). Methods to detect, characterize, and remove motion artifact in resting state fMRI. *Neuroimage*, *84*, 320-341. DOI: 10.1016/j.neuroimage.2013.08.048

Preston, A. R., & Eichenbaum, H. (2013). Interplay of hippocampus and prefrontal cortex in memory. *Current Biology*, *23*(17), R764-R773. DOI: 10.1016/j.cub.2013.05.041

Ralph, M. A. L., Jefferies, E., Patterson, K., & Rogers, T. T. (2017). The neural and computational bases of semantic cognition. *Nature Reviews Neuroscience*, *18*(1), 42. DOI: 10.1038/nrn.2016.150

Ranganath, C., & Ritchey, M. (2012). Two cortical systems for memory-guided behaviour. *Nature Reviews Neuroscience*, *13*(10), 713-726. DOI: 10.1038/nrn3338

Reggente, N., Cohen, M. S., Zheng, Z. S., Castel, A. D., Knowlton, B. J., & Rissman, J. (2018). Memory recall for high reward value items correlates with individual differences in white matter pathways associated with reward processing and fronto-temporal communication. *Frontiers in human neuroscience*, *12*, 241. https://doi.org/10.3389/fnhum.2018.00241

Rekkas, P. V., Westerveld, M., Skudlarski, P., Zumer, J., Pugh, K., Spencer, D. D., & Constable, R. T. (2005). Neural correlates of temporal-order judgments versus those of spatial-location: deactivation of hippocampus may facilitate spatial performance. *Brain and cognition*, *59*(2), 103-113. https://doi.org/10.1016/j.bandc.2005.05.013

Rice, G. E., Hoffman, P., & Ralph, M. A. L. (2015). Graded specialization within and between the anterior temporal lobes. *Annals of the New York Academy of Sciences*, *1359*(1), 84. DOI: 10.1111/nyas.12951

Rosenbaum, R. S., Köhler, S., Schacter, D. L., Moscovitch, M., Westmacott, R., Black, S. E., ... & Tulving, E. (2005). The case of KC: contributions of a memory-impaired person to memory theory. Neuropsychologia, 43(7), 989-1021.

Ross, E. K., Kim, J. P., Settell, M. L., Han, S. R., Blaha, C. D., Min, H. K., & Lee, K. H. (2016). Fornix deep brain stimulation circuit effect is dependent on major excitatory transmission via the nucleus accumbens. *Neuroimage*, *128*, 138-148. DOI: 10.1016/j.neuroimage.2015.12.056

Rudebeck, S. R., Scholz, J., Millington, R., Rohenkohl, G., Johansen-Berg, H., & Lee, A. C. (2009). Fornix microstructure correlates with recollection but not familiarity memory. *Journal of Neuroscience*, *29*(47), 14987-14992. DOI: 10.1523/JNEUROSCI.4707-09.2009

Sampaio-Baptista, C., & Johansen-Berg, H. (2017). White matter plasticity in the adult brain. *Neuron*, *96*(6), 1239-1251. DOI: 10.1016/j.neuron.2017.11.026

Saunders, R. C., & Aggleton, J. P. (2007). Origin and topography of fibers contributing to the fornix in macaque monkeys. Hippocampus, 17(5), 396-411.

Scholz, J., Klein, M. C., Behrens, T. E., & Johansen-Berg, H. (2009). Training induces changes in white-matter architecture. *Nature neuroscience*, *12*(11), 1370-1371. DOI: 10.1038/nn.2412

Schultz W. (2015). Neuronal Reward and Decision Signals: From Theories to Data. Physiological reviews, 95(3), 853–951. https://doi.org/10.1152/physrev.00023.2014

Seghier, M. L., & Price, C. J. (2018). Interpreting and utilising intersubject variability in brain function. *Trends in Cognitive Sciences*, *22*(6), 517-530. DOI: 10.1016/j.tics.2018.03.003

Shin, H., Lee, S. Y., Cho, H. U., Oh, Y., Kim, I. Y., Jang, D. P., & Min, H. K. (2019). Fornix stimulation induces metabolic activity and dopaminergic response in the nucleus accumbens. *Frontiers in neuroscience*, *13*, 1109. https://doi.org/10.3389/fnins.2019.01109

Shohamy, D., & Adcock, R. A. (2010). Dopamine and adaptive memory. *Trends in cognitive sciences*, *14*(10), 464-472. DOI: 10.1016/j.tics.2010.08.002

Singer, A. C., & Frank, L. M. (2009). Rewarded outcomes enhance reactivation of experience in the hippocampus. *Neuron*, *64*(6), 910-921. DOI: 10.1016/j.neuron.2009.11.016

Smith, S. M. (2002). Fast robust automated brain extraction. *Human brain mapping*, *17*(3), 143-155. DOI: 10.1002/hbm.10062

Smitha, K. A., Akhil Raja, K., Arun, K. M., Rajesh, P. G., Thomas, B., Kapilamoorthy, T. R., & Kesavadas, C. (2017). Resting state fMRI: A review on methods in resting state connectivity analysis and resting state networks. *The neuroradiology journal*, *30*(4), 305-317. DOI: 10.1177/1971400917697342

Soares, J., Marques, P., Alves, V., & Sousa, N. (2013). A hitchhiker's guide to diffusion tensor imaging. *Frontiers in neuroscience*, *7*, 31. https://doi.org/10.3389/fnins.2013.00031

Spaniol, J., Schain, C., & Bowen, H. J. (2014). Reward-enhanced memory in younger and older adults. *Journals of Gerontology Series B: Psychological Sciences and Social Sciences*, *69*(5), 730-740. https://doi.org/10.1093/geronb/gbt044

Squire, L. R. (1992). Declarative and nondeclarative memory: Multiple brain systems supporting learning and memory. Journal of cognitive neuroscience, 4(3), 232-243.

St. Jacques, P., Rubin, D. C., LaBar, K. S., & Cabeza, R. (2008). The short and long of it: Neural correlates of temporal-order memory for autobiographical events. Journal of cognitive neuroscience, 20(7), 1327-1341.

Stephan, K. E., & Friston, K. J. (2010). Analyzing effective connectivity with functional magnetic resonance imaging. *Wiley Interdisciplinary Reviews: Cognitive Science*, *1*(3), 446-459. DOI: 10.1002/wcs.58

Stern, C.E., Hasselmo, M.E. (2008). The neurobiological basis of recognition memory. In: J.H. Byrne (Ed.) Learning and Memory: A Comprehensive Reference (pp. 131-141). https://doi.org/10.1016/B978-012370509-9.00109-1.

Strange, B. A., Witter, M. P., Lein, E. S., & Moser, E. I. (2014). Functional organization of the hippocampal longitudinal axis. Nature Reviews Neuroscience, 15(10), 655-669.

Studte, S., Bridger, E., & Mecklinger, A. (2017). Sleep spindles during a nap correlate with post sleep memory performance for highly rewarded word-pairs. *Brain and language*, *167*, 28-35. DOI: 10.1016/j.bandl.2016.03.003

Sullivan, E. V., & Pfefferbaum, A. (2009). Neuroimaging of the Wernicke–Korsakoff syndrome. Alcohol & Alcoholism, 44(2), 155-165.

Tambini, A., Rimmele, U., Phelps, E. A., & Davachi, L. (2017). Emotional brain states carry over and enhance future memory formation. *Nature neuroscience*, *20*(2), 271-278. DOI: 10.1038/nn.4468

Tavor, I., Jones, O. P., Mars, R. B., Smith, S. M., Behrens, T. E., & Jbabdi, S. (2016). Task-free MRI predicts individual differences in brain activity during task performance. *Science*, *352*(6282), 216-220. DOI: 10.1126/science.aad8127

Teipel, S. J., Bokde, A. L., Meindl, T., Amaro Jr, E., Soldner, J., Reiser, M. F., ... & Hampel, H. (2010). White matter microstructure underlying default mode network connectivity in the human brain. Neuroimage, 49(3), 2021-2032.

Templer, V. L., & Hampton, R. R. (2013). Cognitive mechanisms of memory for order in rhesus monkeys (Macaca mulatta). *Hippocampus*, *23*(3), 193-201. DOI: 10.1002/hipo.22082

Tompary, A., Duncan, K., & Davachi, L. (2016). High-resolution investigation of memory-specific reinstatement in the hippocampus and perirhinal cortex. *Hippocampus*, *26*(8), 995-1007. DOI: 10.1002/hipo.22582

Tournier, J. D., Smith, R., Raffelt, D., Tabbara, R., Dhollander, T., Pietsch, M., ... & Connelly, A. (2019). MRtrix3: A fast, flexible and open software framework for medical image processing and visualisation. *Neuroimage*, *202*, 116137. DOI: 10.1016/j.neuroimage.2019.116137

Tubridy, S., & Davachi, L. (2011). Medial temporal lobe contributions to episodic sequence encoding. *Cerebral cortex*, *21*(2), 272-280. DOI: 10.1093/cercor/bhq092

Tulving, E. (1984). Precis of elements of episodic memory. *Behavioral and Brain Sciences*, *7*(2), 223-238. https://doi.org/10.1017/S0140525X0004440X

Tulving, E. (2002). Episodic memory: From mind to brain. *Annual review of psychology*, *53*(1), 1-25. DOI: 10.1146/annurev.psych.53.100901.135114

Tulving, E., Hayman, C. A., & Macdonald, C. A. (1991). Long-lasting perceptual priming and semantic learning in amnesia: a case experiment. *Journal of Experimental Psychology: Learning, Memory, and Cognition*, *17*(4), 595. https://doi.org/10.1037/0278-7393.17.4.595

Tulving, E., & Thomson, D. M. (1973). Encoding specificity and retrieval processes in episodic memory. Psychological review, 80(5), 352.

Van Den Heuvel, M. P., & Pol, H. E. H. (2010). Exploring the brain network: a review on resting-state fMRI functional connectivity. *European neuropsychopharmacology*, *20*(8), 519-534. DOI: 10.1016/j.euroneuro.2010.03.008

van der Meer, M. A., Johnson, A., Schmitzer-Torbert, N. C., & Redish, A. D. (2010). Triple dissociation of information processing in dorsal striatum, ventral striatum, and hippocampus on a learned spatial decision task. *Neuron*, *67*(1), 25-32. DOI: 10.1016/j.neuron.2010.06.023

Veraart, J., Novikov, D. S., Christiaens, D., Ades-Aron, B., Sijbers, J., & Fieremans, E. (2016). Denoising of diffusion MRI using random matrix theory. *Neuroimage*, *142*, 394-406. DOI: 10.1016/j.neuroimage.2016.08.016

Vettel, J. M., Cooper, N., Garcia, J. O., Yeh, F. C., & Verstynen, T. D. (2017). White Matter Tractography and Diffusion-Weighted Imaging. *eLS*, 1-9. https://doi.org/10.1002/9780470015902.a0027162

Wais, P. E., Squire, L. R., & Wixted, J. T. (2010). In search of recollection and familiarity signals in the hippocampus. *Journal of cognitive neuroscience*, *22*(1), 109-123. https://doi.org/10.1162/jocn.2009.21190

Wakana, S., Caprihan, A., Panzenboeck, M. M., Fallon, J. H., Perry, M., Gollub, R. L., ... & Blitz, A. (2007). Reproducibility of quantitative tractography methods applied to cerebral white matter. *Neuroimage*, *36*(3), 630-644. DOI: 10.1016/j.neuroimage.2007.02.049

Wallenstein, G. V., Hasselmo, M. E., & Eichenbaum, H. (1998). The hippocampus as an associator of discontiguous events. *Trends in neurosciences*, *21*(8), 317-323. https://doi.org/10.1016/S0166-2236(97)01220-4

Warthen, K. G., Boyse-Peacor, A., Jones, K. G., Sanford, B., Love, T. M., & Mickey, B. J. (2020). Sex differences in the human reward system: convergent behavioral, autonomic and neural evidence. Social cognitive and affective neuroscience, 15(7), 789-801.

Whitfield-Gabrieli, S., & Nieto-Castanon, A. (2012). Conn: a functional connectivity toolbox for correlated and anticorrelated brain networks. *Brain connectivity*, *2*(3), 125-141. DOI: 10.1089/brain.2012.0073

Wig, G. S., Grafton, S. T., Demos, K. E., Wolford, G. L., Petersen, S. E., & Kelley, W. M. (2008). Medial temporal lobe BOLD activity at rest predicts individual differences in memory ability in healthy young adults. *Proceedings of the National Academy of Sciences*, *105*(47), 18555-18560. https://doi.org/10.1073/pnas.0804546105

Wimmer, G. E., & Büchel, C. (2016). Reactivation of reward-related patterns from single past episodes supports memory-based decision making. Journal of Neuroscience, 36(10), 2868-2880.

Wimmer, G. E., & Shohamy, D. (2012). Preference by association: how memory mechanisms in the hippocampus bias decisions. *Science*, *338*(6104), 270-273. DOI: 10.1126/science.1223252

Wittmann, B. C., Schott, B. H., Guderian, S., Frey, J. U., Heinze, H. J., & Düzel, E. (2005). Reward-related FMRI activation of dopaminergic midbrain is associated with enhanced hippocampus-dependent long-term memory formation. *Neuron*, *45*(3), 459-467. DOI: 10.1016/j.neuron.2005.01.010

Wixted, J. T., & Squire, L. R. (2011). The medial temporal lobe and the attributes of memory. *Trends in cognitive sciences*, *15*(5), 210-217. DOI: 10.1016/j.tics.2011.03.005

Wolosin, S. M., Zeithamova, D., & Preston, A. R. (2012). Reward modulation of hippocampal subfield activation during successful associative encoding and retrieval. *Journal of Cognitive Neuroscience*, *24*(7), 1532-1547. https://doi.org/10.1162/jocn_a_00237

Xiang, J. Z., & Brown, M. W. (1998). Differential neuronal encoding of novelty, familiarity and recency in regions of the anterior temporal lobe. *Neuropharmacology*, *37*(4-5), 657-676. DOI: 10.1016/s0028-3908(98)00030-6

Yonelinas, A. P. (2002). The nature of recollection and familiarity: A review of 30 years of research. *Journal of memory and language*, *46*(3), 441-517. https://doi.org/10.1006/jmla.2002.2864

Yonelinas, A. P., & Jacoby, L. L. (1995). The relation between remembering and knowing as bases for recognition: Effects of size congruency. *Journal of memory and language*, *34*, 622-622. https://doi.org/10.1006/jmla.1995.1028

Zeithamova, D., Dominick, A. L., & Preston, A. R. (2012). Hippocampal and ventral medial prefrontal activation during retrieval-mediated learning supports novel inference. *Neuron*, *75*(1), 168-179. DOI: 10.1016/j.neuron.2012.05.010

Zhang, C., Hu, W. H., Wu, D. L., Zhang, K., & Zhang, J. G. (2015). Behavioral effects of deep brain stimulation of the anterior nucleus of thalamus, entorhinal cortex and

fornix in a rat model of Alzheimer's disease. *Chinese Medical Journal*, *128*(9), 1190. 10.4103/0366-6999.156114

Zhang, H., Schneider, T., Wheeler-Kingshott, C. A., & Alexander, D. C. (2012). NODDI: practical in vivo neurite orientation dispersion and density imaging of the human brain. *Neuroimage*, *61*(4), 1000-1016. DOI: 10.1016/j.neuroimage.2012.03.072

Zhang, P., Hou, F., Yan, F. F., Xi, J., Lin, B. R., Zhao, J., ... & Dosher, B. A. (2018). High reward enhances perceptual learning. *Journal of vision*, *18*(8), 11-11. DOI: 10.1167/18.8.11